UNDERSTANDING HEAT STRESS MECHANISMS IN CREEPING BENTGRASS: FROM PHYSIOLOGY TO MOLECULAR BIOLOGY WITH A FOCUS ON PROTEIN METABOLISM

by

QIANQIAN FAN

(Under the Direction of David Jespersen)

ABSTRACT

Creeping bentgrass (*Agrositis stolonifera* L.) is an economically important perennial grass species which is largely used on high value turf areas but typically show poor performance during summer months due to a lack in heat tolerance. The common symptoms induced by heat stress include photosynthesis inhibition, oxidative damage as well as interruption in metabolism, with interruption in protein metabolism, in turn, exacerbating the former two processes. To accelerate the development of more heat-tolerant cultivars, there is a critical need to better understand the intraspecific diversity in heat tolerance among different lines. Hence, this dissertation aimed to investigate heat stress mechanism in creeping bentgarss from physiology to molecular biology with a focus on protein metabolism, by studying a few promising experimental lines that have demonstrated good summer performance in preliminary trials. A broad range of thermotolerance was found to exist among different creeping bentgrass lines, with S11 729-10 identified as more heat tolerant, supported by its ability to better maintain photosynthetic capacity, regulate protein metabolism, and minimize oxidative damage. The improved physiological performance in S11 729-10 was closely associated with change in protein accumulation at various levels. At the

biochemical level, S11 729-10 maintained lower activities of both protease and the ubiquitin-proteasome system (UPS), two major proteolytic pathways, contributing to its slower protein degradation and higher total protein contents. At the global protein level, S11 729-10 maintain less severe downregulation of proteins involved in the light reactions of photosynthesis, while enhancing the upregulation of antioxidant proteins, particularly during the later phase of stress. This contributed to greater cell membrane integrity and healthier light harvesting components. Additionally, at the level of ubiquitin-tagged proteins targeted by the UPS, the faster turnover of key polyubiquitinated antioxidant proteins in S11 729-10 likely represents a critical mechanism for protecting against oxidative damage and enhancing tolerance under prolonged heat stress. Taken together, this study advances our understanding of global protein accumulation and degradation though protease and the UPS, as well as their associated physiological responses, providing new insights into the thermotolerance mechanisms in creeping bentgrass. The key proteins, pathways, and unique germplasm identified in this research can be utilized for the development of new cultivars with enhanced thermotolerance to help plants cope with climate change.

INDEX WORDS: Creeping Bentgrass, Heat Stress, Protein Metabolism, Proteolysis, Physiology, Protease, the Ubiquitin-Proteasome System

UNDERSTANDING HEAT STRESS MECHANISMS IN CREEPING BENTGRASS: FROM PHYSIOLOGY TO MOLECULAR BIOLOGY WITH A FOCUS ON PROTEIN METABOLISM

by

QIANQIAN FAN

BS, China Agricultural University, P.R. China, 2016

MS, Oregon State University, USA, 2019

A Dissertation Submitted to the Graduate Faculty of The University of Georgia in Partial Fulfillment of the Requirements for the Degree

DOCTOR OF PHILOSOPHY

ATHENS, GEORGIA

2024

UNDERSTANDING HEAT STRESS MECHANISMS IN CREEPING BENTGRASS: FROM PHYSIOLOGY TO MOLECULAR BIOLOGY WITH A FOCUS ON PROTEIN METABOLISM

by

QIANQIAN FAN

Major Professor:	David Jespersen
Committee:	Paul L. Raymer
	Stacy Bonos
	Gerald M. Henry
	Cristiane Pilon

Electronic Version Approved:

Ron Walcott
Vice Provost for Graduate Education and Dean of the Graduate School
The University of Georgia
December 2024

DEDICATION

I dedicate this dissertation to my beloved grandparents, Shixin Fan and Miaozhi Fan, as well as my beloved parents, Fangbing Fan and Zhusun Fan, for their endless love, patience, and for their understanding of my absence over the past six years.

ACKNOWLEDGEMENTS

First, I'd like to express my deep gratitude to my Ph.D. advisor, Dr. David Jespersen, for his insightful mentorship and tremendous support. The Ph.D. journal has been long and challenging, requiring constant learning and critical thinking. Dr. Jespersen, who exemplifies the role of a plant physiologist, has expertly guided my research, helping to shape me into an independent scientist. Joining his lab has been one of the best decisions I've made in the past six years, and I will always cherish my time there.

I'm deeply grateful to my committee members, Dr. Paul Raymer, Dr. Stacy Bonos, Dr. Gerald Henry and Dr. Cristiane Pilon, for their constructive feedback and unwavering support throughout the journey. I'd like to express my sincere appreciation to Dr. Zhengbang Chen, who taught me the genotyping lab technique, and to Dr. Chauwen Chou, who provided detailed insights into proteomics, despite their busy schedules. Your kindness and assistance have been invaluable and unforgettable.

I want to extend my thanks to all my lab members - Somer Rowe, Krishna Katuwal, Ravneet Kaur, Saptarshi Mondal, Ravi Seelam, Kumar Vaibhav, Manveer Singh and Jessica Abi Saab - for their friendship and company. My heartful thanks go to my officemates, Turner Spratling and Harshita Saxena, for sharing the ups and downs of the Ph.D. journey. I wish us all bright futures. I would also like to express my gratitude to Jihong Xue, who provided me with warmth and comfort over the past five years while I was thousands of miles away from my family in China. You have become like family to me here in the U.S., and I hope the bond between us will remain strong.

To my fiancé, Kaiwen Han: Thank you for your unwavering support and patience especially during my challenging times when my research was not going well. Meeting you has been the greatest stroke of luck in my life, and I can't wait to build our future together.

Finally, to my beloved family—my grandparents, Shixin Fan and Miaozhi Fan, my parents, Fangbing Fan and Zhusun Fan, and my younger brother, Yinghao Fan: Your unconditional love has been my greatest source of strength as I pursued my doctoral degree in the U.S. Not being by your side has been the hardest part of this journey. I cannot wait to reunite with you all soon and celebrate the joy of my graduation together.

TABLE OF CONTENTS

Page

LIST OF TABLES

Page

LIST OF FIGURES

Page

CHAPTER 1

LITERATURE REVIEW

1.The Importance of Creeping Bentgrass and Heat Stress

Creeping bentgrass (*Agrostis stolonifera* L.) is a perennial cool-season grass widely used for golf course greens in the United States primarily due to its tolerance to low mowing height and the capacity to form a dense, uniform and fine-textured playing surface. In addition to greens, creeping bentgrass is also planted on fairways because of its superior growth characteristics and playability [1]. Furthermore, creeping bentgrass spreads by stolons, allowing quick recovery from traffic and golf ball marks [2].

As a cool season turfgrass, the growth of creeping bentgrass is often suppressed during summer when temperature is above optimal. High temperature results in reduced photosynthesis and increased respiration, production of reactive oxygen species (ROS), plus damage to proteins and membranes, ultimately causing decline in carbon stores, reduced growth of both above and below ground organs, loss of green color and eventual turf death [3]. Unfortunately, heat stress has become a significant problem due to global warming. Primarily as a consequence of increased amounts of greenhouse gases, global air temperature is predicted to increase by 0.3-4.8 °C by 2100 [4]. This will be detrimental to plant growth and performance as well as crop productivity. Plants, as sessile organisms, cannot move to more favorable environments. Therefore, maintaining quality of creeping bentgrass in response to elevated temperature with minimal inputs and environmental impacts is a challenging concern, making it more crucial to develop more tolerant cultivars to cope

with climate change A key step towards achieving this is to develop a more complete understanding of how plants respond and adapt to heat stress.

The extent to which heat stress causes damage on plants depends on several factors, including location (in the air or the soil), time (day or night), intensity, duration as well as the rate of temperature increase [5, 6]. With the temperature for optimal growth ranging from 18 to 24°C for shoots and from 10 to 18°C for roots, roots and shoots of cool-season turfgrass present different sensitivities to elevated temperature [3, 7]. Lowering soil temperature could significantly improve turf quality, shoot growth rate and chlorophyll content even when shoots were exposed to high air temperature [8] due to enhanced photosynthetic rate and carbohydrate availability [9] plus enhanced water and nutrient uptake [10, 11]. In addition to where heat stress occurs, when it occurs matters as well. High nighttime temperatures have been the main cause of increase in average daily temperature since the 20th century and could be more devastating to plant growth than day-time or mean temperature [12-14]. Respiration activity typically increases with elevated nighttime temperature, leading to an imbalance between carbon consumption and carbon production and resulting in reduced carbohydrate accumulation, which, eventually, accounts for suppressed growth [15]. Intensity is one of the most important factors accounting for the extent of heat stress injury. The higher the temperature is, the greater damage it would cause [16, 17]. Like intensity, rate of temperature rise, too, determines how badly heat stress can damage plants. Thermotolerance improvement by gradual heat stress has been confirmed in turfgrass and other plants, as manifested by increased membrane thermostability, unique heat shock proteins (HSPs) induction, higher total protein content and greater antioxidant enzyme activity compared to sudden heat shock [18, 19]. Furthermore, duration of heat also plays a pivotal role in heat stress injury. Short-term heat stresses, which last for minutes to a few days, primarily result in reversible damage; In contrast, long-term

heat stress, which can persist for weeks or throughout the entire growing season, often leads to irreversible damage due to severe depletion of energy and nutrients, the persistent production of ROS and progressive damage to vital cellular processes [5]. Previous heat-stress studies have mostly focused on short term relative to long term probably because short-term heat stress is often more practical to study in controlled experimental settings, whereas long-term heat stress conditions are more common in natural environments. Considering these factors, Georgia, where there are usually long hot summers combined with high nighttime temperatures as well as high humidity, is a great location to do heat stress screening.

A number of mechanisms have been identified that contribute to enhanced thermotolerance in turfgrasses, including greater maintenance of photosynthesis ability, enhanced antioxidant defense, or altered protein metabolism [3]. Despite this progress, a clear understanding of the mechanisms behind thermotolerance in creeping bentgrass remains elusive, particularly regarding protein metabolism, which is a key driver of plant growth, development, and stress tolerance. Additionally, creeping bentgrass has considerable intraspecific diversity or variability between cultivars or genotypes for its tolerance to heat stress [20, 21]. Previous research has identified differences in creeping bentgrass germplasm for key traits associated with exceptional level of thermotolerance, offering a promising avenue for the development of new cultivars with improved stress resilience [22]. Understanding the mechanisms underlying this variability in tolerance would accelerate the process of cultivar development and provide new insights into the field of stress tolerance.

2. Physiological Responses

2.1. Photosynthesis

Photosynthesis is regarded as one of the most sensitive physiological processes in response to increasing temperature [23]. Photosynthesis capacity of creeping bentgrass typically declines when temperatures are above 23°C [16, 24]. Variations in different photosynthetic attributes, like chlorophyll content and Photosystem II (PSII) activity, are used to indicate heat stress tolerance since any constraints in photosynthesis can limit plant growth [25].

Photosynthesis inhibition is closely related to the heat sensitivity of PSII which is located in the thylakoid membrane and functions to catalyze light-induced water oxidation [26]. PSII is one of the most vulnerable photosynthetic apparatus to heat stress [27]. High temperature can cause denaturation of D1 proteins which make up the core part of PSII [28], and can dissociate the oxygen evolving complex (OEC), resulting in an imbalanced electron flow from OEC to the acceptor side of PSII [29]. The inhibition of PSII can be estimated by changes in chlorophyll fluorescence, which is defined as the re-emission of absorbed light energy and has been shown to be a sensitive and reliable method for detection and quantification of temperature-induced changes in photosynthetic apparatus [23, 30]. For instance, photochemical efficiency, the ratio of variable fluorescence to maximum fluorescence (*Fv/Fm*), is a common parameter used to indicate the health of the PSII reaction center. A higher *Fv/Fm* value generally correlates with a better thermotolerance [20]. As the most thermally labile component of the electron transport chain, the performance of PSII, to a large extent, determines overall photosynthetic capacity of plants under high temperature [31, 32]. Therefore, maintaining normal activity of PSII is a key step in the enhancement of plant thermotolerance.

Photosynthesis inhibition is ascribed to the disturbance of photosynthetic pigments as well, especially chlorophyll [33]. Chlorophyll is responsible for the absorption of light energy for use in photosynthesis. Exposure to high temperature usually leads to the decline in chlorophyll content due to either decreased chlorophyll biosynthesis, increased chlorophyll degradation, or both [30, 34]. A decline in the activity of porphobilinogen deaminase, one major chlorophyll-synthesizing enzyme, in cucumber (*Cucumis sativus* L.), was reported after seedlings were placed under 42°C for 2 days [34]. In another study where creeping bentgrass was exposed to 38°C for 28 days, authors concluded that enhanced gene expression level of chlorophyll-degrading enzymes contributed to the reduced leaf chlorophyll content under high temperature [35].

Inactivation of ribulose-1,5-bisphosphate carboxylase/oxygenase (rubisco), is another main reason for photosynthesis inhibition. Rubisco accounts for catalyzing the carboxylation of ribulose-1,5-bisphosphate (RuBP), which is the first step in Calvin cycle. However, as alternative substrates for rubisco, both CO_2 and O_2 compete for the same active site of rubisco [36]. As temperature increases, rubisco has a higher affinity for O_2 than CO_2 and binds O_2 more strongly, leading to greater oxygenation activities relative to carboxylation, and thereby higher rates of photorespiration, decreasing net photosynthesis [23]. In addition, inhibition of rubisco activase is another primary limiting factor of photosynthesis under heat stress [37, 38]. Rubisco activase is mainly responsible for the removal of sugar-phosphate inhibitors from active sites of rubisco to prepare this enzyme for activation via carbamylation and Mg^+ binding [36]. When the activity of rubisco activase is repressed under high temperature, rubisco's activation state will be reduced, followed by decreased photosynthesis. Previous results have demonstrated that enhanced thermotolerance of rubisco activase improves photosynthesis under moderate heat stress while a

suboptimal level of rubisco activase makes plants more susceptible to photosynthetic inhibition by moderate heat stress [39].

The best performing cultivars of plant species under high temperature maintain not only high photosynthesis activities but also low respiration rates. However, in contrast to photosynthesis, respiration rate generally increases in cool season turfgrasses in response to high temperature [16, 40]. Dramatic increase in carbon consumption has been observed in various cultivars of creeping bentgrass when seedlings were exposed to 34°C and 38°C [16]. A greater ratio of respiration to photosynthesis for a heat-sensitive cultivar of creeping bentgrass than a heat-tolerant one was also reported in an earlier study [41]. Accordingly, total carbohydrate content is another important physiological trait associated with thermotolerance as shown in one study on creeping bentgrass, in which the cultivar with better heat tolerance maintained significantly higher carbohydrate concentration [42]. All in all, controlling the balance between carbon production and carbon consumption to maintain carbohydrate availability could play a critical role in enhancing thermotolerance of plants.

2.2. Oxidative Stress

Reactive oxygen species (ROS) are considered to be unavoidable by-products of aerobic metabolism since the appearance of oxygen-evolving photosynthetic organisms billions years ago [43]. Under normal conditions, plants produce reactive oxygen species (ROS) at a controlled rate. However, elevated temperatures accelerate ROS production due to the disruption of metabolic activities and their role in stress signaling as part of the abiotic stress response network [44, 45]. This leads to an imbalance between ROS generation and the plant's ability to detoxify them, resulting in oxidative stress. ROS are partially reduced or activated forms of O_2, mainly consisting

of singlet oxygen ($^1O_2$), superoxide radical (O^{2-}), hydrogen peroxide (H_2O_2) and hydroxyl radical (OH^-) [46].

Reactive oxygen species are highly active and can damage many important cellular components such as proteins, lipids, carbohydrates [47]. Among these, lipid peroxidation is widely considered as a "hallmark" of oxidative stress [48]. Peroxidation of lipids occurs when ROS react with unsaturated fatty acids, which leads to leakage of cellular contents and decline in cell membrane stability. Heat-induced oxidative stress has been detected in turfgrass species via measuring electrolyte leakage (EL) and a final chemical product derived from lipid peroxidation, malondialdehyde (MDA). It turns out that both contents of EL and MDA increase as temperature rises whereas more thermotolerant species or cultivars typically present less severe oxidative damage in cellular membranes as demonstrated by lower EL and MDA contents when exposed to heat stress [49, 50]. To avoid or minimize oxidative-stress-induced damages to biomolecules, plants have developed scavenging mechanisms to protect cells from ROS attack, including antioxidant enzymatic systems and non-enzymatic systems to ensure cells' normal physiological functions [51]. Non-enzyme compounds are comprised of ascorbic acid, glutathione, α-tocopherol and carotenoids [52]. Major enzymes involved in the antioxidant system include superoxide dismutase (SOD), catalase (CAT), ascorbate peroxidase (APX), and peroxidase (POD) [19, 50, 53, 54]. SOD detoxifies O^{2-} into H_2O_2 and then APX, CAT or POD decompose H_2O_2 into H_2O and O_2 at different cellular locations [5].

How plants alter antioxidant enzyme activities in response to elevated temperature presents more than one pattern. One study reported that prolonged heat stress decreased the activities of SOD and CAT while it increased POD activity in both leaves and roots of creeping bentgrass [20]. Similar patterns of SOD and CAT activities were obtained in another study [50]. Alternatively,

activities of CAT and APX were confirmed to be reduced, whereas SOD activity was not affected under prolonged heat stress in one study on tall fescue (*Festuca arundinacea* L.) and Kentucky bluegrass (*Poa pratensis* L.) [53]. How antioxidant enzymes respond to elevated temperature in Kentucky bluegrass was more specifically demonstrated in a recent study where after exposing Kentucky bluegrass to heat stress for 28 d, the authors found out that, intriguingly, SOD and CAT activities increased and then declined whereas POD and APX activities declined and then increased [55]. It was proposed in this study that for SOD and CAT, their activities were enhanced in response to ROS accumulation during early heat stress but as heat stress progressed, their activities could be reduced due to ROS-mediated damage to cell functions; for POD, accumulation of ROS at early stage of heat stress might suppress its activity and then as POD gene expression increased with elevated temperature, POD's activity could be recovered. Thus, SOD and CAT may be more effective in scavenging ROS under short term heat stress while APX and POD could contribute more to ROS detoxification under prolonged heat stress. The discrepancy among studies on how activities of antioxidant enzymes respond to heat stress is probably influenced by species variation plus difference in stress intensity and duration. However, regardless of whether activities of antioxidant enzymes are enhanced or weakened as temperature increases, greater antioxidant enzyme activities are generally associated with better thermotolerance at both species and cultivar levels [49, 50]. Furthermore, although not reported in turfgrass, endogenous accumulation or exogenous application of antioxidants has been concluded to have a positive relationship with abiotic stress tolerance in other plants [56, 57].

3. Protein Metabolism

Responding to heat stress, proteins will be denatured due to direct damage of extreme temperatures or oxidized due to overproduced ROS [58]. These damaged proteins tend to form

toxic aggregates and precipitate due to structural instability. They have to be removed, otherwise, accumulation of aggregate-prone protein interferes with normal metabolic activities like aforementioned photosynthesis and oxidative defense, accelerating the aging and even death of cells, as proteins are the major effectors of cellular activities [58]. For instance, the metabolism of D1- the core part of PSII, plays a key role in PSII repair [28]. Generally, damaged D1 proteins are degraded [59]. Then a newly synthesized D1 protein is reassembled into PSII, recovering photosynthetic activity. Therefore, minimizing the interruption in D1 protein metabolism is typically associated with greater thermotolerance [28]. In the case of oxidative stress, oxidized proteins undergo proteolysis to be removed. Then the resultant amino acids will be reused for protein biosynthesis and regenerate active proteins [60]. To avoid cellular dysfunction by protein aggregates, plants have evolved multiple levels of protein quality control systems to repair or degrade damaged proteins, where molecular chaperones and proteolytic machinery are central players. Molecular chaperones, namely, heat shock proteins (HSPs), are responsible for the refolding of misfolded or denatured proteins into functional conformation, while proteolytic machinery like proteases and the ubiquitin-proteasome system (UPS) contributes to the degradation of damaged proteins into amino acids for synthesis of new proteins [61]. In principle, molecular chaperones should have the first opportunity to fix damaged proteins by refolding them into functional conformation; When damage is beyond repair, these abnormal proteins will be targeted for degradation by various proteolytic machineries [62]. Unlike normal conditions where there is a balance of proteins constantly being degraded and synthesized, protein degradation is typically accelerated relative to protein synthesis under heat stress [63]. This will lead to decreases in total protein contents, eventually impairing normal metabolic activities and contributing to reduced tolerance levels [64, 65].

3.1. Proteases

Proteases are proteolytic enzymes that account for the breakdown of proteins localized inside organelles by decomposing polypeptide bonds in targeted proteins [66]. They are structurally and functionally diverse and are primarily divided into families of serine proteases, aspartic proteases, cysteine proteases, and metalloproteases, according to the differences in their catalytic mechanism and the nature of their active sites [67]. In addition to performing various functions at every stage of a plant's life, proteases are actively involved in plant responses to environmental conditions as well, such as heat stress [67-69]. To determine how effectively and efficiently proteases break down protein substrates, a common method is to assess protease activity. In line with the need to degrade the increased accumulation of damaged proteins, enhanced protease activities were commonly observed under heat stress, but more-tolerant lines typically presented lower protease activities, contributing to their higher protein contents and greater thermotolerance [70-73]. Furthermore, when protease inhibitors were applied, plants could mitigate the increase in protease activities with concomitant improvement in physiological performance, eventually suppressing proteolysis and delaying heat-induced leaf senescence [69, 74]. Together, these suggest that protease activity could be used as an efficient biochemical marker to assess relative thermotolerance in plants.

Protease concentration is another major determinant of protease activity, with transcription being one of the important layers of regulation for protease concentration [36]. Although closely related, changes in gene expression don't necessarily lead to changes in protein abundance. To gain deeper insights into the role of proteases in heat stress, it is essential to understand both transcriptional and post-transcriptional regulation. Continuous efforts have been made to

investigate their responses at the levels of protein abundance and gene expression, revealing intricate and variable patterns.

3.1.1. Serine protease

Serine proteases are among the most well-studied families of proteases in plants with documented involvement in heat stress [66]. Among three tomato (*Solanum lycopersicum*), genotypes, the abundances of AIR3 didn't change significantly in the heat-tolerant N22 and -sensitive Moroberekan, but presented reductions in the moderately tolerant IR64 compared to those under control conditions [75]. As the most abundant stromal protease, Clp's role in heat stress has received continuous attention. In cultured rice cells, Clp was uniquely accumulated when temperature was elevated to 44°C [76]. Contrastingly, Clp abundance was reduced in leaves of barley (*Hordeum vulgare* L.) under heat stress [77]. At the gene level, heat-induced upregulation of Clp has been detected in different species such as rice, *Arabidopsis thaliana* and *Lolium temulentum* [78-80]. The absence of ClpB protein, a subunit of Clp, in *Arabidopsis thaliana*, resulted in premature plant death under high-temperature conditions [80]. Another serine protease, Deg10, is also essential for the proper functioning of plants exposed to elevated temperatures. The Deg10 mutant of *Arabidopsis thaliana* was reported to cause enhanced impairment in root elongation in response to heat stress, by affecting mitochondrial proteostasis [81],

3.1.2. Cysteine protease

Cysteine proteases (CPs) are the most abundant class of proteases upregulated in response to senescence induced by various stresses, including heat stress [82-84]. As one common heat response, increased accumulation of CPs has been evident in various plant species including peach (*Prunus persica*), rice, Agavaceae (*Agave americana*) and creeping bentgrass, with a negative association typically being found between the abundance of CPs and the level of heat tolerance

[76, 85-88]. For instance, less accumulation of CPs was found in the roots of thermal *Agrostis scabra* compared to that of creeping bentgrass under heat [86]. This was in accordance with the expression level of *AsCP1* encoding CPs in these two grasses [89]. Specifically, the gene expression was upregulated less in heat-tolerant *Agrostis scabra* relative to that in creeping bentgrass [89]. These suggest that reduced upregulation of CPs at both the protein and gene levels may contribute to slower proteolytic degradation processes, thereby improving root thermotolerance in superior *Agrostis scabra.* Intriguingly, contrary to the commonly reported increases in the expression levels of CPs, downregulation of genes encoding CPs in response to heat stress has also been documented in a limited number of studies [90]. This discrepancy may primarily stem from differences in stress intensity and duration. For instance, at the later stage of stress, the extent of damage may be greater, and the plants could be severely senescent with critically depleted energy reserves. In response, plants may reduce ATP investment in energy-intensive processes like protein metabolism, including the production of proteases, and instead, save energy for more immediate needs, such as stress defense, protein transport or cellular repair [91-93]. This strategic redistribution of energy and nutrient resources allows plants to maximize their chances of survival under prolonged stressful conditions by efficiently managing their limited reserves.

3.1.3. Metalloprotease

Among various metalloproteases, FtsH is the most extensively studied in plants. FtsH plays a crucial role in determining a plant's ability to survive under high-temperature conditions, given its essential functions in chloroplast and mitochondria [68, 69, 94]. The involvement of FtsH in heat stress has been documented at the protein level with varying results. For instance, the accumulation of FtsH was reduced in *Populus euphratica* whereas it was enhanced in barley when

heat stress was applied [77, 95]. Intriguingly, in another study where two genotypes of soybean (*Glycine max*) were exposed to heat stress, FtsH8 presented downregulation in one genotype while showing upregulation in another [96]. These findings highlight both interspecific and intraspecific variability in the accumulation of FtsH under heat stress.

Corresponding to the heat-induced differential responses of FtsH at the protein level, significant changes were also observed at the gene level. In *Arabidopsis thaliana*, mutation of FtsH11 gene rendered plants sensitive to elevated temperature by reducing photosynthetic capability, as demonstrated by the declines in chlorophyll content and photosynthetic efficiencies of various light harvesting processes [97-99]. This underscores the necessity of the presence of FtsH11 for regulating the response of photosystem to high-temperature stress, which is not surprising given that FtsH genes are involved in degradation of unassembled thylakoid membrane proteins and photodamaged D1 protein, a core component of heat-labile PSII [94]. In another study, phenotypic abnormalities were seen in the FtsH4 mutant of *Arabidopsis thaliana* when temperature slightly increased above normal, including delayed germination, reduced rosette size, shorter root length as well as irregular serration of leaf blades [100]. This suggested the crucial role of FtsH4 for Arabidopsis's acclimation to moderate, prolonged temperature stress.

In addition to FtsH, efforts have also been made to reveal the responses of other metalloproteases to temperature elevation. As with aforementioned FtsH4 mutant of *Arabidopsis thaliana*, Arabidopsis lacking OMA1 suffered similar phenotypical alterations when exposed to moderate heat stress, like reduced rosette size and root length [100]. Gm1-MMP gene was overexpressed during the development of leaves and roots in *Arabidopsis thaliana* under high temperatures, indicating its essential role for high-temperature tolerance [101]. In tomato, the gene SlEGY2 was significantly upregulated in response to heat stress [102]. However, when the

expression of SlEGY2 was suppressed, plants became more heat sensitive, with greater water loss, seriously damaged membranes, greater decreases in chlorophyll content and photochemical efficiency of PSII, plus lower activities of antioxidant enzymes [102]. These results suggest that SlEGY2 can regulate the thermotolerance of tomatoes by affecting ROS accumulation and photosynthetic activities.

3.1.4. Aspartic protease

Compared to the studies on other families of proteases, the response of aspartic proteases to heat stress remains largely unexplored, although APs genes were found to be highly up-regulated in early grain development in wheat (*Triticum aestivum*) under combined drought and heat [103]. While there is limited research specifically on heat stress, the involvement of APs in leaf senescence induced by various other stresses, such as drought, pathogen attack, and osmotic stress, has been documented [104-106]. This underscores the importance of APs in the complex network of plant stress responses. For instance, the expression of a grape (*Vitis vinifera*) aspartic protease gene in transgenic *Arabidopsis thaliana* conferred increased tolerance to osmotic stress [105]. As osmotic stress often accompanies heat stress, it highlights the potential role that aspartic proteases may play in helping plants cope with heat stress, warranting further investigation.

3.2. The Ubiquitin-Proteosome System

The UPS is a selective degradation pathway that mainly operates in the cytosol and the nucleus, but has also shown involvement in the degradation of endoplasmic reticulum resident proteins as well as chloroplast proteins [107]. The key characteristic of the UPS is ubiquitination, a process where ubiquitin, a highly conserved polypeptide of 76 amino acids, acts as a recyclable recognition signal to tag substrate proteins for proteasomal degradation [108]. This is carried out through the sequential action of three ubiquitin enzymes. namely, ubiquitin-activating enzyme

(E1), ubiquitin-conjugating enzyme (E2) and ubiquitin ligase (E3), with E3 being encoded by a larger number of genes and determining substrate specificity. Specifically, ubiquitin is first activated by E1, followed by the transfer to E2; Then, E3 facilitates the transfer of ubiquitin from the E2-ubiquitin intermediate to one of seven lysine residues (K6, K11, K27, K29, K31, K48, K63) on the substrate proteins [108]. This sequence of reactions repeats itself to yield polyubiquitin chains. The fate of the target proteins varies depending on which specific lysine residues the polyubiquitin chains are linked to. For instance, K63 and K48 are the most extensively studied among various types of polyubiquitin chains. Proteins with K63 polyubiquitination are associated with non-degradative processes such as DNA repair, signal transduction and endocytosis, whereas those with K48 are often directed to the 26S proteasome for degradation [109]. The 26S proteasome is composed of two main components: the 19S regulatory particle and the 20S core proteasome. The 19S regulatory particle is responsible for recognizing and unfolding substrate proteins, as well as guiding polyubiquitinated proteins into the 20S core [62]. The 20S core proteasome then carries out the catalytic degradation of these proteins, eventually releasing free amino acids to be reused for various cellular functions.

As a central player in the protein quality control process, the UPS has garnered continuous attention for its role in removing damaged proteins during heat stress at various levels. A UPS activity assay provides a direct method to measure the efficiency of the UPS in carrying out proteolysis. Although largely unexplored, heat-induced increases in UPS activity have been observed in tobacco (*Nicotiana tabacum* L.) cells [110]. Since polyubiquitination is a typical marker for proteins targeted by the UPS, a few attempts have been made to investigate changes in the ratio of free ubiquitin pools to their conjugated form under heat stress [111-113]. An increase in the high molecular mass conjugates was detected using a ubiquitin antibody when alga

(*Chlamydomonas reinhardii*) cells were exposed to 41.5 °C [113]. In the case of wheat roots, temperature elevation resulted in elevated amounts of high molecular mass conjugates, along with reduced amounts of low molecular mass conjugates and free ubiquitin, suggesting enhanced protein degradation by the UPS [111]. Additionally, heat-induced differential changes were also detected at the gene level, though in a more complex manner. Since E3 and 26S proteasome are more frequently reported as heat-inducible compared to other components of the UPS [109, 114], the gene expression of these two elements was emphasized.

3.2.1. E3

Genes encoding E3 predominantly act as positive regulators of heat stress responses, with their expression often being upregulated under heat stress conditions, as reported in various plant species [79, 115-119]. When E3 genes like AtPPRT1, AtPUB48 and OsHCI1 were overexpressed in *Arabidopsis thaliana*, plants presented enhanced tolerance to high temperature with higher survival rates while mutation of these genes rendered them more susceptible to heat stress with lower germination rates [115, 120, 121]. In the case of tobacco, the overexpression of TaFBA1 led to improved photosynthesis, reduced growth inhibition as well as increased antioxidant defense, eventually contributing to less oxidative damage and improved heat tolerance [117]. Similar findings were found for the overexpression of SISIZ1 in tomato [119]. In addition to their roles as positive regulators, E3 ligases can also act as negative regulators in plant responses to heat stress. For instance, The depletion of BPM expression conferred enhanced thermotolerance in *Arabidopsis thaliana*, as manifested by higher survival rate, greater chlorophyll content and lower ion leakage after heat shock [122]. In another case, overexpression of *AtCHIP* in *Arabidopsis thaliana* reduced heat tolerance [123]. In contrast, silencing *SICHIP* in tomato decreased thermotolerance, evident by reduced photosynthetic activity, elevated electrolyte leakage and

accumulation of insoluble protein aggregates [118]. Notably, the heat tolerance of Arabidopsis *chip* mutant was restored to wild-type levels upon reintroduction of *SICHIP*. These examples highlight the complexity of E3 in regulating heat stress responses, with their effects depending on the specific gene and plant species involved.

3.2.2. The 26S proteasome

Differential expression of genes encoding the 26S proteasome has been confirmed in plants under various stressful conditions, including heat stress, although research on this specific topic remains limited [109]. When genes encoding subunits of the 19S regulatory particle (RPT2a, RPN10, RPN12a and RPN1a) were silenced in *Arabidopsis thaliana*, hypocotyl elongation was inhibited to greater extents in the mutants than in the wild type, leading to reduced tolerance to increased temperatures [124, 125]. In another case, OgTT1, an α2 subunit of the 20S core particle, was found to protect cells from heat stress by removing cytotoxic denatured proteins in African rice (*Oryza glaberrima*); Furthermore, its overexpression significantly enhanced thermotolerance in rice, *Arabidopsis thaliana* and *Festuca elata* [126]. These suggest the protective role of the 26S proteasome in heat stress tolerance across different species. More research efforts should be made to better understand how proteasome components are regulated during heat stress, given the significant gap in this area.

3.2.3. Ubiquitin-Omics

Identifying which proteins are selectively targeted by the UPS pathway promises to be an important area of research because it enables the manipulation of key stress-response proteins and provides deeper insights into various biological processes, particularly related to stress responses and proteostasis in plants [109]. Despite its significance, pinpointing protein substrates for the UPS has remained challenging due to the transient nature of ubiquitination and the dynamic

interaction between substrates and E3 ligases. Ubiquitin-omics, which integrates proteomics with protein ubiquitylation, has emerged more recently as a powerful approach for large-scale identification of the UPS substrates. It has been conducted in a variety of plant species under various conditions, such as osmotic stress, drought, salt stress as well as heat stress [127-131]. For instance, 450 ubiquitinated proteins were identified in Arabidopsis roots under short-term osmotic stress, with most of them being enriched in transporters, regulation of intracellular pH and cellular trafficking processes [128]. Increased and decreased ubiquitination were both observed in this study. However, intriguingly, an inverse relationship between the abundances of proteins and their ubiquitinated form were not found despite the fact that ubiquitination can induce protein degradation. The authors, thereby, proposed that ubiquitination might interfere with protein function or cellular localization rather than with protein stability upon short-term stress. In the case of salt stress, K48-linked polyubiquitination on HSP81-1, aldehyde oxidase 3 and plasma membrane ATPase was detected in rice roots, suggesting the involvement of the UPS [131]. Furthermore, greater upregulation of ubiquitin-modified HSP81-1 and aldehyde oxidase 3 were seen in two rice lines - TNG67 and SA0604, potentially indicating more severe protein degradation. This might contribute to inferior salt tolerance in TNG67 and SA0604 compared to more tolerant SM75. Similarly, enhanced ubiquitination was found when rice roots were exposed to heat stress, with the majority of ubiquitinated proteins being associated with sucrose and starch metabolism, as well as the ribosomal system [129]. The authors speculated that the UPS might be involved in the removal of subunits or entire ribosomes that were improperly folded in high-temperature environments. These studies mostly utilize anti-K-ε-GG antibody to isolate and enrich ubiquitinated peptides after protein digestion, which is a key step in ubiquitin-omics. However, it can’t directly distinguish between different lysine residues on the same proteins. Peptide’s

sequence and fragmentation pattern derived during LC-MS/MS analysis are needed in order to differentiate ubiquitination sites [129]. A relatively new methodology for the isolation of polyubiquitinated proteins is through Tandem Ubiquitin Binding Entities (TUBEs), which are an engineered protein domain. In addition to binding to specific lysine residue, TUBEs offer greater affinity for polyubiquitin chains than most ubiquitin antibodies [132]. Initially developed for mammalian research, the timely adaptation of TUBE technology to plant protocols has allowed it to emerge as an indispensable tool for dissecting the involvement of UPS in plants [133, 134] despite that this remains largely unexplored in the context of heat stress. Therefore, integrating TUBE-based isolation of polyubiquitinated proteins with proteomics may offer new insights into how protein degradation is regulated by the UPS under heat stress.

3.3. HSPs

Although most proteins generally show a decline in their abundance under heat stress, some proteins can be induced or upregulated in response to elevated temperature. HSPs, for example, are probably the most studied proteins induced by heat stress. The common signal for HSPs induction is the formation of aberrant proteins generated as a result of exposure to high temperature that's above normal for plants [135]. Mainly acting as "molecular chaperones", HSPs can prevent other proteins from inappropriate aggregation and assist in protein refolding so as to maintain the functional conformations of proteins and facilitate cell survival under stress conditions [136]. Different HSP activities are required to respond to variable levels of heat shock. For example, in *Saccharomyces cerevisiae,* HSP70 is involved in tolerance to slightly high temperature, while HSP104 is specialized to cope with extreme temperature [135]. Furthermore, different plants employ different HSPs to respond to similar levels of heat stress. HSPs are typically classified into five families based on their size: small HSPs (sHSPs), HSP60, HSP70, HSP90 and HSP100,

among which the importance of small HSPs has received special attention due to their unusual abundance and diversity in plants. Unlike other HSPs, sHSPs fulfill their chaperone function without dependence on ATP. They are able to bind denatured proteins, forming protein complexes, and enable subsequent refolding in cooperation with HSP70 and HSP40, thus allowing proteins to perform their specific function again [137].

The level and specific type of HSPs expression vary with plant species, cultivars and even experimental lines differing in the level of heat tolerance. Synthesis of two 25 kDa HSPs was only detected in heat tolerant line "SB" of creeping bentgrass but not in heat-sensitive line "NSB" [138]. Moreover, the SB line that included the 25 kDa HSP recovered from heat stress faster and enabled resuming typical levels of protein synthesis 2 hours earlier compared to the NSB line, suggesting a protective role that 25 kDa HSP played in conferring better thermotolerance [138]. Three Kentucky bluegrass cultivars with variable levels of thermotolerance (Eagleton >Midnight >Brilliant) were placed under 40 °C and analyzed for HPSs activities [65]. The results interpreted that although some HSPs (64, 78, 85, 39, 45, 66 kDa) were induced in all cultivars, the induction of these proteins was 7 to 14 days earlier in Eagleton or Midnight relative to Brilliant. Combined with higher chlorophyll content, fewer yellow leaves and greater protein abundance in Eagleton and Midnight than Brilliant, this experiment suggested that an earlier induction of HSPs during heat stress could confer better heat tolerance. In addition, one unique HSP, 68 kDa, was only detected in Midnight. HSPs response between different turfgrass species was compared as well. One study where thermal *Agrostis scabra* and heat-sensitive *Agrostis stolonifera* were both exposed to heat stress elucidated that HSP Sti was upregulated in both species but it was increased to a greater level in *Agrostis scabra [17]*. The major function of HSP Sti is to mediate diverse cell activities such as HSP90 signaling and interaction, thus probably contributing to the superior root

heat tolerance in *Agrostis scabra* [17, 139]. Accordingly, HSPs response has been investigated at the molecular level, too. For instance, the expression of a HSP16 gene was detected to be significantly increased in thermal A. *scabra* compared to three heat-sensitive cultivars of *A. stolonifera* ("Penncross", "Pennlinks" and "Kingpin") when exposed to 35 °C, possibly confirming a positive relationship between the expression level of sHSP genes and thermotolerance [3]. All in all, identifying unique HSPs in turfgrass species with superior heat tolerance deserves future investigation.

4. Objectives

The overall objective of my Ph.D. research was to explore physiological, biochemical and molecular mechanisms associated with heat tolerance in creeping bentgrass, with a particular emphasis on proteolysis. The first objective was to screen a collection of creeping bentgrass germplasm for heat tolerance and determine the physiological mechanism leading to the differential tolerance levels. These successfully identified heat-tolerant and heat-sensitive lines would serve for testing in further experiments. The second objective was to identify pathways for increased protein degradation by quantifying proteolytic activity and associated gene expression and understand the associated differences between heat-tolerant and -sensitive lines. The third objective was to quantify changes in overall protein accumulations in contrasting creeping bentgrass lines exposed to heat stress via gel-free proteomics and additionally to identify proteins that have been polyubiquitinated and targeted to the UPS via polyubiquitin-omics to determine proteins subjected to heightened regulation under heat stress. Projects 2 and 3 enabled us to explore different levels of regulation (biochemical level, ubiquitin-tagged, global protein level) in studying protein degradation and metabolism in heat-stressed plants. In the end, such information would allow for a greater understanding of thermotolerance mechanisms in creeping bentgrass. The

identified proteins and pathways plus a better understanding of unique germplasm can be utilized to develop new cultivars with enhanced tolerance to increasing temperature, thereby maintaining economic productivity in the face of climate change.

References

1. Jones, M. *Competitive ability of creeping bentgrass cultivars and their potential for renovating existing putting greens through interseeding*. Researchgate 2010.
2. Peacock, C., *Creeping Bentgarss*, in *NC SATE EXTENSION*. 2017.
3. Huang, B.R., M. DaCosta, and Y.W. Jiang, Research Advances in Mechanisms of Turfgrass Tolerance to Abiotic Stresses: From Physiology to Molecular Biology. *Critical Reviews in Plant Sciences*, 2014. **33**(2-3): p. 141-189 DOI: 10.1080/07352689.2014.870411.
4. Pachauri, R.K. and L. Meyer. *Climate change 2014 Synthesis Report-Summary for Policymakers*. 2014. Geneva, Switzerland: Intergovernmetnal Panel on Climate Change (IPCC).
5. Wahid, A., et al., Heat tolerance in plants: An overview. *Environmental and Experimental Botany*, 2007. **61**(3): p. 199-223 DOI: 10.1016/j.envexpbot.2007.05.011.
6. Sung, D.-Y., et al., Acquired tolerance to temperature extremes. 2003. **8**(4): p. 179-187.
7. Nielsen, K.J.P.P.R.E., Roots and root temperatures. 1974.
8. Xu, Q.Z. and B.R. Huang, Lowering soil temperatures improves creeping bentgrass growth under heat stress. *Crop Science*, 2001. **41**(6): p. 1878-1883 DOI: 10.2135/cropsci2001.1878.
9. Xu, Q. and B.J.C.S. Huang, Effects of differential air and soil temperature on carbohydrate metabolism in creeping bentgrass. 2000. **40**(5): p. 1368-1374.

10. Huang, B. and Q.J.J.o.P.N. Xu, Root growth and nutrient element status of creeping bentgrass cultivars differing in heat tolerance as influenced by supraoptimal shoot and root temperatures. 2000. **23**(7): p. 979-990.

11. Graves, W.R., R.J. Joly, and M.N.J.H. Dana, Water use and growth of honey locust and tree-of-heaven at high root-zone temperature. 1991. **26**(10): p. 1309-1312.

12. Peng, S., et al., Rice yields decline with higher night temperature from global warming. 2004. **101**(27): p. 9971-9975.

13. Kukla, G., T.R.J.E.s. Karl, and technology, Nighttime warming and the greenhouse effect. 1993. **27**(8): p. 1468-1474.

14. Karl, T.R., et al., Global warming: Evidence for asymmetric diurnal temperature change. *Geophysical Research Letters*, 1991. **18**(12): p. 2253-2256.

15. Schmidt, R. and R.J.C.S. Blaser, Effect of Temperature, Light, and Nitrogen on Growth and Metabolism of 'Cohansey'Bentgrass (Agrotis palustris Huds.) 1. 1967. **7**(5): p. 447-451.

16. Huang, B.R. and H.W. Gao, Growth and carbohydrate metabolism of creeping bentgrass cultivars in response to increasing temperatures. *Crop Science*, 2000. **40**(4): p. 1115-1120 DOI: 10.2135/cropsci2000.4041115x.

17. Xu, C.P. and B.R. Huang, Root proteomic responses to heat stress in two Agrostis grass species contrasting in heat tolerance. *Journal of Experimental Botany*, 2008. **59**(15): p. 4183-4194 DOI: 10.1093/jxb/ern258.

18. He, Y.L., X.Z. Liu, and B.R. Huang, Protein changes in response to heat stress in acclimated and nonacclimated creeping bentgrass. *Journal of the American Society for Horticultural Science*, 2005. **130**(4): p. 521-526 DOI: 10.21273/jashs.130.4.521.

19. Gulen, H. and A. Eris, Effect of heat stress on peroxidase activity and total protein content in strawberry plants. *Plant Science*, 2004. **166**(3): p. 739-744 DOI: 10.1016/j.plantsci.2003.11.014.

20. Liu, X. and B. Huang, Heat stress injury in relation to membrane lipid peroxidation in creeping bentgrass. *Crop Science*, 2000. **40**(2): p. 503-510 DOI: 10.2135/cropsci2000.402503x.

21. Heckathorn, S.A., et al., In vivo evidence from an Agrostis stolonifera selection genotype that chloroplast small heat-shock proteins can protect photosystem II during heat stress. *Functional Plant Biology*, 2002. **29**(8): p. 935-946.

22. Jespersen, D., W. Meyer, and B. Huang, Physiological traits and genetic variations associated with drought and heat tolerance in creeping bentgrass. *Int. Turfgrass Soc. Res. J*, 2013. **12**: p. 459-464.

23. Crafts-Brandner, S.J. and M.E. Salvucci, Sensitivity of photosynthesis in a C4 plant, maize, to heat stress. *Plant Physiology*, 2002. **129**(4): p. 1773-1780 DOI: 10.1104/pp.002170.

24. DiPaola, J. and J.J.T. Beard, Physiological effects of temperature stress. 1992: p. 231-267.

25. Fahad, S., et al., Crop Production under Drought and Heat Stress: Plant Responses and Management Options. *Front Plant Sci*, 2017. **8**: p. 1147 DOI: 10.3389/fpls.2017.01147.

26. Shukla, A.K., *Membrane proteins–engineering, purification and crystallization*. Vol. 557. 2015: Academic Press.

27. Sonoike, K., Photoinhibition of photosystem I. *Physiologia plantarum*, 2011. **142**(1): p. 56-64.

28. Li, H., et al., High temperature effects on D1 protein turnover in three wheat varieties with different heat susceptibility. *Plant Growth Regulation*, 2017. **81**(1): p. 1-9 DOI: 10.1007/s10725-016-0179-6.

29. De Ronde, J.A., et al., Photosynthetic response of transgenic soybean plants, containing an Arabidopsis P5CR gene, during heat and drought stress. *Journal of Plant Physiology*, 2004. **161**(11): p. 1211-1224 DOI: 10.1016/j.jplph.2004.01.014.

30. Jespersen, D., J. Zhang, and B.R. Huang, Chlorophyll loss associated with heat-induced senescence in bentgrass. *Plant Science*, 2016. **249**: p. 1-12 DOI: 10.1016/j.plantsci.2016.04.016.

31. Havaux, M., H. Greppin, and R.J. Strasser, Functioning of photosystems I and II in pea leaves exposed to heat stress in the presence or absence of light. *Planta*, 1991. **186**(1): p. 88-98.

32. Havaux, M. and F. Tardy, Temperature-dependent adjustment of the thermal stability of photosystem II in vivo: possible involvement of xanthophyll-cycle pigments. *Planta*, 1996. **198**(3): p. 324-333.

33. Camejo, D., et al., Changes in photosynthetic parameters and antioxidant activities following heat-shock treatment in tomato plants. 2006. **33**(2): p. 177-187.

34. Tewari, A.K. and B.C.J.P.p. Tripathy, Temperature-stress-induced impairment of chlorophyll biosynthetic reactions in cucumber and wheat. 1998. **117**(3): p. 851-858.

35. Rossi, S., et al., Heat-induced leaf senescence associated with Chlorophyll metabolism in Bentgrass lines differing in heat tolerance. 2017. **57**(supplement1): p. S-169-S-178.

36. Taiz, L. and E. Zeiger, *Plant Physiology 5 ed. Sunderland, MA*. 2006, the Sinauer Associates.

37. Feller, U., S.J. Crafts-Brandner, and M.E.J.P.P. Salvucci, Moderately high temperatures inhibit ribulose-1, 5-bisphosphate carboxylase/oxygenase (Rubisco) activase-mediated activation of Rubisco. 1998. **116**(2): p. 539-546.

38. Salvucci, M.E. and S.J.J.P.p. Crafts-Brandner, Inhibition of photosynthesis by heat stress: the activation state of Rubisco as a limiting factor in photosynthesis. 2004. **120**(2): p. 179-186.

39. Kurek, I., et al., Enhanced thermostability of Arabidopsis Rubisco activase improves photosynthesis and growth rates under moderate heat stress. 2007. **19**(10): p. 3230-3241.

40. Liu, X.Z. and B.R. Huang, Seasonal changes and cultivar difference in turf quality, photosynthesis, and respiration of creeping bentgrass. *Hortscience*, 2001. **36**(6): p. 1131-1135 DOI: 10.21273/hortsci.36.6.1131.

41. Huang, B.R., X.Z. Liu, and J.D. Fry, Shoot physiological responses of two bentgrass cultivars to high temperature and poor soil aeration. *Crop Science*, 1998. **38**(5): p. 1219-1224 DOI: 10.2135/cropsci1998.0011183X003800050018x.

42. Liu, X. and B. Huang, Carbohydrate accumulation in relation to heat stress tolerance in two creeping bentgrass cultivars. *Journal of the American Society for Horticultural Science*, 2000. **125**(4): p. 442-447.

43. Mittler, R., A. Finka, and P. Goloubinoff, How do plants feel the heat? *Trends in biochemical sciences*, 2012. **37**(3): p. 118-125.

44. Kovtun, Y., et al., Functional analysis of oxidative stress-activated mitogen-activated protein kinase cascade in plants. 2000. **97**(6): p. 2940-2945.

45. Choudhury, F.K., et al., Reactive oxygen species, abiotic stress and stress combination. *The Plant Journal*, 2017. **90**(5): p. 856-867.

46. Hasanuzzaman, M., et al., Physiological, biochemical, and molecular mechanisms of heat stress tolerance in plants. *Int J Mol Sci*, 2013. **14**(5): p. 9643-84 DOI: 10.3390/ijms14059643.

47. Demidchik, V., Mechanisms of oxidative stress in plants: from classical chemistry to cell biology. *Environmental and experimental botany*, 2015. **109**: p. 212-228.

48. Farmer, E.E. and M.J. Mueller, ROS-mediated lipid peroxidation and RES-activated signaling. *Annual review of plant biology*, 2013. **64**: p. 429-450.

49. Du, H., Z. Wang, and B. Huang, Differential responses of warm-season and cool-season turfgrass species to heat stress associated with antioxidant enzyme activity. *Journal of the American Society for Horticultural Science*, 2009. **134**(4): p. 417-422 DOI: 10.21273/JASHS.134.4.417.

50. Huang, B.R., X.Z. Liu, and Q.Z. Xu, Supraoptimal soil temperatures induced oxidative stress in leaves of creeping bentgrass cultivars differing in heat tolerance. *Crop Science*, 2001. **41**(2): p. 430-435 DOI: 10.2135/cropsci2001.412430x.

51. Smirnof, N.J.N.-t., Therole ofactive oxygenin theresponse ofplantstowaterdeficitand desiccation. 1993. **125**: p. 27-58.

52. Almeselmani, M., et al., Protective role of antioxidant enzymes under high temperature stress. 2006. **171**(3): p. 382-388.

53. Jiang, Y. and B.J.C.s. Huang, Drought and heat stress injury to two cool-season turfgrasses in relation to antioxidant metabolism and lipid peroxidation. 2001. **41**(2): p. 436-442.

54. Feng, X.-H., et al., A small heat shock protein CaHsp25. 9 positively regulates heat, salt, and drought stress tolerance in pepper (Capsicum annuum L.). 2019. **142**: p. 151-162.

55. Li, F.F., et al., Antioxidant and Hormone Responses to Heat Stress in Two Kentucky Bluegrass Cultivars Contrasting in Heat Tolerance. *Journal of the American Society for Horticultural Science*, 2014. **139**(5): p. 587-596 DOI: 10.21273/jashs.139.5.587.

56. Dash, S. and N.J.J.o.P.P. Mohanty, Response of seedlings to heat-stress in cultivars of wheat: growth temperature-dependent differential modulation of photosystem 1 and 2 activity, and foliar antioxidant defense capacity. 2002. **159**(1): p. 49-59.

57. Munné-Bosch, S.J.J.o.p.p., The role of α-tocopherol in plant stress tolerance. 2005. **162**(7): p. 743-748.

58. Goldberg, A.L., Protein degradation and protection against misfolded or damaged proteins. *Nature*, 2003. **426**(6968): p. 895-899 DOI: 10.1038/nature02263.

59. Sun, Y., et al., Regulation of chloroplast protein degradation. *Journal of Genetics and Genomics*, 2023 DOI: 10.1016/j.jgg.2023.02.010.

60. Møller, I.M. and B.K. Kristensen, Protein oxidation in plant mitochondria as a stress indicator. *Photochemical & photobiological sciences*, 2004. **3**(8): p. 730-735 DOI: 10.1039/b315561g.

61. Liu, Y., et al., Proteolysis in plant immunity. *The Plant Cell*, 2024: p. koae142.

62. Shang, F. and A. Taylor, Ubiquitin–proteasome pathway and cellular responses to oxidative stress. *Free Radical Biology and Medicine*, 2011. **51**(1): p. 5-16 DOI: 10.1016/j.freeradbiomed.2011.03.031.

63. Callis, J., Regulation of protein degradation. *The Plant Cell*, 1995. **7**(7): p. 845 DOI: 10.1105/tpc.7.7.845.

64. Fan, Q. and D. Jespersen, Assessing Heat Tolerance in Creeping Bentgrass Lines Based on Physiological Responses. *Plants*, 2023. **12**(1): p. 41 DOI: 10.3390/plants12010041.

65. He, Y. and B. Huang, Protein changes during heat stress in three Kentucky bluegrass cultivars differing in heat tolerance. *Crop Science*, 2007. **47**(6): p. 2513-2520 DOI: 10.2135/cropsci2006.12.0821.

66. Roberts, I.N., et al., Senescence-associated proteases in plants. *Physiologia Plantarum*, 2012. **145**(1): p. 130-139 DOI: 10.1111/j.1399-3054.2012.01574.x.

67. Sharma, P. and D. Gayen, Plant protease as regulator and signaling molecule for enhancing environmental stress-tolerance. *Plant Cell Reports*, 2021. **40**(11): p. 2081-2095 DOI: 10.1007/s00299-021-02739-9.

68. Luciński, R. and M. Adamiec, The role of plant proteases in the response of plants to abiotic stress factors. *Frontiers in Plant Physiology*, 2023. **1**: p. 1330216 DOI: 10.3389/fphgy.2023.1330216.

69. Kidrič, M., J. Kos, and J. Sabotič, Proteases and their endogenous inhibitors in the plant response to abiotic stress. *Botanica serbica*, 2014. **38**(1): p. 139-158.

70. He, Y., X. Liu, and B. Huang, Changes in protein content, protease activity, and amino acid content associated with heat injury in creeping bentgrass. *Journal of the American Society for Horticultural Science*, 2005. **130**(6): p. 842-847 DOI: 10.21273/JASHS.130.6.842.

71. Hameed, A., M. Goher, and N. Iqbal, Heat stress-induced cell death, changes in antioxidants, lipid peroxidation, and protease activity in wheat leaves. *Journal of Plant Growth Regulation*, 2012. **31**: p. 283-291 DOI: 10.1007/s00344-011-9238-4.

72. Veerasamy, M., Y.L. He, and B.R. Huang, Leaf senescence and protein metabolism in creeping bentgrass exposed to heat stress and treated with cytokinins. *Journal of the*

American Society for Horticultural Science, 2007. **132**(4): p. 467-472 DOI: 10.21273/jashs.132.4.467.

73. Li, Z., H. Yue, and D. Xing, MAP Kinase 6-mediated activation of vacuolar processing enzyme modulates heat shock-induced programmed cell death in Arabidopsis. *New Phytologist*, 2012. **195**(1): p. 85-96 DOI: 10.1111/j.1469-8137.2012.04131.x.

74. Rossi, S. and B. Huang, Protease inhibitors suppressed leaf senescence in creeping bentgrass exposed to heat stress in association with inhibition of protein degradation into free amino acids. *Plant Growth Regulation*, 2023: p. 1-11 DOI: 10.1007/s10725-023-00977-3.

75. Jagadish, S., et al., Physiological and proteomic approaches to address heat tolerance during anthesis in rice (Oryza sativa L.). *Journal of experimental botany*, 2010. **61**(1): p. 143-156 DOI: 10.1093/jxb/erp289.

76. Gammulla, C.G., et al., Differential metabolic response of cultured rice (Oryza sativa) cells exposed to high-and low-temperature stress. *Proteomics*, 2010. **10**(16): p. 3001-3019 DOI: 10.1002/pmic.201000054.

77. Rollins, J., et al., Leaf proteome alterations in the context of physiological and morphological responses to drought and heat stress in barley (Hordeum vulgare L.). *Journal of experimental botany*, 2013. **64**(11): p. 3201-3212 DOI: 10.1093/jxb/ert158.

78. Singh, A., et al., Genome-wide analysis of rice ClpB/HSP100, ClpC and ClpD genes. *BMC genomics*, 2010. **11**: p. 1-18 DOI: 10.1186/1471-2164-11-95.

79. Martin, R.C., B.A. Kronmiller, and J.E. Dombrowski, Transcriptome Analysis of Lolium temulentum Exposed to a Combination of Drought and Heat Stress. *Plants*, 2021. **10**(11): p. 2247 DOI: 10.3390/plants10112247.

80. Lee, U., et al., The Arabidopsis ClpB/Hsp100 family of proteins: chaperones for stress and chloroplast development. *The Plant Journal*, 2007. **49**(1): p. 115-127 DOI: 10.1111/j.1365-313X.2006.02940.x.

81. Huber, C.V., et al., DEG10 contributes to mitochondrial proteostasis, root growth, and seed yield in Arabidopsis. *Journal of experimental botany*, 2019. **70**(19): p. 5423-5436 DOI: 10.1093/jxb/erz294.

82. Bhalerao, R., et al., Gene expression in autumn leaves. *Plant physiology*, 2003. **131**(2): p. 430-442 DOI: 10.1104/pp.012732.

83. Lim, P.O., H.J. Kim, and H. Gil Nam, Leaf senescence. *Annu. Rev. Plant Biol.*, 2007. **58**: p. 115-136 DOI: 10.1146/annurev.arplant.57.032905.105316.

84. Diaz-Mendoza, M., et al., Plant senescence and proteolysis: two processes with one destiny. *Genetics and Molecular Biology*, 2016. **39**: p. 329-338 DOI: 10.1590/1678-4685-GMB-2016-0015.

85. Lee, D.G., et al., A proteomic approach in analyzing heat-responsive proteins in rice leaves. *Proteomics*, 2007. **7**(18): p. 3369-3383 DOI: 10.1002/pmic.200700266.

86. Huang, B.R. and C.P. Xu, Identification and characterization of proteins associated with plant tolerance to heat stress. *Journal of Integrative Plant Biology*, 2008. **50**(10): p. 1230-1237 DOI: 10.1111/j.1744-7909.2008.00735.x.

87. Lara, M.V., et al., Biochemical and proteomic analysis of 'Dixiland'peach fruit (Prunus persica) upon heat treatment. *Journal of Experimental Botany*, 2009. **60**(15): p. 4315-4333 DOI: 10.1093/jxb/erp267.

88. Shakeel, S.N., et al., Proteomic and transcriptomic analyses of Agave americana in response to heat stress. *Plant Molecular Biology Reporter*, 2013. **31**: p. 840-851 DOI: 10.1007/s11105-013-0555-6.

89. Huang, B.R., S. Rachmilevitch, and J.C. Xu, Root carbon and protein metabolism associated with heat tolerance. *Journal of Experimental Botany*, 2012. **63**(9): p. 3455-3465 DOI: 10.1093/jxb/ers003.

90. Niño, M.C., et al., Genome-wide identification and molecular characterization of cysteine protease genes in rice. *Plant Biotechnology Reports*, 2020. **14**: p. 69-87 DOI: 10.1007/s11816-019-00583-8.

91. Cao, H., O. Duncan, and A.H. Millar, Protein turnover in the developing Triticum aestivum grain. *New Phytologist*, 2022. **233**(3): p. 1188-1201 DOI: 10.1111/nph.17756.

92. Li, L., et al., Protein degradation rate in Arabidopsis thaliana leaf growth and development. 2017. **29**(2): p. 207-228 DOI: 10.1105/tpc.16.00768.

93. Morales, M. and S. Munné-Bosch, Oxidative stress: a master regulator of plant trade-offs? *Trends in plant science*, 2016. **21**(12): p. 996-999 DOI: 10.1016/j.tplants.2016.09.002.

94. Luo, S. and C. Kim, Current understanding of temperature stress-responsive chloroplast FtsH metalloproteases. *International journal of molecular sciences*, 2021. **22**(22): p. 12106 DOI: 10.3390/ijms222212106.

95. Ferreira, S., et al., Proteome profiling of Populus euphratica Oliv. upon heat stress. *Annals of botany*, 2006. **98**(2): p. 361-377 DOI: 10.1093/aob/mcl106.

96. Das, A., et al., Leaf proteome analysis reveals prospective drought and heat stress response mechanisms in soybean. *BioMed research international*, 2016. **2016**(1): p. 6021047 DOI: 10.1155/2016/6021047.

97. Chen, J., J.J. Burke, and Z. Xin, Chlorophyll fluorescence analysis revealed essential roles of FtsH11 protease in regulation of the adaptive responses of photosynthetic systems to high temperature. *BMC Plant Biology*, 2018. **18**: p. 1-13 DOI: 10.1186/s12870-018-1228-2.

98. Chen, J., et al., FtsH11 protease plays a critical role in Arabidopsis thermotolerance. *The Plant Journal*, 2006. **48**(1): p. 73-84 DOI: 10.1111/j.1365-313X.2006.02855.x.

99. Yue, X., et al., Chloroplast inner envelope protein FtsH11 is involved in the adjustment of assembly of chloroplast ATP synthase under heat stress. *Plant, Cell & Environment*, 2023. **46**(3): p. 850-864 DOI: 10.1111/pce.14525.

100. Maziak, A., et al., FTSH4 and OMA1 mitochondrial proteases reduce moderate heat stress-induced protein aggregation. *Plant physiology*, 2021. **187**(2): p. 769-786 DOI: 10.1093/plphys/kiab296.

101. Liu, S., et al., Gm1-MMP is involved in growth and development of leaf and seed, and enhances tolerance to high temperature and humidity stress in transgenic Arabidopsis. *Plant Science*, 2017. **259**: p. 48-61 DOI: 10.1016/j.plantsci.2017.03.005.

102. Zhang, S., et al., A tomato putative metalloprotease SlEGY2 plays a positive role in thermotolerance. *Agriculture*, 2022. **12**(7): p. 940 DOI: 10.3390/agriculture12070940.

103. Szűcs, A., et al., Histological and microarray analysis of the direct effect of water shortage alone or combined with heat on early grain development in wheat (Triticum aestivum). *Physiologia plantarum*, 2010. **140**(2): p. 174-188 DOI: 10.1111/j.1399-3054.2010.01394.x.

104. Fernando, F.D., D.G. Raúl, and G.M. Gabriela, Overexpression of Arabidopsis aspartic protease APA1 gene confers drought tolerance. *Plant Science*, 2020. **292**: p. 110406 DOI: 10.1016/j.plantsci.2020.110406.

105. Guo, R., et al., Constitutive expression of a grape aspartic protease gene in transgenic Arabidopsis confers osmotic stress tolerance. *Plant Cell, Tissue and Organ Culture (PCTOC)*, 2015. **121**: p. 275-287 DOI: 10.1007/s11240-014-0699-6.

106. Figueiredo, L., R.B. Santos, and A. Figueiredo, Defense and offense strategies: the role of aspartic proteases in plant–pathogen interactions. *Biology*, 2021. **10**(2): p. 75 DOI: 10.3390/biology10020075.

107. van Wijk, K.J. and Z. Adam, Does the polyubiquitination pathway operate inside intact chloroplasts to remove proteins? *The Plant Cell*, 2024: p. koae104 DOI: 10.1093/plcell/koae104.

108. Müller, L. and T. Hoppe, UPS-dependent strategies of protein quality control degradation. *Trends in Biochemical Sciences*, 2024 DOI: 10.1016/j.tibs.2024.06.006.

109. Xu, J., et al., The ubiquitin-proteasome system in the plant response to abiotic stress: potential role in crop resilience improvement. *Plant Science*, 2024: p. 112035 DOI: 10.1016/j.plantsci.2024.112035.

110. Paradiso, A., et al., Cyclic AMP mediates heat stress response by the control of redox homeostasis and ubiquitin-proteasome system. *Plant, Cell & Environment*, 2020. **43**(11): p. 2727-2742 DOI: 10.1111/pce.13878.

111. Ferguson, D.L., J.A. Guikema, and G.M.J.P.P. Paulsen, Ubiquitin pool modulation and protein degradation in wheat roots during high temperature stress. *Plant Physiology*, 1990. **92**(3): p. 740-746 DOI: 10.1104/pp.92.3.740.

112. Ortiz, C. and L. Cardemil, Heat-shock responses in two leguminous plants: a comparative study. *Journal of Experimental Botany*, 2001. **52**(361): p. 1711-1719 DOI: 10.1093/jexbot/52.361.1711.

113. Wettern, M., et al., Ubiquitin in Chlamydomonas reinhardii: distribution in the cell and effect of heat shock and photoinhibition on its conjugate pattern. *European journal of biochemistry*, 1990. **191**(3): p. 571-576 DOI: 10.1111/j.1432-1033.1990.tb19159.x.

114. Xu, F.Q. and H.W. Xue, The ubiquitin-proteasome system in plant responses to environments. *Plant, cell & environment*, 2019. **42**(10): p. 2931-2944 DOI: 10.1111/pce.13633.

115. Lim, S.D., et al., The rice RING finger E3 ligase, OsHCI1, drives nuclear export of multiple substrate proteins and its heterogeneous overexpression enhances acquired thermotolerance. *Journal of experimental botany*, 2013. **64**(10): p. 2899-2914 DOI: 10.1093/jxb/ert143.

116. Kaur, H., et al., PUB63, a novel early heat responsive ubiquitin E3 ligase from rice implicates heat stress tolerance. *Plant Stress*, 2023. **10**(1): p. 100291 DOI: 10.1016/j.stress.2023.100291.

117. Li, Q., et al., Wheat F-box protein gene TaFBA1 is involved in plant tolerance to heat stress. *Frontiers in plant science*, 2018. **9**: p. 521 DOI: 10.3389/fpls.2018.00521.

118. Zhang, Y., et al., Functional analysis of tomato CHIP ubiquitin E3 ligase in heat tolerance. *Scientific Reports*, 2021. **11**(1): p. 1713 DOI: 10.1038/s41598-021-81372-8.

119. Zhang, S., et al., SUMO E3 ligase SlSIZ1 facilitates heat tolerance in tomato. *Plant and Cell Physiology*, 2018. **59**(1): p. 58-71 DOI: 10.1093/pcp/pcx160.

120. Liu, Y., et al., AtPPRT1, an E3 ubiquitin ligase, enhances the thermotolerance in Arabidopsis. *Plants*, 2020. **9**(9): p. 1074 DOI: 10.3390/plants9091074.

121. Peng, L., et al., AtPUB48 E3 ligase plays a crucial role in the thermotolerance of Arabidopsis. *Biochemical and biophysical research communications*, 2019. **509**(1): p. 281-286 DOI: 10.1016/j.bbrc.2018.12.123.

122. Morimoto, K., et al., BPM-CUL3 E3 ligase modulates thermotolerance by facilitating negative regulatory domain-mediated degradation of DREB2A in Arabidopsis. *Proceedings of the National Academy of Sciences*, 2017. **114**(40): p. E8528-E8536 DOI: 10.1073/pnas.1704189114.

123. Yan, J., et al., AtCHIP, a U-box-containing E3 ubiquitin ligase, plays a critical role in temperature stress tolerance in Arabidopsis. *Plant physiology*, 2003. **132**(2): p. 861-869 DOI: 10.1104/pp.103.020800.

124. Wang, S., J. Kurepa, and J.A. Smalle, The Arabidopsis 26S proteasome subunit RPN1a is required for optimal plant growth and stress responses. *Plant and Cell Physiology*, 2009. **50**(9): p. 1721-1725 DOI: 10.1093/pcp/pcp105.

125. Kurepa, J., A. Toh-e, and J.A. Smalle, 26S proteasome regulatory particle mutants have increased oxidative stress tolerance. *The Plant Journal*, 2008. **53**(1): p. 102-114 DOI: 10.1111/j.1365-313X.2007.03322.x.

126. Li, X.-M., et al., Natural alleles of a proteasome α2 subunit gene contribute to thermotolerance and adaptation of African rice. *Nature genetics*, 2015. **47**(7): p. 827-833 DOI: 10.1038/ng.3305.

127. Fan, W., H. Zheng, and G. Wang, Proteomic analysis of ubiquitinated proteins in maize immature kernels. *Journal of Proteomics*, 2021. **243**: p. 104261 DOI: 10.1016/j.jprot.2021.104261.

128. Berger, N., et al., Root membrane ubiquitinome under short-term osmotic stress. *International Journal of Molecular Sciences*, 2022. **23**(4): p. 1956 DOI: 10.1101/2021.12.06.471398.

129. Ying, Y., Y. Pang, and J. Bao, Comparative ubiquitome analysis reveals diverse functions of ubiquitination in rice seed development under high-temperature stress. *Seed Biology*, 2023. **2**(1) DOI: 10.48130/seedbio-2023-0023.

130. Xie, H., et al., Global ubiquitome profiling revealed the roles of ubiquitinated proteins in metabolic pathways of tea leaves in responding to drought stress. *Scientific reports*, 2019. **9**(1): p. 4286 DOI: 10.1038/s41598-019-41041-3.

131. Liu, C.W., et al., Proteomic analysis of salt-responsive ubiquitin-related proteins in rice roots. *Rapid Communications in Mass Spectrometry*, 2012. **26**(15): p. 1649-1660 DOI: 10.1002/rcm.6271.

132. Majer, S.H., Ubiquitin Mass Spectrometry Kit: A Mass Spec Approach to Ubiquitomics. 2024.

133. Ma, X., et al., Ubiquitylome analysis reveals a central role for the ubiquitin-proteasome system in plant innate immunity. *Plant physiology*, 2021. **185**(4): p. 1943-1965 DOI: 10.1093/plphys/kiab011.

134. Kim, D.-Y., et al., Advanced proteomic analyses yield a deep catalog of ubiquitylation targets in Arabidopsis. *The Plant Cell*, 2013. **25**(5): p. 1523-1540 DOI: 10.1105/tpc.112.108613.

135. Wang, W., et al., Role of plant heat-shock proteins and molecular chaperones in the abiotic stress response. 2004. **9**(5): p. 244-252.

136. Parsell, D. and S. Lindquist, The function of heat-shock proteins in stress tolerance: degradation and reactivation of damaged proteins. *Annual review of genetics*, 1993. **27**(1): p. 437-496 DOI: 10.1146/annurev.ge.27.120193.002253.

137. Wang, K., X. Zhang, and E.H. Ervin, *Small heat shock proteins, a key player in grass plant thermotolerance*, in *Heat Shock Proteins and Plants*. 2016, Springer. p. 41-64.

138. Park, S.-Y., et al., Heat-shock response in heat-tolerant and nontolerant variants of Agrostis palustris Huds. 1996. **111**(2): p. 515-524.

139. Flom, G., et al., Effect of mutation of the tetratricopeptide repeat and asparatate-proline 2 domains of Sti1 on Hsp90 signaling and interaction in Saccharomyces cerevisiae. 2006. **172**(1): p. 41-51.

CHAPTER 2

ASSESSING HEAT TOLERANCE IN CREEPING BENTGRASS LINES BASED ON PHYSIOLOGICAL AND BIOCHEMICAL RESPONSES [1]

[1] Q. Fan and D. Jespersen. 2023. *Plants*. 12(1): p. 41 DOI: 10.3390/plants12010041. Reprinted here with permission of the publisher

Abstract

Heat stress is a major concern for the growth of cool-season creeping bentgrass (*Agrostis stolonifera* L.). Nonetheless, there is a lack in a clear and systematic understanding of thermotolerance mechanisms for this species. This study aimed to assess heat tolerance in experimental lines and cultivars to determine important physiological and biochemical traits responsible for improved tolerance, including the use of OJIP fluorescence. Ten creeping bentgrass lines were exposed to either control (20/15°C day/night) or high temperature (38/33°C day/night) conditions for 35 d via growth chambers at Griffin, GA. Principal component analysis and clustering analysis were performed to rank stress performance and divide lines into different groups according to their tolerance similarities, respectively. It was found out that, at the end of the trial, S11 729-10 and BTC032 were in the most thermotolerant group, followed by a group containing BTC011, AU Victory and Penncross. Crenshaw belonged to the most heat-sensitive group while S11 675-02 and Pure Eclipse were in the second most heat-sensitive group. The exceptional thermotolerance in S11 729-10 and BTC032 was associated with their abilities to maintain cell membrane stability and protein metabolism, plus minimize oxidative damages. Additionally, among various light-harvesting steps, energy trapping, dissipation and electron transport from Q_A to PQ were more heat-sensitive than electron transport from Q_A to final PSI acceptors. Along with the strong correlations between multiple OJIP parameters and other traits, it reveals that OJIP fluorescence could be a valuable tool for dissection of photosynthetic processes and identification of the critical steps responsible for photosynthetic declines, enabling a more targeted heat-stress screening. Our results indicated that variability in the level of heat tolerance and associated mechanisms in creeping bentgrass germplasm could be utilized to develop new cultivars with improved thermotolerance.

1. Introduction

As an important cool-season turfgrass, creeping bentgrass (*Agrostis stolonifera* L.**)** is widely used in high value turf areas such as golf courses due to its ability to tolerate low mowing heights and quick recovery from traffic and golf ball marks [140]. Although highly prized for its turf quality, creeping bentgrass has only low to moderate tolerance to high temperatures [141]. This makes heat stress a major concern in many areas such as the southeastern China as well as the southeastern United States where there are typically long hot summers combined with high temperatures, with damages being further exacerbated with more frequent and intense heat wave events as a function of climate change [4, 142]. Many golf courses have been converted from creeping bentgrass to warm-season species, particularly bermudagrass (*Cynodon* sp.), due to a lack of heat tolerance in recent years [143].

High temperature can result in a number of physiological and biochemical injuries to plants, primarily including oxidative stress, photosynthesis inhibition and change in protein metabolism. Oxidative stress results from excess accumulation of reactive oxygen species (ROS) which are a group of free radicals, such as singlet oxygen ($^1O_2$)and hydroxyl radical (OH^-) [144]. They can attack a range of essential cellular components, like proteins, carbohydrates, and lipids in particular to cause leakage of cellular contents, eventually leading to lipid peroxidation and decreased integrity of cell membranes [3]. Photosynthesis inhibition occurs when elevated temperature brings about damages to photosynthetic machinery, including chlorophyll breakdown and reduced photosystem II (PSII) activity [3]. In addition, change in protein metabolism is another common stress symptom. Heat stress generally causes decreased protein abundance, which has been stated in various cool-season turfgrasses including creeping bentgrass [3, 145, 146]. It impacts many important cellular activities including photosynthesis and oxidative stress. The D1

protein plays a key role in PSII repair. Damaged D1 protein undergoes proteolysis to be removed and then a newly synthesized D1 is assembled into PSII, thus recovering PSII activity [147]. One study on wheat (*Triticum aestivum*) suggested that faster turnover of D1 protein contributed to better PSII photochemical efficiency [28]. In the case of oxidative stress, new proteins are synthesized to defend against ROS, and oxidized proteins undergo degradation to be removed, which otherwise would accumulate, causing damage and cell death[60]. These negative effects ultimately result in declines in carbon stores, reduced growth, loss of green color, thinning of the turf canopy and eventual plant death. To this end, development of heat-tolerant creeping bentgrass cultivars is desperately needed.

A few defense pathways have been clarified to be common strategies responding to heat stress in turfgrasses, like enhanced ROS detoxification, greater maintenance of photosynthesis ability, or altered protein metabolism [3]. Nonetheless, it should be noted that the specific changes may differ between species, or even cultivars and genotypes, which plays a pivotal role in the wide divergence in thermotolerance [49, 146, 148]. Creeping bentgrass shows considerable intraspecific diversity among different lines for its tolerance to heat. Previous research has identified differences in germplasm for important stress-related traits and there is potential to develop new cultivars with improved ability to withstand high temperatures [22]. However, despite progress made, comparisons of specific mechanisms, and physiological and biochemical parameters of heat tolerance among creeping bentgrass germplasm are still limited and need to be explored further.

As noted previously, PSII inhibition is a typical heat-stress induced symptom. The chlorophyll fluorescence parameter, photochemical efficiency (TRo/ABS or Fv/Fm), reflects the quantum efficiency of energy trapping by PSII and has been widely used as a reliable and sensitive tool for stress detection in different plant species including creeping bentgrass [20, 149-151]. A

relatively new development in fluorescence methodology is OJIP fluorescence [152]. It monitors rise of fluorescence intensity to a maximum at various states [153]. The O state is dark-adapted state when all the reaction centers, quinone A (Q_A), quinone B (Q_B) and plastoquinone (PQ) are oxidized. Upon exposure to saturating light, electrons will migrate into the PQ pool via Q_A and Q_B. When the majority of electrons have reduced Q_A, the J state is reached (at ~2 ms). When Q_B molecules are also reduced, the I state is reached (at 30 ms). Lastly, the P state is reached when maximum fluorescence intensity is obtained with a concurrent peak reduction in PQ pool, regardless of exposure time. By studying the OJIP curve, multiple photosynthetic component processes unavailable through traditional fluorescence methodologies can be quantified, such as energy trapping by PSII photochemistry, energy dissipation in PSII antennae, as well as electron transport between PSII and photosystem I (PSI), thereby providing a deeper insight into the function of photosynthetic components that might impair plant performance due to unfavorable environmental conditions [154]. To date, the use of OJIP fluorescence in abiotic stress studies have been documented in quite a few species, like tomato [155], cotton [156, 157] and soybean [158]. However, despite its wide-spread application in stress physiology, related reports in creeping bentgrass, to our knowledge, are non-existent.

A number of creeping bentgrass materials were previously screened for summer performance. Within this germplasm collection, several experimental lines were identified with exceptional level of thermotolerance and outperformed commercial cultivars currently available on the market [159]. Nevertheless, the specific physiological or biochemical responses involved in their enhanced tolerance to heat have not yet been clearly revealed. A more complete understanding of the mechanisms conferring improved thermotolerance is essential for the efficient development of elite cultivars. Hence, this project aimed to evaluate heat tolerance in

various creeping bentgrass lines to confirm the exceptional performance under heat stress in these promising experimental lines, as compared to commercial cultivars that form a range of thermotolerance. A number of physiological and biochemical measurements, including OJIP fluorescence, were taken to explore the responses enabling superior lines to outperform others. Integration of multiple stress-related traits will shed further light on heat stress survival strategies in creeping bentgrass, and determine useful traits associated with stress tolerance which can be utilized to develop new cultivars with improved thermotolerance.

2. Materials and Methods

2.1. Growth and Treatment Conditions

A total of ten creeping bentgrass lines were used in this study, including five commercial cultivars ('Crenshaw', 'Pure Eclipse', 'Penn A4', 'Penncross' and 'AU Victory'), and five experimental lines which have shown to perform well during summer in preliminary studies in Georgia, namely, 'GCB2020-1', 'BTC011' and 'BTC032' (Paul Raymer, unpublished work, 2020), plus 'S11 675-02 'and 'S11 729-10' [159]. For each line, 6-cm-diameter plugs were established in plastic pots (10.5 cm long, 10.5 cm wide and 12.5 cm deep) filled with a mixture of 50% sand and 50% calcined clay (Turface; Profile Products LLC, Buffalo Grove, IL) for ten weeks in greenhouse conditions [~23/~15°C (light/dark period temperatures) and 70% relative humidity] before transferred to controlled environmental growth chambers (CG-72; Conviron, Winnipeg, Canada). Plants were allowed one-week acclimation inside the growth chambers under conditions of 20/15°C (day/night), 70% humidity and 14-h photoperiod with 600 μmol m^{-2} s^{-1} photosynthetically active radiation at the canopy level before the onset of different temperature treatments. Plants were maintained well-watered and fertilized weekly with a 24-8-16 (N-P-K) fertilizer (Scotts Miracle-Gro; Marysville, OH) at the rate of 9.8 g N m^{-2} during establishment in

the greenhouse as well as during the treatment period inside growth chambers. Applications of insecticide and fungicide were made as needed for disease control. Plants of each line were exposed to either heat stress (38/33°C day/night) or control (20/15°C day/night) conditions for 35 d after treatments began.

2.2 Measurements

2.2.1 Physiological measurements

Measurements consisted of assessments of whole-plant responses along with physiological and biochemical factors. Overall turf performance was estimated using a visual turf quality (TQ) rating on a scale of 1-9 and percent green cover via digital image analysis. Turf quality was determined according to color, density and uniformity with 1 representing totally dead grass, 9 standing for completely healthy grass with lush green color, and 6 being the minimum acceptable quality [160]. Digital image analysis was conducted through images taken with a digital camera (Canon G9X; Canon, Tokyo, Japan) using a lightbox to ensure a uniform lighting, which were processed using ImageJ v.1.46 to obtain values of percent green cover [161].

Total chlorophyll content and OJIP fluorescence were used to reflect the health status of photosynthetic machinery. Plants were dark adapted overnight (10 h) prior to performing OJIP measurements via a chlorophyll fluorometer (OSP 5+; Opti-sciences, Hudson, NH). This study focused on several energy flux and quantum efficiency parameters to better understand the light-harvesting processes, which included the energy flux absorbed by the antenna of PSII per cross section (ABS/CSm), the excitation energy flux trapped by open PSII reaction centers per cross section leading to the reduction of Q_A (TRo/CSm), the energy flux associated with electron transport from Q_A to PQ per cross section (ETo/CSm), quantum efficiency of energy trapping by PSII (TRo/ABS), quantum efficiency of energy dissipation in PSII antenna (DIo/ABS),quantum

efficiency of electron transport Q_A to PQ (ETo/ABS), and quantum efficiency of electron transport Q_A to final PSI acceptors (REo/ABS) [154]. Four measurements were taken on fully expanded leaves for each replicate. To obtain values of total chlorophyll content, 0.1 g fresh leaves were incubated in 5 mL dimethyl sulfoxide for 7 days to allow for chlorophyll extraction. Then the absorbance of solutions at 665 and 649 nm were read using spectrophotometer (Evolution 300 UV-visible spectrophotometer; Thermo Scientific, Madison, WI) and converted to chlorophyll content according to previously derived equations on a dry weight basis [162].

Electrolyte leakage (EL) serves as an indicator of cell membrane stability. Around 0.1 g fresh leaves were placed in a tube containing 35 mL deionized water. After agitating tubes on a shaker for 16 h, initial conductivity was recorded through a conductivity meter (Radiometer, Copenhagen, Denmark). Next, the samples were autoclaved at 120 °C for 20 min, followed by incubation for another 16 h on a shaker, after which the final conductivity was read. EL then was calculated as the percentage of initial conductivity over total conductivity [163].

2.2.2. Biochemical measurements

Change in protein abundance was measured to represent change in protein metabolism, while malondialdehyde (MDA) content, a final product of lipid peroxidation, was quantified to indicate the extent of oxidative damage. Both analyses were performed through a microplate reader (Epoch 2 microplate reader, BioTek, Winooski, VT). Approximately 50 mg fresh leaves were added into 1.1 mL 50 mM sodium phosphate buffer (pH 7.0 with 1 mM ethylenediaminetetraacetic acid). Supernatants were collected after homogenization and centrifugation at 15000 × g, 4 °C for 20 min. Then total protein content was quantified at 595 nm with Bradford dye reagent and a bovine serum albumin standard [164]. For the quantification of MDA content, 0.25 mL supernatant was mixed and reacted with 0.5 mL reaction solution (20% w/v trichloroacetic acid and 0.5% w/v

thiobarbituric acid) at 95 °C, followed by absorbance measurement at the wavelengths of 532 and 600 nm. MDA content was acquired by subtracting background absorbance at 600 nm from absorbance at 532 nm and then divided by an extinction coefficient of 155 mM^{-1} cm^{-1} [165].

The content of ethanol soluble carbohydrates (ESC) were determined based on the anthrone method [166]. Approximately 30 mg dry leaf tissues were homogenized in 5 mL of 95 % (v/v) ethanol and centrifuged at 3500 rpm, 4 °C for 10 min. The pellet was washed with 5 mL of 70% (v/v) ethanol twice. Then all soluble portions were pooled, vortexed and centrifuged again to remove debris. Next, 100 μL of the ethanolic extract was added into 3 mL of anthrone-sulfuric acid reagent [200 mg anthrone dissolved in 100 mL 72 % (v/v) H_2SO_4]. After incubation in boiling water for 10 min, the absorbance of the resultant reaction mixture was recorded at 630 nm, and compared against glucose standards in the range of 20-100 μg mL^{-1}. All measurements were taken weekly except for contents of protein, MDA and ESC with the former two being measured every other week while the latter was analyzed once at the end of the trial.

2.3. Statistical Analysis

A completely randomized split-plot design was applied with temperature as the whole plot and line as the subplot, with each combination of temperature and line having four replications. During the trial, each temperature was repeated in four growth chambers. Inside each chamber, there were two pots for every line and the average of these two pots was used to represent an individual replicate.

Data were analyzed via ANOVA using a mixed model in JMP Pro 16.0.0 (SAS Institute, 2021). Date, temperature, line, and their interactions were treated as fixed effects whereas experimental run and the whole plot were random effects. Before ANOVA, normal distribution of residuals and the homogeneity of variance were checked according to normal quantile-quantile

plots and residuals versus fitted plots, respectively, to make sure data met ANOVA assumptions. Means were separated by Fisher's protected least significant difference (LSD) at the 0.05 probability level. Correlation analysis and K-means clustering analysis were performed using corrplot and cluster packages, respectively, while principal component analysis was conducted through plotly and ggfortify packages in RStudio (R 3.6.0, 2019).

3. Results

Since significant effects of temperature, line, date, and their interactions were detected for most parameters (Table 2.1) and the focus is mainly on exploring variations among lines under stress, differences among lines were analyzed for a given day under individual treatment.

For TQ, there were no significant differences for control plants over the duration of the trial, with all lines maintaining values greater than 8.5, representing a lack of stress (Figure 2.1; Table S2.1). Conversely, TQ scores declined throughout the trial for heat-stressed plants, to a greater extent in Crenshaw, Pure Eclipse as well as S11 675-02 than others, presenting variations in thermotolerance. These were in accordance with the significant effects of temperature and temperature × line interaction (Table 2.1). TQ scores were not significantly different among lines until heat progressed beyond 14 d, with differences being more pronounced over time. At the end of the trial, Crenshaw had the worst performance with an average score of 1.9 but not significantly different from Pure Eclipse and S11 675-02. The two top performers, S11 729-10 and BTC032, had values of 5.8 and 5.6, respectively, without significant differences relative to BTC011, AU Victory, Penn A4 and Penncross. As with TQ, change in percent green cover followed a similar pattern (Figure 2.2; Table S2.2). All lines experienced significant drops in percent cover by 35 d of stress and the declines were greater in Crenshaw, Pure Eclipse and S11 675-02 than other lines.

At 35 d, these three lines were also the poorest performers, whereas BTC032 was the top performer but was not significantly differed from S11 729-10, BTC011, AU Victory and Penncross.

Regarding photosynthetic attributes, consistent values of total chlorophyll content, TRo/ABS and DIo/ABS were maintained in most lines with little variation among lines on most sampling dates under control conditions (Figure 2.3-2.5; Table S2.3-S2.5). For ETo/ABS, no significant difference was found between 0 d and 35 d under control conditions despite variations over time, with differences among lines detected within sampling dates (Figure 2.6; Table S2.6). Intriguingly, DIo/ABS significantly rose while the other three parameters fell as a result of heat stress. At the end of week 5, the top statistical group contained S11 729-10, AU Victory, BTC032 and BTC011 for TRo/ABS as well as DIo/ABS measurements, S11 729-10, Penncross and AU Victory for chlorophyll content, and AU Victory, BTC032 and S11 729-10 for ETo/ABS. Crenshaw consistently presented the lowest values regarding TRo/ABS, total chlorophyll content and ETo/ABS but was not significantly different compared to Pure Eclipse for TRo/ABS, or to S11 675-02 and Pure Eclipse for chlorophyll levels or ETo/ABS at 35 d. Regarding DIo/ABS, the highest values were also found in Crenshaw at 35 d although it showed no significant difference compared to Pure Eclipse. As for REo/ABS, only the main effect of date was significant.

As for the phenomenological energy fluxes involved in light-harvesting processes, significant differences were not found between 0 d and 35 d under control conditions for all parameters (ABS/CSm, TRo/CSm and ETo/CSm) although variations existed over time potentially as a consequence of chamber acclimation effects or natural genotypic variations, with differences detected within certain sampling dates (Figure 2.7-2.9; Table S2.7-S2.9). In contrast with control, heat stress caused significant reductions in every line for all three parameters, with pronounced separations being observed from 14 d onwards. At 35 d, Crenshaw, Pure Eclipse and S11 675-02

were the three poorest performers whose values were significantly lower than S11 729-10, Penncross and BTC032 in terms of ABS/CSm, and all the remainging lines except for GCB2020-1 regarding TRo/CSm and ETo/CSm.

For EL under control conditions, no significant difference was seen between 0 d and 35 d despite some variance over time (Figure 2.10; Table S2.10). Contrastingly, values went up dramatically in response to heat stress in all lines with the exception of S11 729-10. Similar to most parameters mentioned above, variation among lines became apparent after two-weeks of stress with divergence increasing over time until 35 d. At 35 d of treatment, EL of S11 729-10 was the lowest but was not statistically different from BTC032, AU Victory, or BTC011, whereas Crenshaw had the highest value and was in the same statistical group as Pure Eclipse and S11 675-02.

For MDA content, plants under control conditions maintained mostly consistent values over time whereas significant rises were detected in all lines under heat stress, with the exception of S11 729-10 and AU Victory (Figure 2.11; Table S2.11). Pronounced variation among lines was found in response to stress at 21 d and continued to diverge through the end of the experiment. At 35 d, S11 729-10, as the top performer, presented a significantly lower MDA content than Crenshaw, Pure Eclipse, GCB2020-1 and S11 675-02.

For protein abundance, plants followed similar patterns of change over time when exposed to control conditions, with greater values generally found at 0 d and 7 d potentially due to variations in fresh weight (Figure 2.12; Table S2.12). On the contrary, heat stress caused an obvious separation among lines with prominent differences detected over the last two weeks of stress. Specifically, at 35 d, S11 729-10 was the top performer, showing greater contents than the other lines with the exception of BTC032 and BTC011, whereas Crenshaw's protein content was

significantly lower than all others except Penn A4. Moreover, protein abundances presented no significant changes over the course of the five-week stress period for S11 729-10, BTC032 and BTC011 while the remaining lines all presented dramatic decreases.

For ESC, lines exposed to elevated temperature presented increases compared to those under control conditions, with an average of 81.0 and 37. 0 mg g^{-1} dry weight under heat stress and control conditions, respectively (data not shown). No significant differences existed for the line or line × temperature interaction effects. In this study ESC was not a useful parameter for separating heat tolerance among lines.

Correlation analysis was conducted for all parameters except for ESC since there was limited data with no significant variation among lines. It revealed that all the parameters excluding protein content and REo/ABS were significantly and strongly correlated with each other, with the absolute values ranging from 0.70 to 0.99 (Figure 2.13). Conversely, the absolute values were not greater than 0.23 for the correlation coefficients between protein and other parameters, and not over 0.21 between REo/ABS and other parameters.

To take all the measurements into account to rank stress performance of lines, principal component analysis was conducted. Analysis determined the contribution of each component to the overall variation among lines due to differences after five weeks of heat stress, and also revealed to what extent different parameters contributed to stress tolerance (Figure 2.14). The first principal component (PC1) explained 89.2% of variance while the second principal component accounted for only 4.6% of variance. Except for total protein content and REo/ABS accounting for 5.7% and 6.6% of PC1, respectively, the contribution to PC1 made by the remaining traits ranged from 7.3% to 8.4%. Furthermore, clustering analysis was performed to divide lines into different groups according to their similarities (within-group variation is minimized). Together

with results of principal component analysis, it revealed that S11 729-10 and BTC032 were in the most thermotolerant group. The second most thermotolerant group contained BTC011, AU Victory and Penncross, followed by the group containing Penn A4 as well as GCB2020-1. Crenshaw belonged to the most heat-sensitive group while S11 675-02 and Pure Eclipse were in the second most heat-sensitive group.

4. Discussion

Although elevated temperature caused damages to all plants over the course of the 35 d stress period, a wide range of thermotolerance was observed among lines as evidenced by the differences in their visual characteristics. Specifically, S11 729-10, BTC032, BTC011 and AU Victory were the four top performers, outperforming others by maintaining greater overall quality as measured by TQ and green cover. Conversely, heat-sensitive lines, such as Crenshaw, S11 675-02 and Pure Eclipse, consistently performed poorly in terms of these two measured parameters, while the remaining lines were intermediate in their performances. Moreover, superior visual characteristics in the more heat-tolerant lines were attributed to their improved physiological as well as biochemical responses. These included greater abilities to withstand injuries to photosynthetic machinery as reflected in chlorophyll content and OJIP fluorescence traits (TRo/ABS, DIo/ABS, ETo/ABS, ABS/CSm, TRo/CSm and ETo/CSm), maintain cell membrane stability as evaluated by EL, minimize oxidative damage as measured by MDA content, and reduce change in protein metabolism as indicated by total protein content.

Maintaining chlorophyll levels and chlorophyll fluorescence traits is critically important for cool-season grass survival during heat stress. The former contributes to the absorption of light energy for use in photosynthesis while the latter estimates the health of PSII reaction centers which are the most thermally labile component of the electron transport chain, with constraints in either

of them impairing photosynthetic capacity [167, 168]. Within this study, despite heat-induced declines in chlorophyll content, TRo/ABS, ETo/ABS, ABS/CSm, TRo/CSm and ETo/CSm and increases in DIo/ABS over time, more heat-tolerant lines S11 719-10, AU Victory, BTC032 and BTC011 generally better maintained these characteristics, revealing less damage to their photosynthetic systems, which is in accordance with previous research [20, 169, 170]. Chlorophyll loss is one major characteristic of leaf senescence induced by heat stress damage [5]. The lesser decline in chlorophyll content in heat-tolerant plants could be a consequence of slower chlorophyll degradation resulting from relatively lower gene expression levels of chlorophyll-degrading enzymes, like chlorophyllase, pheophytinase and chlorophyll-degrading peroxidases [30, 35].

The light energy absorbed by photosynthetic pigments is either used in PSII photochemistry or dissipated through heat and fluorescence [36]. Energy absorption decreased as measured by ABS/CSm, potentially as a result of heat-induced chlorophyll reduction or damage to photosynthetic complexes. With reduced energy absorption, the resulting energy trapped by PSII reaction centers, as measured by TRo/CSm, would also be expected to go down, reducing the efficiency of trapping and ultimately causing declines in the light-harvesting abilities of the leaf [155]. As noted previously, electrons migrate from PSII to PSI via Q_A and PQ during light harvesting. When the electron flow to Q_A declined (TRo/CSm), there would generally be a concomitant decline in energy flux from Q_A to PQ too, as evaluated by ETo/CSm [155, 171]. Likewise, when OJIP traits were expressed as energy fluxes per absorbed photo flux, declines in TRo/ABS and ETo/ABS were detected as well. A decrease in the quantum efficiency of light photochemical reactions in PSII (TRo/ABS) resulted in a rise of energy dissipation as heat and fluorescence, as evidenced by increases in DIo/ABS, highlighting that stress-induced damage required the leaves to dissipate excess excitation energy instead of utilizing it for photosynthetic

processes [172]. Intriguingly, in contrast with the significances observed for TRo/ABS, DIo/ABS and ETo/ABS, neither temperature effects nor line effects were significant for the quantum efficiency of electron transport from Q_A to final PSI acceptors, as measured by REo/ABS, despite heat-induced numerical declines over time among all lines (data not shown). This suggested that during light-harvesting processes, energy trapping, energy dissipation and electron transport from Q_A to PQ were more sensitive to temperature rise than electron transport from Q_A to final PSI acceptors [155, 173]. Identifying these critical steps responsible for photosynthetic inhibitions would allow for a more targeted screening and improvement of plants with enhanced heat tolerance.

Previous studies pointed out that heat stress impaired a range of OJIP fluorescence traits in croftonweed (*Ageratina adenophora* (Spreng.) King & H. Rob) and peony (*P. lactiflora*) [171, 172]. However, more heat-tolerant populations or cultivars typically better maintained absorbed energy flux, energy flux trapped by PSII, electron transport from Q_A to PQ, as well as quantum efficiencies of energy trapping, dissipation, and electron transport from Q_A to PQ. Similarly, another study on tall fescue (*Festuca arundinacea* Schreb.), stated that at the end of heat treatments, the heat-tolerant "TF71" presented significantly higher values in absorbed energy flux, energy flux trapped by PSII, and quantum efficiencies of energy trapping and electron transport from Q_A to PQ than the heat-sensitive "TF133", maintaining better photosynthetic capacity thus contributing to its enhanced adaptation to high temperature [170]. These are all in agreement with our findings. Additionally, the close associations among ABS/CSm, TRo/CSm, ETo/CSm, TRo/ABS, ETo/ABS and DIo/ABS were also supported by their significantly strong correlation coefficients among each other. Along with concurrent declines in ABS/CSm, TRo/CSm, ETo/CSm from 21 d onwards, and concurrent declines or increases in TRo/ABS,ETo/ABS and DIo/ABS

from 7 d onwards, it could be inferred that injuries to photosynthetic components were wide spread in the chloroplast and these light-harvesting steps might be concomitantly damaged by heat stress. Furthermore, our study also detected strong correlations of physiological factors plus MDA content with all fluorescence traits except for REo/ABS. As a reliable parameter commonly used in heat stress screening, it was not surprising that TRo/ABS showed the strongest associations with other factors [148, 149, 174]. Nevertheless, it's noteworthy that DIo/ABS had the same correlation coefficients as TRo/ABS did, indicating its potential as another rapid and reliable measurement for thermotolerance evaluation in turfgrasses. The second strongest correlations with physiological traits plus MDA content were observed for ETo/ABS, which were close to those for TRo/ABS and DIo/ABS. Stronger relationships between whole-plant seedling vigor and ETo/ABS than other OJIP traits were reported in cotton previously and the authors proposed that ETo/ABS could be used as a surrogate for more time-consuming seedling vigor measurement [156, 157]. To our knowledge, this is the first time that the application of OJIP fluorescence in abiotic stress response has been reported in creeping bentgrass. It could serve as a valuable tool for actual dissection of photosynthetic processes and help understand which steps of light-harvesting electron transport were more sensitive to heat stress [171, 172]. Such information would provide deeper insights into heat-induced photosynthetic declines, allowing for a more targeted screening and improvement of heat tolerance in plants.

Accumulated ROS triggered by heat stress can attack lipids, resulting in decreased membrane integrity and lipid peroxidation, so typically the EL value increases with a concomitant increase in MDA content during plants' exposure to stress [20]. However, these responses could be specific at both species and cultivar levels with lower EL and MDA content representing improved thermotolerance [49, 50]. This corroborates the results found in our study where, compared to

heat-sensitive lines, lower values of EL and MDA content were detected in heat-tolerant lines at 35 d, particularly S11 729-10. S11 729-10 had relatively little increase in these two parameters during the entire period of stress, suggesting its superior ability to maintain cell membrane integrity and to minimize oxidative damage. Furthermore, although not measured in the current study, greater activities of antioxidant enzymes, for instance, superoxide dismutase, catalase, ascorbate peroxidase, and peroxidase, can result in lower MDA abundances in heat-tolerant lines by scavenging excess ROS to protect cells or macromolecules from severe oxidative damage [20, 55]. This may also have contributed to better maintenance of chlorophyll content and fluorescence traits and lower EL, eventually leading to better overall quality. Strong correlations between MDA and many other physiological traits support that reduced oxidative damage may result in the maintenance of photosynthetic processes such as light harvesting, reduced cellular damage, and maintenance of overall turf quality.

Protein metabolism, a process controlled by the balance between protein synthesis and protein degradation, impacts many cellular activities such as the aforementioned photosynthesis and oxidative stress. Decrease in protein abundance is a typic stress-induced characteristic, which has been confirmed in a wide range of plant species besides creeping bentgrass, including but not limited to strawberry (*Fragaria x ananassa* cv. Camarosa) [19], tomato (*Lycopersicon esculentum* Mill.) and maize (*Zea mays* L.) [175]. In general, protein catabolism is accelerated to a greater degree compared to the biosynthesis process under unfavorable environmental conditions, taking major responsibility for reduced protein content in response to elevated temperature [63, 176]. However, it was previously documented that heat-tolerant plants typically had lower declines in protein abundance [65, 89]. This agrees with our findings among which, greater protein contents were seen in more heat-tolerant lines like S11 729-10 and BTC032 at the end of the experiment.

The higher protein abundance in heat-tolerant plants could be a consequence of faster protein synthesis, slower protein degradation, or both. Proteins synthesized abundantly under heat are primarily heat shock proteins, functioning as chaperones by preventing other proteins from aggregation and refolding stress-damaged proteins [135], contributing to the maintenance of protein metabolism. Hence, a greater and earlier induction of heat shock proteins in the heat-tolerant plants could be one reason for their improved thermotolerance [65, 177]. As an opposing process to protein synthesis, less protein catabolism or slower degradation may be due to reduced proteolysis activity carried out by the coordinated action of the ubiquitin-proteasome system and various proteases [66, 111]. One previous study stated that less enhanced gene expression of cysteine protease and a slower rate of overall protein degradation were detected in heat-adapted *Agrostis scabra*, contributing to its higher protein thermostability, and thereby greater protein abundance compared creeping bentgrass [89]. Thus, in order to develop a further understanding of protein regulation in response to heat stress in turfgrasses, more research is needed to understand proteolysis activity of both the ubiquitin-proteasome system and proteases.

As with the defense mechanisms discussed above, accumulation of sugars can be another important contributor to heat tolerance. It not only contributes to increased osmotic adjustment but also improves the integrity of cellular membranes, helping relieve plants from heat-induced damages, which has been documented in creeping bentgrass [178] and other plant species [179, 180]. Moreover, ESC turned out to accumulate more in creeping bentgrass cultivars with better summer performance [148]. The authors proposed that elevated temperature resulted in rapid loss of water, causing dehydration, as manifested by the declines in leaf relative water content and osmotic potential, while accumulation of sugars could produce positive effects on water homeostasis, thus explaining the higher sugar contents along with better leaf water status and

osmotic adjustment abilities found in the more heat-tolerant cultivars. These findings were not consistent with our research where no significance was shown among various lines in terms of ESC. The discrepancy between studies is likely due to differences in creeping bentgrass lines, environmental conditions such as stress duration and stress intensity, and measurement techniques.

5. Conclusions

In summary, a broad range of thermotolerance exists among creeping bentgrass lines At the end of the trial, the overall ranking for heat tolerance of lines was that S11 729-10 and BTC032 were in the most thermotolerant group while BTC011, AU Victory and Penncross were in the second most thermotolerant group; Crenshaw belonged to the most heat-sensitive group while S11 675-02 and Pure Eclipse were in the second most heat-sensitive group; The group containing Penn A4 and GCB202-1 was intermediate in their tolerance ranking. The exceptional thermotolerance in S11 729-10 and BTC032 was mainly associated with their greater abilities to maintain integrity of cellular membranes, as well as protein metabolism, and the ability to minimize oxidative damages. In addition, among various light-harvesting steps, energy trapping, dissipation and electron transport from Q_A to PQ were more heat-sensitive than electron transport from Q_A to final PSI acceptors. Moreover, strong significant correlations were detected among multiple OJIP parameters and other stress-related factors. These suggest that OJIP fluorescence could be a valuable tool for dissection of photosynthetic processes and identification of the critical steps responsible for photosynthetic declines, enabling a more targeted screening and improvement of plants for enhanced heat tolerance. This is also the first time that the potential application of rapid OJIP assessments is addressed in creeping bentgrass. Additional research is needed to further reveal how heat-tolerant and heat-sensitive creeping bentgrass lines respond to high temperature from physiological, biochemical and molecular mechanisms, particularly regarding proteolysis.

Author Contributions: Formal analysis, investigation, project administration, visualization, writing—original draft preparation and editing, Q. F.; conceptualization, resources, supervision, writing—review and editing, D. J. Both authors have read and agreed to the published version of the manuscript.

Acknowledgments: Thanks go to Paul Raymer and Stacy Bonos for providing experimental materials. Technical assistance from Somer Rowe and assistance on data analysis from Kaiwen Han is much appreciated. Support was provided by the University of Georgia Research Foundation.

Conflicts of Interest: The authors declare no conflict of interest.

References

1. Fry, J. and B. Huang, Applied turfgrass science and physiology. 2004.
2. Turgeon, A.J.N., Turfgrass management 5th ed Prentice Hall Upper Saddle. 1999. **4**: p. 225.
3. Pachauri, R.K. and L. Meyer, *Climate change 2014 Synthesis Report-Summary for Policymakers*. 2014, Intergovernmetnal Panel on Climate Change (IPCC).
4. Zhou, Y., M. Yin, and F. Liu, First Report of Summer Patch of Creeping Bentgrass Caused by Magnaporthiopsis poae in Southeastern China. *Plant Disease*, 2022. **106**(5): p. 1527 DOI: 10.1094/PDIS-09-21-1892-PDN.
5. O'Brien, P. and C. Hartwiger, A time to change: The ultradwarf bermudagrass putting green golf model is solid in the southern USA. *USGA Green Section Record. February*, 2011. **25**(49): p. 8.

6. Mansoor, S., et al., Reactive Oxygen Species in Plants: From Source to Sink. *Antioxidants*, 2022. **11**(2): p. 225 DOI: 10.3390/antiox11020225.

7. Huang, B.R., M. DaCosta, and Y.W. Jiang, Research Advances in Mechanisms of Turfgrass Tolerance to Abiotic Stresses: From Physiology to Molecular Biology. *Critical Reviews in Plant Sciences*, 2014. **33**(2-3): p. 141-189 DOI: 10.1080/07352689.2014.870411.

8. Alam, M.N., et al., Role of melatonin in inducing the physiological and biochemical processes associated with heat stress tolerance in tall fescue (Festuca arundinaceous). *Journal of Plant Growth Regulation*, 2022. **41**(7): p. 2759-2768 DOI: 10.1007/s00344-021-10472-6.

9. Jespersen, D., C.P. Xu, and B.R. Huang, Membrane Proteins Associated with Heat-Induced Leaf Senescence in a Cool-Season Grass Species. *Crop Science*, 2015. **55**(2): p. 837-850 DOI: 10.2135/cropsci2014.04.0335.

10. Balfagón, D., et al., Jasmonic acid is required for plant acclimation to a combination of high light and heat stress. *Plant Physiology*, 2019. **181**(4): p. 1668-1682 DOI: 10.1104/pp.19.00956.

11. Li, H., et al., High temperature effects on D1 protein turnover in three wheat varieties with different heat susceptibility. *Plant Growth Regulation*, 2017. **81**(1): p. 1-9 DOI: 10.1007/s10725-016-0179-6.

12. Møller, I.M. and B.K. Kristensen, Protein oxidation in plant mitochondria as a stress indicator. *Photochemical & photobiological sciences*, 2004. **3**(8): p. 730-735 DOI: 10.1039/b315561g.

13. Du, H., Z. Wang, and B. Huang, Differential responses of warm-season and cool-season turfgrass species to heat stress associated with antioxidant enzyme activity. *Journal of the American Society for Horticultural Science*, 2009. **134**(4): p. 417-422 DOI: 10.21273/JASHS.134.4.417.

14. Li, Z., et al., Turf Quality and Physiological Responses to Summer Stress in Four Creeping Bentgrass Cultivars in a Subtropical Zone. *Plants (Basel)*, 2022. **11**(5): p. 665 DOI: 10.3390/plants11050665.

15. Jespersen, D., W. Meyer, and B. Huang, Physiological traits and genetic variations associated with drought and heat tolerance in creeping bentgrass. *Int. Turfgrass Soc. Res. J*, 2013. **12**: p. 459-464.

16. Liu, X. and B. Huang, Heat stress injury in relation to membrane lipid peroxidation in creeping bentgrass. *Crop Science*, 2000. **40**(2): p. 503-510 DOI: 10.2135/cropsci2000.402503x.

17. Zhou, R., et al., Screening and validation of tomato genotypes under heat stress using Fv/Fm to reveal the physiological mechanism of heat tolerance. *Environmental and Experimental Botany*, 2015. **118**: p. 1-11 DOI: 10.1016/j.envexpbot.2015.05.006.

18. Pirdashti, H., Z.T. Sarvestani, and M.A. Bahmanyar, Comparison of physiological responses among four contrast rice cultivars under drought stress conditions. *World Academy of Science, Engineering and Technology*, 2009. **49**: p. 52-53.

19. Zhang, X., et al., Phosphatidic acid and hydrogen peroxide coordinately enhance heat tolerance in tall fescue. *Plant Biology*, 2021. **23**: p. 142-151 DOI: 10.1111/plb.13215.

20. Strasser, R.J., A. Srivastava, and M. Tsimilli-Michael, The fluorescence transient as a tool to characterize and screen photosynthetic samples. *Probing photosynthesis: mechanisms, regulation and adaptation*, 2000: p. 445-483.

21. Küpper, H., et al., Analysis of OJIP chlorophyll fluorescence kinetics and QA reoxidation kinetics by direct fast imaging. *Plant physiology*, 2019. **179**(2): p. 369-381 DOI: 10.1104/pp.18.00953.

22. Stirbet, A., D. Lazár, and J. Kromdijk, Chlorophyll a fluorescence induction: can just a one-second measurement be used to quantify abiotic stress responses? *Photosynthetica*, 2018. **56**(1): p. 86-104 DOI: 10.1007/s11099-018-0770-3.

23. Zushi, K., S. Kajiwara, and N. Matsuzoe, Chlorophyll a fluorescence OJIP transient as a tool to characterize and evaluate response to heat and chilling stress in tomato leaf and fruit. *Scientia Horticulturae*, 2012. **148**: p. 39-46 DOI: 10.1016/j.scienta.2012.09.022.

24. Snider, J.L., et al., OJIP-fluorescence parameters as rapid indicators of cotton (Gossypium hirsutum L.) seedling vigor under contrasting growth temperature regimes. *Plant physiology and biochemistry*, 2018. **132**: p. 249-257 DOI: 10.1016/j.plaphy.2018.09.015.

25. Virk, G., et al., Extreme temperatures affect seedling growth and photosynthetic performance of advanced cotton genotypes. *Industrial Crops and Products*, 2021. **172**: p. 114025 DOI: 10.1016/j.indcrop.2021.114025.

26. Strauss, A., et al., Ranking of dark chilling tolerance in soybean genotypes probed by the chlorophyll a fluorescence transient OJIP. *Environmental and experimental botany*, 2006. **56**(2): p. 147-157 DOI: 10.1016/j.envexpbot.2005.01.011.

27. Jespersen, D., et al., Association of SSR and candidate gene markers with genetic variations in summer heat and drought performance for creeping bentgrass. 2018. **58**(6): p. 2644-2656 DOI: 10.2135/cropsci2018.05.0299.

28. Krans, J.V. and K. Morris, Determining a profile of protocols and standards used in the visual field assessment of turfgrasses: A survey of national turfgrass evaluation program-sponsored university scientists. 2007 DOI: 10.1094/ATS-2007-1130-01-TT.

29. Karcher, D.E. and M.D. Richardson, Digital image analysis in turfgrass research. *Turfgrass: Biology, use, and management*, 2013. **56**: p. 1133-1149-2 DOI: 10.2134/agronmonogr56.c29.

30. Wellburn, A.R., The spectral determination of chlorophylls a and b, as well as total carotenoids, using various solvents with spectrophotometers of different resolution. *Journal of plant physiology*, 1994. **144**(3): p. 307-313 DOI: 10.1016/S0176-1617(11)81192-2.

31. Blum, A. and A.J.C.S. Ebercon, Cell membrane stability as a measure of drought and heat tolerance in wheat 1. 1981. **21**(1): p. 43-47 DOI: 10.2135/cropsci1981.0011183X002100010013x.

32. Bradford, M.M., A rapid and sensitive method for the quantitation of microgram quantities of protein utilizing the principle of protein-dye binding. *Analytical biochemistry*, 1976. **72**(1-2): p. 248-254 DOI: 10.1016/0003-2697(76)90527-90523.

33. Hodges, D.M., et al., Improving the thiobarbituric acid-reactive-substances assay for estimating lipid peroxidation in plant tissues containing anthocyanin and other interfering compounds. *Planta*, 1999. **207**(4): p. 604-611 DOI: 10.1007/s004250050524.

34. Irigoyen, J., D. Einerich, and M. Sánchez-Díaz, Water stress induced changes in concentrations of proline and total soluble sugars in nodulated alfalfa (Medicago sativd) plants. *Physiologia plantarum*, 1992. **84**(1): p. 55-60 DOI: 10.1111/j.1399-3054.1992.tb08764.x.

35. Allakhverdiev, S.I., et al., Heat stress: an overview of molecular responses in photosynthesis. *Photosynthesis research*, 2008. **98**(1): p. 541-550 DOI: 10.1007/s11120-008-9331-0.

36. Xu, Y. and B. Huang, Heat-induced leaf senescence and hormonal changes for thermal bentgrass and turf-type bentgrass species differing in heat tolerance. *Journal of the American Society for Horticultural Science*, 2007. **132**(2): p. 185-192 DOI: 10.21273/JASHS.132.2.185.

37. Xu, C.P. and B.R. Huang, Comparative Analysis of Proteomic Responses to Single and Simultaneous Drought and Heat Stress for Two Kentucky Bluegrass Cultivars. *Crop Science*, 2012. **52**(3): p. 1246-1260 DOI: 10.2135/cropsci2011.10.0551.

38. Hu, L., et al., Antioxidant metabolism, photosystem II, and fatty acid composition of two tall fescue genotypes with different heat tolerance under high temperature stress. *Frontiers in Plant Science*, 2018. **9**: p. 1242 DOI: 10.3389/fpls.2018.01242.

39. Wahid, A., et al., Heat tolerance in plants: An overview. *Environmental and Experimental Botany*, 2007. **61**(3): p. 199-223 DOI: 10.1016/j.envexpbot.2007.05.011.

40. Jespersen, D., J. Zhang, and B.R. Huang, Chlorophyll loss associated with heat-induced senescence in bentgrass. *Plant Science*, 2016. **249**: p. 1-12 DOI: 10.1016/j.plantsci.2016.04.016.

41. Rossi, S., et al., Heat-induced leaf senescence associated with Chlorophyll metabolism in Bentgrass lines differing in heat tolerance. 2017. **57**(supplement1): p. S-169-S-178 DOI: 10.2135/cropsci2016.06.0542.

42. Taiz, L. and E. Zeiger, *Plant Physiology 5 ed. Sunderland, MA*. 2006, the Sinauer Associates.

43. Zhang, L., et al., The Effect of high-temperature stress on the physiological indexes, chloroplast ultrastructure, and photosystems of two herbaceous peony cultivars. *Journal of Plant Growth Regulation*, 2022: p. 1-16 DOI: 10.1007/s00344-022-10647-9.

44. Chen, S., et al., Classification and characteristics of heat tolerance in Ageratina adenophora populations using fast chlorophyll a fluorescence rise OJIP. *Environmental and Experimental Botany*, 2016. **122**: p. 126-140 DOI: 10.1016/j.envexpbot.2015.09.011.

45. Chen, L.-S. and L. Cheng, Photosystem 2 is more tolerant to high temperature in apple (Malus domestica Borkh.) leaves than in fruit peel. *Photosynthetica*, 2009. **47**(1): p. 112-120 DOI: 10.1007/s11099-009-0017-4.

46. Sharma, D.K., et al., Wheat cultivars selected for high Fv/Fm under heat stress maintain high photosynthesis, total chlorophyll, stomatal conductance, transpiration and dry matter. *Physiologia plantarum*, 2015. **153**(2): p. 284-298 DOI: 10.1111/ppl.12245.

47. Huang, B.R., X.Z. Liu, and Q.Z. Xu, Supraoptimal soil temperatures induced oxidative stress in leaves of creeping bentgrass cultivars differing in heat tolerance. *Crop Science*, 2001. **41**(2): p. 430-435 DOI: 10.2135/cropsci2001.412430x.

48. Li, F.F., et al., Antioxidant and Hormone Responses to Heat Stress in Two Kentucky Bluegrass Cultivars Contrasting in Heat Tolerance. *Journal of the American Society for Horticultural Science*, 2014. **139**(5): p. 587-596 DOI: 10.21273/jashs.139.5.587.

49. Gulen, H. and A. Eris, Effect of heat stress on peroxidase activity and total protein content in strawberry plants. *Plant Science*, 2004. **166**(3): p. 739-744 DOI: 10.1016/j.plantsci.2003.11.014.

50. Ayub, M., et al., Growth and physio-biochemical responses of maize (Zea mays L.) to drought and heat stresses. *Plant Biosystems-An International Journal Dealing with all Aspects of Plant Biology*, 2021. **155**(3): p. 535-542 DOI: 10.1080/11263504.2020.1762785.

51. Huffaker, R., Proteolytic activity during senescence of plants. *New Phytologist*, 1990. **116**(2): p. 199-231 DOI: 10.1111/j.1469-8137.1990.tb04710.x.

52. Callis, J.J.T.P.C., Regulation of protein degradation. 1995. **7**(7): p. 845 DOI: 10.1105/tpc.7.7.845.

53. He, Y. and B. Huang, Protein changes during heat stress in three Kentucky bluegrass cultivars differing in heat tolerance. *Crop Science*, 2007. **47**(6): p. 2513-2520 DOI: 10.2135/cropsci2006.12.0821.

54. Huang, B.R., S. Rachmilevitch, and J.C. Xu, Root carbon and protein metabolism associated with heat tolerance. *Journal of Experimental Botany*, 2012. **63**(9): p. 3455-3465 DOI: 10.1093/jxb/ers003.

55. Parsell, D. and S. Lindquist, The function of heat-shock proteins in stress tolerance: degradation and reactivation of damaged proteins. *Annual review of genetics*, 1993. **27**(1): p. 437-496 DOI: 10.1146/annurev.ge.27.120193.002253.

56. Xu, Y. and B. Huang, Differential protein expression for geothermal Agrostis scabra and turf-type Agrostis stolonifera differing in heat tolerance. *Environmental and Experimental Botany*, 2008. **64**(1): p. 58-64 DOI: 10.1016/j.envexpbot.2008.02.002.

57. Roberts, I.N., et al., Senescence-associated proteases in plants. *Physiologia Plantarum*, 2012. **145**(1): p. 130-139 DOI: 10.1111/j.1399-3054.2012.01574.x.

58. Ferguson, D.L., J.A. Guikema, and G.M.J.P.P. Paulsen, Ubiquitin pool modulation and protein degradation in wheat roots during high temperature stress. 1990. **92**(3): p. 740-746 DOI: 10.1104/pp.92.3.740.

59. DUFF, D.T. and J.B. BEARD, Supraoptimal Temperature Effects upon Agrostis palustris: Part II. Influence on Carbohydrate Levels, Photosynthetic Rate, and Respiration Rate. *Physiologia Plantarum*, 1974. **32**(1): p. 18-22 DOI: 10.1111/j.1399-3054.1974.tb03720.x.

60. Du, H., et al., Differential metabolic responses of perennial grass Cynodon transvaalensis× Cynodon dactylon (C4) and Poa Pratensis (C3) to heat stress. *Physiologia Plantarum*, 2011. **141**(3): p. 251-264 DOI: 10.1111/j.1399-3054.2010.01432.x.

61. Wahid, A. and T.J.B.P. Close, Expression of dehydrins under heat stress and their relationship with water relations of sugarcane leaves. 2007. **51**(1): p. 104-109 DOI: 10.1007/s10535-007-0021-0.

Tables and Figures

Table 2.1 ANOVA results for heat stress trials of creeping bentgrass.

Parameter†	*P* value						
	Date (D)	Temperature (T)	Line (L)	D×T	D×L	L×T	D×T×L
TQ	<0.0001	0.0004	<0.0001	<0.0001	<0.0001	<0.0001	<0.0001
Percent green cover	<0.0001	0.0025	<0.0001	<0.0001	0.0002	<0.0001	<0.0001
EL	<0.0001	0.0064	<0.0001	<0.0001	0.0400	<0.0001	0.1994
Total chlorophyll content	<0.0001	0.0004	0.0044	<0.0001	0.4223	<0.0001	0.7669
MDA content	<0.0001	0.0004	0.0016	<0.0001	0.5540	0.0006	0.7585
Total protein content	<0.0001	0.0316	0.0002	<0.0001	0.7554	0.0001	0.0102
ABS/CSm	<0.0001	0.0008	0.0002	<0.0001	0.8551	0.0001	0.6623
TRo/CSm	<0.0001	0.0004	<0.0001	<0.0001	0.7140	<0.0001	0.4652
ETo/CSm	<0.0001	0.0005	0.0002	<0.0001	0.8837	<0.0001	0.7059
TRo/ABS	<0.0001	0.0010	<0.0001	<0.0001	<0.0001	<0.0001	<0.0001
DIo/ABS	<0.0001	0.001	<0.0001	<0.0001	<0.0001	<0.0001	<0.0001
ETo/ABS	<0.0001	0.0025	<0.0001	<0.0001	0.1282	<0.0001	0.0608
REo/ABS	<0.0001	0.0572	0.4620	0.0834	1.0000	0.1614	1.0000
ESC	\	0.0097	0.3803	\	\	0.9539	\

†TQ, turf quality; EL, electrolyte leakage; MDA, malondialdehyde; ABS/CSm, the energy flux absorbed by the antenna of photosystem II (PSII) per cross section; TRo/CSm, the excitation energy flux trapped by open PSII reaction centers per cross section, leading to the reduction of quinone A (Q_A); ETo/CSm, the energy flux associated with electron transport from Q_A to PQ per cross section; TRo/ABS, quantum efficiency of energy trapping by PSII; DIo/ABS, quantum efficiency of energy dissipation in PSII antenna; ETo/ABS, quantum efficiency of electron transport from Q_A to plastoquinone; REo/ABS, quantum efficiency of electron transport from Q_A to final photosynstem I acceptors; ESC, ethanol soluble carbohydrate.

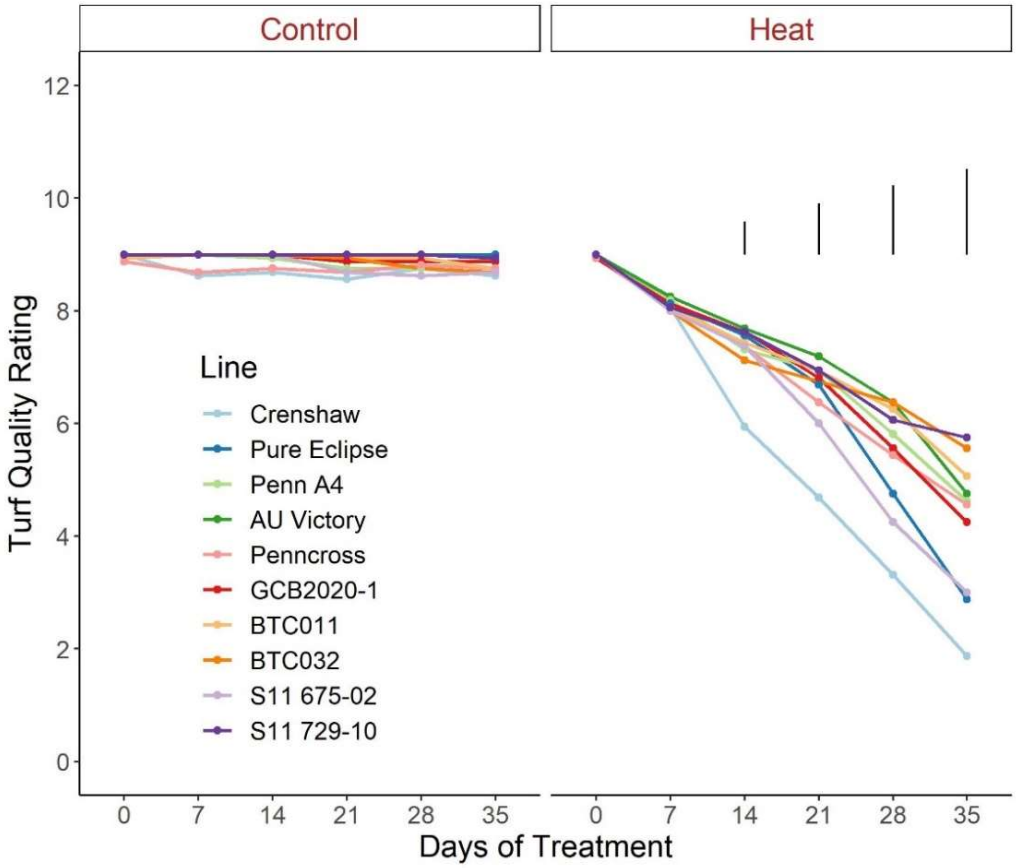

Figure 2.1 Change in visual turf quality rating for creeping bentgrass lines over time under control (20/15°C day/night) and heat stress (38/33°C day/night) conditions. Bars represent LSD values at $p = 0.05$ on days when significant differences among lines were found.

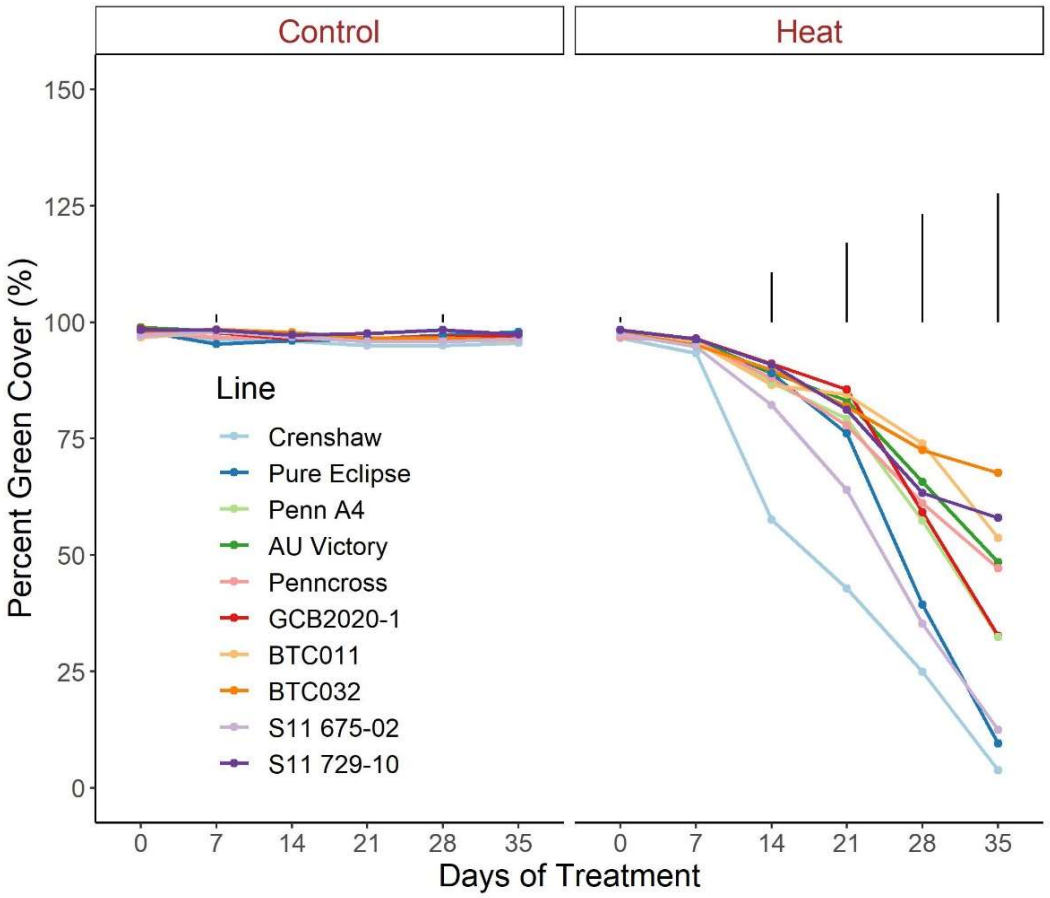

Figure 2.2 Change in percent green cover for creeping bentgrass lines over time under control (20/15°C day/night) and heat stress (38/33°C day/night) conditions. Bars represent LSD values at $p = 0.05$ on days when significant differences among lines were found.

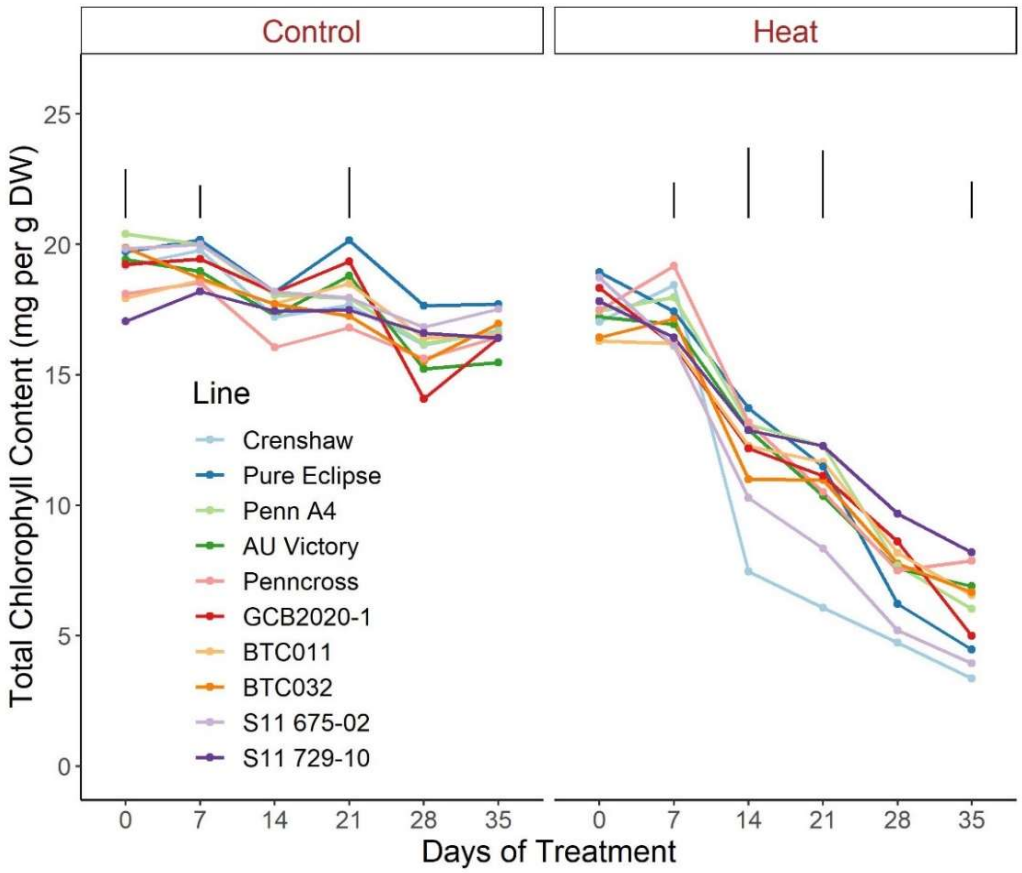

Figure 2.3 Change in total chlorophyll content for creeping bentgrass lines over time under control (20/15°C day/night) and heat stress (38/33°C day/night) conditions. Bars represent LSD values at $p = 0.05$ on days when significant differences among lines were found. DW, dry weight.

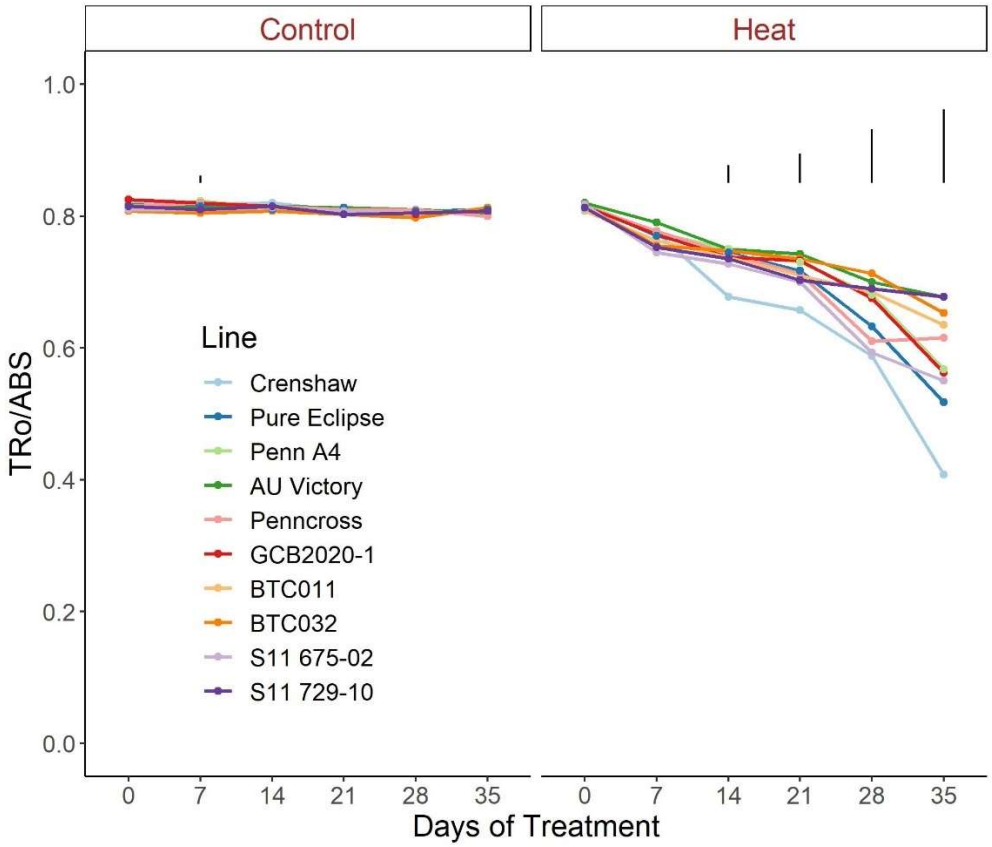

Figure 2.4 Change in TRo/ABS for creeping bentgrass lines over time under control (20/15°C day/night) and heat stress (38/33°C day/night) conditions. Bars represent LSD values at $p = 0.05$ on days when significant differences among lines were found.

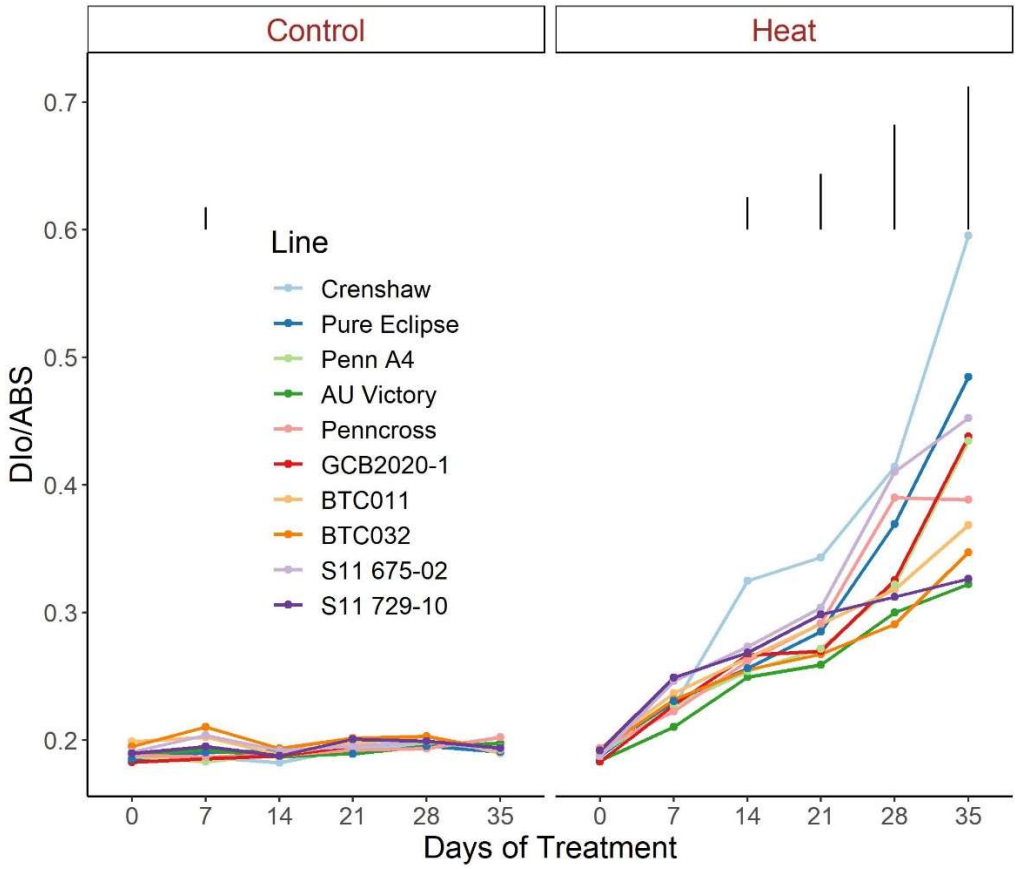

Figure 2.5 Change in DIo/ABS for creeping bentgrass lines over time under control (20/15°C day/night) and heat stress (38/33°C day/night) conditions. Bars represent LSD values at $p = 0.05$ on days when significant differences among lines were found.

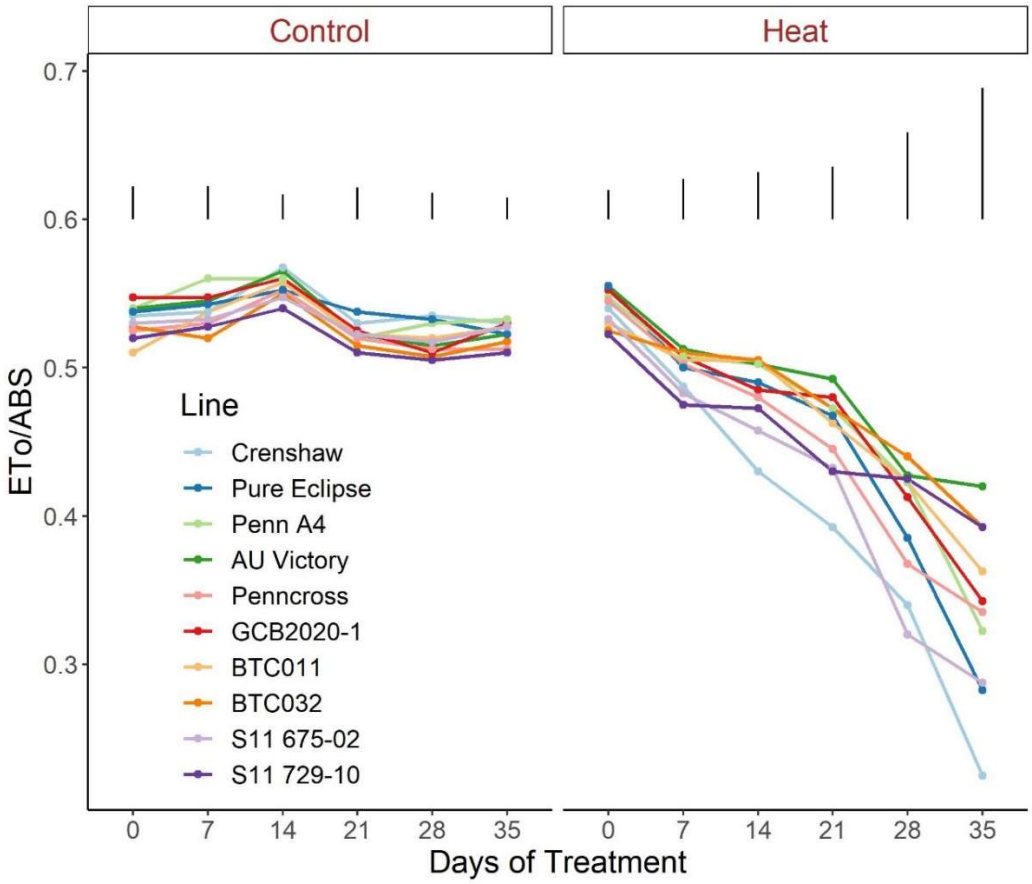

Figure 2.6 Change in ETo/ABS for creeping bentgrass lines over time under control (20/15°C day/night) and heat stress (38/33°C day/night) conditions. Bars represent LSD values at $p = 0.05$ on days when significant differences among lines were found.

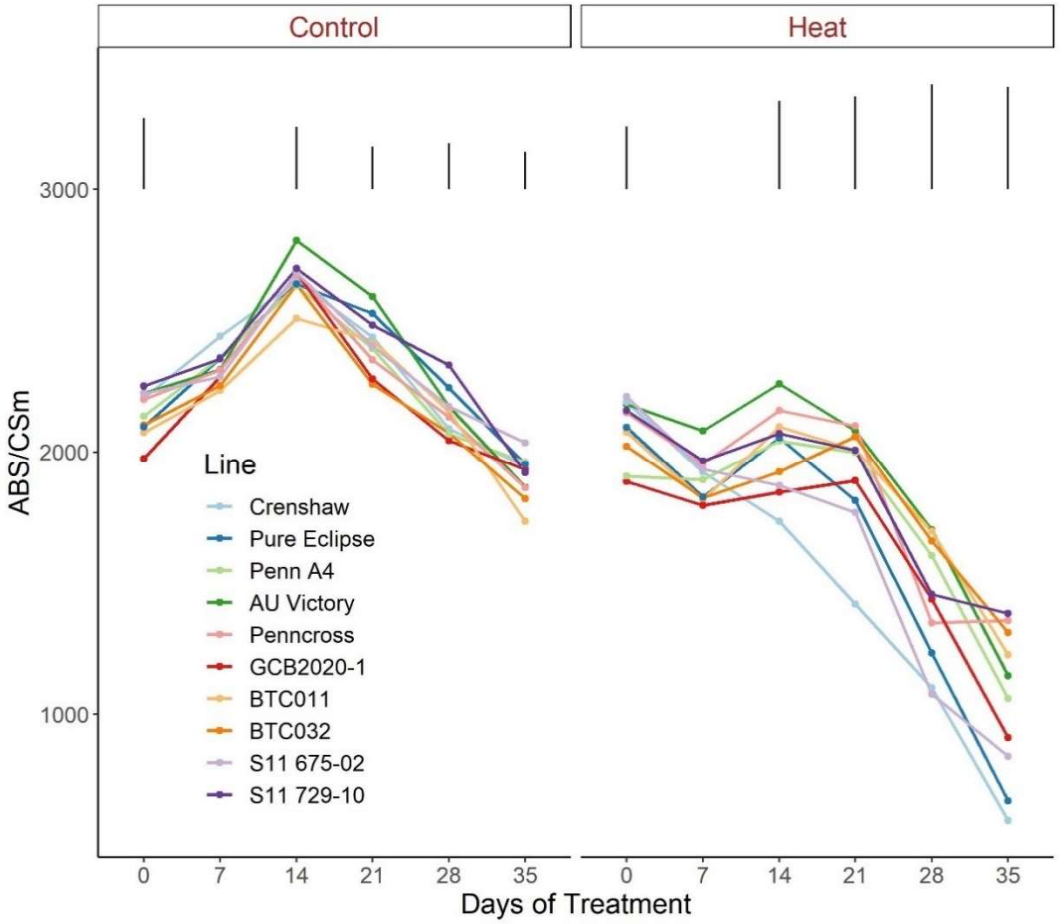

Figure 2.7 Change of ABS/CSm for creeping bentgrass lines over time under control (20/15°C day/night) and heat stress (38/33°C day/night) conditions. Bars represent LSD values at $p = 0.05$ on days when significant differences mong lines were found.

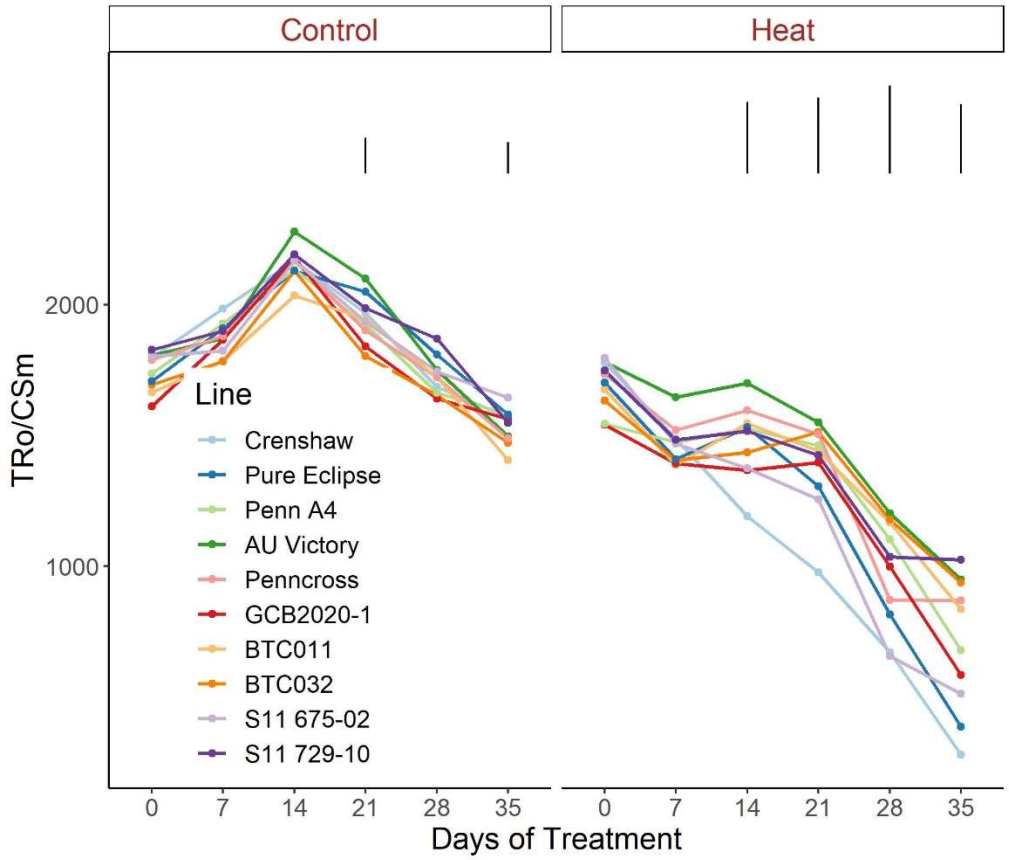

Figure 2.8 Change in TRo/CSm for creeping bentgrass lines over time under control (20/15°C day/night) and heat stress (38/33°C day/night) conditions. Bars represent LSD values at $p = 0.05$ on days when significant differences among lines were found.

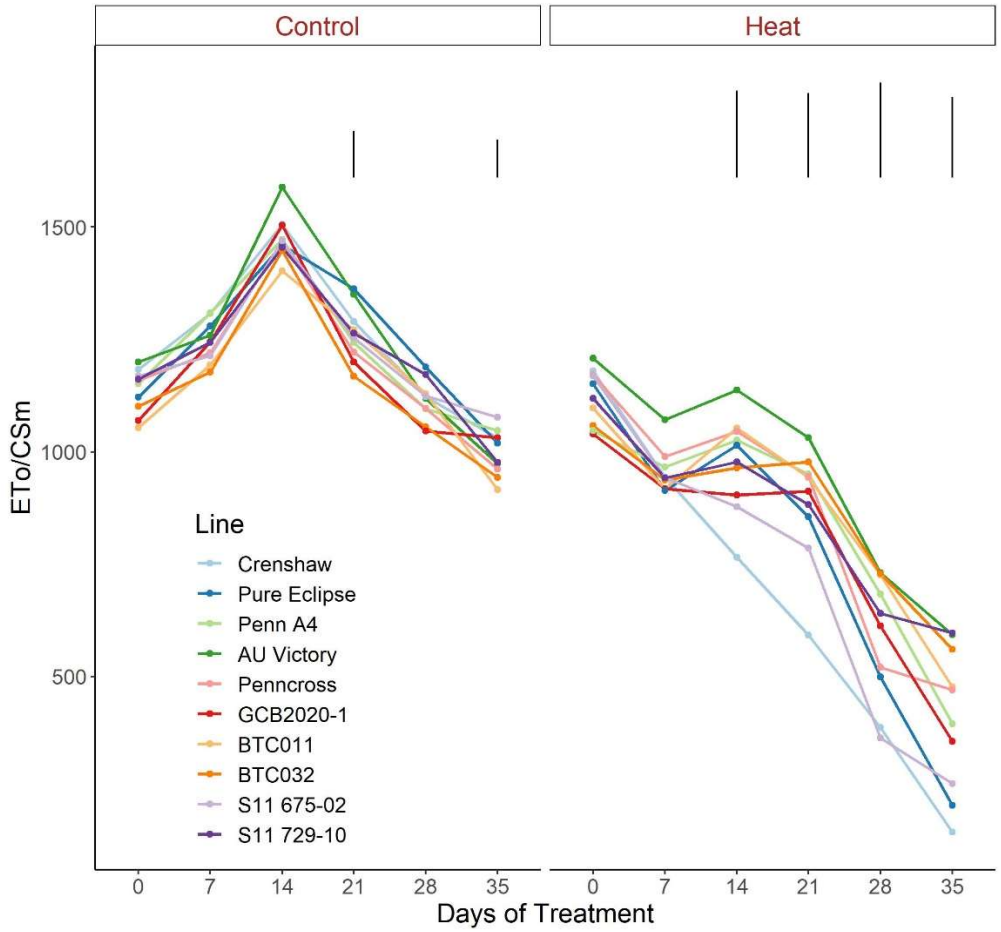

Figure 2.9 Change in ETo/CSm for creeping bentgrass lines over time under control (20/15°C day/night) and heat stress (38/33°C day/night) conditions. Bars represent LSD values at $p = 0.05$ on days when significant differences among lines were found.

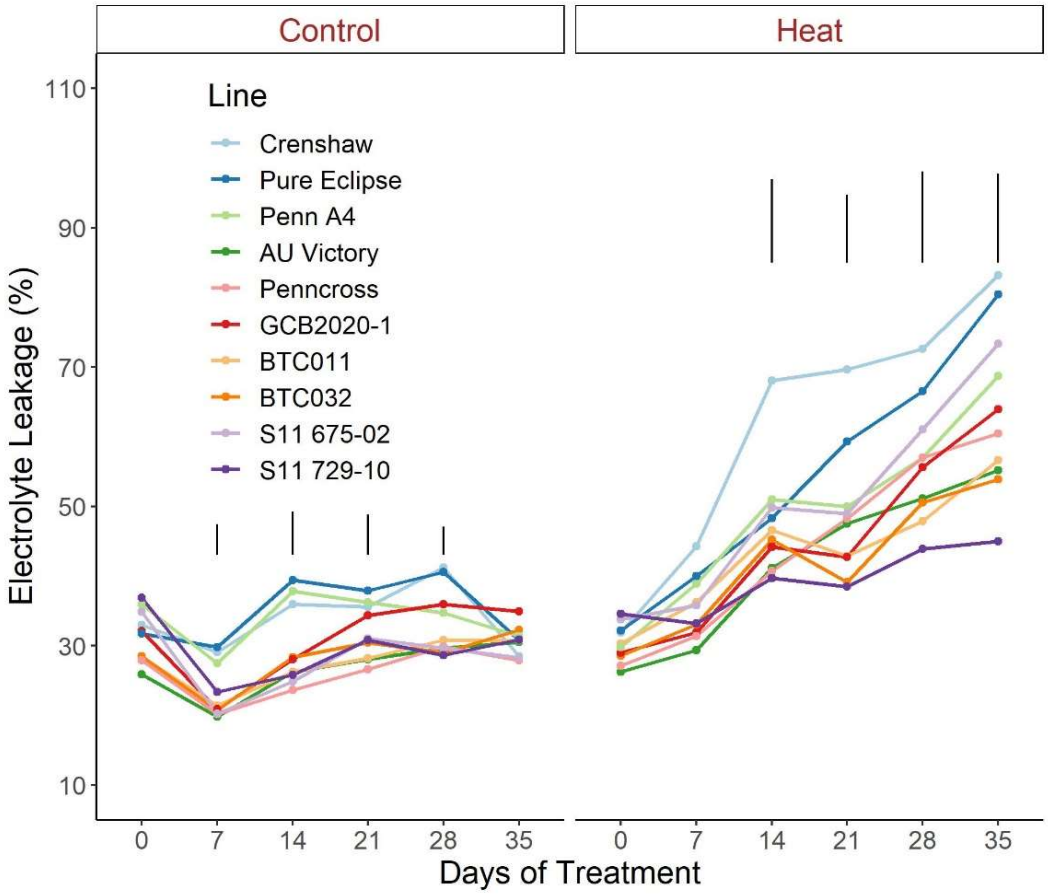

Figure 2.10 Change in electrolyte leakage for creeping bentgrass lines over time under control (20/15°C day/night) and heat stress (38/33°C day/night) conditions. Bars represent LSD values at $p = 0.05$ on days when significant differences among lines were found.

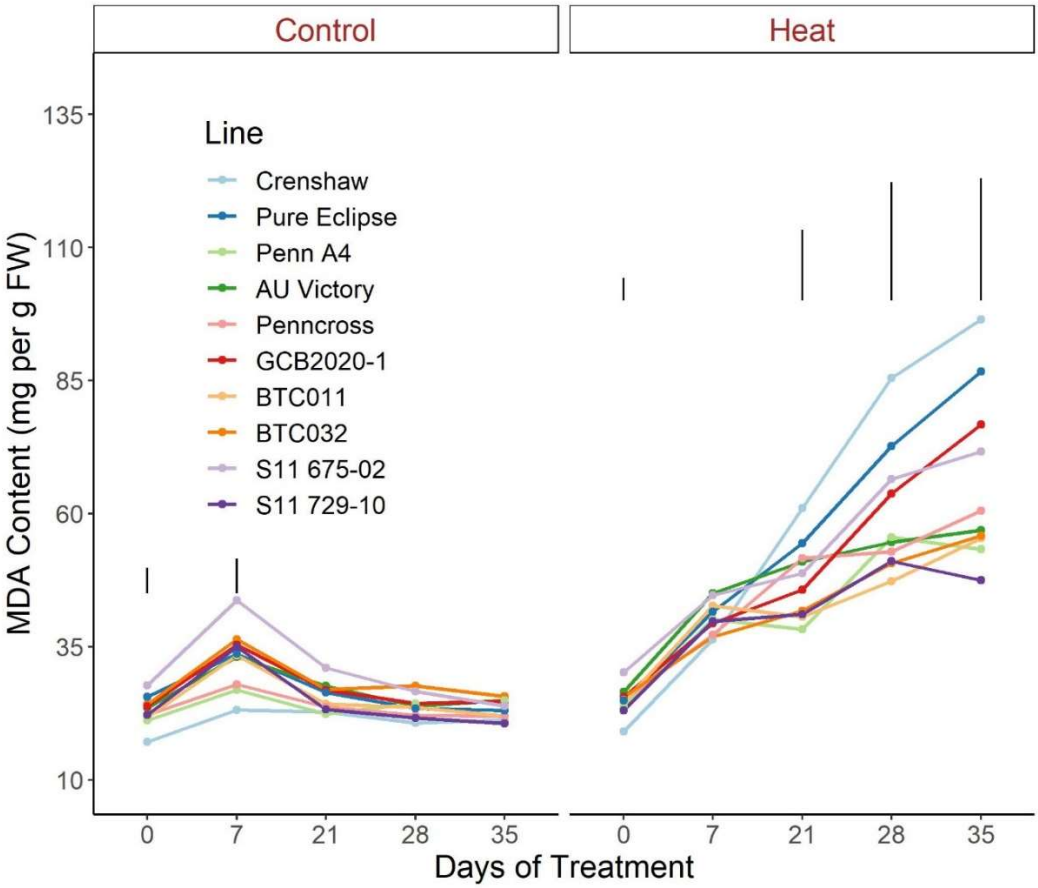

Figure 2.11 Change in MDA content for creeping bentgrass lines over time under control (20/15°C day/night) and heat stress (38/33°C day/night) conditions. Bars represent LSD values at $p = 0.05$ on days when significant differences among lines were found. FW, fresh weight.

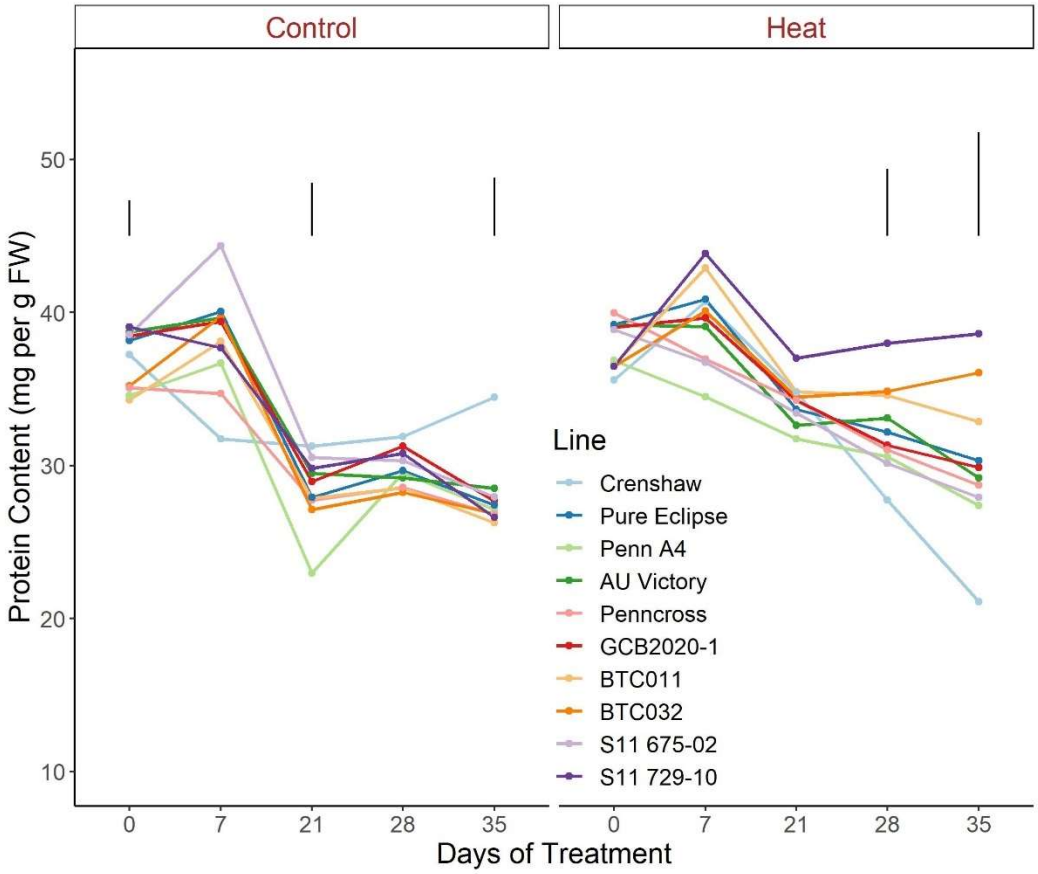

Figure 2.12 Change in total protein content for creeping bentgrass lines over time under control (20/15°C day/night) and heat stress (38/33°C day/night) conditions. Bars represent LSD values at $p = 0.05$ on days when significant differences among lines were found.

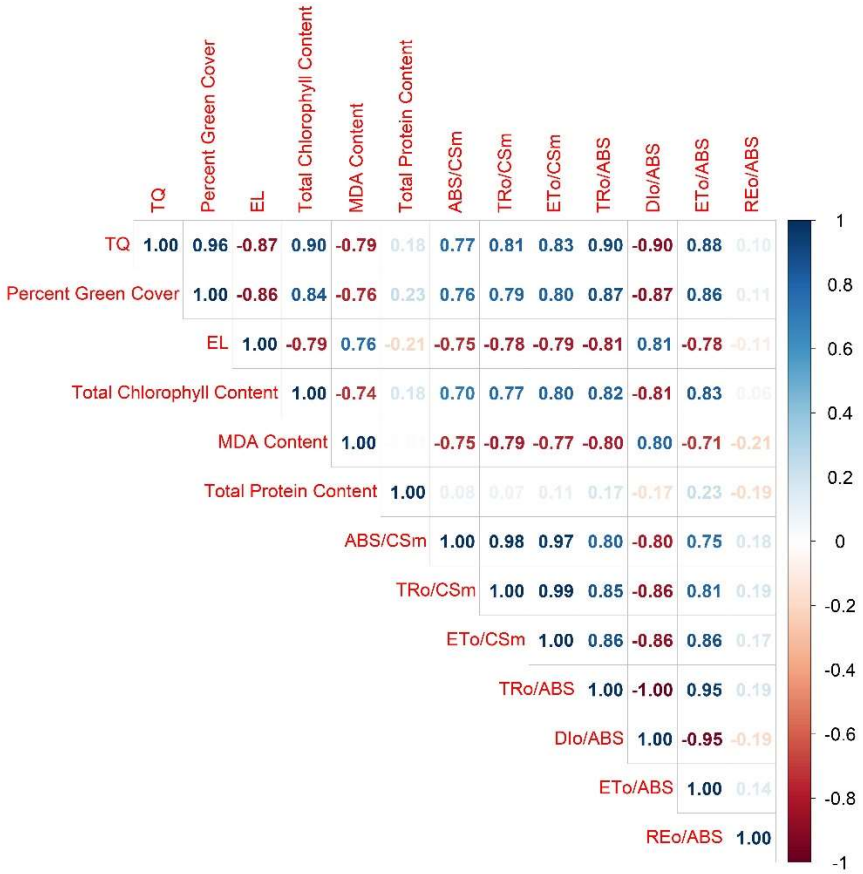

Figure 2.13 Correlation plot for different parameters of creeping bentgrass under control (20/15°C day/night) and heat stress (38/33°C day/night) conditions. Numbers indicate correlation coefficients. Color intensity is proportional to the correlation coefficients with blue indicating positive correlations and red representing negative correlations. Correlation coefficient values were left blank when not significant at $p = 0.05$.

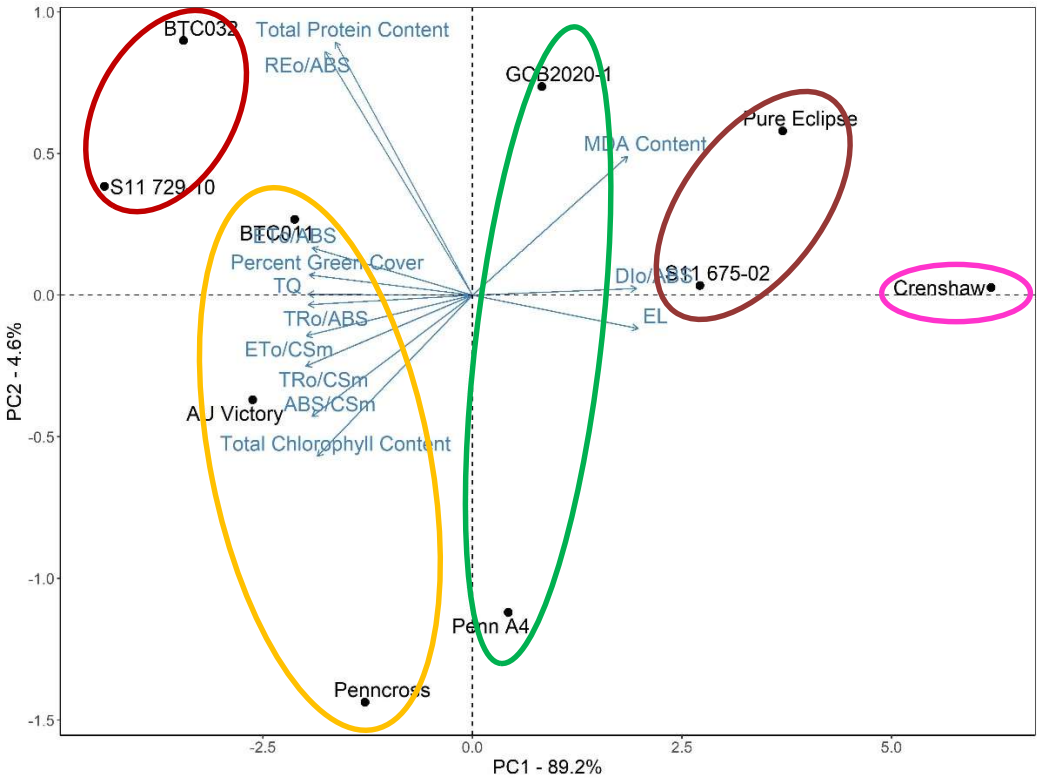

Figure 2.14 Principal component analysis for different parameters of creeping bentgrass at 35 d under heat stress (38/33°C day/night) condition. Principal component 1 is represented on the X axis while principal component 2 is represented on the Y axis. Vectors indicate the direction and contribution of each parameter to the overall distribution of various lines. Circles of different colors indicate different clusters.

Supplemental Materials

Table S2.1 Change in visual turf quality rating for creeping bentgrass lines over time under control (20/15°C day/night) and heat stress (38/33°C day/night) conditions

Lines	Control						Heat					
	0	**7**	**14**	**21**	**28**	**35**	**0**	**7**	**14**	**21**	**28**	**35**
Crenshaw	9.0	8.6	8.7	8.6	8.8	8.6	9.0	8.1	5.9 b	4.7 c	3.3 d	1.9 c
Pure Eclipse	9.0	9.0	9.0	9.0	9.0	9.0	9.0	8.1	7.6 a	6.7 ab	4.8 bc	2.9 bc
Penn A4	9.0	9.0	8.9	8.8	8.8	8.9	9.0	8.2	7.3 a	6.9 a	5.8 ab	4.6 a
AU Victory	9.0	9.0	9.0	9.0	8.9	8.9	9.0	8.3	7.7 a	7.2 a	6.4 a	4.8 a
Penncross	8.9	8.7	8.8	8.7	8.8	8.8	8.9	8.1	7.4 a	6.4 ab	5.4 abc	4.6 a
GCB2020-1	9.0	9.0	9.0	8.9	8.9	8.9	8.9	8.1	7.6 a	6.8 ab	5.6 ab	4.3 ab
BTC011	8.9	9.0	9.0	8.9	8.9	8.8	9.0	8.1	7.4 a	6.9 a	6.3 a	5.1 a
BTC032	9.0	9.0	9.0	8.9	8.8	8.7	9.0	8.0	7.1 a	6.8 ab	6.4 a	5.6 a
S11 675-02	9.0	9.0	9.0	8.7	8.6	8.7	9.0	8.0	7.4 a	6.0 b	4.3 cd	3.0 bc
S11 729-10	9.0	9.0	9.0	9.0	9.0	8.9	9.0	8.1	7.6 a	6.9 a	6.1 a	5.8 a
LSD	ns	ns	ns	ns	ns	ns	ns	ns	0.59	0.91	1.2	1.5

Note: values followed by a common lowercase letter within each column indicate no significant difference among various lines at $p = 0.05$; ns, not significant

Table S2.2 Change in green cover (%) for creeping bentgrass lines over time under control (20/15°C day/night) and heat stress (38/33°C day/night) conditions

Lines	Control						Heat					
	0	**7**	**14**	**21**	**28**	**35**	**0**	**7**	**14**	**21**	**28**	**35**
Crenshaw	98.0	96.3 bc	96.0	95.0	95.0 c	95.5	96.7 b	93.4	57.6 b	42.8 c	24.9 d	3.8 d
Pure Eclipse	98.1	95.4 c	96.1	96.5	97.3 ab	97.9	98.4 a	95.9	89.1 a	76.1 ab	39.3 bcd	9.6 cd
Penn A4	98.3	98.0 ab	96.6	96.1	96.4 bc	97.4	97.5 ab	95.7	87.0 a	79.3 ab	57.4 abc	32.4 bc
AU Victory	98.9	98.2 a	96.9	96.1	96.5 bc	96.9	98.1 a	96.2	89.3 a	83.2 a	65.8 a	48.5 ab
Penncross	97.9	96.8 abc	96.8	95.9	96.7 b	96.7	96.7 b	95.9	87.9 a	77.9 ab	61.1 ab	47.2 ab
GCB2020-1	98.6	97.9 ab	96.5	96.6	96.9 ab	97.0	97.8 a	96.5	91.1 a	85.5 a	59.2 ab	32.6 bc
BTC011	96.7	97.9 ab	97.2	96.6	96.2 bc	96.1	97.8 a	95.7	86.5 a	84.5 a	73.9 a	53.7 ab
BTC032	98.1	98.5 a	97.8	96.6	96.6 bc	96.3	97.7 ab	95.1	89.8 a	81.9 a	72.6 a	67.6 a
S11 675-02	97.1	98.1 a	96.8	95.9	95.9 bc	96.5	97.5 ab	94.8	82.2 a	64.0 b	35.2 cd	12.4 cd
S11 729-10	98.3	98.4 a	97.2	97.6	98.4 a	97.4	98.4 a	96.5	90.9 a	81.2 a	63.3 a	58.0 ab
LSD	ns	1.7	ns	ns	1.7	ns	1.0	ns	10.8	17.1	23.2	27.7

Note: values followed by a common lowercase letter within each column indicate no significant difference among various lines at $p = 0.05$; ns, not significant

Table S2.3 Change in total chlorophyll content (mg per g DW) for creeping bentgrass lines over time under control (20/15°C day/night) and heat stress (38/33°C day/night) conditions

Lines	Control						Heat					
	0	**7**	**14**	**21**	**28**	**35**	**0**	**7**	**14**	**21**	**28**	**35**
Crenshaw	19.6 abc	20.0 ab	17.2	17.7 bcd	16.2	16.7	17.0	18.8 ab	7.5 d	6.1 c	4.7 d	3.4 f
Pure Eclipse	19.7 abc	20.4 a	18.2	20.2 a	17.7	17.7	18.9	17.8 bcd	13.7 a	11.5 a	6.2 bcd	4.5 ef
Penn A4	20.4 a	20.3 a	18.1	17.9 bcd	16.2	16.6	17.5	18.3 abc	13.1 ab	12.3 a	7.7 abcd	6.0 cd
AU Victory	19.4 abc	19.2 abc	17.3	18.8 abc	15.2	15.5	17.2	17.3 cd	12.9 abc	10.4 ab	7.6 abcd	6.9 abc
Penncross	18.1 bcd	18.8 bc	16.1	16.8 d	15.6	16.5	17.5	19.5 a	13.2 ab	10.5 ab	7.5 abcd	7.9 ab
GCB2020-1	19.2 abc	19.7 abc	18.2	19.4 ab	14.1	16.4	18.3	16.5 d	12.2 abc	11.1 a	8.6 ab	5.0 de
BTC011	17.9 cd	18.9 bc	17.7	18.5 abcd	16.4	16.6	16.3	16.5 d	12.3 abc	11.7 a	8.2 abc	6.6 bc
BTC032	19.9 ab	19.0 bc	17.7	17.3 cd	15.5	17.0	16.4	17.5 bcd	11.0 bc	11.0 a	7.8 abc	6.7 bc
S11 675-02	19.8 ab	20.3 a	18.2	18.0 bcd	16.8	17.5	18.7	16.4 d	10.3 c	8.4 bc	5.2 cd	4.0 ef
S11 729-10	17.1 d	18.5 c	17.5	17.5 bcd	16.6	16.4	17.8	16.8 d	12.9 abc	12.3 a	9.7 a	8.2 a
LSD	1.9	1.3	ns	2.0	ns	ns	ns	1.4	2.7	2.6	ns	1.4

Note: values followed by a common lowercase letter within each column indicate no significant difference among various lines at $p = 0.05$; ns, not significant

Table S2.4 Change in TRo/ABS for creeping bentgrass lines over time under control (20/15°C day/night) and heat stress (38/33°C day/night) conditions

Lines	Control						Heat					
	0	**7**	**14**	**21**	**28**	**35**	**0**	**7**	**14**	**21**	**28**	**35**
Crenshaw	0.82	0.818 ab	0.82	0.81	0.81	0.81	0.81	0.78	0.68 b	0.658 b	0.588 c	0.41 d
Pure Eclipse	0.82	0.815 abc	0.81	0.81	0.81	0.81	0.82	0.77	0.75 a	0.718 a	0.633 abc	0.52 cd
Penn A4	0.81	0.823 a	0.81	0.81	0.81	0.81	0.82	0.78	0.75 a	0.730 a	0.680 ab	0.57 abc
AU Victory	0.82	0.813 abc	0.82	0.81	0.81	0.81	0.82	0.79	0.75 a	0.743 a	0.700 a	0.68 a
Penncross	0.82	0.82 ab	0.82	0.81	0.81	0.80	0.82	0.78	0.74 a	0.713 a	0.610 bc	0.62 abc
GCB2020-1	0.83	0.82 ab	0.82	0.81	0.80	0.81	0.82	0.77	0.74 a	0.733 a	0.675 ab	0.56 bc
BTC011	0.81	0.805 c	0.82	0.81	0.80	0.81	0.81	0.76	0.74 a	0.710 a	0.685 ab	0.64 ab
BTC032	0.81	0.805 c	0.81	0.80	0.80	0.81	0.82	0.76	0.75 a	0.735 a	0.713 a	0.65 ab
S11 675-02	0.81	0.810 bc	0.81	0.81	0.81	0.81	0.82	0.75	0.73 a	0.700 ab	0.593 c	0.55 bc
S11 729-10	0.82	0.810 bc	0.82	0.80	0.81	0.81	0.81	0.75	0.74 a	0.703 a	0.690 ab	0.68 a
LSD	ns	0.011	ns	ns	ns	ns	ns	ns	0.027	0.044	0.082	0.11

Note: values followed by a common lowercase letter within each column indicate no significant difference among various lines at $p = 0.05$; ns, not significant

Table S2.5 Change in ETo/ABS for creeping bentgrass lines over time under control (20/15°C day/night) and heat stress (38/33°C day/night) conditions

Lines	Control						Heat					
	0	**7**	**14**	**21**	**28**	**35**	**0**	**7**	**14**	**21**	**28**	**35**
Crenshaw	0.535 ab	0.538 abc	0.568 a	0.530 ab	0.535 a	0.530 ab	0.540 abc	0.488 abc	0.430 d	0.393 e	0.340 cd	0.225 d
Pure Eclipse	0.538 ab	0.543 abc	0.553 abcd	0.538 a	0.532 ab	0.523 abc	0.555 a	0.500 abc	0.490 ab	0.468 abc	0.385 abc	0.283 cd
Penn A4	0.540 ab	0.560 a	0.560 abc	0.520 ab	0.530 abc	0.533 a	0.548 ab	0.508 ab	0.503 ab	0.473 ab	0.423 ab	0.323 bc
AU Victory	0.540 ab	0.545 ab	0.565 ab	0.523 ab	0.515 bcd	0.523 abc	0.555 a	0.513 a	0.503 ab	0.493 a	0.428 a	0.420 a
Penncross	0.525 bc	0.530 bc	0.553 abcd	0.520 ab	0.513 cd	0.513 c	0.545 ab	0.503 ab	0.480 abc	0.445 bcd	0.368 bcd	0.335 abc
GCB2020-1	0.548 a	0.548 ab	0.560 abc	0.525 ab	0.510 d	0.530 ab	0.553 a	0.508 ab	0.485 abc	0.480 ab	0.413 ab	0.343 abc
BTC011	0.510 c	0.538 abc	0.558 abc	0.523 ab	0.520 abcd	0.528 ab	0.530 bc	0.505 ab	0.505 a	0.463 abcd	0.423 ab	0.363 abc
BTC032	0.528 abc	0.520 c	0.550 bcd	0.515 b	0.508 d	0.518 bc	0.525 c	0.510 a	0.505 a	0.473 ab	0.440 a	0.393 ab
S11 675-02	0.530 abc	0.533 bc	0.548 cd	0.523 ab	0.518 abcd	0.528 ab	0.533 bc	0.483 bc	0.458 cd	0.433 cd	0.320 d	0.288 cd
S11 729-10	0.520 bc	0.528 bc	0.540 d	0.510 b	0.505 d	0.510 c	0.523 c	0.475 c	0.473 bc	0.430 d	0.425 ab	0.393 ab
LSD	0.022	0.023	0.017	0.021	0.018	0.015	0.020	0.027	0.032	0.036	0.059	0.088

Note: values followed by a common lowercase letter within each column indicate no significant difference among various lines at $p = 0.05$; ns, not significant

Table S2.6 Change in DIo/ABS for creeping bentgrass lines over time under control (20/15°C day/night) and heat stress (38/33°C day/night) conditions

Lines	Control						Heat					
	0	**7**	**14**	**21**	**28**	**35**	**0**	**7**	**14**	**21**	**28**	**35**
Crenshaw	0.18	0.186 bcd	0.18	0.19	0.20	0.19	0.19	0.23	0.32 a	0.343 a	0.414 a	0.595 a
Pure Eclipse	0.19	0.191 bcd	0.19	0.19	0.20	0.19	0.19	0.23	0.26 b	0.285 bc	0.369 abc	0.484 ab
Penn A4	0.19	0.183 d	0.19	0.20	0.20	0.19	0.19	0.23	0.25 b	0.271 bc	0.322 bc	0.434 bcd
AU Victory	0.19	0.192 bcd	0.19	0.19	0.19	0.20	0.18	0.21	0.25 b	0.260 c	0.300 c	0.322 e
Penncross	0.19	0.187 bcd	0.19	0.19	0.19	0.20	0.19	0.22	0.26 b	0.291 bc	0.390 ab	0.388 bcde
GCB2020-1	0.18	0.185 cd	0.19	0.20	0.20	0.19	0.18	0.23	0.27 b	0.270 bc	0.325 bc	0.438 bcd
BTC011	0.20	0.202 abc	0.19	0.20	0.20	0.19	0.19	0.24	0.26 b	0.291 bc	0.318 bc	0.369 cde
BTC032	0.20	0.210 a	0.19	0.20	0.20	0.19	0.19	0.23	0.26 b	0.267 bc	0.291 c	0.347 cde
S11 675-02	0.19	0.204 ab	0.19	0.20	0.20	0.19	0.19	0.25	0.27 b	0.304 ab	0.410 a	0.452 bc
S11 729-10	0.19	0.195 abcd	0.19	0.20	0.20	0.19	0.19	0.25	0.27 b	0.298 bc	0.312 bc	0.326 de
LSD	ns	0.018	ns	ns	ns	ns	ns	ns	0.026	0.044	0.082	0.11

Note: values followed by a common lowercase letter within each column indicate no significant difference among various lines at $p = 0.05$; ns, not significant

Table S2.7 Change in ABS/CSm for creeping bentgrass lines over time under control (20/15°C day/night) and heat stress (38/33°C day/night) conditions

Lines	Control						Heat					
	0	**7**	**14**	**21**	**28**	**35**	**0**	**7**	**14**	**21**	**28**	**35**
Crenshaw	2205.4 ab	2440.4	2650.8 ab	2437.8 abcd	2088.9 bc	1944.0 ab	2191.4 a	1921.9	1733.2 c	1419.1 b	1100.3 c	595.5 c
Pure Eclipse	2095.5 ab	2359.0	2639.8 ab	2527.2 ab	2244.3 ab	1951.2 ab	2093.7 ab	1827.3	2053.5 abc	1812.2 a	1231.5 bc	670.0 c
Penn A4	2136.5 ab	2360.1	2632.9 ab	2393.8 bcde	2068.6 c	1961.1 ab	1906.2 b	1892.8	2041.7 abc	1998.3 a	1603.2 ab	1059.1 ab
AU Victory	2224.7 ab	2313.5	2804.6 a	2591.8 a	2173.5 abc	1864.6 bc	2182.3 a	2081.3	2260.7 a	2080.8 a	1701.0 a	1145.3 ab
Penncross	2200.4 ab	2312.5	2672.2 ab	2351.8 cde	2132.5 bc	1861.6 bc	2150.5 a	1954.3	2157.6 ab	2099.3 a	1346.6 abc	1356.2 a
GCB2020-1	1973.6 b	2286.3	2682.2 ab	2278.2 de	2042.7 c	1931.5 ab	1885.8 b	1794.9	1845.8 bc	1889.4 a	1436.4 abc	911.0 bc
BTC011	2072.9 ab	2234.5	2508.6 b	2424.5 bcd	2154.6 bc	1733.5 c	2075.7 ab	1816.8	2096.4 ab	2007.6 a	1696.2 a	1224.7 ab
BTC032	2102.6	2254.0	2637.6 ab	2258.0 e	2071.3 bc	1819.5 bc	2021.2 ab	1822.6	1922.8 bc	2057.7 a	1658.9 a	1310.3 a
S11 675-02	2222.8 ab	2286.7	2680.8 ab	2403.5 bcde	2174.5 abc	2035.3 a	2210.2 a	1933.3	1871.4 bc	1766.6 ab	1075.8 c	838.7 bc
S11 729-10	2251.5 a	2355.6	2698.1 ab	2484.1 abc	2331.0 a	1919.4 ab	2157.7 a	1966.0	2070.0 ab	2005.8 a	1455.6 abc	1382.0 a
LSD	271.1	ns	236.6	162.1	174.7	143.1	238.7	ns	335.4	352.4	398.6	388.7

Note: values followed by a common lowercase letter within each column indicate no significant difference among various lines at $p = 0.05$; ns, not significant

Table S2.8 Change in TRo/CSm for creeping bentgrass lines over time under control (20/15°C day/night) and heat stress (38/33°C day/night) conditions

Lines	Control						Heat					
	0	**7**	**14**	**21**	**28**	**35**	**0**	**7**	**14**	**21**	**28**	**35**
Crenshaw	1797.9	1984.5	2167.6	1967.1 abcd	1684.2	1570.6 ab	1779.3	1487.6	1191.4 c	976.0 c	672.1 cd	280.6 f
Pure Eclipse	1706.7	1909.7	2128.9	2049.2 ab	1808.9	1579.7 ab	1701.7	1410.0	1532.1 ab	1305.8 ab	815.4 bcd	386.2 ef
Penn A4	1736.8	1926.8	2134.5	1923.7 bcde	1663.5	1580.1 ab	1545.0	1473.4	1525.7 ab	1461.4 ab	1103.5 ab	679.2 bcd
AU Victory	1807.1	1870.6	2279.1	2100.0 a	1750.0	1496.8 bc	1781.7	1646.4	1700.0 a	1550.9 a	1203.1 a	949.2 a
Penncross	1788.9	1879.7	2168.0	1901.4 cde	1721.6	1488.8 bc	1734.6	1520.0	1596.4 ab	1505.4 ab	870.7 abcd	869.0 ab
GCB2020-1	1611.7	1866.5	2178.1	1840.2 de	1641.0	1563.6 ab	1541.2	1392.0	1367.2 bc	1396.1 ab	999.4 abc	585.0 cde
BTC011	1663.9	1785.0	2035.4	1946.0 bcd	1722.0	1406.5 c	1676.5	1386.7	1545.5 ab	1440.1 ab	1167.1 a	835.6 abc
BTC032	1695.0	1783.6	2129.0	1802.7 e	1654.0	1472.1 bc	1632.3	1405.8	1435.3 abc	1513.0 ab	1177.7 a	937.2 ab
S11 675-02	1803.6	1823.6	2168.2	1935.1 bcde	1743.6	1644.4 a	1796.8	1468.2	1374.6 bc	1256.3 bc	656.7 d	513.6 def
S11 729-10	1828.0	1890.0	2190.9	1987.2 abc	1870.7	1548.4 ab	1747.8	1484.0	1517.5 ab	1424.1 ab	1036.8 ab	1024.4 a
LSD	ns	ns	ns	137.2	ns	120.6	ns	ns	274.1	290.8	336.9	265.3

Note: values followed by a common lowercase letter within each column indicate no significant difference among various lines at $p = 0.05$; ns, not significant

Table S2.9 Change in ETo/CSm for creeping bentgrass lines over time under control (20/15°C day/night) and heat stress (38/33°C day/night) conditions

Lines	Control						Heat					
	0	**7**	**14**	**21**	**28**	**35**	**0**	**7**	**14**	**21**	**28**	**35**
Crenshaw	1182.8	1307.5	1506.3	1289.8 abc	1122.7	1030.8 abc	1180.1	943.4	765.2 c	592.5 c	386.1 c	153.7 f
Pure Eclipse	1121.9	1279.8	1460.1	1363.0 a	1188.5	1019.1 abcd	1151.5	914.4	1014.5 ab	855.4 ab	499.1 bc	213.4 ef
Penn A4	1151.4	1309.0	1472.4	1243.6 cd	1095.9	1047.2 ab	1047.0	966.0	1025.3 ab	950.1 ab	683.7 ab	395.1 bcd
AU Victory	1200.0	1258.9	1588.6	1350.8 ab	1119.1	973.9 bcde	1207.9	1070.9	1137.6 a	1031.6 a	730.5 a	592.8 a
Penncross	1158.8	1220.0	1468.2	1221.9 cd	1096.0	961.3 cde	1172.1	989.5	1045.1 ab	944.8 ab	520.5 abc	470.4 abc
GCB2020-1	1069.7	1244.5	1504.3	1199.3 cd	1045.8	1031.1 abc	1039.5	918.1	904.0 bc	912.6 ab	612.3 ab	355.5 cde
BTC011	1053.8	1193.6	1403.1	1271.3 abcd	1129.4	916.0 e	1097.5	917.6	1053.1 ab	942.6 ab	726.2 a	476.9 abc
BTC032	1101.1	1177.3	1448.1	1167.9 d	1055.7	942.5 de	1058.6	937.5	964.1 ab	977.4 a	729.1 a	560.4 ab
S11 675-02	1168.3	1213.9	1469.5	1253.6 bcd	1124.7	1076.9 a	1169.2	943.0	877.4 bc	786.0 b	363.5 c	262.1 def
S11 729-10	1162.0	1243.9	1455.1	1263.9 abcd	1172.2	976.5 bcde	1118.3	941.8	977.1 ab	882.7 ab	640.8 ab	596.9 a
LSD	ns	ns	ns	103.6	ns	84.7	ns	ns	193.3	188.0	211.0	180.0

Note: values followed by a common lowercase letter within each column indicate no significant difference among various lines at $p = 0.05$; ns, not significant

Table S2.10 Change in electrolyte leakage (%) for creeping bentgrass lines over time under control (20/15°C day/night) and heat stress (38/33°C day/night) conditions

Lines	Control						Heat					
	0	**7**	**14**	**21**	**28**	**35**	**0**	**7**	**14**	**21**	**28**	**35**
Crenshaw	33.0	29.1 a	35.9 a	35.6 abc	41.2 a	30.5	31.9	44.3	68.0 a	69.7 a	72.6 a	83.2 a
Pure Eclipse	31.7	29.8 a	39.4 a	37.9 a	40.6 a	35.8	32.2	40.0	48.3 b	59.3 b	66.5 ab	80.5 ab
Penn A4	36.0	27.5 ab	37.8 a	36.3 ab	34.7 bc	33.4	29.8	38.9	51.0 b	50.0 bc	57.0 bcd	68.7 bcd
AU Victory	25.9	19.8 c	26.3 b	28.0 d	29.7 d	30.5	26.3	29.4	41.1 b	47.5 cde	51.1 cd	55.2 ef
Penncross	27.9	20.2 c	23.7 b	26.6 d	29.9 d	27.9	27.1	31.4	40.7 b	48.2 cd	57.0 bcd	60.5 de
GCB2020-1	32.1	20.9 c	28.1 b	34.4 abc	35.9 b	34.9	29.0	31.9	44.2 b	42.7 cde	55.6 bcd	63.9 cde
BTC011	28.4	21.4 c	26.3 b	28.2 d	30.8 cd	30.7	30.3	36.2	46.6 b	42.9 cde	47.9 d	56.7 def
BTC032	28.5	20.8 c	28.3 b	30.4 cd	29.0 d	32.2	28.6	33.1	45.2 b	39.2 de	50.5 cd	53.9 ef
S11 675-02	33.6	20.3 c	24.9 b	31.0 bcd	29.7 d	28.3	33.8	35.8	49.8 b	49.0 c	61.0 abc	73.3 abc
S11 729-10	36.9	23.3 bc	25.8 b	30.8 bcd	28.7 d	30.9	34.6	33.2	39.7 b	38.5 e	43.9 d	45.0 f
LSD	ns	4.5	6.2	5.8	4.0	ns	ns	ns	12.0	9.7	13.1	12.8

Note: values followed by a common lowercase letter within each column indicate no significant difference among various lines at $p = 0.05$; ns, not significant

Table S2.11 Change in MDA content (mg per g FW) for creeping bentgrass lines over time under control (20/15°C day/night) and heat stress (38/33°C day/night) conditions

Lines	Control					Heat				
	0	**7**	**21**	**28**	**35**	**0**	**7**	**21**	**28**	**35**
Crenshaw	17.1 c	23.2 e	22.8	20.7	21.2	19.1 c	36.4	61.0 a	85.4 a	96.5 a
Pure Eclipse	25.6 ab	33.7 bcd	26.4	23.4	23.0	24.9 b	41.6	54.5 ab	72.7 ab	86.7 ab
Penn A4	21.1 bc	26.9 de	22.3	24.4	24.9	23.8 b	40.2	38.3 d	55.6 bc	53.3 de
AU Victory	23.5 ab	33.1 bcd	27.7	23.9	24.9	26.5 ab	45.0	51.0 abcd	54.7 bc	56.9 cde
Penncross	22.2 b	28.0 cde	23.7	22.1	22.0	25.0 b	37.3	51.7 abc	52.8 bc	60.5 cde
GCB2020-1	23.8 ab	35.4 b	26.9	24.4	24.7	25.5 b	39.4	45.7 bcd	63.7 abc	76.8 abc
BTC011	21.7 bc	33.4 bcd	24.3	23.6	22.0	24.6 b	42.7	40.6 cd	47.3 c	55.4 cde
BTC032	24.2 ab	36.4 b	27.0	27.6	25.7	25.6 b	36.9	41.8 bcd	50.7 bc	55.8 cde
S11 675-02	27.8 a	43.7 a	31.0	26.6	23.9	30.2 a	44.7	48.8 abcd	66.5 abc	71.6 bcd
S11 729-10	22.2 b	35.0 bc	23.2	21.7	20.6	23.1 bc	39.8	41.1 cd	51.1 bc	47.5 e
LSD	4.8	6.5	ns	ns	ns	4.2	ns	13.3	22.2	23.0

Note: values followed by a common lowercase letter within each column indicate no significant difference among various lines at $p = 0.05$; ns, not significant

Table S2.12 Change in protein content (mg per g FW) for creeping bentgrass lines over time under control (20/15°C day/night) and heat stress (38/33°C day/night) conditions

Lines	Control					Heat				
	0	**7**	**21**	**28**	**35**	**0**	**7**	**21**	**28**	**35**
Crenshaw	37.3 ab	31.8	31.3 a	31.9	34.5 a	35.6	40.7	34.8	27.8 d	21.1 d
Pure Eclipse	38.2 a	40.1	27.9 ab	29.7	27.4 b	39.2	40.9	33.7	32.2 bc	30.3 bc
Penn A4	34.6 c	36.7	23.0 c	29.5	27.1 b	36.9	34.5	31.7	30.6 bcd	27.4 cd
AU Victory	38.7 a	39.7	29.5 ab	29.2	28.5 b	39.2	39.1	32.6	33.1 bc	29.2 c
Penncross	35.1 bc	34.7	27.8 b	28.6	26.8 b	40.0	37.0	34.3	31.0 bcd	28.7 c
GCB2020-1	38.5 a	39.4	29.0 ab	31.3	27.7 b	39.0	39.7	34.3	31.3 bcd	29.9 bc
BTC011	34.3 c	38.1	27.9 ab	28.5	26.3 b	36.6	42.9	34.8	34.6 ab	32.9 abc
BTC032	35.2 bc	39.8	27.1 b	28.3	26.9 b	36.5	40.1	34.5	34.9 ab	36.1 ab
S11 675-02	38.6 a	44.4	30.5 ab	30.3	28.0 b	38.9	36.8	33.4	30.2 cd	27.9 c
S11 729-10	39.1 a	37.7	29.8 ab	30.8	26.6 b	36.5	43.9	37.0	38.0 a	38.6 a
LSD	2.3	ns	3.5	ns	3.8	ns	ns	ns	4.4	6.8

Note: values followed by a common lowercase letter within each column indicate no significant difference among various lines at $p = 0.05$; ns, not significant

CHAPTER 3

PROTEOLYSIS ACTIVITIES IN CREEPING BENTGRASS LEAVES SUBJECTED TO HEAT STRESS[1]

[1] Q. Fan and D. Jespersen. Submitted to *Physiologia Plantarum*, 08/30/2024.

Abstract

Enhanced protein degradation, typically conducted by the coordinated action of proteases and the ubiquitin-proteasome system (UPS), is a common response to heat stress. It works by removing nonfunctional or damaged proteins to maintain normal cell function and to allow for the remobilization of nutrients, enabling plants to respond rapidly to environmental perturbation. Despite its crucial role, there has been limited research addressing proteolysis activities from both proteases and the UPS in grasses exposed to heat stress. This project aims to quantify activities of proteases and the UPS in different lines of creeping bentgrass (*Agrostis stolonifera* L.), a cool-season turfgrass that's prized for its functional and aesthetic qualities and detect changes in expression levels of known proteases and the UPS genes. Previously identified heat-tolerant and -sensitive creeping bentgrass lines were selected for this study. They were exposed to either control (20/15°C day/night) or heat stress (38/33°C day/night) treatments for 35 d. Protein degradation was enhanced under heat as demonstrated by significant increases in protease activity and the UPS activity over time. A more heat-tolerant line, S11 729-10, maintained lower activities of both protease and the UPS, contributing to its higher protein contents, and thereby greater thermotolerance. Additionally, cysteine protease was more heat-inducible than serine protease during the midpoint phase of leaf senescence. This is the first time that the roles of protease activity and the UPS activity in heat stress were simultaneously analyzed in a perennial grass species. Such information will broaden the understanding of how protein degradation is regulated in response to heat stress, providing a deeper insight into thermotolerance mechanisms in creeping bentgrass.

1. Introduction

Protein metabolism, and ultimately the levels of specific proteins within a cell, are controlled by the balance between protein synthesis and protein degradation. Degradation of proteins is typically achieved via two proteolytic pathways, namely, proteases and the ubiquitin-proteasome system (UPS). Proteases are divided into families of serine proteases, aspartic proteases, cysteine proteases, and metalloproteases. They are mainly responsible for the breakdown of proteins localized inside organelles by decomposing polypeptide bonds in targeted proteins [66]. The UPS utilizes the protein – ubiquitin, as the recognition signal and is a rapid regulatory mechanism for selective degradation of proteins primarily in the cytosol and nucleus [107, 114]. Ubiquitin units are attached to substrate proteins through three enzymes, namely, ubiquitin-activating enzyme (E1), ubiquitin-conjugating enzyme (E2), and ubiquitin ligase (E3). The resultant polyubiquitinated proteins are then recognized and degraded by the 26S proteasome with the release of intact ubiquitin [109]. Together with proteases, the UPS is employed by plants to efficiently and effectively control the abundance of numerous cellular proteins and plays a significant role in plant growth and development, and responses to abiotic stress [114, 181, 182].

Heat stress is a significant issue in many areas with the ever-increasing trend of climate change [4], creating challenging environmental conditions for the growth of plants, particularly cool-season plants. A series of damages occur in plants as temperature increases above optimal, such as photosynthetic inhibition as a consequence of chlorophyll breakdown and reduced photosystem II (PSII) activity, and oxidative stress due to overproduction of reactive oxygen species (ROS) [3]. When not sufficiently scavenged, ROS can damage many essential molecules such as lipids, resulting in lipid peroxidation and decreased integrity of cell membranes [144]. In

addition to decreased photosynthesis and oxidative damage, interruption in protein metabolism is another common symptom under heat stress.

Proteins may become misfolded or denatured due to direct exposure to heat stress or oxidized due to excess ROS induced by heat stress [58]. These damaged proteins need to be repaired or degraded to be removed due to their structural instability. Otherwise, they tend to aggregate and precipitate, interfering with normal cellular functions and potentially leading to cell aging and even death [183]. In principle, molecular chaperones should have the first opportunity to fix damaged proteins by refolding them into functional conformation; When damage is beyond repair, these abnormal proteins will be targeted for degradation by various proteolytic machineries like proteases and the UPS [62]. The timely degradation of damaged proteins enables recycling of resources for new protein synthesis and is highly associated with many critical cellular activities like aforementioned photosynthesis and ROS defense, as proteins are the major driving force behind physiological responses and performance in plants. As the core part of PSII, D1 metabolism plays a key role in PSII repair [28]. Generally, damaged D1 proteins are degraded through the cooperation of Deg, a serine protease, and FtsH, a metalloprotease [59]. Then a newly synthesized D1 protein is reassembled into PSII, recovering photosynthetic activity. Therefore, minimizing the interruption in D1 protein metabolism is typically associated with greater thermotolerance [28]. In the case of oxidative stress, oxidized proteins undergo proteolysis to be removed. Then the resultant amino acids will be reused for protein biosynthesis and regenerate active proteins to defend against ROS [60]. Unlike normal conditions where there is a balance of proteins constantly being degraded and synthesized, degradation of proteins is typically accelerated relative to protein synthesis under heat stress [63, 176]. It implies that proteins being degraded can't be replaced by newly synthesized proteins in time. This will lead to decreases in total protein contents, eventually

resulting in disfunction in plant cells and impacting normal metabolic activities [63, 176]. Enhanced protease activities responding to heat stress have been documented in several plant species, such as *Agrostis scabra*, creeping bentgrass as well as wheat (*Triticum aestivum*) [71, 74, 89]. In the case of creeping bentgrass, protease activities increased under heat stress; However, the application of protease inhibitors mitigated the increase while better maintaining physiological performance, contributing to suppressed proteolysis and delayed heat-induced leaf senescence [74]. Similarly, in the case of wheat seedlings, while heat stress caused increases in protease activity, more heat-tolerant genotypes generally possessed weaker protease activities, resulting in slower proteolytic degradation and in turn higher protein contents and enhanced overall performance [71]. These studies further point out that protease activity could be used as an efficient biochemical marker to assess relative thermotolerance of genotypes. Comparatively, studies on quantifying heat-induced UPS activity are largely lacking, although such activity has been found in tobacco (*Nicotiana tabacum* L.) cells [110]. Other studies investigated the expression of UPS genes under heat stress and reported differential regulation of a few key components, such as E3 and 26S proteasome, while not measuring the UPS activity directly [109, 182, 184, 185]. All suggest the significant role the UPS pathway could play in heat-induced interruption in protein metabolism. However, despite the importance of protein degradation, to our knowledge, there are no reports detailing the underlying molecular mechanisms against heat stress involving both protease activity and the UPS activity in any grass species.

Creeping bentgrass is an economically important cool-season turfgrass with excellent tolerance to low mowing height, and quick recovery from traffic [140]. It has been widely used on high-value and high-input turf areas like golf courses. However, due to a lack of heat tolerance, creeping bentgarss is actively being displaced by climate change, with a 35% and 22% decrease

in acreage on golf courses in the Southeastern and Transition regions of the U.S. between 2015 and 2021 [186]. A collection of creeping bentgrass germplasm, including commercial cultivars and experimental breeding lines, were previously screened for heat tolerance, with differential accumulations of total proteins being detected in association with varying levels of tolerance [64]. However, the specific pathways responsible for protein degradation, a key contributor to changes in protein abundance, remains to be documented. A more complete understanding of the mechanisms conferring improved thermotolerance will facilitate the more efficient development of lines into elite cultivars. Hence, this project aimed to explore the underlying molecular mechanisms responsible for protein degradation by quantifying proteolysis activities and detecting changes in expression levels of known proteases and UPS genes. This would enable a better understanding of the pathways responsible for heat-induced protein degradation as well as the associated differences between contrasting creeping bentgrass lines. Such information would provide further insights into the thermotolerance mechanisms and be an important step to the development of elite creeping bentgrass cultivars with exceptional resilience to climate change.

2. Materials and Methods

2.1. Experimental description

Five creeping bentgrass lines with differential heat tolerance levels were selected for this study, namely, heat-tolerant ‘S11 729-10’ and ‘BTC032’, heat-sensitive ‘S11 675-02’ and ‘Crenshaw’, plus ‘AU Victory’ with intermediate heat tolerance [64]. Among these five lines, ‘AU Victory’ and ‘Crenshaw’ are commercial cultivars while the rest are experimental lines. For each line, 6-cm-diameter plugs were established in plastic pots (10.5 cm long, 10.5 cm wide and 12.5 cm deep) filled with a mixture of 50% sand and 50% calcined clay (Turface; Profile Products LLC, Buffalo Grove, IL) for ten weeks in a greenhouse [~23/~15°C (light/dark period temperatures) and

70% relative humidity] before being transferred to controlled environmental growth chambers (CG-72; Conviron, Winnipeg, Canada). Plants were allowed one-week acclimation inside the growth chambers under conditions of 20/15°C (day/night), 70% humidity and 14-h photoperiod with 600 μmol m^{-2} s^{-1} photosynthetically active radiation at the canopy level before the onset of different temperature treatments. Plants were well-watered and fertilized weekly with a 24-8-16 (N-P-K) fertilizer (Scotts Miracle-Gro; Marysville, OH) at the rate of 9.8 g N m^{-2} during establishment in the greenhouse as well as during the treatment period inside growth chambers. Applications of insecticide and fungicide were made as needed for disease control. Plants of each line were exposed to either heat stress (38/33°C day/night) or control (20/15°C day/night) conditions for 35 d after treatments began, with other conditions remaining the same.

2.2. Measurements

Weekly measurements included visual turf quality ratings (TQ), percent green cover, photochemical efficiency (Fv/Fm), electrolyte leakage (EL), total protein content and protease activity. Biweekly measurements were performed for the UPS activity. In addition, at 21 d and 35 d, corresponding to the midpoint and late stages of heat-induced leaf senescence, respectively, gene expression for cysteine protease, serine protease and E3 was analyzed using real-time quantitative reverse transcription polymerase chain reaction (qRT-PCR). These genes were selected for analysis because serine proteases are among the most well-studied families of proteases in plants with documented involvement in heat stress, while cysteine proteases consistently appear as the most abundant class of proteases upregulated in response to stress-induced senescence in various plants [82-84]. E3 was also analyzed as it determines the substrate specificity in the UPS and is more commonly reported to be heat-inducible compared to other components of the UPS [109, 114].

2.2.1. Physiological traits

Turf quality ratings and percent green cover represent overall turf performance. Turf quality scores were assessed based on color, density and uniformity with 1 representing totally dead grass, 9 for completely healthy grass, and 6 being the minimum acceptable quality [160]. Percent green cover was acquired through images taken with a digital camera (Canon G9X; Canon, Tokyo, Japan) using a lightbox to ensure uniform lighting, and processed via ImageJ v.1.46 [161].

Photochemical efficiency reflects the health status of photosynthetic machinery. Plants were dark adapted overnight (10 h) prior to performing the measurements via a chlorophyll fluorometer (OSP 5+; Opti-sciences, Hudson, NH). At least two fluorometry measurements were taken on fully expanded leaves for each replicate. Electrolyte leakage (EL) serves as an indicator of cell membrane stability. Around 0.1 g fresh leaves were placed in a tube containing 35 mL deionized water. After agitating tubes on a shaker for 16 h, initial conductivity was recorded through a conductivity meter (Radiometer, Copenhagen, Denmark). Next, the samples were autoclaved at 120 °C for 20 min, followed by incubation for another 16 h on a shaker, after which the total conductivity was read. EL was then calculated as the percentage of initial conductivity compared to total conductivity [187].

Change in protein abundance was measured to represent disruption in protein accumulation. Analyses were performed with a microplate reader (Epoch 2 microplate reader, BioTek, Winooski, VT). Approximately 50 mg fresh leaves were added into 1.1 mL 50 mM sodium phosphate buffer (pH 7.0 with 1 mM ethylenediaminetetraacetic acid). Supernatants were collected after homogenization and centrifugation. Then total protein content was quantified at 595 nm with Bradford dye reagent and a bovine serum albumin standard [164].

2.2.2. Measurement of total protease activity

Protease activity was quantified based on the rate of release of tyrosine using casein as substrate[188]. Specifically, ~200 mg fresh leaf tissues were added into 2 mL 50 mM sodium phosphate buffer (pH 7.5) for the extraction of crude proteases. Following homogenization and centrifugation, supernatants were collected. Then a reaction mixture containing 0.5 mL 0.65% casein and 0.8 mL supernatant was incubated at 37 °C for 10 minutes. The reaction was terminated by the addition of 4 mL 110 mM trichloroacetic acid. Non-hydrolyzed casein was filtered with filter paper (Grade 42, 90 mm, Whatman International Ltd., Maidstone, England). Next, 2 mL of the filtrate was mixed with 5 mL 500 mM Na_2CO_3 and 1 mL 2N Folin-Ciocalteu reagent, followed by incubation at 37°C for 30 minutes. The absorbance of the resultant blue-color complex was measured at 660 nm via a microplate reader (Epoch 2 microplate reader, BioTek, Winooski, VT) along with a tyrosine standard.

2.2.3. Measurement of the UPS activity

The UPS activity was determined spectrofluorometrically based on the rate of release of amino-methyl-coumarin (AMC) using a fluorogenic peptide Suc-LLVY-AMC (Calbiochem) as the substrate [189]. In brief, ~20 mg fresh leaf tissues were homogenized in 5 mL extraction buffer (50 mM Hepes-KOH, pH 7.2, 2 mM ATP, 2 mM DTT, 250 mM sucrose). After centrifugation, 250 µL of the supernatant was added into 250 µL proteolysis buffer (100 mM Hepes-KOH, pH 7.8, 2 mM ATP, 5 mM $MgCl_2$, 10 mM KCl), followed by a 5-minute incubation at 30 °C. Then the reaction was started by the addition of 2 µL 5 mM Suc-LLVY-AMC. A proteasome inhibitor MG132 (Sigma) was added into half samples to differentiate proteasome activity from protease activity. Lastly, the fluorescence of released AMC was monitored every 2 minutes between 0 and 120 minutes via a fluorescence microplate reader (SpectraMax M2; Molecular Devices,

Sunnyvale, CA) with an excitation wavelength of 360 nm and an emission wavelength of 460 nm. A standard curve utilizing AMC of different concentrations was used to interpret results.

2.2.4. Total mRNA extraction and expression analysis

Total RNA was extracted from fresh leaves using TRIZOL reagent (Invitrogen, Carlsbad, CA). The extracted RNA was purified with a PureLink RNA mini kit (Invitrogen, Carlsbad, CA) and TURBO DNA-free kit (Invitrogen, Vilnius, Lithuania) successively, following manufacturers' instructions. After checking the concentration of the purified RNA with nanophotometer (IMPLEN GMBH, Germany), cDNA synthesis was performed using the high-capacity cDNA synthesis kit (Applied Biosystems, Vilnius, Lithuania). The primers for selected genes (Table 3.1) were either designed via online Primer3Plus or acquired from previous literature [190]. For primers designed by Primer3Plus, their corresponding gene sequences were obtained from tblastn of protein query with available nucleotide databases of creeping bentgrass and wheat in the National Center for Biotechnology Information database. Then, qPCR assays were conducted on the QuantStudio 3 PCR instrument (Applied Biosystems, Marsiling, Singapore) using Power SYBR Green Master Mix (Applied Biosystems, Warrington, England). Three biological replicates for each treatment combination and three technical replicates for each sample were conducted. Relative gene expression was calculated based on the $\Delta\Delta C_t$ method with actin as the reference gene [110].

2.3. Experimental design and statistical analysis

A completely randomized design was adopted within each temperature. There were four and five replicates for each line under control and heat stress conditions, respectively. Within each temperature, analysis of variance (ANOVA) was conducted by fitting a linear regression model in RStudio (R 4.2.1, Boston, MA, USA, 2022) with both line and date as fixed effects. Before

ANOVA, normal distribution of residuals and the homogeneity of variance were checked according to normal quantile-quantile plots and residuals versus fitted plots, respectively, to make sure data met ANOVA assumption. Multiple comparison was performed using the Fisher's protected least significant difference (LSD) test at the 0.05 probability level. Correlation analysis was performed using corrplot package while other figures were made via the ggplot2 package in RStudio (R 3.6.0, 2019).

3. Results

Regarding TQ, plants under control conditions maintained values of 9 for the duration of the trial (Figure 3.1). Contrastingly, TQ decreased consistently under heat stress, with significant differences starting to be seen among lines beyond 7 d. These agreed with the ANOVA results where effects of line, date and their interaction were all significant under heat stress whereas no significant effects were found under control conditions (Table S3.1). At 35 d, S11 729-10 and BTC032 were the two top performers with significantly higher TQ values than those of S11 675-02 and Crenshaw. Oppositely, Crenshaw, as the worst performer, had lower values than all the rest except S11 675-02. As with TQ, heat stress caused dramatic reductions in green cover and Fv/Fm regardless of lines, with pronounced separations being observed from 14 d and 7 d onwards, respectively (Figure 3.2 and 3.3). At 35 d, heat-tolerant S11 729-10 and BTC032 showed higher values than heat-sensitive S11 675-02 and Crenshaw in terms of green cover, and Crenshaw in terms of Fv/Fm.

For EL, unlike control conditions where plants maintained consistent values over time, heat stress caused marked rises in every line (Figure 3.4). At the conclusion of this study (35 d), S11 729-10 had lower EL than the remaining lines with the exception of BTC032. Still, Crenshaw was the worst performer, but it didn't significantly differ relative to S11 675-02 and AU Victory.

Regarding total protein concentration, each line showed insignificant changes over time under control conditions despite significant differences among lines on most sampling dates (Figure 3.5). In contrast, protein concentrations presented pronounced declines in response to elevated temperature in all lines. At 35 d, S11 729-10 outperformed others with significantly greater values than all the other lines with the exception of AU Victory, while Crenshaw had the lowest protein concentrations.

In terms of proteolysis activity, no significant differences were observed between 0 d and 35 d under control for both protease activity and the UPS activity despite some variations during the trial (Figure 3.6 and 3.7). Contrastingly, heat stress resulted in marked increases in both proteolysis pathways' activities. At 35 d, for protease activity, S11 729-10 and AU Victory presented significantly lower values than the remaining lines except BTC032 while Crenshaw had the highest values although not statistically different from S11 675-02. For the UPS activity, S11 729-10 outperformed other lines with significantly lower values than BTC032 at the end of the trial while no prominent differences were seen among the rest of the lines.

For cysteine protease, upregulated gene expression was observed in response to heat stress in all lines at 21 d (Figure 3.8). However, at 35 d, heat stress caused downregulated gene expression in Crenshaw and AU Victory while no statistical differences relative to control in other lines. In addition, at 35 d, heat stress caused significant differences in gene expression among lines. Specifically, S11 675-02 showed the highest values but it was in the same statistical group as BTC032; These two both had greater relative gene expression than AU Victory.

Regarding serine protease, there were no significant differences in gene expression between temperature treatments for any line at 21 d (Figure 3.9). At 21 d of heat stress, S11 729-10 showed the greatest upregulation in expression for the serine protease gene with no significant

difference compared to S11 675-02; Serine protease expression was greater in S11 729-10 and S11 675-02 than BTC032. Contrastingly, at 35 d, gene expression was downregulated in all lines as a consequence of heat stress. As with serine protease, downregulation of E3 was found in all lines subjected to heat stress at 35 d (Figure 3.10). Comparatively, at 21 d, AU Victory and BTC032 showed upregulation under heat while the rest presented no pronounced differences relative to control. No significant differences were seen among heat-stressed lines at both 21 d and 35 d.

Correlation analysis was conducted for all parameters except for gene expression of serine protease, cysteine protease and E3 given the limited amount of the data. It revealed that all the parameters were significantly and strongly correlated with each other, with the absolute values ranging from 0.67 to 0.96 (Figure 3.11).

4. Discussion

The levels of heat tolerance showed significant variations among these creeping bentgrass lines. More heat-tolerant S11 729-10 and BTC032 had superior overall performance compared to the rest as demonstrated by greater TQ and green cover. This is associated with their improved physiological responses, namely, enhanced cell membrane stability as measured by EL, plus greater maintenance of photosynthetic capacity as indicated by Fv/Fm. Comparatively, S11 675-02 and Crenshaw were more heat sensitive, while the performance of AU Victory was intermediate. Heat tolerance levels observed in this study agree with the thermotolerance ranking in a previous study [64]. Interruption in protein metabolism is an important stress-related trait under elevated temperature [3]. In our study, heat-tolerant S11 729-10 presented a greater ability to maintain protein metabolism which was evident from its higher protein content relative to other lines at 35 d. Similar findings were drawn from previous research where greater protein content was typically associated with higher tolerance level despite heat-induced common declines in

protein contents for different plants [64, 65, 191]. Intriguingly, under heat stress, the protein content of heat-tolerant BTC032 was similar to that of sensitive S11 675-02 at the conclusion of the trial. This implies that BTC032 might employ a different mechanism to regulate protein metabolism compared to S11 729-10, or it might utilize additional mechanisms beyond protein regulation to tolerate heat stress.

Proteases and the UPS are enzymes whose activities are determined by various factors, like temperature, pH, their own concentration as well as substrate concentration [36]. Proteins may become misfolded as a direct consequence of exposure to heat stress or oxidized due to excess ROS accumulation induced by heat stress [192]. These damaged proteins serve as major substrates to proteases and the UPS pathways. As heat stress progressed, non-functional proteins would accumulate due to increased damage or deficiency in repair or removal, leading to varying increases in proteolysis activities across different lines. The increased proteolysis activities indicated enhanced protein degradation, which might explain the declines in total protein contents for heat-stressed plants. Moreover, S11 729-10 presented weaker proteolytic process as evidenced by its lower activities of the UPS and protease enzymes, contributing to its higher protein contents, and eventually conferring its greater thermotolerance. These were further supported by the strong correlations among TQ, green cover, protein content, protease activity and the UPS activity. Heat-induced increases in protease activities have been documented in many studies [70, 71, 74, 89]. In the case of wheat, protease activity was significantly increased in all genotypes under heat stress, with a significant positive correlation with heat susceptibility index [71]. The authors, therefore, concluded that protease activity could be used as a biochemical marker to assess the relative degree of heat tolerance of wheat genotypes. Similarly, when *Agrostis scabra* and creeping bentgrass were both placed under 35 °C, rises in protease activities were observed in both species relative to

control but more heat-tolerant *Agrostis scabra* was able to maintain lower values [89]. In another study, application of protease inhibitors led to lower protease activity and higher protein content with concurrent improvements in TQ, Fv/Fm, and chlorophyll content in heat-stressed creeping bentgrass [74]. The findings highlight that protease inhibitors can mitigate heat-induced leaf senescence and enhance turf performance by suppressing proteolysis. Compared to the studies on protease activity, the role of the UPS in heat-induced senescence remains largely unexplored although heat-induced UPS activity has been found in tobacco cells [110]. While not measuring the UPS activity directly, another study on wheat reported that when roots were exposed to increased temperature, elevated amounts of high molecular mass conjugates while significantly lower amounts of low molecular mass conjugates and free ubiquitin were detected [111]. The UPS works by adding polyubiquitin onto target proteins to form protein-ubiquitin substrates for the 26S proteasome to be degraded [108]. Hence, the authors proposed that high temperatures increased breakdown of root proteins via enhanced ubiquitin proteolytic pathways, namely, the UPS pathway.

Enzyme concentration, regulated at both the transcriptional and translational levels, positively correlates with enzyme activity, provided there is sufficient substrate availability [36]. While additional factors influence this relationship, increased gene expression typically plays a key role in driving higher enzyme production, which subsequently enhances catalytic efficiency. To assess whether increases in gene expression accompanied the observed rise in proteolysis activities, qRT-PCR was performed on selected proteases and key components of the UPS, specifically serine protease, cysteine protease, and E3 ligase. In our study, at 21 d when stress symptoms started to be observed visually, the genes encoding cysteine protease showed upregulation in all lines under heat stress while no significant differences were seen between

temperature treatments regarding the expression level of the serine protease gene. When leaf senescence is induced, chloroplast will be the first organelle to be disorganized [83]. Degradation of stromal proteins like Rubisco activase, and Rubisco which is the most abundant protein in leaves, occurs earlier than degradation of chlorophyll and thylakoidal proteins, including D1, light harvesting complex II and PSII antenna [84]. Principal targets for cysteine proteases during leaf senescence are Rubisco and Rubisco activase in cool-season plants, while serine proteases are more involved in degradation of D1 and light harvesting complex II [59, 66, 84]. Therefore, during the midpoint phase of stress, cysteine protease can be more heat-inducible to accumulate in sufficient amount for the early breakdown of damaged stromal proteins like Rubisco. This might help explain the differences in terms of gene expression for cysteine protease and serine protease at 21 d in our study. The expression of proteolysis-related genes responding to heat stress has been explored in several studies. The expression levels of *AsCP1* encoding cysteine proteases were upregulated in the roots at the end of heat stress trial, but this upregulation was less pronounced in the more heat-tolerant *Agrostis scabra* compared to creeping bentgrass [89]. Another transcriptome study on *Lolium temulentum,* a model grass species, revealed upregulation of most genes encoding serine protease in response to combined heat and drought stress [79]. While not analyzing gene expression, some papers reported increased protein expression of cysteine proteases and serine proteases upon heat shock, with most studies being conducted on rice (*Oryza sativa* L.) [76, 85, 193]. Similarly, heat-induced upregulation of genes encoding E3 has been stated in a few studies, too, with various types of E3 ligases exhibiting differential responses to heat stress [79, 117, 123, 182]. For example, the overexpression of *AtCHIP* encoding a U-Box-Containing E3 rendered Arabidopsis more sensitive to elevated temperature whereas the overexpression of an F-box E3 gene *TaFBA,* improved heat tolerance in tobacco seedlings [117, 123].

In contrast to the upregulation observed at Day 21, at 35 d in our study, we noted marked gene downregulation in serine protease, cysteine protease as well as E3 in almost all lines as a consequence of temperature elevation. The discrepancies could arise from the differences in heat stress intensity and stress duration. While most studies cited applied heat stress for no more than 14 days, our experiment extended to 35 days. High temperatures downregulate and damage proteins involved in the glycolytic pathways, reducing energy generation, while respiration rates rise to meet increased demands for protein repair/degradation and stress defense [16, 40, 76, 135, 194]. When the heat stress trial progressed into Day 35, the extent of damage was severe, and the plants had entered an advanced state of senescence with critically depleted energy reserves. In response, plants would shift ATP from energy-intensive processes like protein synthesis, including the production of proteases and components of the UPS, to more immediate needs, such as stress defense, protein transport or cellular repair [91-93]. This strategic redistribution of energy and nutrient resources allows plants to maximize their chances of survival under prolonged stressful conditions by efficiently managing their limited reserves. Interestingly, the maximal proteolysis activities were observed at 35 d when gene expression exhibited declines. This suggests that gene expression and enzyme activity are not always synchronized, with transcriptional regulation for proteolysis likely occurring earlier in the stress response. Additionally, transcript levels can only explain a fraction of variation in protein abundance in plants [195-197]. Decreases in gene expression don't necessarily correspond to decreases in protein levels, as protein abundance is governed by the dynamic balance between protein degradation and protein synthesis [91]. These might explain the decreases in gene expression of serine proteases, cysteine protease and E3 while the increases in proteolysis activities under heat stress at 35 d.

5. Conclusions

Heat-tolerant S11 729-10 and BTC032 presented better overall performance under heat stress, with improved physiological responses, including better maintenance in photosynthetic efficiency and cell membrane stability. Protein degradation was enhanced under heat as demonstrated by significant increases in protease activity and the UPS activity over time. Nevertheless, more heat-tolerant S11 729-10 maintained lower activities of both protease and the UPS, contributing to its higher protein content, thereby greater thermotolerance. Additionally, cysteine protease could be more heat-inducible than serine protease during the midpoint stage of heat stress. To our knowledge, this is the first time that the roles of protease activity and the UPS activity in heat stress were simultaneously analyzed in a perennial grass species. Such information will provide a favorable steppingstone for elucidating protein metabolism underlying heat stress responses, furthering the understanding of the thermotolerance mechanisms in creeping bentgrass. Acquiring more precise information about the molecular regulation of proteolysis pathways as well as their substrates will be an important direction for future research.

Author Contributions

QF designed the study, conducted the study, performed data collection, analysis, and visualization, prepared the original draft and edited it. DJ designed the study, provided resources as well as supervision, reviewed and edited the manuscript.

Funding

This project was funded by the Georgia Golf Environmental Foundation.

Conflict of Interest

The authors declare that there is no conflict of interest.

Data Availability Statement

All data supporting the findings of this study are available within the manuscript and within its supplemental materials published online.

References

1. Roberts, I.N., et al., Senescence-associated proteases in plants. *Physiologia Plantarum*, 2012. **145**(1): p. 130-139 DOI: 10.1111/j.1399-3054.2012.01574.x.
2. Xu, F.Q. and H.W. Xue, The ubiquitin-proteasome system in plant responses to environments. *Plant, cell & environment*, 2019. **42**(10): p. 2931-2944 DOI: 10.1111/pce.13633.
3. van Wijk, K.J. and Z. Adam, Does the polyubiquitination pathway operate inside intact chloroplasts to remove proteins? *The Plant Cell*, 2024: p. koae104 DOI: 10.1093/plcell/koae104.
4. Xu, J., et al., The ubiquitin-proteasome system in the plant response to abiotic stress: potential role in crop resilience improvement. *Plant Science*, 2024: p. 112035 DOI: 10.1016/j.plantsci.2024.112035.
5. Stone, S.L., Role of the ubiquitin proteasome system in plant response to abiotic stress. *International review of cell and molecular biology*, 2019. **343**: p. 65-110 DOI: 10.1016/bs.ircmb.2018.05.012.
6. Zhang, X., et al., Transcriptome profile reveals heat response mechanism at molecular and metabolic levels in rice flag leaf. *Gene*, 2013. **530**(2): p. 185-192 DOI: 10.1016/j.gene.2013.08.048.
7. Pachauri, R.K. and L. Meyer. *Climate change 2014 Synthesis Report-Summary for Policymakers*. 2014. Geneva, Switzerland: Intergovernmetnal Panel on Climate Change (IPCC).

8. Huang, B.R., M. DaCosta, and Y.W. Jiang, Research Advances in Mechanisms of Turfgrass Tolerance to Abiotic Stresses: From Physiology to Molecular Biology. *Critical Reviews in Plant Sciences*, 2014. **33**(2-3): p. 141-189 DOI: 10.1080/07352689.2014.870411.

9. Mansoor, S., et al., Reactive Oxygen Species in Plants: From Source to Sink. *Antioxidants*, 2022. **11**(2): p. 225 DOI: 10.3390/antiox11020225.

10. Goldberg, A.L., Protein degradation and protection against misfolded or damaged proteins. *Nature*, 2003. **426**(6968): p. 895-899 DOI: 10.1038/nature02263.

11. Planas-Marquès, M., S. Lema A, and N.S. Coll, Detection and quantification of protein aggregates in plants. *Plant proteostasis: methods and protocols*, 2016: p. 195-203 DOI: 10.1007/978-1-4939-3759-2_15.

12. Shang, F. and A. Taylor, Ubiquitin–proteasome pathway and cellular responses to oxidative stress. *Free Radical Biology and Medicine*, 2011. **51**(1): p. 5-16 DOI: 10.1016/j.freeradbiomed.2011.03.031.

13. Li, H., et al., High temperature effects on D1 protein turnover in three wheat varieties with different heat susceptibility. *Plant Growth Regulation*, 2017. **81**(1): p. 1-9 DOI: 10.1007/s10725-016-0179-6.

14. Sun, Y., et al., Regulation of chloroplast protein degradation. *Journal of Genetics and Genomics*, 2023 DOI: 10.1016/j.jgg.2023.02.010.

15. Møller, I.M. and B.K. Kristensen, Protein oxidation in plant mitochondria as a stress indicator. *Photochemical & photobiological sciences*, 2004. **3**(8): p. 730-735 DOI: 10.1039/b315561g.

16. Huffaker, R., Proteolytic activity during senescence of plants. *New Phytologist*, 1990. **116**(2): p. 199-231 DOI: 10.1111/j.1469-8137.1990.tb04710.x.

17. Callis, J., Regulation of protein degradation. *The Plant Cell*, 1995. **7**(7): p. 845 DOI: 10.1105/tpc.7.7.845.

18. Hameed, A., M. Goher, and N. Iqbal, Heat stress-induced cell death, changes in antioxidants, lipid peroxidation, and protease activity in wheat leaves. *Journal of Plant Growth Regulation*, 2012. **31**: p. 283-291 DOI: 10.1007/s00344-011-9238-4.

19. Rossi, S. and B. Huang, Protease inhibitors suppressed leaf senescence in creeping bentgrass exposed to heat stress in association with inhibition of protein degradation into free amino acids. *Plant Growth Regulation*, 2023: p. 1-11 DOI: 10.1007/s10725-023-00977-3.

20. Huang, B.R., S. Rachmilevitch, and J.C. Xu, Root carbon and protein metabolism associated with heat tolerance. *Journal of Experimental Botany*, 2012. **63**(9): p. 3455-3465 DOI: 10.1093/jxb/ers003.

21. Paradiso, A., et al., Cyclic AMP mediates heat stress response by the control of redox homeostasis and ubiquitin-proteasome system. *Plant, Cell & Environment*, 2020. **43**(11): p. 2727-2742 DOI: 10.1111/pce.13878.

22. Kim, J.H., S.D. Lim, and C.S. Jang, Oryza sativa heat-induced RING finger protein 1 (OsHIRP1) positively regulates plant response to heat stress. *Plant molecular biology*, 2019. **99**: p. 545-559.

23. Doroodian, P. and Z. Hua, The ubiquitin switch in plant stress response. *Plants*, 2021. **10**(2): p. 246 DOI: 10.3390/plants10020246.

24. Fry, J. and B. Huang, Applied turfgrass science and physiology. 2004.

25. Shaddox, T.W., et al., Turfgrass Use on US Golf Courses. *HortTechnology*, 2023. **33**(4): p. 367-376 DOI: 10.21273/HORTTECH05238-23.

26. Fan, Q. and D. Jespersen, Assessing Heat Tolerance in Creeping Bentgrass Lines Based on Physiological Responses. *Plants*, 2023. **12**(1): p. 41 DOI: 10.3390/plants12010041.

27. Bhalerao, R., et al., Gene expression in autumn leaves. *Plant physiology*, 2003. **131**(2): p. 430-442 DOI: 10.1104/pp.012732.

28. Lim, P.O., H.J. Kim, and H. Gil Nam, Leaf senescence. *Annu. Rev. Plant Biol.*, 2007. **58**: p. 115-136 DOI: 10.1146/annurev.arplant.57.032905.105316.

29. Diaz-Mendoza, M., et al., Plant senescence and proteolysis: two processes with one destiny. *Genetics and Molecular Biology*, 2016. **39**: p. 329-338 DOI: 10.1590/1678-4685-GMB-2016-0015.

30. Krans, J.V. and K. Morris, Determining a profile of protocols and standards used in the visual field assessment of turfgrasses: A survey of national turfgrass evaluation program-sponsored university scientists. 2007 DOI: 10.1094/ATS-2007-1130-01-TT.

31. Karcher, D.E. and M.D. Richardson, Digital image analysis in turfgrass research. *Turfgrass: Biology, use, and management*, 2013. **56**: p. 1133-1149-2 DOI: 10.2134/agronmonogr56.c29.

32. Blum, A. and A. Ebercon, Cell membrane stability as a measure of drought and heat tolerance in wheat 1. *Crop Science*, 1981. **21**(1): p. 43-47 DOI: 10.2135/cropsci1981.0011183X002100010013x.

33. Bradford, M.M., A rapid and sensitive method for the quantitation of microgram quantities of protein utilizing the principle of protein-dye binding. *Analytical biochemistry*, 1976. **72**(1-2): p. 248-254 DOI: 10.1016/0003-2697(76)90527-90523.

34. Cupp-Enyard, C., Sigma's non-specific protease activity assay-casein as a substrate. *JoVE (Journal of Visualized Experiments)*, 2008(19): p. e899 DOI: 10.3791/899.

35. Üstün, S., et al., The proteasome acts as a hub for plant immunity and is targeted by Pseudomonas type III effectors. *Plant physiology*, 2016. **172**(3): p. 1941-1958 DOI: 10.1104/pp.16.00808.

36. Xu, Y., P. Burgess, and B. Huang, Transcriptional regulation of hormone-synthesis and signaling pathways by overexpressing cytokinin-synthesis contributes to improved drought tolerance in creeping bentgrass. *Physiologia Plantarum*, 2017. **161**(2): p. 235-256 DOI: 10.1111/ppl.12588.

37. He, Y. and B. Huang, Protein changes during heat stress in three Kentucky bluegrass cultivars differing in heat tolerance. *Crop Science*, 2007. **47**(6): p. 2513-2520 DOI: 10.2135/cropsci2006.12.0821.

38. Chen, W., et al., Morphological, physiological and biochemical responses of gerbera cultivars to heat stress. *Horticultural Science & Technology*, 2016. **34**(1): p. 1-14 DOI: 10.12972/kjhst.20160018.

39. Taiz, L. and E. Zeiger, *Plant Physiology 5 ed. Sunderland, MA*. 2006, the Sinauer Associates.

40. Vierstra, R.D., Protein degradation in plants. *Annual review of plant biology*, 1993. **44**(1): p. 385-410 DOI: 10.1146/annurev.pp.44.060193.002125.

41. He, Y., X. Liu, and B. Huang, Changes in protein content, protease activity, and amino acid content associated with heat injury in creeping bentgrass. *Journal of the American Society for Horticultural Science*, 2005. **130**(6): p. 842-847 DOI: 10.21273/JASHS.130.6.842.

42. Ferguson, D.L., J.A. Guikema, and G.M.J.P.P. Paulsen, Ubiquitin pool modulation and protein degradation in wheat roots during high temperature stress. *Plant Physiology*, 1990. **92**(3): p. 740-746 DOI: 10.1104/pp.92.3.740.

43. Müller, L. and T. Hoppe, UPS-dependent strategies of protein quality control degradation. *Trends in Biochemical Sciences*, 2024 DOI: 10.1016/j.tibs.2024.06.006.

44. Martin, R.C., B.A. Kronmiller, and J.E. Dombrowski, Transcriptome Analysis of Lolium temulentum Exposed to a Combination of Drought and Heat Stress. *Plants*, 2021. **10**(11): p. 2247 DOI: 10.3390/plants10112247.

45. Gammulla, C.G., et al., Differential metabolic response of cultured rice (Oryza sativa) cells exposed to high-and low-temperature stress. *Proteomics*, 2010. **10**(16): p. 3001-3019 DOI: 10.1002/pmic.201000054.

46. Jagadish, S., et al., Physiological and proteomic approaches to address heat tolerance during anthesis in rice (Oryza sativa L.). *Journal of experimental botany*, 2010. **61**(1): p. 143-156 DOI: 10.1093/jxb/erp289.

47. Lee, D.G., et al., A proteomic approach in analyzing heat-responsive proteins in rice leaves. *Proteomics*, 2007. **7**(18): p. 3369-3383 DOI: 10.1002/pmic.200700266.

48. Li, Q., et al., Wheat F-box protein gene TaFBA1 is involved in plant tolerance to heat stress. *Frontiers in plant science*, 2018. **9**: p. 521 DOI: 10.3389/fpls.2018.00521.

49. Yan, J., et al., AtCHIP, a U-box-containing E3 ubiquitin ligase, plays a critical role in temperature stress tolerance in Arabidopsis. *Plant physiology*, 2003. **132**(2): p. 861-869 DOI: 10.1104/pp.103.020800.

50. Huang, B.R. and H.W. Gao, Growth and carbohydrate metabolism of creeping bentgrass cultivars in response to increasing temperatures. *Crop Science*, 2000. **40**(4): p. 1115-1120 DOI: 10.2135/cropsci2000.4041115x.

51. Liu, X.Z. and B.R. Huang, Seasonal changes and cultivar difference in turf quality, photosynthesis, and respiration of creeping bentgrass. *Hortscience*, 2001. **36**(6): p. 1131-1135 DOI: 10.21273/hortsci.36.6.1131.

52. Parsell, D. and S. Lindquist, The function of heat-shock proteins in stress tolerance: degradation and reactivation of damaged proteins. *Annual review of genetics*, 1993. **27**(1): p. 437-496 DOI: 10.1146/annurev.ge.27.120193.002253.

53. Zou, J., C. Liu, and X. Chen, Proteomics of rice in response to heat stress and advances in genetic engineering for heat tolerance in rice. *Plant Cell Reports*, 2011. **30**: p. 2155-2165 DOI: 10.1007/s00299-011-1122-y.

54. Cao, H., O. Duncan, and A.H. Millar, Protein turnover in the developing Triticum aestivum grain. *New Phytologist*, 2022. **233**(3): p. 1188-1201 DOI: 10.1111/nph.17756.

55. Li, L., et al., Protein degradation rate in Arabidopsis thaliana leaf growth and development. 2017. **29**(2): p. 207-228 DOI: 10.1105/tpc.16.00768.

56. Morales, M. and S. Munné-Bosch, Oxidative stress: a master regulator of plant trade-offs? *Trends in plant science*, 2016. **21**(12): p. 996-999 DOI: 10.1016/j.tplants.2016.09.002.

57. Zander, M., et al., Integrated multi-omics framework of the plant response to jasmonic acid. *Nature plants*, 2020. **6**(3): p. 290-302 DOI: 10.1038/s41477-020-0605-7.

58. Reich, S., et al., A multi-omics analysis reveals the unfolded protein response regulon and stress-induced resistance to folate-based antimetabolites. *Nature communications*, 2020. **11**(1): p. 2936 DOI: 0.1038/s41467-020-16747-y.

59. McLoughlin, F., et al., Maize multi-omics reveal roles for autophagic recycling in proteome remodelling and lipid turnover. *Nature plants*, 2018. **4**(12): p. 1056-1070 DOI: 10.1038/s41477-018-0299-2.

Tables and Figures

Table 3.1 List of primers for real-time quantitative reverse transcription polymerase chain reaction (qRT-PCR)

Gene name	Accession number	Forward primer	Reverse primer	Reference
Serine protease	GFQK01035040.1	TTTCAATTTGGCCGCCTCTG	TTCGCTGCTGCTAATTGCTG	-
Cysteine protease	-	GGTTGATGAGGAACAGATTGC	CAGATGTATGGGCACGACAC	[190]
E3	GFJH01061614.1	AACACGCTGTGCATAGCATG	TTGTGGCATTGTTGGTACGG	-
Actin	-	CCTTTTCCAGCCATCTTTCA	GAGGTCCTTCCTGATATCCA	[190]

E3, ubiquitin ligase.

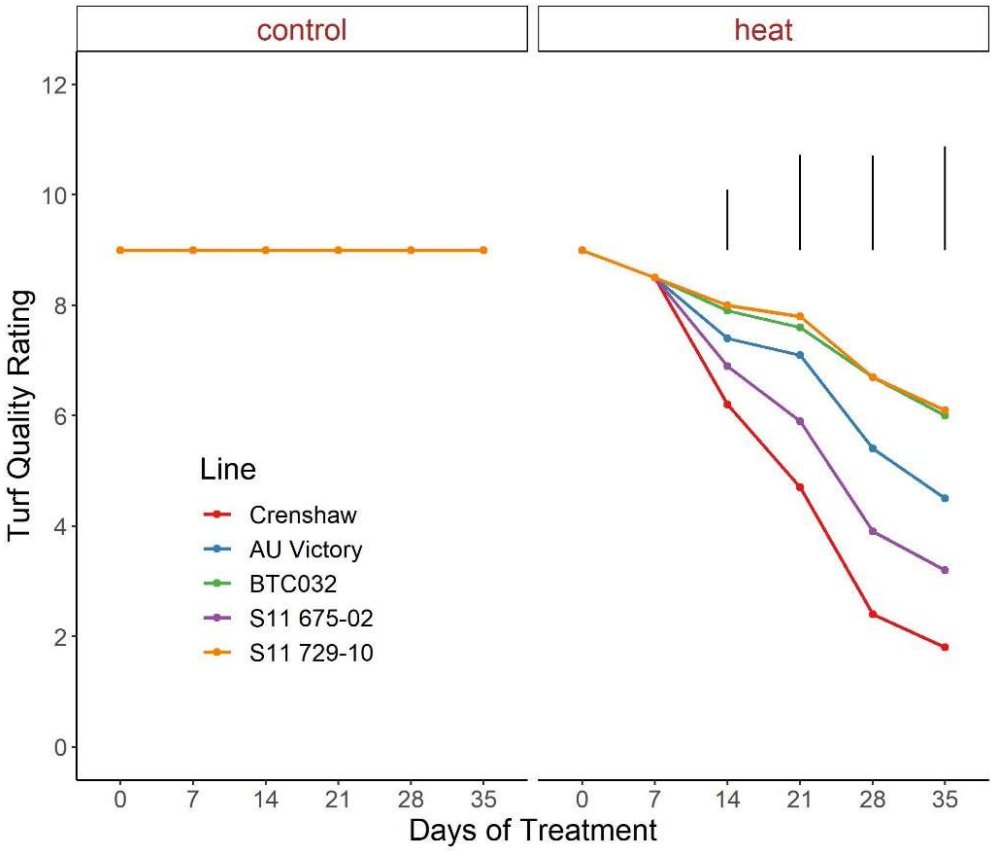

Figure 3.1 Change in visual turf quality rating for creeping bentgrass lines over time under control (20/15°C day/night) and heat stress (38/33°C day/night) conditions. Bars represent LSD values at $p = 0.05$ on days when significant differences among lines were found.

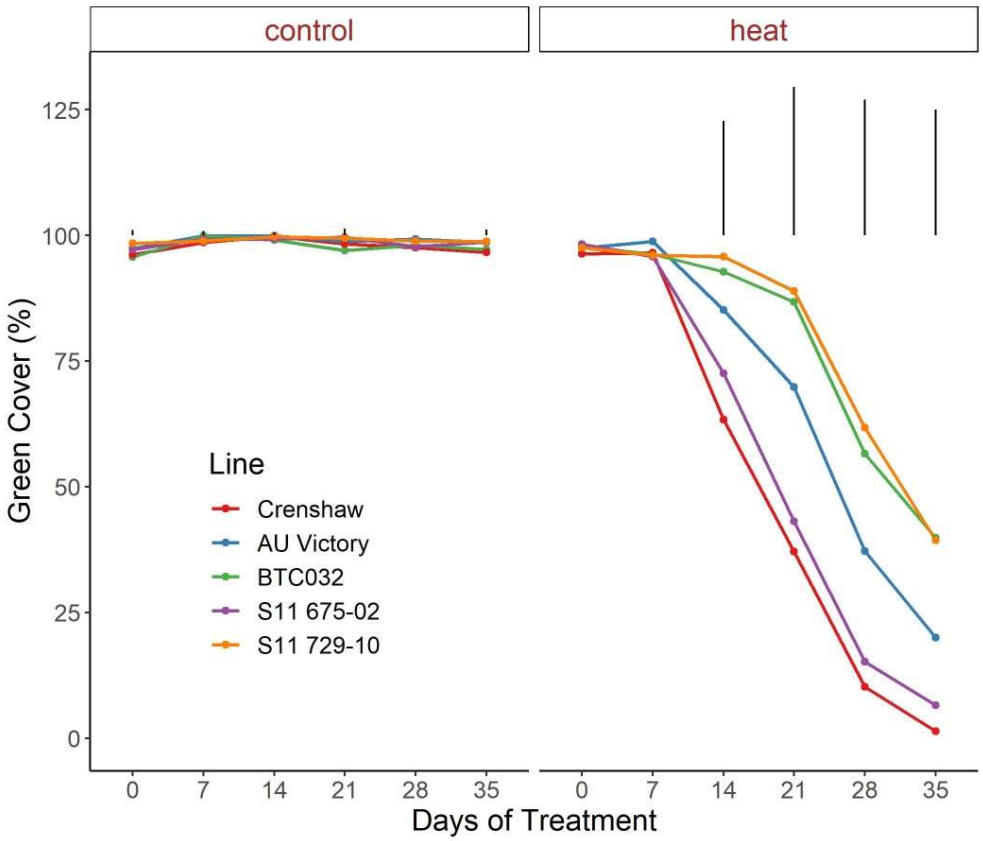

Figure 3.2 Change in percent green cover rating for creeping bentgrass lines over time under control (20/15°C day/night) and heat stress (38/33°C day/night) conditions. Bars represent LSD values at $p = 0.05$ on days when significant differences among lines were found.

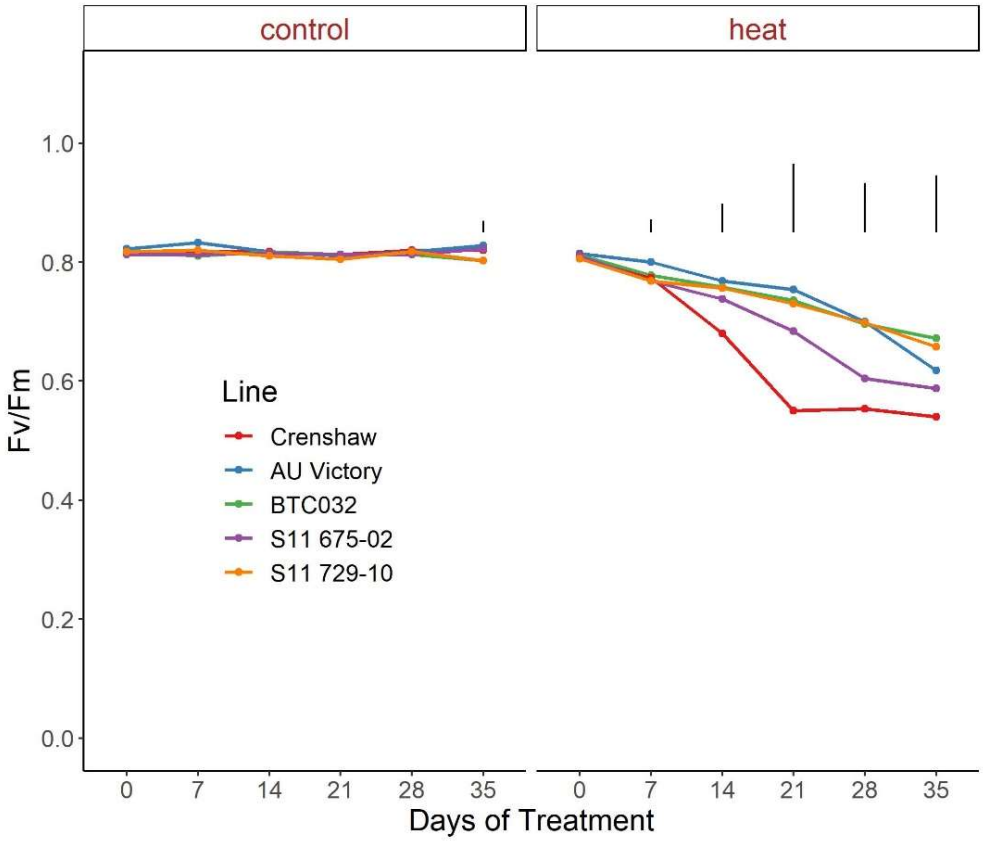

Figure 3.3 Change in Fv/Fm for creeping bentgrass lines over time under control (20/15°C day/night) and heat stress (38/33°C day/night) conditions. Bars represent LSD values at $p = 0.05$ on days when significant differences among lines were found.

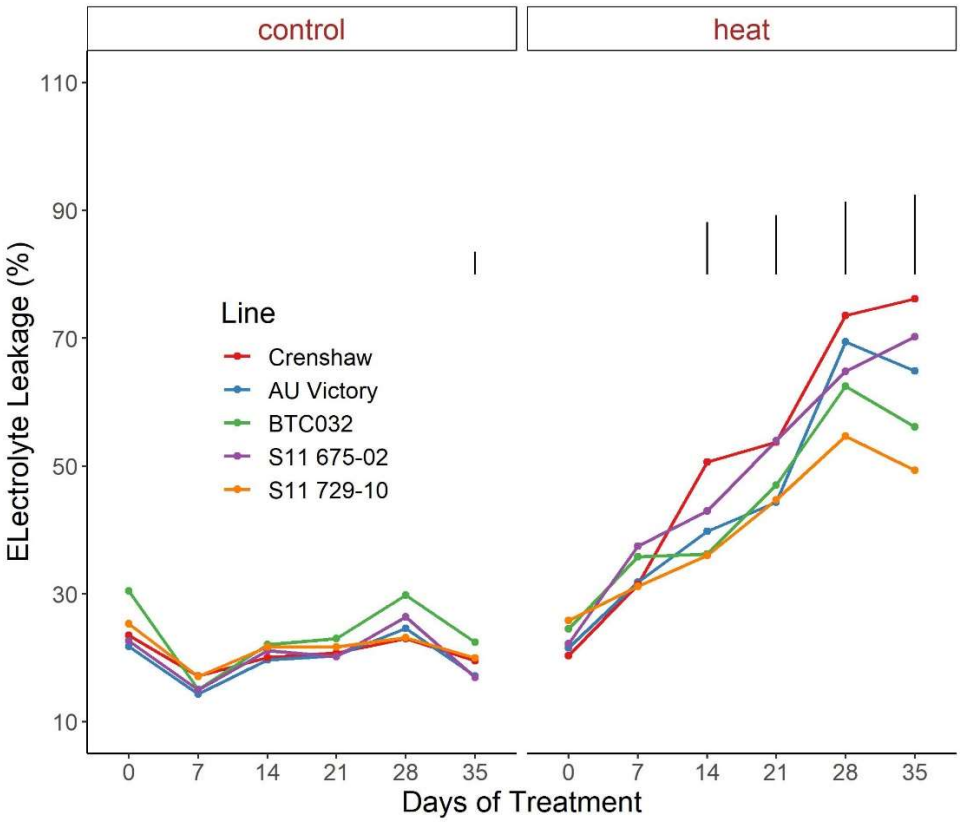

Figure 3.4 Change in electrolyte leakage for creeping bentgrass lines over time under control (20/15°C day/night) and heat stress (38/33°C day/night) conditions. Bars represent LSD values at $p = 0.05$ on days when significant differences among lines were found.

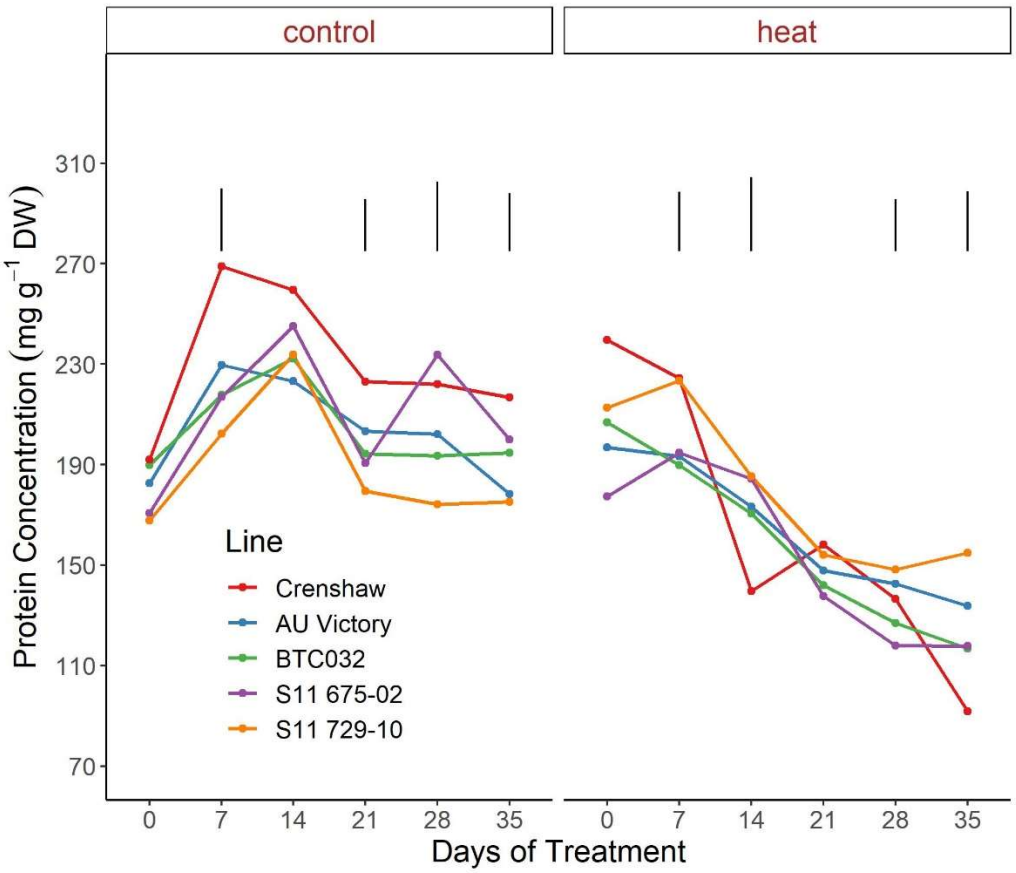

Figure 3.5 Change in total protein concentration for creeping bentgrass lines over time under control (20/15°C day/night) and heat stress (38/33°C day/night) conditions. Bars represent LSD values at $p = 0.05$ on days when significant differences among lines were found.

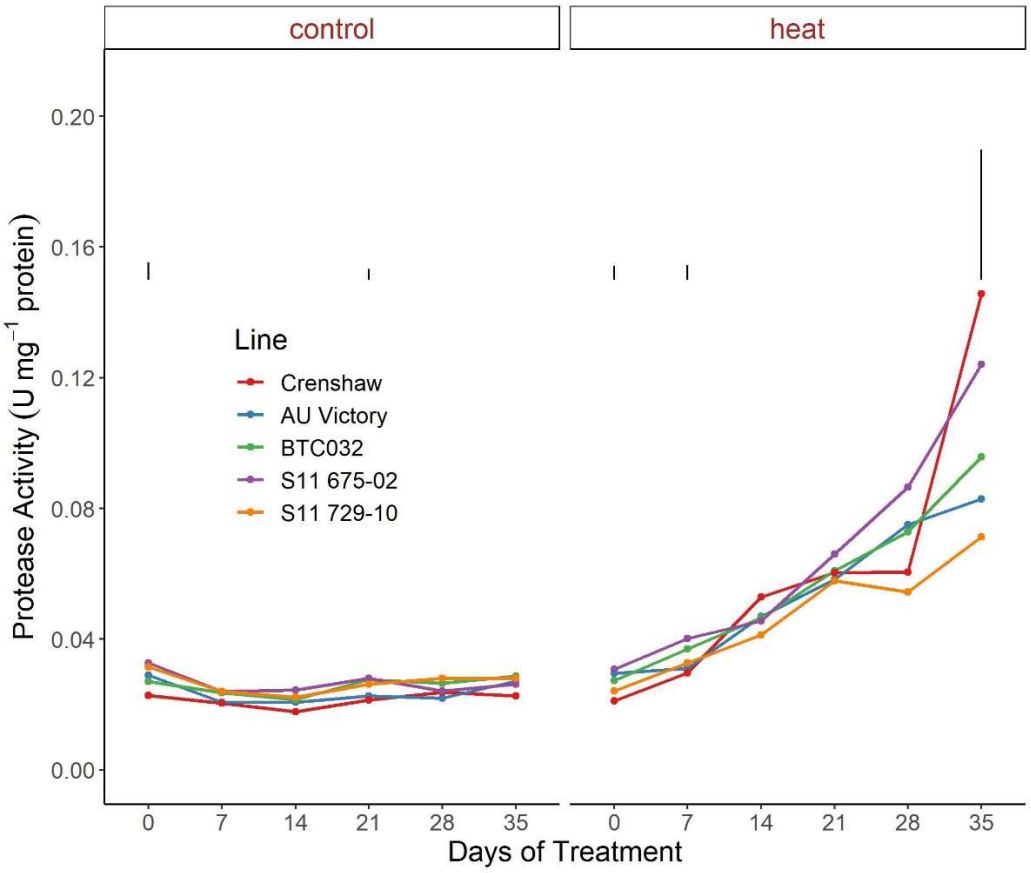

Figure 3.6 Change in total protease activity for creeping bentgrass lines over time under control (20/15°C day/night) and heat stress (38/33°C day/night) conditions. Bars represent LSD values at $p = 0.05$ on days when significant differences among lines were found.

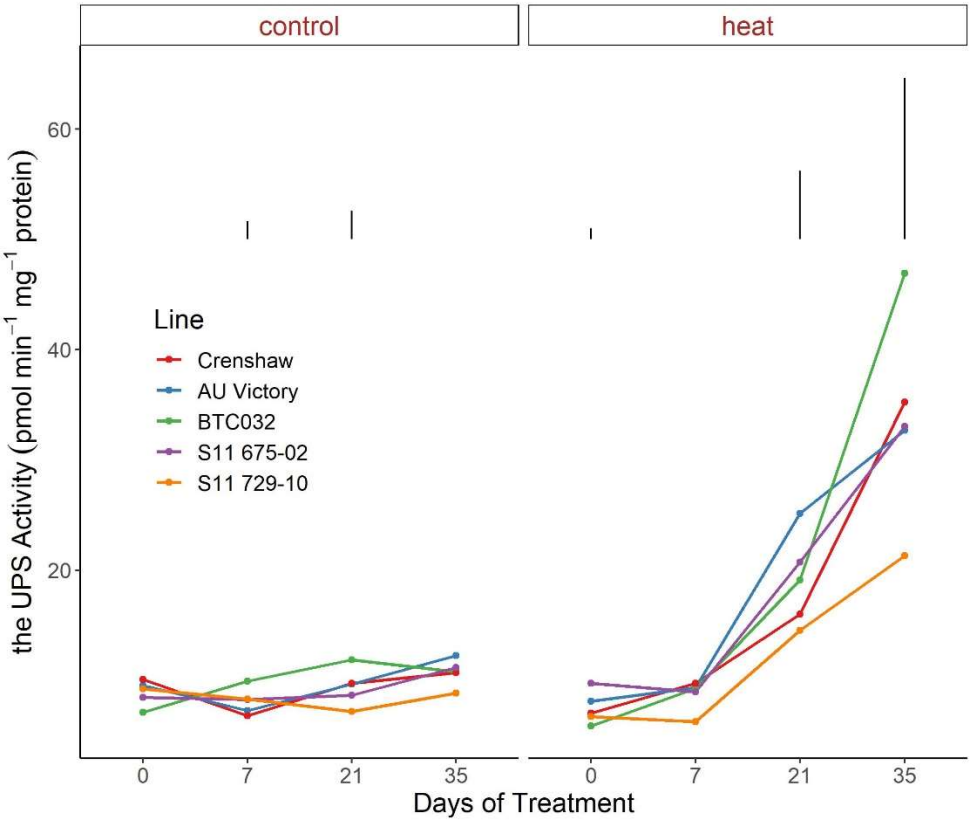

Figure 3.7 Change in the UPS activity for creeping bentgrass lines over time under control (20/15°C day/night) and heat stress (38/33°C day/night) conditions. Bars represent LSD values at $p = 0.05$ on days when significant differences among lines were found.

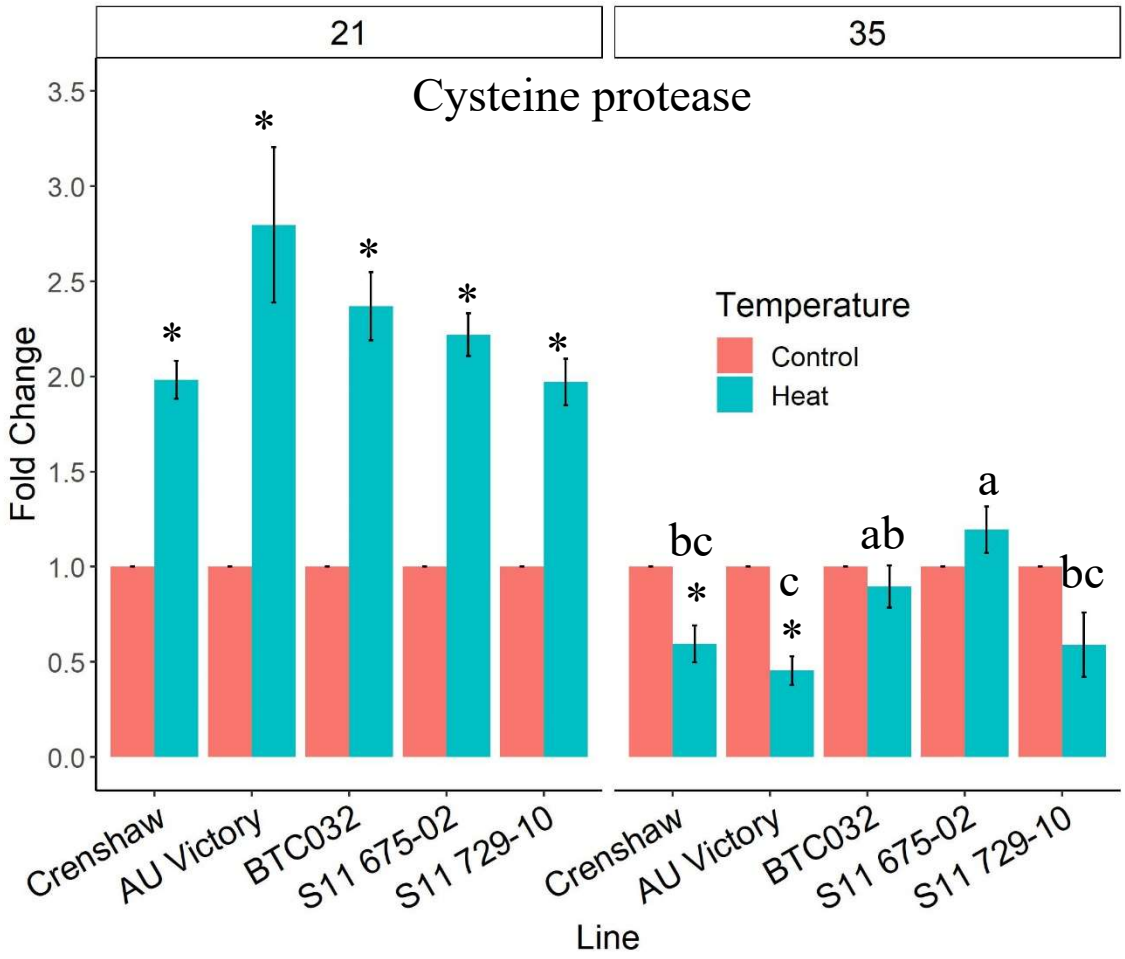

Figure 3.8 Relative gene expression of cysteine protease for creeping bentgrass lines at 21 d and 35 d under control (20/15°C day/night) and heat stress (38/33°C day/night) conditions. Bars represent standard errors. Columns marked with the same lowercase letters are not significantly different within each sampling date at $p = 0.05$. The asterisk above each column indicates there is a significant difference between control and heat stress for each line at $p = 0.05$.

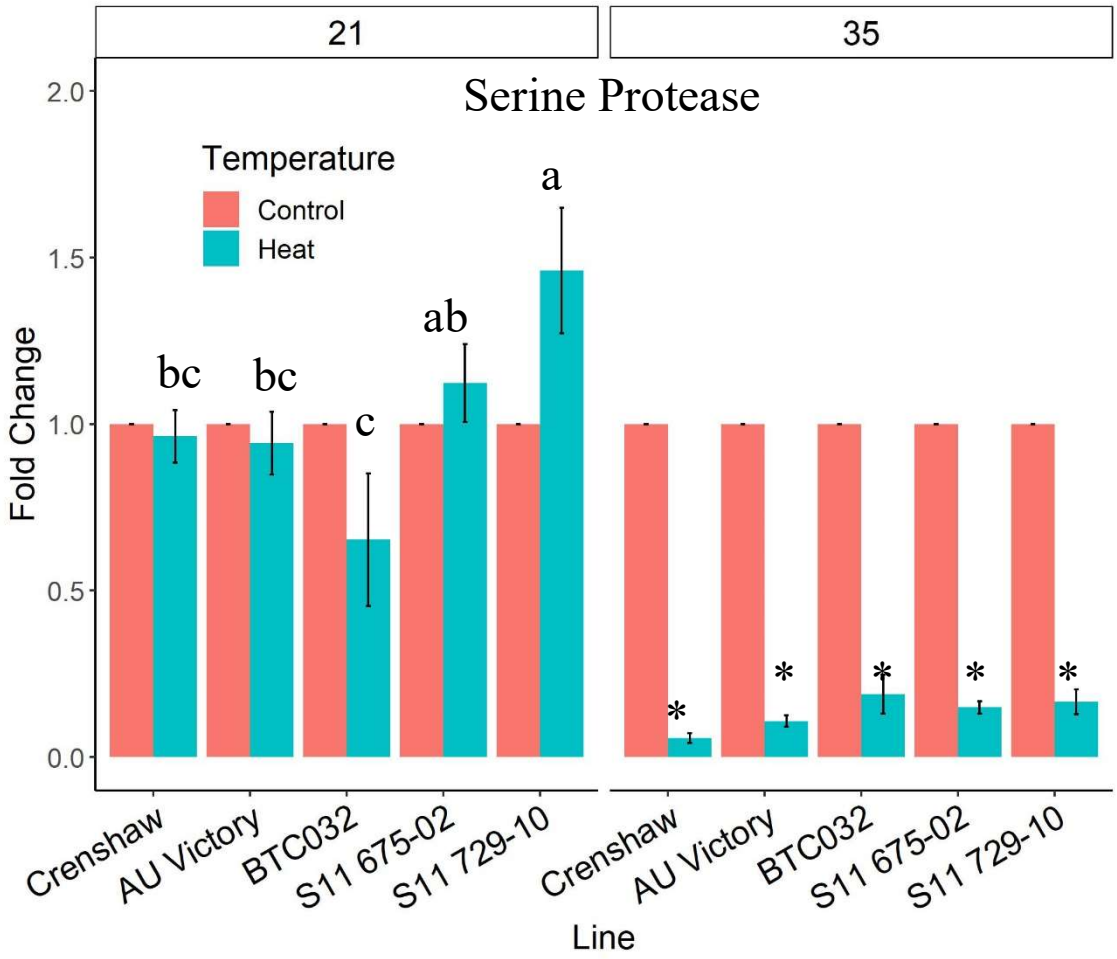

Figure 3.9 Relative gene expression of serine protease for creeping bentgrass lines at 21 d and 35 d under control (20/15°C day/night) and heat stress (38/33°C day/night) conditions. Bars represent standard errors. Columns marked with the same lowercase letters are not significantly different within each sampling date at $p = 0.05$. The asterisk above each column indicates there is a significant difference between control and heat stress for each line at $p = 0.05$.

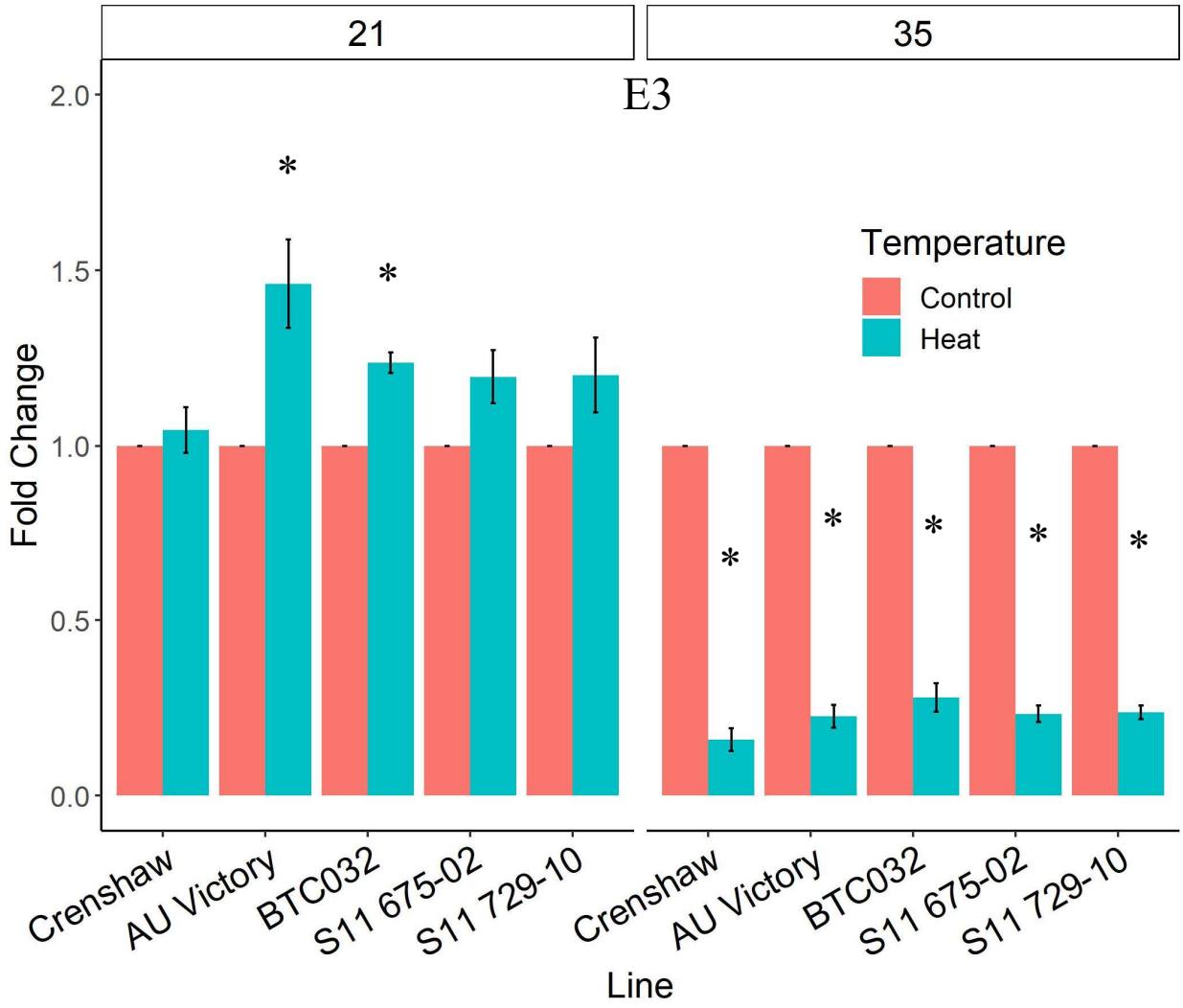

Figure 3.10 Relative gene expression of E3 for creeping bentgrass lines at 21 d and 35 d under control (20/15°C day/night) and heat stress (38/33°C day/night) conditions. Bars represent standard errors. Columns marked with the same lowercase letters are not significantly different within each sampling date at p = 0.05. The asterisk above each column indicates there is a significant difference between control and heat stress for each line at p = 0.05.

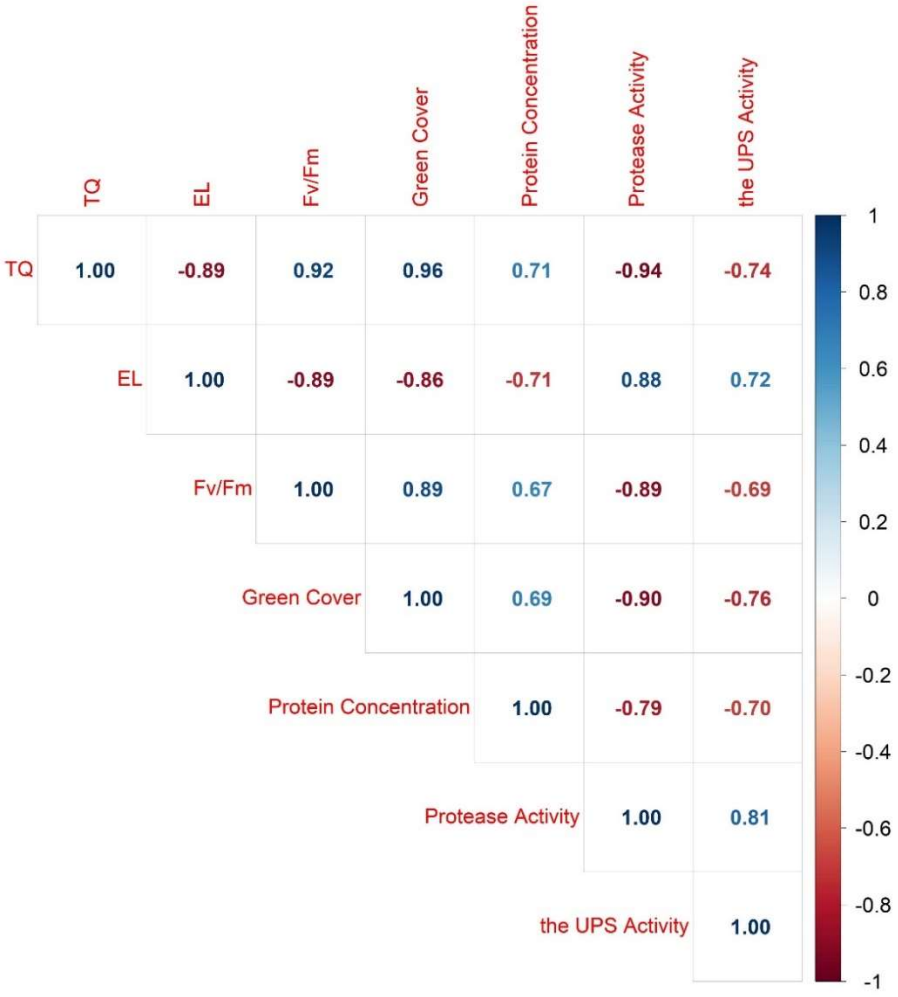

Figure 3.11 Correlation plot for different parameters of creeping bentgrass under control (20/15°C day/night) and heat stress (38/33°C day/night) conditions. Numbers indicate correlation coefficients. Color intensity is proportional to the correlation coefficients with blue indicating positive correlations and red representing negative correlations.

Supplemental Materials

Table S3.1 ANOVA results for heat stress trial of creeping bentgrass

Parameter	*P* value					
	Control			Heat stress		
	Line	Date	Line × Date	Line	Date	Line × Date
TQ	0.3825	0.1356	0.0672	< 2.2e-16	< 2.2e-16	1.299e-11
Green cover	0.0004887	0.6750	0.9405	1.644e-11	< 2.2e-16	5.426e-05
EL	0.04878	0.9528	0.9743	0.0006646	< 2.2e-16	2.213e-06
Fv/Fm	0.05887	0.3325	0.2655	7.930e-09	< 2.2e-16	8.037e-05
Total protein content	5.494e-05	0.3982	0.5040	0.0006595	< 2.2e-16	0.001322
Protease activity	3.222e-05	0.9622	0.2703	0.003045	< 2.2e-16	0.000185
The UPS activity	0.171364	0.000239	0.2401	0.002414	< 2.2e-16	0.0007177

TQ, turf quality; EL, electrolyte leakage; Fv/Fm, quantum efficiency of energy flux trapped by photosystem II (PSII) photochemistry; UPS, ubiquitin-proteasome system.

CHAPTER 4

PROTEIN METABOLISM UNDERLYING HEAT TOLERANCE IN CONTRASTING CREEPING BENTGASS LINES: INSIGHTS FROM GEL-FREE PROTEOMICS AND POLYUBIQUITIN-OMICS[1]

[1] Q. Fan and D. Jespersen. To be submitted to *International Journal of Molecular Sciences*.

Abstract

One of the major disfunctions that occurs in heat-stressed plants is enhanced protein damage and a consequent decline in cellular protein content. Creeping bentgrass (*Agrositis stolonifera* L.) is an economically important perennial grass species which is largely used on high value turf areas but experiences frequent damage due to heat stress. Several promising experimental lines of creeping bentgrass showed various tolerance levels to heat stress, with differential responses observed in physiological traits, total protein content and rates of protein degradation. The ubiquitin-proteasome system (UPS) plays a crucial role in the removal of damaged proteins, and there is a critical need to better understand the changes in protein accumulations and degradation via the UPS that occur during heat stress. Hence, we aimed to estimate change in global protein accumulations by performing gel-free proteomics as well as identify proteins that have been polyubiquitinated and targeted to the UPS pathway via polyubiquitin-omics in contrasting creeping bentgrass lines exposed to heat stress. It was found that heat-tolerant S11 729-10 was able to maintain less severe downregulation of proteins involved in the light reactions of photosynthesis, while enhancing the upregulation of antioxidant proteins, particularly during the later phase of stress. These contributed to its improved physiological performance including greater cell membrane integrity as well as healthier light harvesting components. Additionally, the faster turnover of key polyubiquitinated antioxidant proteins in S11 729-10 likely represents a critical mechanism for protecting against oxidative damage and enhancing tolerance under prolonged heat stress. This is the first time that the application of polyubiquitin-omics has been utilized in turfgrass. These findings provide deeper insights into protein metabolism underlying heat tolerance. Key stress-related traits or proteins identified in this study could be utilized to help develop new cultivars with enhanced tolerance to heat stress.

1. Introduction

Maintenance of protein metabolism is of utmost importance for the normal cellular activities of plants as proteins are the major driving force behind plant growth, development and stress tolerance. Unfavorable environmental conditions, however, can induce proteome disruption. One such stressor is heat stress, which is a major threat to many economically important plant species, with damages being further exacerbated with more frequent and intense heat wave events as a function of climate change [4]. Heat stress leads to large scale protein misfolding and aggregation, resulting in a decline in protein content, with concomitant impairment of various physiological activities, including inhibition of photosynthesis caused by degradation of photosynthetic machinery, plus oxidative stress resulting from the overproduction of reactive oxygen species (ROS) [58, 64]. To prevent cellular dysfunction and injuries to cells, plants can adjust their proteome to inhibit the formation or promote the removal of these damaged proteins. These mechanisms include refolding by heat shock proteins (HSPs) or degradation through various proteolytic pathways including the ubiquitin-proteasome system (UPS). HSPs are well-known molecular chaperones that work by preventing proteins from inappropriate aggregation and promoting refolding of damaged proteins to maintain their functional conformations [135]. Many HSPs are initially induced upon temperature elevation, contributing to protein stabilization under stressful conditions [3]. Similar to HSPs, a series of antioxidant enzymes and non-enzymatic antioxidants are also upregulated in response to heat stress to scavenge excessive ROS, protecting cellular components like proteins from being oxidized and maintaining cell membrane stability [3]. Despite the observed accumulation of heat-protective proteins, other essential proteins, such as those involved in photosynthesis and electron transport are often downregulated by heat, suggesting impairment to those pathways or related machinery [3, 198, 199]. This differential

changes in the proteome demonstrates that plants' response to environmental perturbation is an intricate process at the molecular level. A better understanding of the changes in protein accumulation will assist in dissecting physiological responses, thereby providing deeper insights into the molecular basis of heat tolerance.

Proteomics has been a powerful approach to discover the proteins and pathways that are crucial for stress tolerance and has been addressed in a wide range of plant species, including creeping bentgarss (*Agrositis stolonifera* L.) [3, 198, 200-202]. Creeping bentgrass, an economically important perennial grass species, is largely used on high value turf areas such as putting greens on golf courses and courts for lawn tennis given its fine texture and tolerance to low mowing height [140]. However, due to its low to moderate tolerance to high temperature, heat stress has been one major factor limiting the performance of creeping bentgrass worldwide [140]. To further understand thermotolerance mechanisms and accelerate the development of elite cultivars with enhanced tolerance levels, attempts have been made to investigate proteomics in heat-stressed creeping bentgrass [86, 203-205]. It was found from these studies that compared to heat-sensitive lines/cultivars, heat-tolerant ones had lesser extents of downregulation of the proteins involved in important pathways like photosynthesis and energy metabolism while greater upregulation or even unique induction of stress-responsive proteins like HSPs and certain antioxidants. These, collectively, contributed to the enhanced thermotolerance in the heat-tolerant plants. Nevertheless, the majority of these studies use gel-based methods from the previous generation of technology. Gel-free proteomics, as a relatively newer methodology, possesses several advantages over gel-based ones, such as broader dynamic range and greater sensitivity, higher reproducibility, improved quantification accuracy, and more efficient protein identification

[206]. Exploring protein metabolism from the point of gel-free proteomics, thus, may offer some new insights into the survival strategies creeping bentgrass utilizes to cope with heat stress.

The UPS is a key proteolytic pathway responsible for maintaining protein homeostasis by targeting damaged proteins for degradation, primarily in the cytosol and nucleus, but also in organelles like chloroplasts and the endoplasmic reticulum [107]. It relies on a cascade of ubiquitin enzymes—E1, E2, and E3—to attach ubiquitin molecules to substrate proteins, forming polyubiquitin chains that are recognized and degraded by the 26S proteasome [109]. This process eventually results in the release of free amino acids and ubiquitin molecules to be reused for various cellular functions. Given the importance of the UPS in protein quality control, there has been a growing body of research which investigated its role in plant responses to various abiotic stresses, including heat stress [62, 109, 185, 207]. In the case of tobacco (*Nicotiana tabacum* L.) cells, heat-induced increases in UPS activity have been observed [110]. Similarly, another study on wheat (*Triticum aestivum*) proposed accelerated breakdown of root proteins via enhanced UPS pathway, as manifested by elevated amounts of ubiquitin-protein conjugates while lower amounts of free ubiquitin [111]. The integration of proteomics with protein ubiquitylation, referred to as ubiquitin-omics, is a relatively new and promising area of research. It enables the large-scale identification of substrate proteins targeted by the UPS, offering valuable insights into the regulation of key stress-response proteins and various biological processes, particularly those related to stress responses and proteostasis in plants [109]. Despite its significance, identifying UPS substrates has been challenging due to the transient nature of ubiquitination and the dynamic interactions between substrates and E3 ligases. However, ubiquitin-omics has emerged as a powerful tool to overcome these challenges, and it has been applied to a variety of plant species, such as maize (*Zea mays*), *Arabidopsis thaliana* and rice (*Oryza sativa* L.) [127-129]. The key step

of this procedure is the efficient enrichment of ubiquitin conjugates. Traditional strategies for the isolation of poly-ubiquitinated proteins often require immuno-precipitation of epitope-tagged ubiquitin, which however displays a lack of affinity [208]. Tandem Ubiquitin Binding Entities (TUBEs), which are an engineered protein domain, can overcome this problem. This technology shows greater affinity for polyubiquitin chains than most ubiquitin antibodies and is emerging as an indispensable strategy for further understanding of the UPS [132]. Integrating TUBE-based isolation of polyubiquitinated proteins with proteomics, thus, may offer new insights into how protein degradation is regulated by the UPS under heat stress.

Recent studies on several promising experimental lines of creeping bentgrass revealed various tolerance levels to heat stress, with differential responses identified in terms of physiological traits and total protein content [64]. Stronger UPS activity induced by heat stress was also observed in more heat-sensitive lines of creeping bentgrass (Qianqian Fan, unpublished). However, the substrate proteins for the UPS pathway and how these individual proteins were regulated under heat stress remain elusive. The development of elite cultivars will be more efficient with a more complete understanding of the mechanisms conferring improved thermotolerance. There is a critical need to better understand the changes in protein accumulation that are driving the differences in heat tolerance as well as underlying regulation of these changes. Hence, we aimed to estimate global proteomic changes due to heat stress by performing gel-free proteomics in contrasting creeping bentgrass lines and identify proteins that have been polyubiquitinated and targeted to the UPS pathway via polyubiquitin-omics. Findings from this study would enable a more complete picture of protein metabolism underpinning thermotolerance and identify stress-related proteins and pathways that can be utilized for new cultivar development.

2. Materials and methods

2.1. Growth and Treatment Conditions

Three creeping bentgrass lines with varying levels of heat stress tolerance were selected for this study based on previous findings [64]. These included two experimental lines ('S11 675-02', 'S11 729-10') and one commercial cultivar ('Crenshaw'), with S11 729-10 being heat-tolerant while S11 675-02 and Crenshaw being heat-sensitive. For each line, 6-cm-diameter plugs were established in plastic pots (10.5 cm long, 10.5 cm wide and 12.5 cm deep) filled with a mixture of 50% sand and 50% calcined clay (Turface; Profile Products LLC, Buffalo Grove, IL, USA), and placed in greenhouse conditions [~23/~15 °C (light/dark period temperatures) and 70% relative humidity] for two months. Then plants were transferred to controlled environmental growth chambers (CG-72; Conviron, Winnipeg, MB, Canada) for one-week acclimation under conditions of 20/15 °C (day/night), 70% humidity and 14 h photoperiod with 600 μmol m^{-2} s^{-1} photosynthetically active radiation at the canopy level before treatments began. Plants were maintained well-watered and fertilized weekly with a 24-8-16 (N-P-K) fertilizer (Scotts Miracle-Gro; Marysville, OH, USA) at the rate of 9.8 g N m^{-2} during establishment in the greenhouse as well as during the treatment period inside growth chambers. Applications of insecticides and fungicides were made as needed for disease control. Plants of each line were placed under either heat stress (38/33 °C day/night) or control (20/15 °C day/night) conditions for 28 d after the initiation of treatments.

2.2. Physiological Measurements

Weekly measurements of visual turf quality (TQ) rating, percent green cover, electrolyte leakage (EL) and chlorophyll fluorescence were performed. TQ and green cover represent overall turf performance. TQ was rated on a scale of 1–9 according to color, density and uniformity with

1 representing totally dead grass while 9 standing for completely healthy grass [160]. Percent green cover was acquired through images taken with a digital camera (Canon G9X; Canon, Tokyo, Japan) using a lightbox to ensure a uniform lighting, which were then processed via ImageJ v.1.46. [161].

Chlorophyll fluorescence reflects the health status of photosynthetic light harvesting. To conduct chlorophyll fluorescence measurements, plants were dark-adapted for at least 30 min prior to measurement via a chlorophyll fluorometer (OSP 5+; Opti-sciences, Hudson, NH). Fluorescence traits consisted of absorbed energy flux per cross section (ABS/CSm), quantum efficiency of energy dissipation in photosystem II (PSII) antenna (DIo/ABS), quantum efficiency of energy flux trapped by PSII photochemistry leading to reduction of quinone A (Q_A) (Fv/Fm), the energy flux associated with electron transport from Q_A to intersystem electron acceptors such as plastoquinone pool per cross section (ETo/CSm), and the energy flux associated with electron transport from intersystem electron acceptors to final PSI acceptors per cross section (REo/ CSm) [154]. Three measurements were taken on fully expanded leaves for each replicate.

Cell membrane stability, as estimated by EL, is widely used as an indicator for membrane damage in plants [64]. To quantify EL, around 0.1 g fresh leaves were placed in a tube containing 35 mL deionized water. After agitating tubes on a shaker for 16 h, initial conductivity was recorded through a conductivity meter (Radiometer, Copenhagen, Denmark). Next, the samples were autoclaved at 120 °C for 20 min, followed by incubation for another 16 h on a shaker, after which the final conductivity was read. EL then was calculated as the percentage of initial conductivity over total conductivity [163].

2.3. Polyubiquitin-Omics and Gel-Free Proteomics

Gel-free proteomics for global proteins at 14 d and 28 d and polyubiquitin-omics at 28 d were performed by the Proteomics and Mass Spectrometry Facility at University of Georgia. Since the most significant differences in physiological responses were found between Crenshaw and S11 729-10, both proteomic analyses focused on these two lines for comparison. Approximately 500 mg leaf tissues were harvested from each plot at 14 d and 28 d and immediately flash frozen in liquid nitrogen. Frozen leaves were stored at -80 °C until further analysis.

2.3.1. Global Protein Extraction, Purification and Digestion

Protein was extracted according to the trichloroacetic acid/acetone method with minor modification [209]. Around 150 mg leaves of each sample were homogenized in 1.5 mL sodium phosphate buffer (50 mM, pH 7.5 pH with 1 mM ethylenediaminetetraacetic acid), followed by centrifuge (10,000× *g*, 4 °C for 20 min) to obtain 0.4 mL supernatant containing crude proteins. The crude protein supernatant was transferred to a solution containing 20% TCA and 0.14% 2-mercaptoethanol in acetone (pH 7.5). The mixture was fully vortexed, placed on ice for 5 min and then centrifuged (15,000 × *g* for 3 min). The resultant tissue pellets were washed using 0.07% 2-mercaptoethanol in acetone and 0.07% 2-mercaptoethanol in 80% acetone, successively, then air dried for 9 min at 37 °C. The final pellets were resuspended by vortexing at 25 °C in 0.4 mL resolubilization buffer [7 M urea, 2 M thiourea, 5% (m/v) CHAPS, and 2 mM tributylphosphine, pH 7.5], followed by centrifuge at 21,000 × g, 25 °C for 20 min. The resulting supernatant was collected as protein extract. Total protein content was quantified at 595 nm using a Bradford dye reagent with a bovine serum albumin standard [164].

Proteins were further purified according to a modified filter-assisted sample preparation [210].Ten µg of protein sample was mixed with 5 µL of 0.05 M dithiothreitol and then denatured by a heat block at 100 °C for ~10 minutes. After cooling down to room temperature, the mixture

was incubated for an additional 30 minutes. The protein samples were diluted with 100 µL of 20 mM triethylamine bicarbonate (Millipore-Sigma), and then transferred into Vivacon® 500 (10K MWCO Hydrosart) filters (Sartorius). The filter units were spun at 14,000 g in a microcentrifuge (Sorvall Legend Micro17, Thermo Scientific, Madison, WI, USA) for 15 minutes, and the flow-throughs were discarded. The resultant proteins were alkylated by adding 50 µL 0.02 M iodoacetamide to the filters and were allowed to react in the dark for 30 minutes. The filters were washed/spun with 400 µL 20 mM triethylamine bicarbonate (TEAB) for 2 times. Then 0.2 µg Trypsin in 50 µL 20 mM TEAB was dispended into each filter to digest proteins at room temperature overnight. The next day, the filters were spun at 14,000 g for 10 minutes to allow for the elution of tryptic peptides to the collection tubes, followed by a wash with 100 µL water to elute the residual peptides. The collected peptide solutions were dried in a vacuum concentrator (RC1010 centrifuge, Jouan).

2.3.2. Enrichment, Purification and Digestion of Polyubiquitinated Proteins

Polyubiquitinated proteins were isolated according to TUBE technology using K48 version of ubiquitin mass spectrometry kit (LifeSensors, Malvern, PA, USA), with minor modification [132]. Around 100 mg leaves of each sample were homogenized in 1.0 mL sodium phosphate buffer (50 mM, pH 7.5 pH with 1 mM ethylenediaminetetraacetic acid), followed by the addition of 10 µL of UPS inhibitor cocktail. After centrifuge (14,000× *g*, 4 °C for 20 min), 5 µL of decomplexing buffer was added to the resultant 500 µL supernatant, followed by 15-minute incubation over ice. The total protein content was quantified at 595 nm using a Bradford dye reagent with a bovine serum albumin standard [164]. A total 100 µL of slurry containing magnetic beads bound with TUBEs was added into the supernatant containing 1-3 mg of total proteins, and PBS buffer was used to adjust the final volume to 1 mL. After incubation overnight at 4 °C using

an end-to-end rotator (Benchmark, Edison, NJ, USA), the beads of the mixture were collected using a magnetic stand (VWR). Following three washes with PBS-T and another wash with 80 µL of TUBE wash buffer. The beads were resuspended and incubated in 30 µL TUBE elution buffer at room temperature for 15 minutes with mixing. The resulting eluate contained polyubiquitinated proteins.

A total of 3.3 µL neutralization buffer was added into the eluted proteins, followed by centrifuge. Then, 4 µL of 6X Laemmli buffer (Thermo Fisher Scientific, Ward Hill, MA, USA) was added into 20 µL of the resultant supernatant. After boiling at 90 °C for 5 minutes, the mixture was loaded into a Bolt 4%-12% acrylamide gel (Invitrogen, Carlsbad, CA, USA) for SDS-PAGE via a mini gel tank (Invitrogen, Kiryat Shmona, Israel) in order to remove detergents. The gel was run at 150 V for 2 minutes and then stained using SimpleBlue SafeStain (Invitrogen, Carlsbad, CA, USA). After destaining in DI water for 1 h, the gel bands with stain were carefully excised. After three washes with gel wash buffer, gel alkylation was performed in the dark. Specifically, 100 µL of reducing solution was added to the excised gel and incubated for 15 minutes at 37 °C. After removing the solution, 100 µL of alkylating solution was added and incubated for 1 hour at 37 °C, then discarded. The gel fragments were successively washed with 400 µL gel wash buffer, digestion buffer and gel wash buffer, each with a 15-minute incubation at 37 °C. After air-drying for 10 minutes, the samples were incubated with trypsin overnight at room temperature with mixing to generate peptides.

2.3.3. Analysis through Tandem Mass Spectrometry coupled with Liquid Chromatography (LC-MS/MS)

The downstream analysis for digested global proteins and polyubiquitinated proteins are performed the same. The mass spectrometry analyses were performed on a Thermo-Fisher LTQ

Orbitrap Elite Mass Spectrometer coupled with a Proxeon Easy NanoLC system (Waltham, MA, USA). Approximate 0.5 μg peptides were loaded into a reversed-phase (RP) column (100 μm inner-diameter, ~15 cm long, ReperoSil-Pur 120 C18-AQ, Dr. Maisch, Ammerbuch, Germany) and then directly eluted into the mass spectrometer for 90-minute run. A two-buffer gradient elution consisting of 0.1% formic acid as buffer A and 99.9% acetonitrile with 0.1% formic acid as buffer B, was used for analysis. The gradients were as follows: 0-2 minutes, 5% buffer B; 2-60 minutes, 20% buffer B; 60-85 minutes, 50% buffer B; 85-95 minutes, 95% buffer B. Data was acquired using Xcalibur software (version 3.0, Thermo Fisher Scientific). The data-dependent acquisition method was used to acquire MS data. A survey MS scan was acquired first, and then the top 10 ions in the MS scan were selected for following collision-induced dissociation analysis. Both MS and MS/MS scans were acquired by Orbitrap at the resolutions of 120,000 and 15,000, respectively.

2.3.4. Protein Identification, Quantification and Classification

Protein identification was performed using Proteome Discoverer 3.0 (Thermo) with Mascot 2.8 (Matrix Science) against the Poaceae database of UniProt (downloaded on 12/2023) and a modified contaminations database containing commonly known contaminating proteins (Mascot). The search parameters were as follows: precursor mass tolerance 10 ppm, fragment mass tolerance 0.02 Da, trypsin full specificity, maximum number of missed cleavages 1, false discovery rate <0.01; Methionine oxidation was set as variable modifications and cysteine carbamidomethylation was designated as fixed modification. The semi-quantitative analyses were achieved using a label-free quantification workflow within Proteome Discoverer. Specifically, a Precursor Ion Quantifier node calculated the summated peak areas of the peptide matches of protein matches in the Extracted Ion Chromatograms (mass precision, 5 ppm). Protein was

identified to be differentially expressed proteins (DEPs) when it showed a fold change (FC) of no less than 1.2 or no larger than 0.83 in the heat-stressed condition compared with the control condition with P-value ≤ 0.05 [211, 212].

Gene ontology (GO) is an international classification system which describes biological functions at various levels, from molecular to organismal. The Kyoto Encyclopedia of Genes and Genomes (KEGG) is a database of manually drawn pathway maps representing our knowledge of molecular interaction and reaction networks. In our study, GO analysis including biological process (BP) and molecular function (MF) was performed using the Blast2GO program (OmicsBox 3.1.11) against the non-redundant protein database [213]. KEGG pathway annotation was conducted via g:Profiler (https://biit.cs.ut.ee/gprofiler/gost, accessed on 03/2024) [214]; Pathways were identified to be enriched with P-value ≤ 0.05 using the Benjamini-Hochberg approach.

2.4. Statistical Analysis

A completely randomized design was adopted within each temperature. There were four replicates for each line under control and heat stress conditions, respectively. Within each temperature, analysis of variance was performed by fitting a linear regression model for physiological measurements in RStudio (R 4.3.3, Boston, MA, USA, 2024), with both line and date as fixed effects. Means were separated by Fisher's protected least significant difference at the 0.05 probability level. For the visualization of proteomics data, venn plot, PCA plot as well as radar plot were made using ggvenn, ggfortify and ggradar packages, respectively in RStudio; Additional figures were created using either Hiplot (https://hiplot.com.cn/) or SRplot platforms (https://www.bioinformatics.com.cn/srplot).

3. Results

3.1. Overall Performance, Electrolyte Leakage and Chlorophyll Fluorescence Traits

Temperature effects were mostly significant according to the preliminary analysis. The three-way interaction, however, was difficult to interpret. Investigating the interaction between date and line under heat stress conditions may offer more valuable insights into tolerance differences among lines than focusing on the interaction between temperature and other treatments due to the temporal differences in the onset of heat stress symptoms at the experiment progressed [64].

In contrast to control conditions, heat stress caused dramatical decreases in TQ and green cover (up to 55.6% and 77.2% declines, respectively, relative to 0 d) while significant increases in EL (up to 401.4% relative to 0 d) over time (Figure 4.1; Table S4.1-S4.5). Prominent separations among lines were observed from the second measurement at 7 d for TQ and EL, and from the fourth measurement at 21 d for green cover. At the end of the trial (28 d), Crenshaw was the worst performer with the lowest TQ and green cover, while having the highest EL. No significant differences were found between the other two lines in terms of TQ and green cover. However, S11 729-10 showed significantly lower values of EL than S11 675-02 at 28 d.

Similar to TQ and green cover, Fv/Fm was reduced by heat stress throughout the trial with the greatest extent of decrease (up to 40.0% relative to 0 d) seen in Crenshaw (Figure 4.2). Additional differences were detected during the later phase of stress (21 d and 28 d). At 28 d, S11 729-10 was the best line whose value was 43.1% higher than Crenshaw; No significant differences were seen between S11 729-10 and S11 675-02, or between Crenshaw and S11 675-02. In addition to Fv/Fm, other traits indicating various light harvest processes, also showed significant changes in response to heat stress, with declines observed for ABS/CSm, ETo/CSm and REo/CSm while

increases detected for DIo/ABS in all the three lines (Figure 4.3). Again, S11 729-10 outperformed others in terms of these traits at 28 d, having significantly higher values relative to Crenshaw and S11 675-02 for ABS/CSm, ETo/CSm and REo/ CSm, while showing significantly lower values relative to Crenshaw for DIo/ABS.

3.2. Gel-Free Proteomics

Out of a total of 373 putative proteins identified, 240 proteins were successfully quantified via LC-MS/MS. Specifically, 131, 85, 146 and 101 proteins were considered to be DEPs in the heat-stressed group compared with the control group for Crenshaw at 14 d, Crenshaw at 28 d, S11 729-10 at 14 d and S11 729-10 at 28 d, respectively (Figure 4.4a, Table S4.2, S4.3, S4.4, S4.5). 44 DEPs were commonly shared across different groups while 11, 6, 29 and 7 DEPs were uniquely found for Crenshaw at 14 d, Crenshaw at 28 d, S11 729-10 at 14 d and S11 729-10 at 28 d, respectively. For Crenshaw, at 14 d, 48 DEPs were upregulated while 83 were downregulated; at 28 d, 37 DEPs were upregulated while 48 were downregulated (Figure 4.4b). For S11 729-10, at 14 d, 27 DEPs were upregulated while 119 were downregulated; at 28 d, 37 DEPs were upregulated while 64 were downregulated. Additionally, principal component analysis showed clear separation in terms of DEPs between heat-stressed and control samples for each group (Figure S4.1).

To evaluate the function of DEPs, GO analysis was performed. The distribution of the top ten GO terms for biological process and molecular function, respectively, mostly overlapped across lines within each time point (Figure 4.5). At 14 d, top biological process categories included the generation of precursor metabolites and energy, carbohydrate metabolic process, carbohydrate derivative metabolite process, photosynthesis, and nucleobase-containing small molecule metabolic process, whereas the top molecular function categories included oxidoreductase activity,

transferase activity, hydrolase activity and ATP-dependent activity. At 28 d, the most represented GO terms for biological processes were typically photosynthesis, phosphorylation, response to hydrogen peroxidase, electron transport and protein folding across lines. Nevertheless, response to water deprivation, glycolytic process and gluconeogenesis were uniquely included in the top ten terms for S11 729-10. Regarding molecular functions, the top GO categories associated with DEPs were ATP binding, metal ion binding, structural constituent of ribosome as well as protein binding at the end of the trial (28 d).

To investigate the involvement of DEPs in crucial pathways, DEPs within each group were annotated according to the KEGG database using gProfiler. A total of 77, 89, 53, and 62 proteins were assigned KEGG annotations in the heat-stressed samples for Crenshaw at 14 days, Crenshaw at 28 days, S11 729-10 at 14 days, and S11 729-10 at 28 days, respectively. These represented 58.8%, 62.4%, 61.0%, and 61.4% of all DEPs within their respective groups (Figure S4.2). These DEPs with KEGG annotation were enriched into 13, 16, 12, and 11 pathways for Crenshaw at 14 d, Crenshaw at 28 d, S11 729-10 at 14 d and S11 729-10 at 28 d, respectively. Most DEPs associated with KEGG pathways were classified into carbohydrate metabolism like glyoxylate and dicarboxylate metabolism, energy metabolism including photosynthesis and carbon fixation, as well as amino acid metabolism such as arginine biosynthesis or alanine, aspartate and glutamate metabolism. Additionally, the majority of them overlapped across different groups. To maximize the number of DEPs within annotated pathways, for those DEPs without KEGG annotation, their sequences were blasted against the UniProt database to determine putative functions and pathways. Similarly, most DEPs fell into carbohydrate metabolism, energy metabolism and amino acid metabolism after combining results from gProfiler and UniProt blast results. Since photosynthesis inhibition, oxidative stress and protein damage are the most common symptoms induced by heat

stress, with a large number of identified DEPs associated with these processes as supported by previous literature [205, 211] as well as the GO term analysis in our study, we put additional focus on the DEPs related to light reactions, antioxidant defense, and protein refolding.

In terms of photosynthesis-light reactions, heat stress caused dramatic downregulation of all related DEPs except Photosystem I assembly protein Ycf4 (A0A5J9WER5) in Crenshaw at 14 d, with FC ranging from 0.16 to 0.82 (Figure 4.6a). Comparatively, in S11 729-10 at 14 d, the number of downregulated proteins and the extent of decrease were both smaller. When heat stress progressed into Day 28, these DEPs were mostly further decreased in Crenshaw while in S11 729-10, some of them showed no significant change (cytochrome b6-f complex iron-sulfur subunit [Q7X9A6,]; Photosystem I assembly protein Ycf4 [A0A5J9WER5]; Photosystem I P700 chlorophyll a apoprotein A1 [A0A2U9DRJ5]; Photosystem I P700 chlorophyll a apoprotein A2 [A0A4P8F6B8]; Ferredoxin--NADP reductase [P41345]; ATP synthase subunit alpha [A0A2L0VAS4]) or even upregulation (Chlorophyll a-b binding protein [A2XJ35]; Photosystem II 22 kDa protein 1 [Q943K1]) compared to control condition (Figure 4.6b and 4.6c).

Regarding ROS scavenging, 7 out of 11 identified antioxidant proteins showed upregulation in heat-stressed Crenshaw at 14 d while there were 4 out of 11 in heat-stressed S11 729-10 (Figure 4.7a). At the end of the trial (28 d), the number of upregulated proteins decreased to 3 in Crenshaw; Contrastingly, it was increased to 7 in S11 729-10, with the rest showing no differential expression except superoxide dismutase [Cu-Zn] (Figure 4.7b). For protein refolding, eight DEPs belonging to HSP families including HSP60, 70, 80 and 90, were identified (Figure 4.8). They were heat-induced and mostly showed continuous increase over time. At 28 d, Hsp70-Hsp90 organizing protein (HOP) and Heat shock 70 kDa protein BIP1 were uniquely accumulated in S11 729-10 and Crenshaw, respectively.

3.3. Polyubiquitin-omics

Out of a total of 138 putative polyubiquitinated proteins identified under heat stress, 6 (2,3-bisphosphoglycerate-independent phosphoglycerate mutase [P30792]; 6-phosphogluconate dehydrogenase, decarboxylating [A0A1D6LJP0]; Cysteine synthase [A0A0E0GTN2]; DNA-directed RNA polymerase [A0A3L6EAY7]; Ferredoxin-dependent glutamate synthase (Fragment) [Q08258]; Inositol-3-phosphate synthase 1 [O64437]) were uniquely identified in Crenshaw while 3 (Beta-fructofuranosidase, insoluble isoenzyme 4 [Q5JJV0]; Peroxidase [A0A1D5UL37]; Superoxide dismutase [Cu-Zn] 4AP [P23346]) were only identified in S11 729-10 (Figure 4.9a). A total of 129 polyubiquitinated proteins were identified in both lines. According to GO analysis on these polyubiquitinated proteins, the most represented GO terms for biological processes were small molecular metabolic process, biosynthetic process, response to stress, generation of precursor metabolites and energy, carbohydrate metabolic process (Figure 4.9b). A few other important heat-responsive processes were also included, such as photosynthesis, proteolysis and protein binding. Regarding molecular function, the top GO categories associated with identified polyubiquitinated proteins were metal ion binding, nucleotide binding, ion binding, oxidoreductase binding as well as protein binding.

Among 138 identified polyubiquitinated proteins, 20 of them were considered to be DEPs when comparing heat-stressed S11 729-10 against heat-stressed Crenshaw (Table 4.1). Specifically, 8 polyubiquitinated DEPs showed significant downregulation in S11 729-10, with FC values ranging from 0.2 to 0.6. Among these downregulated polyubiquitinated DEPs, one was identified as an E3 ligase while half were members of the histone family. Contrastingly, 12 polyubiquitinated DEPs were upregulated instead in heat-stressed S11 729-10, with FC values

ranging from 1.2 to 6.0. The majority of the upregulated polyubiquitinated DEPs were involved in antioxidant defense, chaperone activity and energy metabolism.

4. Discussion

These three lines showed differential levels of heat tolerance, as reflected by the differences in their overall performance (TQ, green cover). In accordance with the tolerance ranking in previous findings [64], S11 729-10 was the best performer while Crenshaw was a relatively poor performer; S11 675- 02 was intermediate in its responses. Superior overall performance in the more heat-tolerant S11 729-10 was associated with its improved physiological responses, including greater cell membrane stability as measured by EL, and healthier photosynthetic status as evaluated by chlorophyll fluorescence traits (ABS/CSm, DIo/ABS, Fv/Fm, ETo/CSm and REo/ CSm). Accumulated ROS triggered by heat stress can attack lipids resulting in decreased membrane stability with concomitant peroxidation of lipids [20]. Hence, EL increases during exposure to stress but plants with greater thermotolerance typically have lower values of EL [49, 64], which corroborates the results found in our study. By monitoring the rise of fluorescence intensity to a maximum at various states, chlorophyll fluorescence parameters can quantify sequential light harvesting processes, including light absorption by PSII antenna (ABS/CSm), energy trapping by PSII reaction centers (Fv/Fm), energy dissipation (DIo/ABS), electrons migration towards intersystem acceptors from PSII (ETo/CSm) as well as electron transport into PSI end acceptors (REo/ CSm) [154]. This tool is gaining increasing popularity for stress detection in various plant species due to its rapidness, sensitivity, and reliability [64, 156, 215, 216]. In our study, at 28 d, heat stress resulted in different extents of decreases in ABS/CSm, Fv/Fm, ETo/CSm and REo/CSm while concurrent increases in DIo/ABS among lines relative to control. The increase in DIo/ABS highlighted that stress-induced damage required the leaves to dissipate excess

excitation energy instead of utilizing it for photosynthetic processes, thus being negatively correlated with heat tolerance ranking [172]. Collectively, these changes in fluorescence traits indicated that the injuries to photosynthetic components were widespread in the chloroplast and these light-harvesting steps might be concomitantly damaged by heat stress [64]. Although interruption to photosynthetic machinery was a common response, S11 729-10 was able to minimize the damage as evidenced by greater values for ABS/CSm, Fv/Fm, ETo/CSm and REo/CSm while smaller values for DIo/ABS, compared to the other two lines. Similar findings have been documented in previous literature where more heat-tolerant cultivars or lines typically exhibited less variation in fluorescence parameters although photosynthetic components were commonly damaged [64, 171, 172].

Proteins are important drivers behind physiological responses. Stress not only triggers differences in physiological performance, but also elicits differential accumulation of proteins involved in those activities correspondingly [146, 198, 217]. Since the most significant differences in terms of physiological traits were detected between S11 729-10 and Crenshaw as discussed above, analysis of global protein accumulation was performed for these two lines. Differential changes in protein accumulation resulted in clear separation between the two contrasting lines based on PCA analysis, which explained a large proportion of the observed variance. This implied that the difference in heat tolerance between the two lines could be attributed, at least in large part, to these DEPs. Interestingly, more DEPs were detected at 14 d compared to 28 d for both lines. During the early phase of stress, proteomic alterations could occur rapidly and robustly to help plants adapt to stress and maintain cellular homeostasis under challenging conditions. However, when stress treatments are prolonged, plants could fail to maintain stress-induced homeostasis and enter an exhaustion phase when they became less responsive to the stressor [218]. The reduced

responsiveness is resulted from the depletion of essential resources, such as energy and nutrients, required for defense or repair pathways, as well as the accumulation of damages [218]. As a result, there would be a reduction in the number of DEPs compared to the early phase. Additionally, DEPs related to carbohydrate metabolism, antioxidant defense and protein metabolism were major categories identified by both GO term and pathway analysis, which were highly regulated during both time points, particularly during the later phase of heat stress.

4.1. DEPs Associated with Photosynthesis

Photosynthesis is the basis of plant growth. It consists of two phases, light reactions and dark reactions. During light reactions, light is absorbed by chlorophyll and then transported along an electron transport chain, leading to the production of ATP and NADPH, which are essential for the subsequent dark reactions. Four major protein complexes are involved in light reactions: PSII, Cytochrome b_6f, PSI and ATP synthase [36]. Impairment of these complexes can weaken photosynthetic ability. Declines in the abundance of light-reaction-related proteins have been documented to be common responses under heat stress in various plant species besides creeping bentgrass [146], such as *Arabidopsis thaliana* [219], soybean (*Glycine max* L.*)* [220], wheat (*Triticum aestivum*) [28] and rice (*Oryza sativa* L.) [221]. Nevertheless, more heat-tolerant plants generally possessed less severe downregulation of these proteins [28, 146, 169]. For instance, photosynthesis-related proteins including ATP-synthase, cytochrome b6f and chloroplast oxygen-evolving enhancer proteins were downregulated in two lines of bentgrass (ColxCB169 and ColxCB190) due to heat stress, but they were decreased later and to a lesser extent in leaves of more heat-tolerant ColxCB169 [146]. These corroborate the results found in our study where heat stress mostly caused downregulation of DEPs involved in the electron transport chain, but the number of downregulated DEPs as well as the extent of decreases were both smaller in S11 729-

10 relative to Crenshaw. Furthermore, as heat stress progressed into 28 d, the accumulation of most proteins involved in light reactions was further reduced in Crenshaw, reflecting more severe damage under prolonged stress. However, this was not observed in S11 729-10. Instead, quite a few proteins showed unchanged (Cytochrome b6-f complex iron-sulfur subunit, PSI assembly protein Ycf4, PSI chlorophyll a apoprotein A1/A2, Ferredoxin--NADP reductase, and ATP synthase subunit alpha) or increased (Chlorophyll a-b binding protein, PSII 22 kDa protein 1) accumulation in stressed S11 729-10 relative to control conditions at 28 d. Furthermore, these proteins were specifically involved in light absorption by PSII antenna, energy trapping by PSII reaction centers and energy flux associated with electron transport from intersystem to final PSI acceptors, suggesting better maintenance of sequential photosynthetic component processes in heat-tolerant S11 729-10 especially during the later phase of stress. These were consistent with the measurements of chlorophyll fluorescence traits in our study. Healthier light harvesting components, eventually, could lead to greater production of ATP and NADPH, which are an important energy source and reducing agent, respectively, and could impact numerous cellular activities beyond the dark reaction [36].

4.2. DEPs Associated with Antioxidant Defense

High temperature accelerates ROS production resulting in oxidative stress, making enhanced antioxidant capacity one of the most fundamental protective responses [222]. Increased activity or accumulation of antioxidants, like peroxidase, superoxide dismutase and ascorbate peroxidase, have been reported previously when plants were exposed to heat stress [55, 211, 223]. Typically, more heat-tolerant plants would present stronger antioxidant activity due to greater accumulation of antioxidants as supported by these studies. In addition to cultivar or line differences, antioxidant capacity was also affected by stress duration. For instance, the activity of

superoxide dismutase increased in creeping bentgrass leaves at 18 d of heat stress, but then presented significant declines at 28 d and 35 d [205, 224]. The authors highlighted that plants could activate antioxidant defense to acclimate to oxidative damage in response to an earlier phase of heat stress, but antioxidant defense decreased as a consequence of damage accumulation when plants suffered from severe stress at a later phase. Similar findings were confirmed in our study. Specifically, the expression of identified antioxidant proteins was mostly enhanced in Crenshaw at 14 d. Moreover, the responses were stronger compared to S11 729-10 on the same day as evidenced by a larger number of upregulated DEPs as well as greater extents of upregulation, indicating that Crenshaw might be experiencing a more severe ROS attack. From 14 d to 28 d, the number of upregulated DEPs (catalase, superoxide dismutase [Mn], thioredoxin reductase) decreased for Crenshaw although the extents of upregulation were enhanced. When stress persisted for longer durations, antioxidant proteins can become denatured and nonfunctional due to accumulated damage from heat stress and ROS, which might explain the fewer upregulated DEPs. In contrast to the decrease for Crenshaw, an increase in the number of upregulated DEPs (catalase, superoxide dismutase [Mn], L-ascorbate peroxidase, probable L-ascorbate peroxidase 8, ferritin, peptide methionine sulfoxide reductase A4, probable glutathione S-transferase DHAR2) was detected for S11 729-10 at 28 d relative to 14 d, indicating improved antioxidant defense. Furthermore, at 28 d, antioxidant proteins in S11 729-10 mostly showed enhanced expression or better maintenance of accumulation compared to the corresponding ones in Crenshaw. This might contribute to the reduced oxidative stress observed in the heat-tolerant S11 729-10, as supported by its greater cell membrane stability, as evaluated by EL. Overall, these suggested that Crenshaw experienced more severe oxidative stress during the early phase of heat stress, while S11 729-10

enhanced its survival by increasing the accumulation of antioxidant proteins during the later phase, thereby leading to improved performance under prolonged stress [55].

4.3. DEPs Associated with Protein Folding and Degradation

The induction of HSPs is a common response to the formation of aberrant proteins induced by heat stress [135]. HSPs work by promoting refolding of misfolded proteins, thereby helping maintain proteins' functional conformations. Consistent with previous literature [205, 211, 225], enhanced accumulation of HSPs of different sizes, such as HSP60, HSP70, HSP80, were detected under temperature elevation in both lines. Plus, the level of upregulation for these HSPs continued to rise from 14 d to 28 d, possibly suggesting increased accumulation of damaged proteins. Particularly, Chaperonin CPN60-1 belonging to the HSP60 family, was upregulated prominently, by 9.4, and 9.5 fold in stressed Crenshaw and S11 729-10, respectively, at 28 d. This dramatic upregulation might suggest its crucial role in protein repair in both lines. Despite the common induction, line-specific protein induction was also observed. For example, HOP was uniquely induced in S11 729-10 while BIP1 was only upregulated in Crenshaw at 28 d. HOP is a family of cytosolic co-chaperones whose role in thermotolerance is deeply analyzed in other eukaryotes, but is largely unexplored in plants with exception of a few studies [226]. In Arabidopsis, HOP3 was highly induced in response to temperature elevation and HOP-overexpressing plants displayed enhanced tolerance to heat [227, 228]. Contrastingly, the HOP mutants rendered Arabidopsis sensitive to heat stress with an unusual high accumulation of insoluble and ubiquitinated proteins, which underscores the crucial role of HOP in protein quality control under heat [227]. Unlike the significant gap in the study of HOP in heat stress, more efforts have been made to advance the understanding of BIP in thermotolerance. BIP expression was reported to be upregulated in response to temperature elevation in various plants [229-232]. In pepper (*Capsicum annuum* L.),

a BIP-overexpression line displayed improved heat tolerance with reduced oxidative damage, as manifested by lower contents of malondialdehyde and H_2O_2, while the silencing of the BIP1 gene resulted in more severe injury symptoms, rendering it susceptible to heat stress [230]. Similar results were also found in Arabidopsis [229], suggesting the protective role of BIP1 against heat stress. The unique induction of these HSPs might indicate activation of different defense pathways and contribute to the contrasting heat tolerance in the two creeping bentgrass lines.

In addition to being repaired, another fate for damaged proteins is to be degraded through proteolytic machinery like proteases and the UPS, as described earlier. Lower proteolysis activity typically corresponded to less severe protein damage and higher protein content, in turn associated with greater thermotolerance [74, 233]. In our study, two proteolysis-related proteins were identified to be differentially expressed, which were proteasome subunit beta and endopeptidase Clp (Table S2, S3, S4, S5). The former is an integral component of the UPS while the latter belongs to the category of serine proteases [66, 181]. Intriguingly, no matter at 14 d or at 28 d, both proteasome subunit beta and endopeptidase Clp were downregulated to greater extents in S11 729-10 than in Crenshaw, possibly suggesting lower proteolytic activity and slower protein degradation in S11 729-10, as enzyme concentration typically correlates positively with catalytic activity [36]. This could be associated with less severe downregulation of proteins involved in important pathways, like the aforementioned light reaction of photosynthesis, conferring greater thermotolerance in heat-tolerant S11 729-10.

4.4. Differentially and Uniquely Expressed Polyubiquitinated Proteins

Using polyubiquitin-omics, a number of polyubiquitinated proteins were identified to be associated with various important cellular activities, including photosynthesis, protein folding, proteolysis, transport, signal transduction and redox homeostasis, as supported by GO term

analysis. In addition to line-unique expression, differential accumulation of polyubiquitinated proteins was detected in S11 729-10 relative to Crenshaw in response to temperature elevation, with most of these proteins enriched in antioxidant defense, energy metabolism and protein metabolism. Similar attempts on the identification of substrate proteins targeted by the UPS pathway have also been made previously under various environmental conditions [109]. For instance, enhanced ubiquitination was found when rice roots were exposed to heat stress, with the majority of polyubiquitinated proteins being associated with sucrose and starch metabolism, as well as the ribosomal system [129]. In the case of salt stress, greater upregulation of ubiquitin-modified HSP81-1 and aldehyde oxidase 3 were seen in rice lines - TNG67 and SA0604, indicating more severe protein degradation via the UPS, which might contribute to the inferior salt tolerance in TNG67 and SA0604 compared to the more tolerant SM75 [131].

Among those differentially and uniquely expressed polyubiquitinated proteins identified in our study, antioxidant proteins were either significantly upregulated (Catalase, Germin-like protein 8-14, L-ascorbate peroxidase, Plant heme peroxidase family profile domain-containing protein, Probable glutathione S-transferase DHAR2) or uniquely induced (Peroxidase, Superoxide dismutase [Cu-Zn] 4AP) in S11 729-10 compared to Crenshaw, potentially suggesting a faster turnover. Heat stress leads to accumulation of damaged proteins and an elevated need for ROS detoxication. To meet this demand, plants might rapidly degrade antioxidant proteins that were denatured or oxidized though the UPS, while synthesizing more new antioxidant proteins for replacement, contributing to reduced oxidative damage and thereby improved tolerance [234, 235]. This is consistent with the enhanced expression of several antioxidant proteins (Catalase, L-ascorbate peroxidase, Plant heme peroxidase family profile domain-containing protein, Probable glutathione S-transferase DHAR2) in S11 729-10 when heat-stressed samples were compared

against control ones at 28 d according to the gel-free proteomics results (Figure 4.7b). Similarly, greater upregulation of polyubiquitinated proteins involved in energy metabolism (Cytochrome c, Photosystem I iron-sulfur center, Pyruvate kinase), chaperone activity (18.1 kDa class I heat shock protein, Peptidyl-prolyl cis-trans isomerase) and transport (Kinesin-like protein) was observed in S11 729-10 than Crenshaw. The faster turnover of those might enable more efficient ATP production, protein refolding of damaged proteins, as well as transport of key molecules involved in stress responses, leading to improved tolerance in S11 729-10. These are in accordance with previous research where higher degradation rates of HSPs, antioxidant proteins (catalases and peroxidases) and photorespiration-related proteins were detected when *Arabidopsis thaliana* seedlings were exposed to elevated temperature [234]. The authors proposed that the faster turnover might represent an important adaptive mechanism to maintain cellular homeostasis and improve plant survival under stressful conditions. In contrast to the upregulation mostly observed, polyubiquitinated E3 ligase showed significant downregulation in heat-stressed S11 729-10 compared to heat-stressed Crenshaw, potentially indicating greater stability. This is further supported by the gel-free proteomics results, which found that E3 ligase levels were better maintained in S11 729-10 compared to Crenshaw under heat stress, relative to control conditions. Given the role of E3 ligase in tagging substrate protein for degradation via the UPS, better maintenance of E3 ligase levels enables more effective removal of heat-induced damaged proteins, reducing cellular toxicity and preserving protein quality [236]. On the other hand, E3 ligases are involved in modulating key stress-responsive proteins, including transcription factors and signaling molecules [236]. By ensuring that these regulatory proteins are activated or degraded as needed, better maintenance of E3 ligase levels allows plants to adjust more rapidly and robustly to heat stress. Taken together, the accumulation of polyubiquitinated proteins in plants during heat

stress is a complex process, and changes in the levels of proteins and their polyubiquitinated forms are not always synchronized, despite that ubiquitination typically leads to protein degradation.

5. Conclusions

Gel-free proteomics were applied to heat-stressed creeping bentgrass to reveal the change in proteome profile determining differential physiological performance among lines. It showed that some common metabolic processes, like photosynthesis, antioxidant defense and protein refolding, could be responsible for regulating heat tolerance in contrasting lines. Heat-tolerant S11 729-10 was able to maintain less severe downregulation of the proteins involved in the light reactions of photosynthesis, while enhancing the upregulation of antioxidant proteins, particularly during the later phase of stress. These contributed to improved physiological responses including greater cell membrane stability as well as healthier light-harvesting components, eventually leading to higher overall tolerance levels in S11 729-10. For the first time, polyubiquitin-omics analysis was applied to turfgrass research, revealing differentially or uniquely expressed polyubiquitinated proteins in S11 729-10, with enrichment in antioxidant defense, energy production, and protein metabolism. Notably, the faster turnover of key polyubiquitinated antioxidant proteins in S11 729-10 likely represents a critical mechanism for protecting against oxidative damage and enhancing tolerance under prolonged heat stress. Our findings suggest the power of gel-free proteomics and polyubiquitin-omics in improving the understanding of global protein accumulation and degradation though the UPS, as well as their associated physiological responses. The stress-related traits or proteins identified in this study could be utilized for the development of new cultivars with enhanced thermotolerance to help plants cope with climate change. Further studies are needed to gain a more complete picture of how protein metabolism is regulated at multiple levels.

Acknowledgements

Sincere thanks go to Dr. Stacy Bonos for providing the plant materials. We'd like to thank Proteomics and Mass Spectrometry Facility at the University of Georgia (UGA) for LC-MS/MS analysis. The Orbitrap Elite Mass Spectrometer was purchased using a NIH grant (Grant number: S10RR028859) from Professor I. Jonathan Amster at the Department of Chemistry, UGA.

Author Contributions

QF designed the study, conducted the study, performed data collection, analysis, and visualization, prepared the original draft and edited it. DJ designed the study, provided resources as well as supervision, reviewed and edited the manuscript.

Conflict of Interest

The authors declare that there is no conflict of interest.

References

1. Pachauri, R.K. and L. Meyer. *Climate change 2014 Synthesis Report-Summary for Policymakers*. 2014. Geneva, Switzerland: Intergovernmetnal Panel on Climate Change (IPCC).
2. Fan, Q. and D. Jespersen, Assessing Heat Tolerance in Creeping Bentgrass Lines Based on Physiological Responses. *Plants*, 2023. **12**(1): p. 41 DOI: 10.3390/plants12010041.
3. Goldberg, A.L., Protein degradation and protection against misfolded or damaged proteins. *Nature*, 2003. **426**(6968): p. 895-899 DOI: 10.1038/nature02263.
4. Parsell, D. and S. Lindquist, The function of heat-shock proteins in stress tolerance: degradation and reactivation of damaged proteins. *Annual review of genetics*, 1993. **27**(1): p. 437-496 DOI: 10.1146/annurev.ge.27.120193.002253.

5. Huang, B.R., M. DaCosta, and Y.W. Jiang, Research Advances in Mechanisms of Turfgrass Tolerance to Abiotic Stresses: From Physiology to Molecular Biology. *Critical Reviews in Plant Sciences*, 2014. **33**(2-3): p. 141-189 DOI: 10.1080/07352689.2014.870411.

6. Zhao, Y. and Z. Hou, Application of proteomics to determine the mechanism of ozone on sweet cherries (Prunus avium L.) by time-series analysis. *Frontiers in Plant Science*, 2023. **14**: p. 66 DOI: 10.3389/fpls.2023.1065465.

7. Wang, X., et al., Heat-responsive photosynthetic and signaling pathways in plants: insight from proteomics. *International journal of molecular sciences*, 2017. **18**(10): p. 2191 DOI: 10.3390/ijms18102191.

8. Lyon, D., et al., Drought and recovery: independently regulated processes highlighting the importance of protein turnover dynamics and translational regulation in Medicago truncatula. *Molecular & Cellular Proteomics*, 2016. **15**(6): p. 1921-1937 DOI: 10.1074/mcp.M115.049205.

9. Ali, A.E.E., et al., Comparative Proteomics Analysis between Maize and Sorghum Uncovers Important Proteins and Metabolic Pathways Mediating Drought Tolerance. *Life*, 2023. **13**(1): p. 170 DOI: 10.3390/life13010170.

10. Sinha, R., et al., The effects of multifactorial stress combination on rice and maize. *Plant Physiology*, 2024. **194**(3): p. 1358-1369 DOI: 10.1093/plphys/kiad557.

11. Fry, J. and B. Huang, Applied turfgrass science and physiology. 2004.

12. Jespersen, D. and B. Huang, Proteins associated with heat-induced leaf senescence in creeping bentgrass as affected by foliar application of nitrogen, cytokinins, and an ethylene inhibitor. *Proteomics*, 2015. **15**(4): p. 798-812 DOI: 10.1002/pmic.201400393.

13. Huang, B.R. and C.P. Xu, Identification and characterization of proteins associated with plant tolerance to heat stress. *Journal of Integrative Plant Biology*, 2008. **50**(10): p. 1230-1237 DOI: 10.1111/j.1744-7909.2008.00735.x.

14. Xu, C.P. and B.R. Huang, Differential proteomic response to heat stress in thermal Agrostis scabra and heat-sensitive Agrostis stolonifera. *Physiologia Plantarum*, 2010. **139**(2): p. 192-204 DOI: 10.1111/j.1399-3054.2010.01357.x.

15. Li, Z., et al., γ-Aminobutyric acid enhances heat tolerance associated with the change of proteomic profiling in creeping bentgrass. *Molecules*, 2020. **25**(18): p. 4270 DOI: 10.3390/molecules25184270.

16. Zargar, S., et al., Shift from gel based to gel free proteomics to unlock unknown regulatory network in plants: a comprehensive review. *J. Adv. Res. Biotechnol*, 2016. **1**(19.10): p. 15226 DOI: 10.15226/2475-4714/1/2/00107.

17. van Wijk, K.J. and Z. Adam, Does the polyubiquitination pathway operate inside intact chloroplasts to remove proteins? *The Plant Cell*, 2024: p. koae104 DOI: 10.1093/plcell/koae104.

18. Xu, J., et al., The ubiquitin-proteasome system in the plant response to abiotic stress: potential role in crop resilience improvement. *Plant Science*, 2024: p. 112035 DOI: 10.1016/j.plantsci.2024.112035.

19. Zhang, Z., et al., Roles of ubiquitination-mediated protein degradation in plant responses to abiotic stresses. *Environmental and Experimental Botany*, 2015. **114**: p. 92-103.

20. Doroodian, P. and Z. Hua, The ubiquitin switch in plant stress response. *Plants*, 2021. **10**(2): p. 246 DOI: 10.3390/plants10020246.

21. Shang, F. and A. Taylor, Ubiquitin–proteasome pathway and cellular responses to oxidative stress. *Free Radical Biology and Medicine*, 2011. **51**(1): p. 5-16 DOI: 10.1016/j.freeradbiomed.2011.03.031.

22. Paradiso, A., et al., Cyclic AMP mediates heat stress response by the control of redox homeostasis and ubiquitin-proteasome system. *Plant, Cell & Environment*, 2020. **43**(11): p. 2727-2742 DOI: 10.1111/pce.13878.

23. Ferguson, D.L., J.A. Guikema, and G.M.J.P.P. Paulsen, Ubiquitin pool modulation and protein degradation in wheat roots during high temperature stress. *Plant Physiology*, 1990. **92**(3): p. 740-746 DOI: 10.1104/pp.92.3.740.

24. Fan, W., H. Zheng, and G. Wang, Proteomic analysis of ubiquitinated proteins in maize immature kernels. *Journal of Proteomics*, 2021. **243**: p. 104261 DOI: 10.1016/j.jprot.2021.104261.

25. Berger, N., et al., Root membrane ubiquitinome under short-term osmotic stress. *International Journal of Molecular Sciences*, 2022. **23**(4): p. 1956 DOI: 10.1101/2021.12.06.471398.

26. Ying, Y., Y. Pang, and J. Bao, Comparative ubiquitome analysis reveals diverse functions of ubiquitination in rice seed development under high-temperature stress. *Seed Biology*, 2023. **2**(1) DOI: 10.48130/seedbio-2023-0023.

27. Olzmann, J.A. and L.-S. Chin, Parkin-mediated K63-linked polyubiquitination: a signal for targeting misfolded proteins to the aggresome-autophagy pathway. *Autophagy*, 2008. **4**(1): p. 85-87.

28. Majer, S.H., Ubiquitin Mass Spectrometry Kit: A Mass Spec Approach to Ubiquitomics. 2024.

29. Krans, J.V. and K. Morris, Determining a profile of protocols and standards used in the visual field assessment of turfgrasses: A survey of national turfgrass evaluation program-sponsored university scientists. 2007 DOI: 10.1094/ATS-2007-1130-01-TT.

30. Karcher, D.E. and M.D. Richardson, Digital image analysis in turfgrass research. *Turfgrass: Biology, use, and management*, 2013. **56**: p. 1133-1149-2 DOI: 10.2134/agronmonogr56.c29.

31. Stirbet, A., D. Lazár, and J. Kromdijk, Chlorophyll a fluorescence induction: can just a one-second measurement be used to quantify abiotic stress responses? *Photosynthetica*, 2018. **56**(1): p. 86-104 DOI: 10.1007/s11099-018-0770-3.

32. Blum, A. and A.J.C.S. Ebercon, Cell membrane stability as a measure of drought and heat tolerance in wheat 1. 1981. **21**(1): p. 43-47 DOI: 10.2135/cropsci1981.0011183X002100010013x.

33. Niu, L., et al., Modified TCA/acetone precipitation of plant proteins for proteomic analysis. *PLoS One*, 2018. **13**(12): p. e0202238 DOI: 10.1371/journal.pone.0202238.

34. Bradford, M.M., A rapid and sensitive method for the quantitation of microgram quantities of protein utilizing the principle of protein-dye binding. *Analytical biochemistry*, 1976. **72**(1-2): p. 248-254 DOI: 10.1016/0003-2697(76)90527-90523.

35. Nagaraj, N., et al., Detergent-based but gel-free method allows identification of several hundred membrane proteins in single LC-MS runs. *Journal of proteome research*, 2008. **7**(11): p. 5028-5032 DOI: 10.1021/pr800412j.

36. Li, J., et al., Differential proteomic analysis of soybean anthers by iTRAQ under high-temperature stress. *Journal of proteomics*, 2020. **229**: p. 103968 DOI: 10.1016/j.jprot.2020.103968.

37. Li, Z., et al., iTRAQ-based proteomics reveals key role of γ-aminobutyric acid (GABA) in regulating drought tolerance in perennial creeping bentgrass (Agrostis stolonifera). *Plant Physiology and Biochemistry*, 2019. **145**: p. 216-226.

38. Conesa, A., et al., Blast2GO: a universal tool for annotation, visualization and analysis in functional genomics research. *Bioinformatics*, 2005. **21**(18): p. 3674-3676 DOI: 10.1093/bioinformatics/bti610.

39. Kolberg, L., et al., gprofiler2--an R package for gene list functional enrichment analysis and namespace conversion toolset g: Profiler. *F1000Research*, 2020. **9** DOI: 10.12688/f1000research.24956.2.

40. Liu, X. and B. Huang, Heat stress injury in relation to membrane lipid peroxidation in creeping bentgrass. *Crop Science*, 2000. **40**(2): p. 503-510 DOI: 10.2135/cropsci2000.402503x.

41. Du, H., Z. Wang, and B. Huang, Differential responses of warm-season and cool-season turfgrass species to heat stress associated with antioxidant enzyme activity. *Journal of the American Society for Horticultural Science*, 2009. **134**(4): p. 417-422 DOI: 10.21273/JASHS.134.4.417.

42. Snider, J.L., et al., OJIP-fluorescence parameters as rapid indicators of cotton (Gossypium hirsutum L.) seedling vigor under contrasting growth temperature regimes. *Plant physiology and biochemistry*, 2018. **132**: p. 249-257 DOI: 10.1016/j.plaphy.2018.09.015.

43. Fan, Q., et al., Dose-dependent physiological effects of UV-C radiation on seashore paspalum. *Plant Physiology and Biochemistry*, 2024. **208**: p. 108514 DOI: 10.1016/j.plaphy.2024.108514.

44. Zhou, L., et al., Application of Chlorophyll Fluorescence Analysis Technique in Studying the Response of Lettuce (Lactuca sativa L.) to Cadmium Stress. *Sensors*, 2024. **24**(5): p. 1501 DOI: 10.3390/s24051501.

45. Chen, S., et al., Classification and characteristics of heat tolerance in Ageratina adenophora populations using fast chlorophyll a fluorescence rise OJIP. *Environmental and Experimental Botany*, 2016. **122**: p. 126-140 DOI: 10.1016/j.envexpbot.2015.09.011.

46. Zhang, L., et al., The Effect of high-temperature stress on the physiological indexes, chloroplast ultrastructure, and photosystems of two herbaceous peony cultivars. *Journal of Plant Growth Regulation*, 2022: p. 1-16 DOI: 10.1007/s00344-022-10647-9.

47. Jespersen, D., C.P. Xu, and B.R. Huang, Membrane Proteins Associated with Heat-Induced Leaf Senescence in a Cool-Season Grass Species. *Crop Science*, 2015. **55**(2): p. 837-850 DOI: 10.2135/cropsci2014.04.0335.

48. Schmitt, K.F.M., et al., Decoding the effects of drought stress on popcorn (Zea mays var. everta) flowering combining proteomics and physiological analysis. *Plant Physiology and Biochemistry*, 2024. **208**: p. 108444 DOI: 10.1016/j.plaphy.2024.108444.

49. Kosová, K., et al., Plant proteome changes under abiotic stress—contribution of proteomics studies to understanding plant stress response. *Journal of proteomics*, 2011. **74**(8): p. 1301-1322 DOI: 10.1016/j.jprot.2011.02.006.

50. Taiz, L. and E. Zeiger, *Plant Physiology 5 ed. Sunderland, MA*. 2006, the Sinauer Associates.

51. Rocco, M., et al., Proteomic analysis of temperature stress-responsive proteins in Arabidopsis thaliana rosette leaves. *Molecular BioSystems*, 2013. **9**(6): p. 1257-1267 DOI: 10.1039/c3mb70137a.

52. Ahsan, N., et al., Tissue-specific defense and thermo-adaptive mechanisms of soybean seedlings under heat stress revealed by proteomic approach. *Journal of proteome research*, 2010. **9**(8): p. 4189-4204 DOI: 10.1021/pr100504j.

53. Li, H., et al., High temperature effects on D1 protein turnover in three wheat varieties with different heat susceptibility. *Plant Growth Regulation*, 2017. **81**(1): p. 1-9 DOI: 10.1007/s10725-016-0179-6.

54. Han, F., et al., A comparative proteomic analysis of rice seedlings under various high-temperature stresses. *Biochimica et Biophysica Acta (BBA)-Proteins and Proteomics*, 2009. **1794**(11): p. 1625-1634 DOI: 10.1016/j.bbapap.2009.07.013.

55. Xu, C.P. and B.R. Huang, Comparative Analysis of Proteomic Responses to Single and Simultaneous Drought and Heat Stress for Two Kentucky Bluegrass Cultivars. *Crop Science*, 2012. **52**(3): p. 1246-1260 DOI: 10.2135/cropsci2011.10.0551.

56. Wang, P., et al., Reactive oxygen species: multidimensional regulators of plant adaptation to abiotic stress and development. *Journal of Integrative Plant Biology*, 2024. **66**(3): p. 330-367 DOI: 10.1111/jipb.13601.

57. Li, F.F., et al., Antioxidant and Hormone Responses to Heat Stress in Two Kentucky Bluegrass Cultivars Contrasting in Heat Tolerance. *Journal of the American Society for Horticultural Science*, 2014. **139**(5): p. 587-596 DOI: 10.21273/jashs.139.5.587.

58. Li, Z., et al., Proteomic and metabolomic profilings reveal crucial functions of γ-aminobutyric acid in regulating Ionic, water, and metabolic homeostasis in creeping bentgrass under salt stress. *Journal of proteome research*, 2020. **19**(2): p. 769-780 DOI: 10.1021/acs.jproteome.9b00627.

59. Li, Z., et al., Metabolic pathways regulated by γ-aminobutyric acid (GABA) contributing to heat tolerance in creeping bentgrass (Agrostis stolonifera). *Scientific Reports*, 2016. **6**(1): p. 1-16 DOI: 10.1038/srep30338.

60. Wang, K., et al., Heat shock proteins in relation to heat stress tolerance of creeping bentgrass at different N levels. *PLoS One*, 2014. **9**(7): p. e102914 DOI: 10.1371/journal.pone.0102914.

61. Toribio, R., et al., HOP, a co-chaperone involved in response to stress in plants. *Frontiers in Plant Science*, 2020. **11**: p. 591940 DOI: 10.3389/fpls.2020.591940.

62. Fernández-Bautista, N., et al., HOP family plays a major role in long-term acquired thermotolerance in Arabidopsis. *Plant, cell & environment*, 2018. **41**(8): p. 1852-1869 DOI: 10.1111/pce.13326.

63. Wang, Y.-X., et al., Heat shock protein TaHSP17. 4, a TaHOP interactor in wheat, improves plant stress tolerance. *International Journal of Biological Macromolecules*, 2023. **246**: p. 125694 DOI: 10.1016/j.ijbiomac.2023.125694.

64. Yang, X., et al., Activation of autophagy by unfolded proteins during endoplasmic reticulum stress. *The Plant Journal*, 2016. **85**(1): p. 83-95 DOI: 10.1111/tpj.13091.

65. Wang, H., et al., Characterization of BiP genes from pepper (Capsicum annuum L.) and the role of CaBiP1 in response to endoplasmic reticulum and multiple abiotic stresses. *Frontiers in Plant Science*, 2017. **8**: p. 1122 DOI: 10.3389/fpls.2017.01122.

66. Zhang, L., et al., Genome-wide analysis and expression profiling under heat and drought treatments of HSP70 gene family in soybean (Glycine max L.). *Frontiers in plant science*, 2015. **6**: p. 773 DOI: 10.3389/fpls.2015.00773.

67. Jung, K.-H., et al., Genome-wide expression analysis of HSP70 family genes in rice and identification of a cytosolic HSP70 gene highly induced under heat stress. *Functional & integrative genomics*, 2013. **13**: p. 391-402 DOI: 10.1007/s10142-013-0331-6.

68. Rossi, S. and B. Huang, Protease inhibitors suppressed leaf senescence in creeping bentgrass exposed to heat stress in association with inhibition of protein degradation into free amino acids. *Plant Growth Regulation*, 2023: p. 1-11 DOI: 10.1007/s10725-023-00977-3.

69. Chauhan, S., et al., Wheat cultivars differing in heat tolerance show a differential response to monocarpic senescence under high-temperature stress and the involvement of serine proteases. 2009. **47**(4): p. 536-547 DOI: 10.1007/s11099-009-0079-3.

70. Stone, S.L., Role of the ubiquitin proteasome system in plant response to abiotic stress. *International review of cell and molecular biology*, 2019. **343**: p. 65-110 DOI: 10.1016/bs.ircmb.2018.05.012.

71. Roberts, I.N., et al., Senescence-associated proteases in plants. *Physiologia Plantarum*, 2012. **145**(1): p. 130-139 DOI: 10.1111/j.1399-3054.2012.01574.x.

72. Liu, C.W., et al., Proteomic analysis of salt-responsive ubiquitin-related proteins in rice roots. *Rapid Communications in Mass Spectrometry*, 2012. **26**(15): p. 1649-1660 DOI: 10.1002/rcm.6271.

73. Fan, K.-T., Y. Xu, and A.D. Hegeman, Elevated Temperature Effects on Protein Turnover Dynamics in Arabidopsis thaliana Seedlings Revealed by 15N-Stable Isotope Labeling and ProteinTurnover Algorithm. *International Journal of Molecular Sciences*, 2024. **25**(11): p. 5882 DOI: 10.3390/ijms25115882.

74. Li, L., et al., Enzymes degraded under high light maintain proteostasis by transcriptional regulation in Arabidopsis. *Proceedings of the National Academy of Sciences*, 2022. **119**(20): p. e2121362119 DOI: 10.1101/2021.10.03.462903.

75. Shu, K. and W. Yang, E3 ubiquitin ligases: ubiquitous actors in plant development and abiotic stress responses. *Plant and Cell Physiology*, 2017. **58**(9): p. 1461-1476 DOI: 10.1093/pcp/pcx071.

Tables and Figures

Table 4.1 List of differentially expressed polyubiquitinated proteins with their accession ID, description and fold change (FC) when comparing S11 729-10 against Crenshaw under heat stress at 28 d.

Accession	Description	FC
A0A3B6KQP3	Catalase OS=Triticum aestivum	1.2
Q6ZBZ2	Germin-like protein 8-14 OS=Oryza sativa subsp. Japonica	2.7
A0A3B6PVU5	L-ascorbate peroxidase OS=Triticum aestivum	2.2
A0A0E0QCR5	Plant heme peroxidase family profile domain-containing protein OS=Oryza rufipogon	5.7
Q67UK9	Probable glutathione S-transferase DHAR2, chloroplastic OS=Oryza sativa subsp. Japonica	2.5
Q84Q72	18.1 kDa class I heat shock protein OS=Oryza sativa subsp. japonica	3.9
P21569	Peptidyl-prolyl cis-trans isomerase OS=Zea mays	4.8
P00068	Cytochrome c OS=Triticum aestivum	3.6
Q7FAH2	Glyceraldehyde-3-phosphate dehydrogenase 2, cytosolic OS=Oryza sativa subsp. Japonica	0.6
A0A0E0EN62	Photosystem I iron-sulfur center OS=Oryza meridionalis	6.0
A0A0E0HXE6	Pyruvate kinase OS=Oryza nivara	5.8
Q8L5C6	Xylanase inhibitor protein 1 OS=Triticum aestivum	0.6
A0A1D6HLU2	Kinesin-like protein OS=Zea mays	1.5
P02276	Histone H2A.2.1 OS=Triticum aestivum	0.3
A2WKT4	Histone H2B.5 OS=Oryza sativa subsp. indica	0.2
P68428	Histone H3.2 OS=Triticum aestivum	0.3
P62787	Histone H4 OS=Zea mays	0.4
A0A0E0D0N3	RING-type E3 ubiquitin transferase OS=Oryza meridionalis	0.3
C5WVT9	Guanine nucleotide-binding protein alpha subunit OS=Sorghum bicolor	5.9
Q7F8T6	Tricin synthase 2 OS=Oryza sativa subsp. japonica	0.3

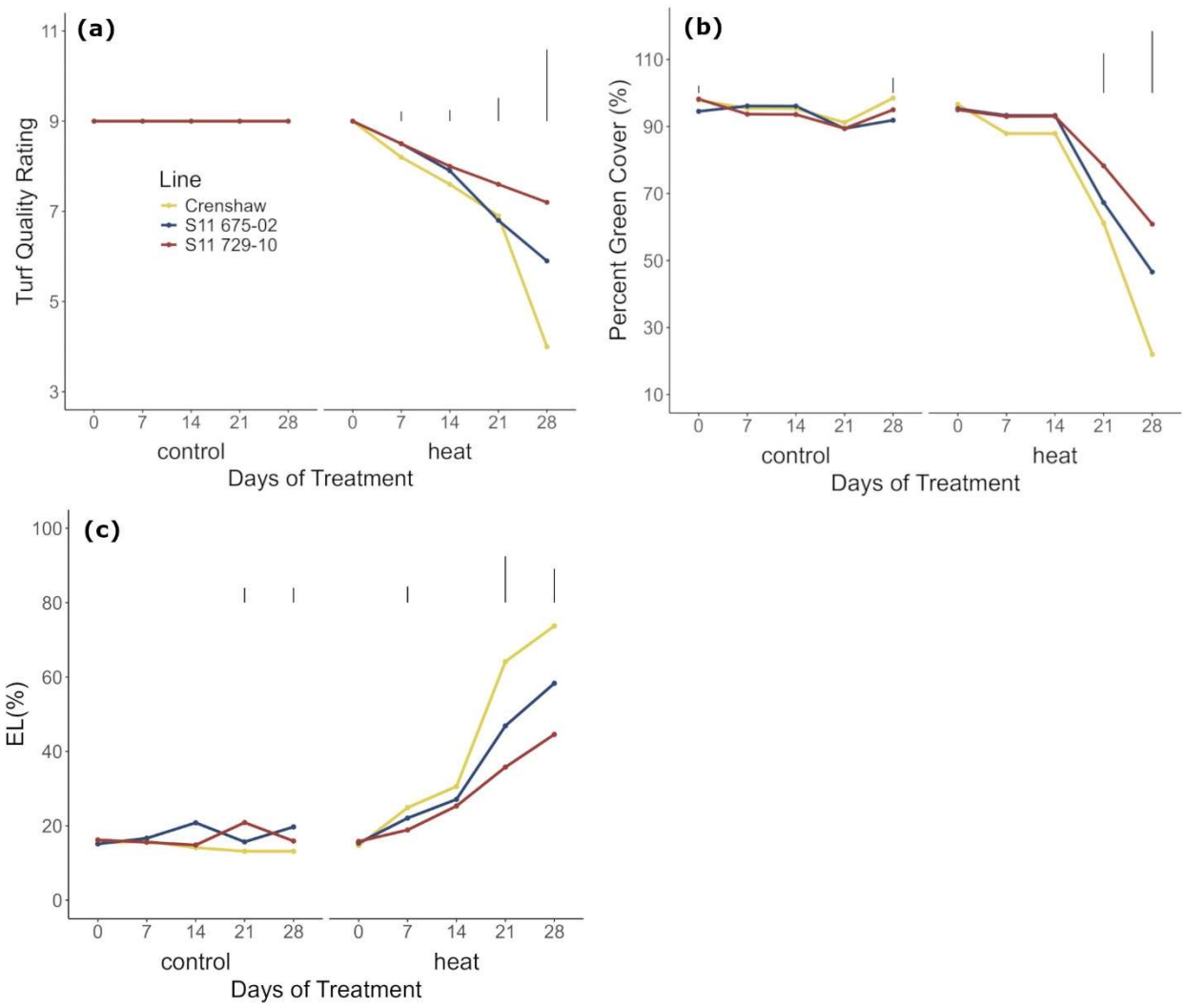

Figure 4.1 Change in turf quality ratings (a), green cover (b) and electrolyte leakage (EL) (c) for creeping bentgrass lines over time under control (20/15 °C day/night) and heat stress (38/33 °C day/night) conditions. Bars represent LSD values at $p = 0.05$ on days when significant differences among lines were found.

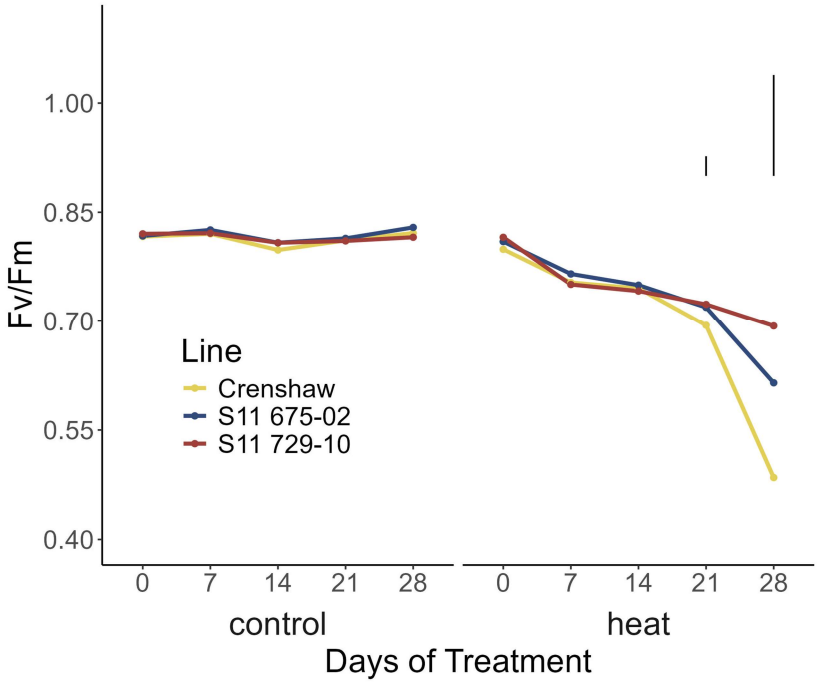

Figure 4.2 Change in Fv/Fm for creeping bentgrass lines over time under control (20/15 °C day/night) and heat stress (38/33 °C day/night) conditions. Bars represent LSD values at $p = 0.05$ on days when significant differences among lines were found. Fv/Fm, quantum efficiency of energy flux trapped by photosystem II photochemistry.

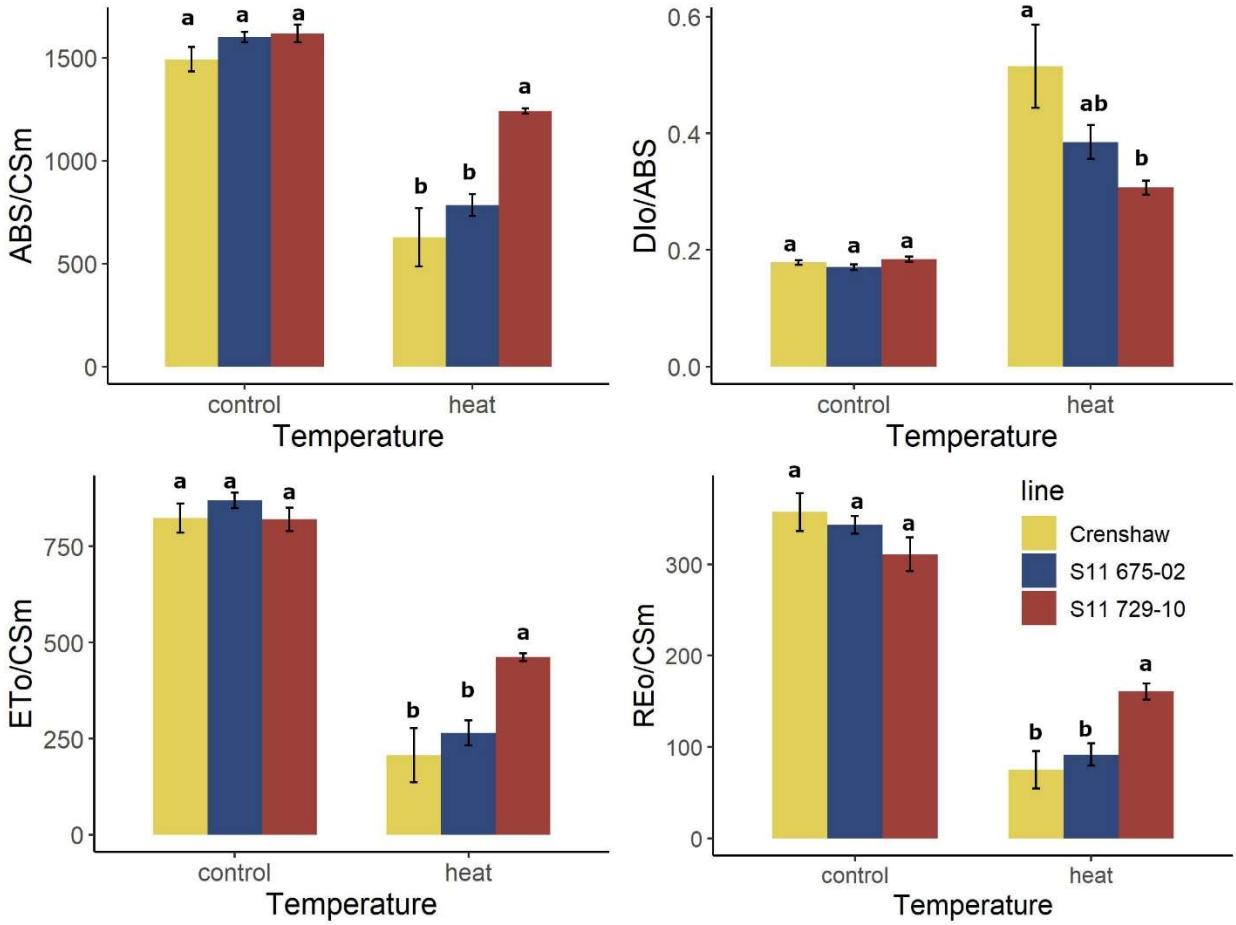

Figure 4.3 Chlorophyll fluorescence traits for creeping bentgrass lines under control (20/15 °C day/night) and heat stress (38/33 °C day/night) conditions at 28 d. Data are presented as means ± standard errors. Columns marked with the same lowercase letters are not significantly different at $p = 0.05$ within each temperature condition. ABS/CSm, absorbed energy flux per cross section; DIo/ABS, quantum efficiency of energy dissipation in PSII antenna; ETo/CSm, the energy flux associated with electron transport from quinone A to intersystem electron acceptors such as plastoquinone pool per cross section; REo/ CSm, the energy flux associated with electron transport from intersystem electron acceptors to final photosystem I acceptors per cross section.

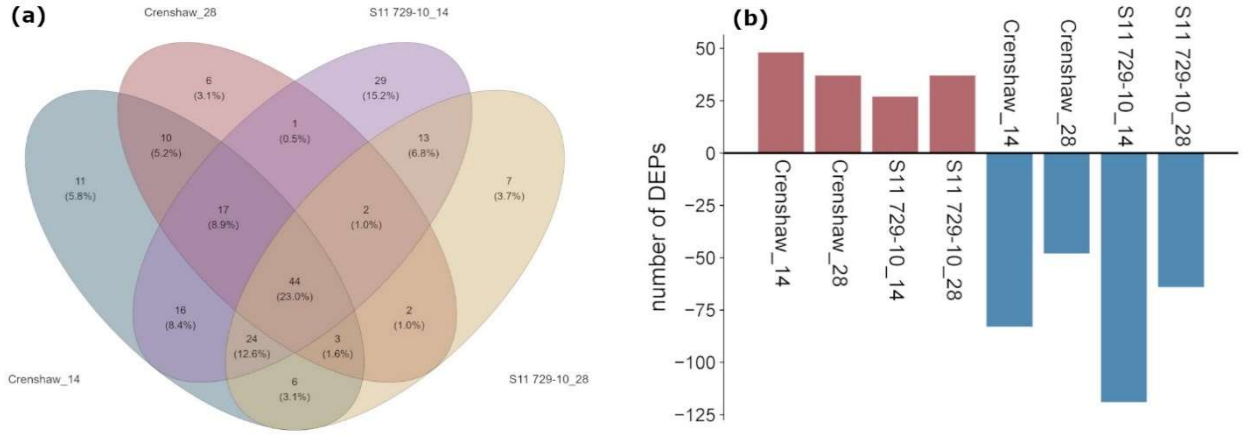

Figure 4.4 Overall change in differentially expressed proteins (DEPs) of two creeping bentgrass lines (Crenshaw and S11 729-10) at 14 d and 28 d. Venn diagram showing common and unique DEPs among different groups (a). Bar plot showing upregulated and downregulated proteins for each group (b). Red bars represented upregulation while blue bars represented downregulation.

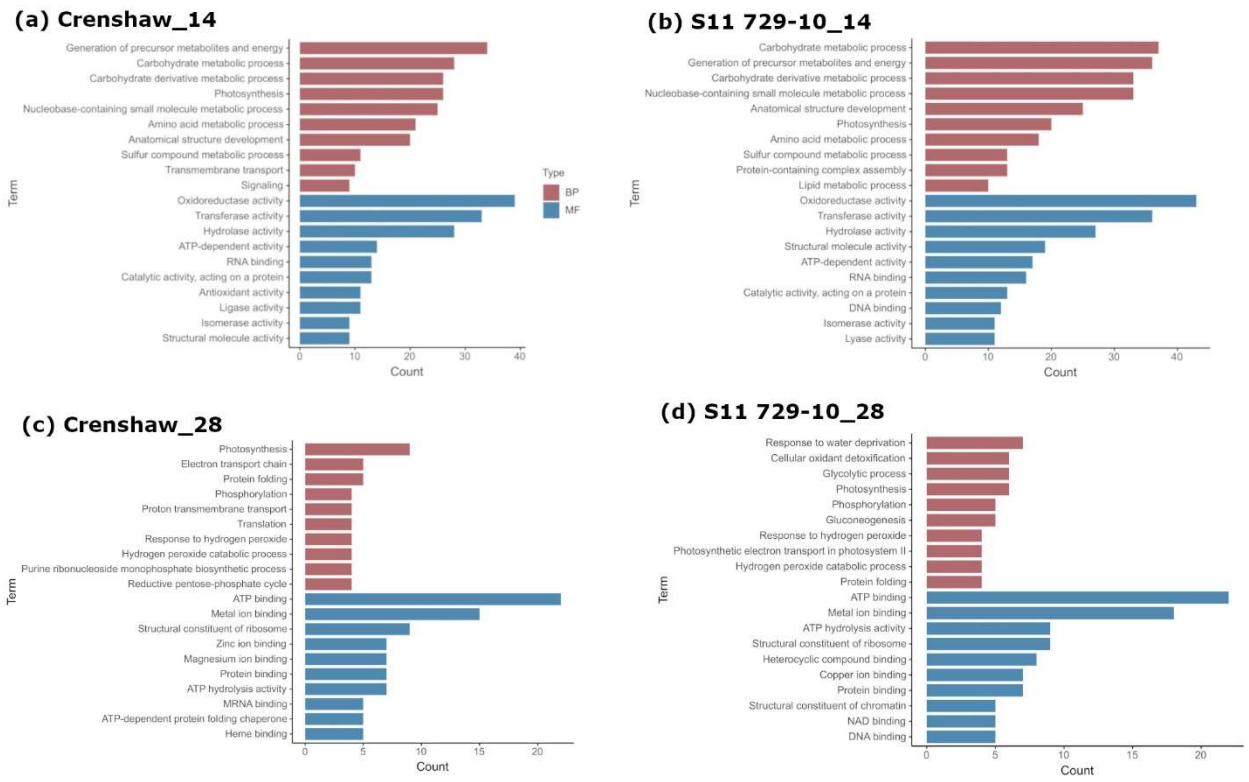

Figure 4.5 Top twenty terms of gene ontology (GO) for differentially expressed proteins (DEPs) of two creeping bentgrass lines (Crenshaw and S11 729-10) at 14 d (a, b) and 28 d (c, d) responding to heat stress. BP, biological process; MF, molecular function. Count was the number of DEPs falling into each GO term.

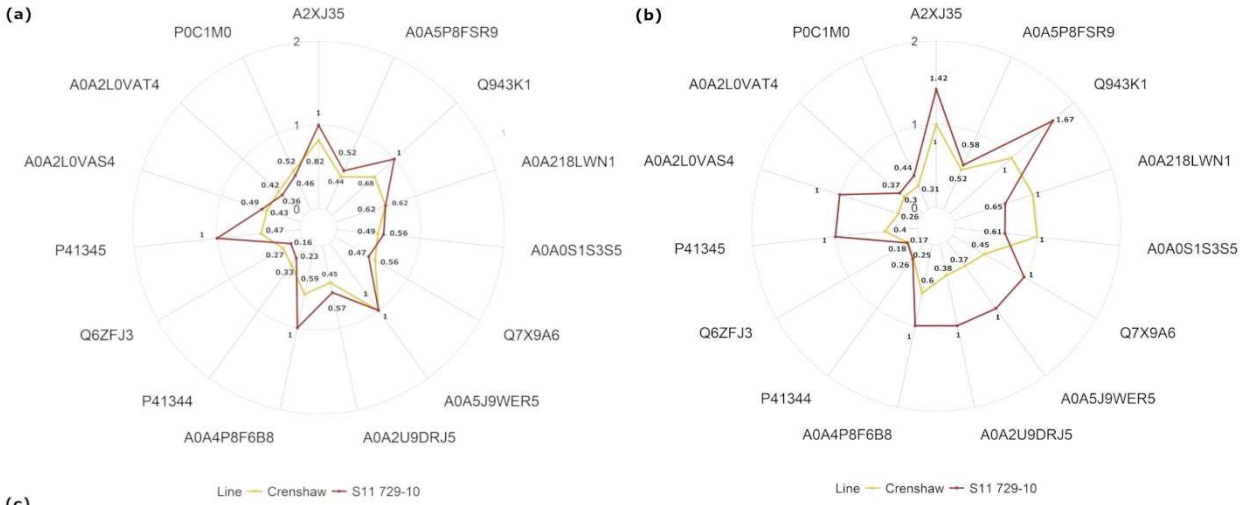

(c)

Accession ID	Description
A2XJ35	Chlorophyll a-b binding protein
A0A5P8FSR9	Photosystem II protein D1
Q943K1	Photosystem II 22 kDa protein 1
A0A218LWN1	Photosystem II CP43 reaction center protein
A0A0S1S3S5	Photosystem II D2 protein
Q7X9A6	Cytochrome b6-f complex iron-sulfur subunit,
A0A5J9WER5	Photosystem I assembly protein Ycf4 (Fragment)
A0A2U9DRJ5	Photosystem I P700 chlorophyll a apoprotein A1
A0A4P8F6B8	Photosystem I P700 chlorophyll a apoprotein A2
P41344	Ferredoxin--NADP reductase, leaf isozyme
Q6ZFJ3	Ferredoxin--NADP reductase, leaf isozyme 2
P41345	Ferredoxin--NADP reductase, root isozyme
A0A2L0VAS4	ATP synthase subunit alpha
A0A2L0VAT4	ATP synthase subunit beta
P0C1M0	ATP synthase subunit gamma

Figure 4.6 Fold change of the differentially expressed proteins involved in photosynthesis-electron transport chain for creeping bentgrass (Crenshaw and S11 729-10) when heat-stressed samples were compared against control samples at 14 d (a) and 28 d (b). The corresponding protein description for each accession ID was attached (c).

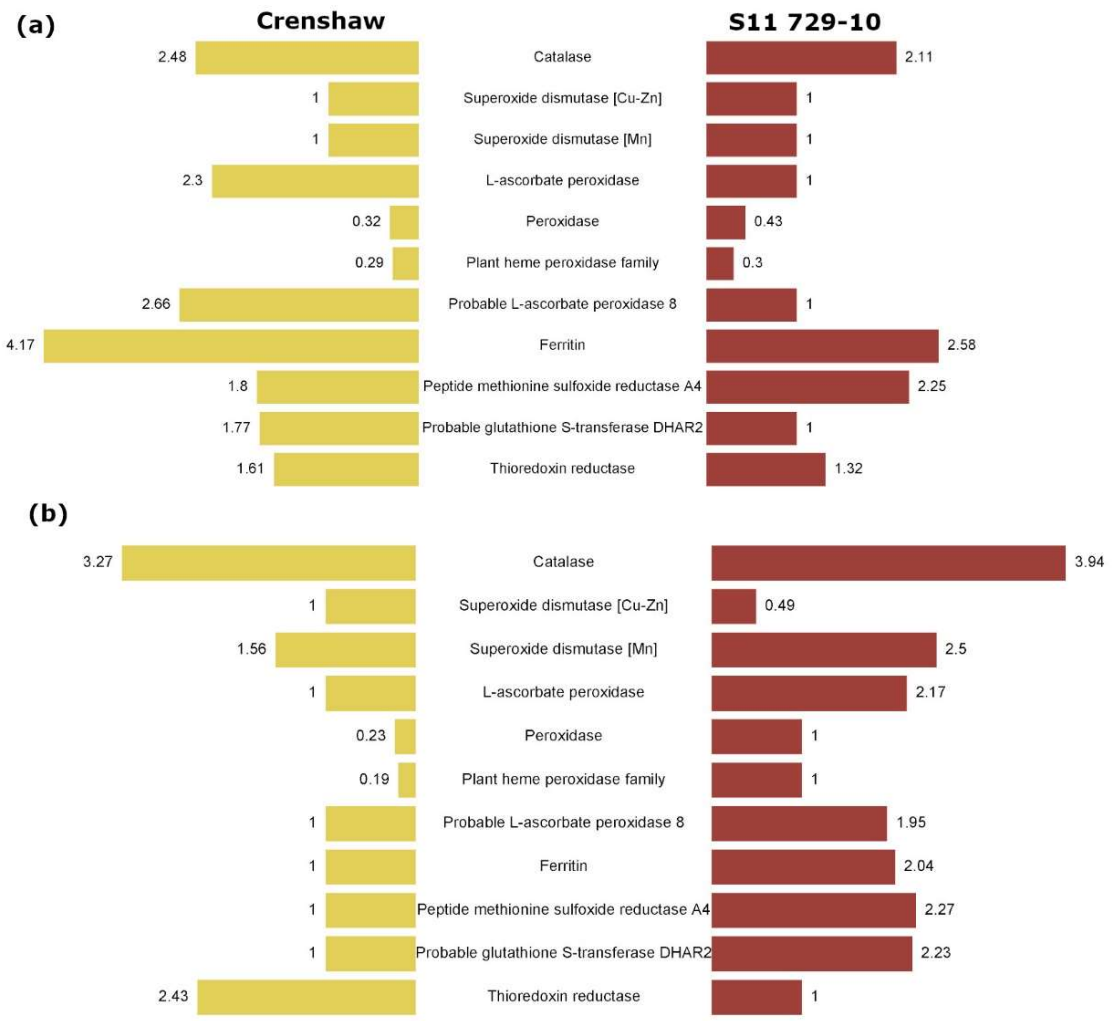

Figure 4.7 Fold change of the differentially expressed proteins involved in antioxidant defense for creeping bentgrass (Crenshaw and S11 729-10) when heat-stressed samples were compared against control samples at 14 d (a) and 28 d (b). Yellow represented Crenshaw while red represented S11 729-10.

(a)

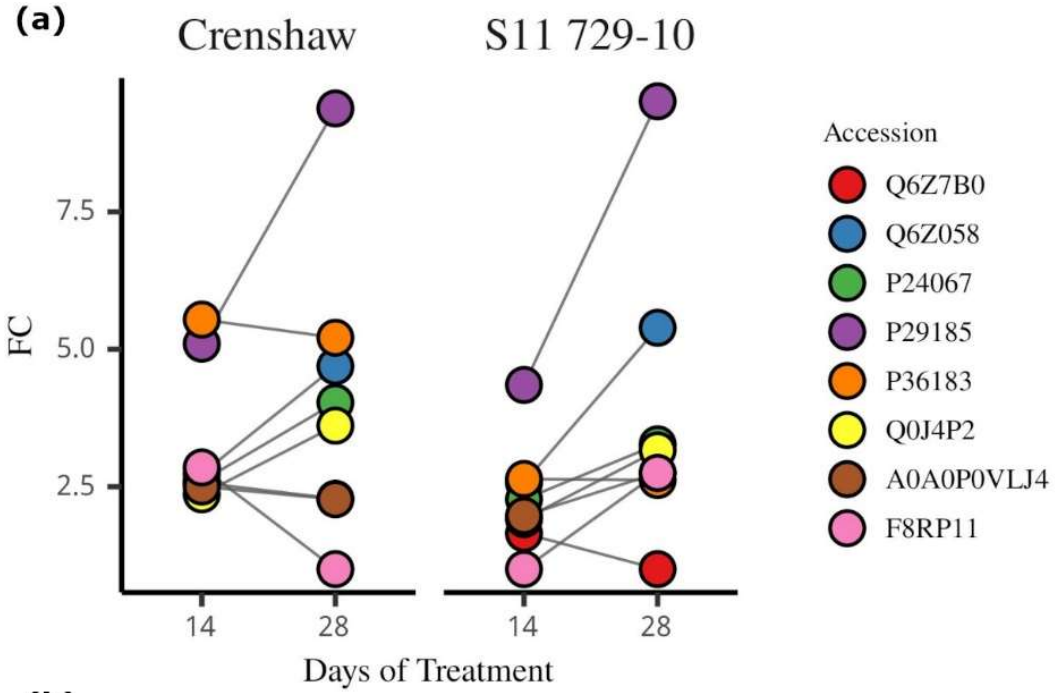

(b)

Accession ID	Description
Q6Z7B0	Heat shock 70 kDa protein BIP1
Q6Z058	Heat shock 70 kDa protein BIP5
P24067	Luminal-binding protein 2, HSP70
P29185	Chaperonin CPN60-1, HSP60
P36183	Endoplasmin homolog, HSP70
Q0J4P2	Heat shock protein 81-1, HSP80
A0A0P0VLJ4	GrpE protein homolog, critical regulators of Hsp70/Dnak chaperone activity
F8RP11	Hsp70-Hsp90 organizing protein

Figure 4.8 Fold change of the differentially expressed proteins involved in protein refolding for creeping bentgrass (Crenshaw and S11 729-10) when heat-stressed samples were compared against control samples at 14 d and 28 d (a). The corresponding protein description for each accession ID (b).

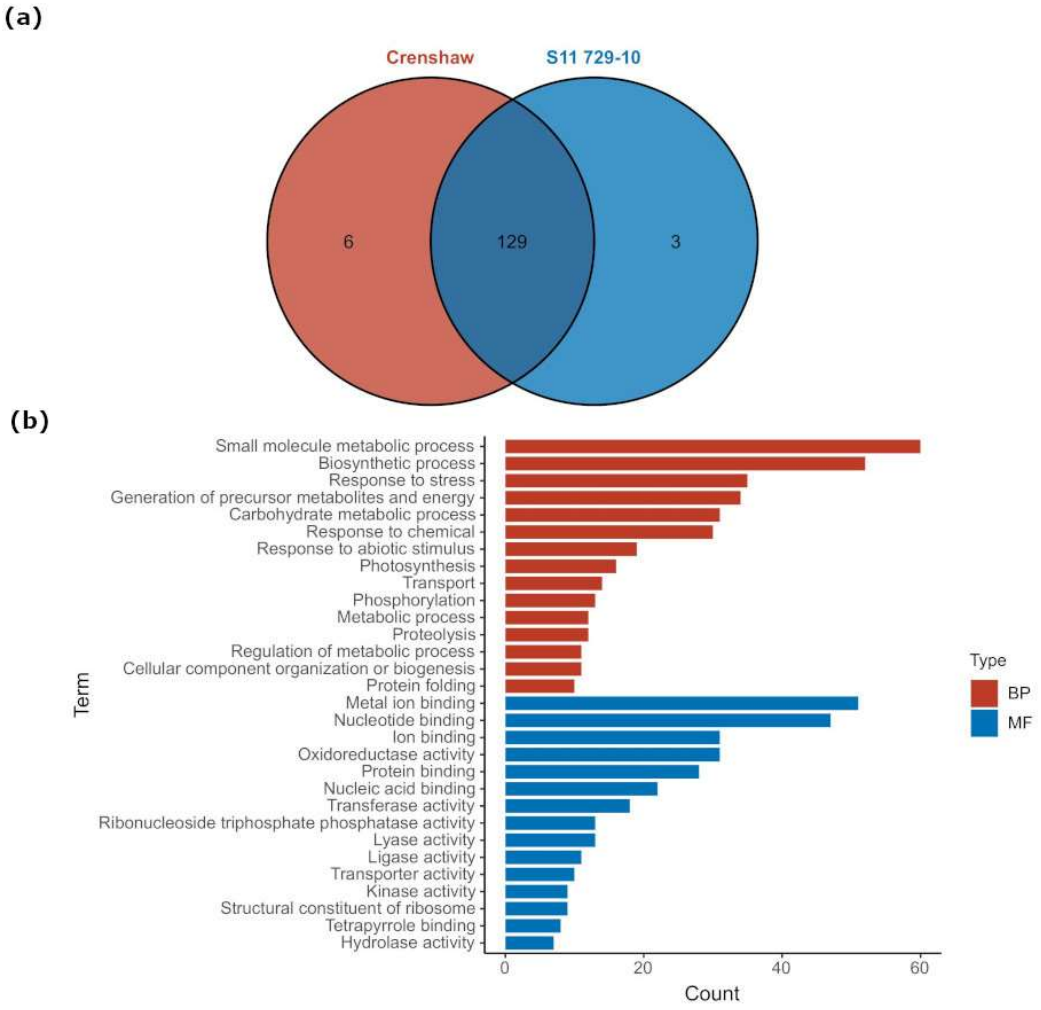

Figure 4.9 Identified polyubiquitinated proteins of two heat-stressed creeping bentgrass lines (Crenshaw and S11 729-10) at 28 d. Venn diagram showing common and unique polyubiquitinated proteins (a). Bar plot showing top thirty GO terms for commonly identified polyubiquitinated proteins. BP, biological process; MF, molecular function. Count was the number of polyubiquitinated proteins falling into each GO term.

Supplemental Materials

Table S4.1 ANOVA results for heat stress trial of creeping bentgrass

Parameter	*P* value					
	Control			Heat stress		
	Line	Date	Line × Date	Line	Date	Line × Date
TQ	0.354	0.151	0.130	<0.001	<0.001	<0.001
Green cover	0.081	0.003	0.359	<0.001	<0.001	<0.001
EL	0.012	0.543	0.118	<0.001	<0.001	<0.001
Fv/Fm	0.332	0.014	0.578	0.011	<0.001	0.016
ABS/CSm	0.151	-	-	<0.001	-	-
DIo/ABS	0.146	-	-	0.021	-	-
ETo/CSm	0.468	-	-	0.004	-	-
REo/CSm	0.194	-	-	0.003	-	-

TQ, turf quality; EL, electrolyte leakage; Fv/Fm, quantum efficiency of energy flux trapped by photosystem II (PSII) photochemistry; ABS/CSm, absorbed energy flux per cross section; DIo/ABS, quantum efficiency of energy dissipation in PSII antenna; ETo/CSm, the energy flux associated with electron transport from quinone A to intersystem electron acceptors such as plastoquinone pool per cross section; REo/ CSm, the energy flux associated with electron transport from intersystem electron acceptors to final photosystem I acceptors per cross section

Table S4.2 Change in visual turf quality rating for creeping bentgrass lines over time under control (20/15°C day/night) and heat stress (38/33°C day/night) conditions

Lines	Control					Heat				
	0	**7**	**14**	**21**	**28**	**0**	**7**	**14**	**21**	**28**
Crenshaw	9.0	9.0	9.0	9.0	9.0	9.0	8.2b	7.6b	6.9b	4.0b
S11 675-02	9.0	9.0	9.0	9.0	9.0	9.0	8.5a	7.9a	6.8b	5.9a
S11 729-10	9.0	9.0	9.0	9.0	9.0	9.0	8.5a	8.0a	7.6a	7.2a
LSD	ns	ns	ns	ns	ns	ns	0.22	0.25	0.52	1.6

Note: values followed by a common lowercase letter within each column indicate no significant difference among various lines at $p = 0.05$; ns, not significant

Table S4.3 Change in green cover for creeping bentgrass lines over time under control (20/15°C day/night) and heat stress (38/33°C day/night) conditions

Lines	Control					Heat				
	0	**7**	**14**	**21**	**28**	**0**	**7**	**14**	**21**	**28**
Crenshaw	97.8a	95.4	95.4	91.2	98.5a	96.6	87.9	87.9	61.2b	22.0b
S11 675-02	94.5b	96.1	96.1	89.4	91.9b	95.3	93.3	93.3	67.3ab	46.6a
S11 729-10	98.2a	93.7	93.6	89.4	95.0ab	95.0	93.0	93.0	78.3a	60.9a
LSD	2.2	ns	ns	ns	4.6	ns	ns	ns	11.9	18.5

Note: values followed by a common lowercase letter within each column indicate no significant difference among various lines at $p = 0.05$; ns, not significant

Table S4.4 Change in electrolyte leakage for creeping bentgrass lines over time under control (20/15°C day/night) and heat stress (38/33°C day/night) conditions

Lines	Control					Heat				
	0	**7**	**14**	**21**	**28**	**0**	**7**	**14**	**21**	**28**
Crenshaw	15.4	15.8	14.1	13.2b	13.2b	14.7	24.9a	30.6	64.2a	73.7a
S11 675-02	15.1	16.7	20.8	15.7b	15.7b	15.4	22.1ab	27.1	46.9b	58.3b
S11 729-10	16.2	15.6	14.8	20.9a	20.9a	15.8	18.9b	25.3	35.8b	44.6c
LSD	ns	ns	ns	4.0	4.0	ns	4.3	ns	12.5	9.1

Note: values followed by a common lowercase letter within each column indicate no significant difference among various lines at $p = 0.05$; ns, not significant

Table S4.5 Change in Fv/Fm for creeping bentgrass lines over time under control (20/15°C day/night) and heat stress (38/33°C day/night) conditions

Lines	Control					Heat				
	0	**7**	**14**	**21**	**28**	**0**	**7**	**14**	**21**	**28**
Crenshaw	0.82	0.82	0.80	0.81	0.82	0.80	0.75	0.75	0.694b	0.48b
S11 675-02	0.82	0.83	0.81	0.81	0.83	0.81	0.77	0.75	0.719ab	0.61ab
S11 729-10	0.82	0.82	0.81	0.81	0.82	0.82	0.75	0.74	0.723a	0.69a
LSD	ns	ns	ns	ns	ns	ns	ns	ns	0.027	0.14

Note: values followed by a common lowercase letter within each column indicate no significant difference among various lines at $p = 0.05$; ns, not significant; Fv/Fm, quantum efficiency of energy flux trapped by photosystem II photochemistry.

Table S4.6 List of differentially expressed proteins with their accession ID, description and log2 fold change (logFC) when comparing heat stress condition against control condition for Crenshaw at 14 d

Accession	Description	logFC
P30792	2,3-bisphosphoglycerate-independent phosphoglycerate mutase OS=Zea mays	-0.52
W5EP13	2-carboxy-D-arabinitol-1-phosphatase OS=Triticum aestivum	1.46
Q6AVG6	4-hydroxy-3-methylbut-2-enyl diphosphate reductase, chloroplastic OS=Oryza sativa subsp. japonica	0.46
A0A2S3IJL2	5-methyltetrahydropteroyltriglutamate--homocysteine S-methyltransferase OS=Panicum hallii	-1.55
A0A2T7DTW1	AAA+ ATPase domain-containing protein OS=Panicum hallii var. hallii	-1.71
A0A3B6NJT0	Acetyltransferase component of pyruvate dehydrogenase complex OS=Triticum aestivum	0.81
P32112	Adenosylhomocysteinase OS=Triticum aestivum	-0.97
A0A3B6PR10	ADP/ATP translocase OS=Triticum aestivum	-0.37
P34106	Alanine aminotransferase 2 OS=Panicum miliaceum	0.82
A0A1D6HR58	alanine transaminase OS=Zea mays	-1.3
Q0DWH1	Alcohol dehydrogenase class-3 OS=Oryza sativa subsp. japonica	0.67
A0A1B6QHW4	Alpha-1,4 glucan phosphorylase OS=Sorghum bicolor	-0.86
Q9FXT4	Alpha-galactosidase OS=Oryza sativa subsp. japonica	-1.57
A0A453NS22	Aminopeptidase OS=Aegilops tauschii subsp. strangulata	0.34
Q9XJ29	Anthranilate synthase alpha subunit 2, chloroplastic OS=Oryza sativa subsp. japonica	0.46
B8AU84	Arginase 1, mitochondrial OS=Oryza sativa subsp. indica	2.42
P37833	Aspartate aminotransferase, cytoplasmic OS=Oryza sativa subsp. japonica	-1.1
A0A1B6PGM0	aspartate carbamoyltransferase OS=Sorghum bicolor	1.37
A0A3B5ZZW5	assimilatory sulfite reductase (ferredoxin) OS=Triticum aestivum	-1.19
A0A2L0VAS4	ATP synthase subunit alpha, chloroplastic OS=Lamarckia aurea	-1.22
A0A2L0VAT4	ATP synthase subunit beta, chloroplastic OS=Lamarckia aurea	-1.26
P0C1M0	ATP synthase subunit gamma, chloroplastic OS=Zea mays	-0.94
A0A317YBF8	ATP-dependent DNA helicase OS=Zea mays	1.73
P16098	Beta-amylase OS=Hordeum vulgare	-1.91
A0A3L6FGN4	carbamoyl-phosphate synthase (glutamine-hydrolyzing) OS=Zea mays	0.7

B9EXM2	Carbamoyl-phosphate synthase large chain, chloroplastic OS=Oryza sativa subsp. japonica	0.76
A0A3B6KQP3	Catalase OS=Triticum aestivum	1.31
A0A1W0VZF1	CBM20 domain-containing protein OS=Sorghum bicolor	3.11
P29185	Chaperonin CPN60-1, mitochondrial OS=Zea mays	2.35
A2XJ35	Chlorophyll a-b binding protein, chloroplastic OS=Oryza sativa subsp. indica	-0.29
A0A0E0GTN2	Cysteine synthase OS=Oryza nivara	-2.28
A0A024BKI8	Cytochrome b559 subunit alpha OS=Cenchrus americanus	-0.63
A0A3G1AT48	Cytochrome b6 OS=Bromus vulgaris	-1.16
Q7X9A6	Cytochrome b6-f complex iron-sulfur subunit, chloroplastic OS=Triticum aestivum	-0.83
A0A0E0E626	Delta-aminolevulinic acid dehydratase OS=Oryza meridionalis	0.81
A0A0E0JJD7	Endopeptidase Clp OS=Oryza punctata	-1.16
P36183	Endoplasmin homolog OS=Hordeum vulgare	2.47
A4KAG8	Ent-isokaur-15-ene synthase OS=Oryza sativa subsp. japonica	-0.57
Q6Z2Z4	Eukaryotic initiation factor 4A-3 OS=Oryza sativa subsp. japonica	-0.6
Q69RJ0	Ferredoxin-dependent glutamate synthase, chloroplastic OS=Oryza sativa subsp. japonica	-0.73
P41344	Ferredoxin--NADP reductase, leaf isozyme 1, chloroplastic OS=Oryza sativa subsp. japonica	-1.59
Q6ZFJ3	Ferredoxin--NADP reductase, leaf isozyme 2, chloroplastic OS=Oryza sativa subsp. japonica	-1.88
P41345	Ferredoxin--NADP reductase, root isozyme, chloroplastic OS=Oryza sativa subsp. japonica	-1.1
A0A0E0N8J2	ferredoxin--NADP(+) reductase OS=Oryza rufipogon	-1.32
Q42997	Ferredoxin--nitrite reductase, chloroplastic OS=Oryza sativa subsp. japonica	-2.05
A0A1D5YQ12	Ferritin OS=Triticum aestivum	2.06
Q84N28	Flavone O-methyltransferase 1 OS=Triticum aestivum	-1.22
A0A4V6DBK4	Formate dehydrogenase, mitochondrial OS=Setaria viridis	0.59
Q0JGZ6	Fructokinase-1 OS=Oryza sativa subsp. japonica	-0.59
Q0J8G4	Fructokinase-2 OS=Oryza sativa subsp. japonica	-1.38
A0A2K2DTT5	fructose-bisphosphatase OS=Brachypodium distachyon	-0.45
Q40677	Fructose-bisphosphate aldolase, chloroplastic OS=Oryza sativa subsp. japonica	0.95

Q6AVT2	Glucose-1-phosphate adenylyltransferase large subunit 1, chloroplastic/amyloplastic OS=Oryza sativa subsp. japonica	-0.98
P55239	Glucose-1-phosphate adenylyltransferase large subunit 2 (Fragment) OS=Hordeum vulgare	-1
A0A3B6KSU0	Glucose-1-phosphate adenylyltransferase OS=Triticum aestivum	-0.72
A0A0E0CZR5	Glucose-6-phosphate 1-dehydrogenase OS=Oryza meridionalis	1.09
Q33E23	Glutamate dehydrogenase 2, mitochondrial OS=Oryza sativa subsp. japonica	-0.99
I1HQF1	glutamate synthase (NADH) OS=Brachypodium distachyon	-2.22
P13564	Glutamine synthetase leaf isozyme, chloroplastic OS=Hordeum vulgare	0.37
P14655	Glutamine synthetase, chloroplastic OS=Oryza sativa subsp. japonica	0.63
A0A3B6JM67	Glutathione reductase OS=Triticum aestivum	-0.62
P08735	Glyceraldehyde-3-phosphate dehydrogenase 1, cytosolic OS=Zea mays	0.62
A0A077S2R7	Glycine cleavage system P protein OS=Triticum aestivum	0.34
Q10CE4	Glycolate oxidase 1 OS=Oryza sativa subsp. japonica	-0.7
B8B7C5	Glycolate oxidase 5 OS=Oryza sativa subsp. indica	-0.35
A0A0P0VLJ4	GrpE protein homolog OS=Oryza sativa subsp. japonica	1.32
C5WVT9	Guanine nucleotide-binding protein alpha subunit OS=Sorghum bicolor	-0.61
Q0J4P2	Heat shock protein 81-1 OS=Oryza sativa subsp. japonica	1.24
F8RP11	Hsp70-Hsp90 organizing protein OS=Triticum aestivum	1.51
O64437	Inositol-3-phosphate synthase 1 OS=Oryza sativa subsp. japonica	-0.79
P17788	Large ribosomal subunit protein uL2cz/uL2cy OS=Zea mays	-0.87
Q10N21	L-ascorbate peroxidase 1, cytosolic OS=Oryza sativa subsp. japonica	1.55
Q9FE01	L-ascorbate peroxidase 2, cytosolic OS=Oryza sativa subsp. japonica	0.61
A0A3B6PVU5	L-ascorbate peroxidase OS=Triticum aestivum	1.2
Q6K669	Leucine aminopeptidase 2, chloroplastic OS=Oryza sativa subsp. japonica	-0.32
P24067	Luminal-binding protein 2 OS=Zea mays	1.38
A0A0Q3LQ58	Malate dehydrogenase OS=Brachypodium distachyon	0.5
Q9SE94	Methylenetetrahydrofolate reductase (NADH) 1 OS=Zea mays	-0.68
A0A0E0EWM9	Mevalonate kinase OS=Oryza meridionalis	0.75
A0A0E0D501	Multifunctional fusion protein OS=Oryza meridionalis	0.3
A0A1E5VRY2	N-acyl-aliphatic-L-amino acid amidohydrolase OS=Dichanthelium oligosanthes	0.87

A6N0M9	Nucleoside diphosphate kinase 1 OS=Oryza sativa subsp. indica	0.44
B4FK49	Nucleoside diphosphate kinase 1 OS=Zea mays	-0.94
B8AW64	Nucleosome assembly protein 1;2 OS=Oryza sativa subsp. indica	-1.21
A0A0Q3RM53	ornithine aminotransferase OS=Brachypodium distachyon	3.01
A0A3B6LEJ3	Pectinesterase OS=Triticum aestivum	-2.54
Q336R9	Peptide methionine sulfoxide reductase A4, chloroplastic OS=Oryza sativa subsp. japonica	0.85
A0A0D9UZT5	Peptidyl-prolyl cis-trans isomerase OS=Leersia perrieri	-3.62
P27337	Peroxidase 1 OS=Hordeum vulgare	-1.48
A0A453APJ3	Peroxidase OS=Aegilops tauschii subsp. strangulata	-1.64
Q9FR35	Peroxiredoxin-2C OS=Oryza sativa subsp. japonica	1.08
P29195	Phosphoenolpyruvate carboxylase 1 OS=Sorghum bicolor	0.35
A0A0Q3JDL9	phosphoglucomutase (alpha-D-glucose-1,6-bisphosphate-dependent) OS=Brachypodium distachyon	-2.16
Q43007	Phospholipase D alpha 1 OS=Oryza sativa subsp. japonica	-0.42
A0A3B6HT18	Phosphomannomutase OS=Triticum aestivum	1.53
A0A220IHK0	Photosystem I iron-sulfur center OS=Aegilops uniaristata	-0.6
A0A2U9DRJ5	Photosystem I P700 chlorophyll a apoprotein A1 OS=Campeiostachys nutans	-1.16
A0A4P8F6B8	Photosystem I P700 chlorophyll a apoprotein A2 OS=Triodia mallota	0.76
Q943K1	Photosystem II 22 kDa protein 1, chloroplastic OS=Oryza sativa subsp. japonica	-0.56
Q0J8R9	Photosystem II 22 kDa protein 2, chloroplastic OS=Oryza sativa subsp. japonica	-0.92
A0A218LWN1	Photosystem II CP43 reaction center protein OS=Triticum monococcum	-0.7
A0A0S1S3S5	Photosystem II D2 protein OS=Stipa lipskyi	1.02
A0A5P8FSR9	Photosystem II protein D1 OS=Bambusa variostriata	-1.2
A0A0E0QCR5	Plant heme peroxidase family profile domain-containing protein OS=Oryza rufipogon	-1.79
O64411	Polyamine oxidase 1 OS=Zea mays	-2.21
Q2QP54	Polyprotein of EF-Ts, chloroplastic OS=Oryza sativa subsp. japonica	-1.56

Q6H6D2	Porphobilinogen deaminase, chloroplastic OS=Oryza sativa subsp. japonica	-0.58
A0A0E0NUQ9	Potassium transporter OS=Oryza rufipogon	-1.23
Q69SV0	Probable L-ascorbate peroxidase 8, chloroplastic OS=Oryza sativa subsp. japonica	1.41
P80607	Probable UDP-arabinopyranose mutase 1 OS=Zea mays	-0.94
O22655	Profilin-4 OS=Zea mays	-0.82
A0A3B6RCJ8	Proteasome subunit beta OS=Triticum aestivum	-0.62
Q2RAK2	Pyruvate kinase 1, cytosolic OS=Oryza sativa subsp. japonica	0.36
A0A0E0HXE6	Pyruvate kinase OS=Oryza nivara	-1.23
A0A2S3ID39	Receptor-like serine/threonine-protein kinase OS=Panicum hallii	-0.93
A0A2T7CH14	Ribulose-phosphate 3-epimerase OS=Panicum hallii var. hallii	-1.23
A0A0E0D0N3	RING-type E3 ubiquitin transferase OS=Oryza meridionalis	-0.58
A0A077RWS5	S-adenosylmethionine synthase OS=Triticum aestivum	-1.28
P46285	Sedoheptulose-1,7-bisphosphatase, chloroplastic OS=Triticum aestivum	-1.64
P49027	Small ribosomal subunit protein RACK1z OS=Oryza sativa subsp. japonica	-1.37
Q6YXW6	Sucrose-phosphatase 2 OS=Oryza sativa subsp. japonica	1.3
A0A3B6RMJ1	Thiamine thiazole synthase, chloroplastic OS=Triticum aestivum	-2.05
A0A0Q3NCX3	Thioredoxin reductase OS=Brachypodium distachyon	0.69
Q7SIC9	Transketolase, chloroplastic OS=Zea mays	-1.22
P46225	Triosephosphate isomerase, chloroplastic OS=Secale cereale	-1.05
Q9ZRB0	Tubulin beta-3 chain OS=Triticum aestivum	2.1
Q8H8T0	UDP-arabinopyranose mutase 1 OS=Oryza sativa subsp. japonica	-1.03
Q6Z7B0	Heat shock 70 kDa protein BIP1 OS=Oryza sativa subsp. japonica	1.36
Q6Z058	Heat shock 70 kDa protein BIP5 OS=Oryza sativa subsp. japonica	1.45
A0A0E0PRJ8	very-long-chain 3-oxoacyl-CoA synthase OS=Oryza rufipogon	1.33
P49087	V-type proton ATPase catalytic subunit A (Fragment) OS=Zea mays	-0.28

Table S4.7 List of differentially expressed proteins with their accession ID, description and log2 fold change (logFC) when comparing heat stress condition against control condition for Crenshaw at 28 d

Accession	Description	logFC
W5EP13	2-carboxy-D-arabinitol-1-phosphatase OS=Triticum aestivum	2.76
A0A2S3IJL2	5-methyltetrahydropteroyltriglutamate--homocysteine S-methyltransferase OS=Panicum hallii	-1.22
A0A2T7DTW1	AAA+ ATPase domain-containing protein OS=Panicum hallii var. hallii	-2.03
A0A3B6NJT0	Acetyltransferase component of pyruvate dehydrogenase complex OS=Triticum aestivum	1.9
A0A3B6PR10	ADP/ATP translocase OS=Triticum aestivum	0.62
P34106	Alanine aminotransferase 2 OS=Panicum miliaceum	2.14
A0A1D6HR58	alanine transaminase OS=Zea mays	-1.21
Q0DWH1	Alcohol dehydrogenase class-3 OS=Oryza sativa subsp. japonica	0.94
Q9FXT4	Alpha-galactosidase OS=Oryza sativa subsp. japonica	-1.63
A0A0E0L2W9	Amidophosphoribosyltransferase OS=Oryza punctata	0.7
B8AU84	Arginase 1, mitochondrial OS=Oryza sativa subsp. indica	2.84
A0A1B6PGM0	aspartate carbamoyltransferase OS=Sorghum bicolor	1.36
A0A3B5ZZW5	assimilatory sulfite reductase (ferredoxin) OS=Triticum aestivum	-1.69
A0A2L0VAS4	ATP synthase subunit alpha, chloroplastic OS=Lamarckia aurea	-1.93
A0A2L0VAT4	ATP synthase subunit beta, chloroplastic OS=Lamarckia aurea	-1.74
P0C1M0	ATP synthase subunit gamma, chloroplastic OS=Zea mays	-1.71
A0A317YBF8	ATP-dependent DNA helicase OS=Zea mays	3.26
B9EXM2	Carbamoyl-phosphate synthase large chain, chloroplastic OS=Oryza sativa subsp. japonica	2.1
A0A3B6KQP3	Catalase OS=Triticum aestivum	1.71
A0A1W0VZF1	CBM20 domain-containing protein OS=Sorghum bicolor	4.04
P29185	Chaperonin CPN60-1, mitochondrial OS=Zea mays	3.23
A0A0E0GTN2	Cysteine synthase OS=Oryza nivara	-0.9
Q7X9A6	Cytochrome b6-f complex iron-sulfur subunit, chloroplastic OS=Triticum aestivum	-1.14
A0A0E0E626	Delta-aminolevulinic acid dehydratase OS=Oryza meridionalis	1.19
P36183	Endoplasmin homolog OS=Hordeum vulgare	2.38
Q69RJ0	Ferredoxin-dependent glutamate synthase, chloroplastic OS=Oryza sativa subsp. japonica	-1.1
P41344	Ferredoxin--NADP reductase, leaf isozyme 1, chloroplastic OS=Oryza sativa subsp. japonica	-1.98
Q6ZFJ3	Ferredoxin--NADP reductase, leaf isozyme 2, chloroplastic OS=Oryza sativa subsp. japonica	-2.56
P41345	Ferredoxin--NADP reductase, root isozyme, chloroplastic OS=Oryza sativa subsp. japonica	-1.32
A0A0E0N8J2	ferredoxin--NADP(+) reductase OS=Oryza rufipogon	-1.78

Q42997	Ferredoxin--nitrite reductase, chloroplastic OS=Oryza sativa subsp. japonica	-1.83
Q84N28	Flavone O-methyltransferase 1 OS=Triticum aestivum	-0.99
A0A4V6DBK4	Formate dehydrogenase, mitochondrial OS=Setaria viridis	2.39
Q40677	Fructose-bisphosphate aldolase, chloroplastic OS=Oryza sativa subsp. japonica	1.33
Q6AVT2	Glucose-1-phosphate adenylyltransferase large subunit 1, chloroplastic/amyloplastic OS=Oryza sativa subsp. japonica	-0.88
A0A3B6KSU0	Glucose-1-phosphate adenylyltransferase OS=Triticum aestivum	-0.95
I1HQF1	glutamate synthase (NADH) OS=Brachypodium distachyon	-2.01
P13564	Glutamine synthetase leaf isozyme, chloroplastic	1.24
P38562	Glutamine synthetase root isozyme 4 OS=Zea mays	-1.16
P14655	Glutamine synthetase, chloroplastic OS=Oryza sativa subsp. japonica	0.88
Q10CE4	Glycolate oxidase 1 OS=Oryza sativa subsp. japonica	-1.2
B8B7C5	Glycolate oxidase 5 OS=Oryza sativa subsp. indica	-0.82
A0A0P0VLJ4	GrpE protein homolog OS=Oryza sativa subsp. japonica	1.18
Q0J4P2	Heat shock protein 81-1 OS=Oryza sativa subsp. japonica	1.85
O64437	Inositol-3-phosphate synthase 1 OS=Oryza sativa subsp. japonica	-2.22
P17788	Large ribosomal subunit protein uL2cz/uL2cy OS=Zea mays	-1.67
P24067	Luminal-binding protein 2 OS=Zea mays	2.01
Q9SE94	Methylenetetrahydrofolate reductase (NADH) 1 OS=Zea mays	0.87
A0A0D9UZT5	Peptidyl-prolyl cis-trans isomerase OS=Leersia perrieri	-3.7
A0A453APJ3	Peroxidase OS=Aegilops tauschii subsp. strangulata	-2.13
P29195	Phosphoenolpyruvate carboxylase 1 OS=Sorghum bicolor	0.93
A0A0Q3JDL9	phosphoglucomutase (alpha-D-glucose-1,6-bisphosphate-dependent) OS=Brachypodium distachyon	-2.11
A0A3B6HT18	Phosphomannomutase OS=Triticum aestivum	-1.31
A0A5J9WER5	Photosystem I assembly protein Ycf4 (Fragment) OS=Eragrostis curvula	-1.45
A0A2U9DRJ5	Photosystem I P700 chlorophyll a apoprotein A1 OS=Campeiostachys nutans	-1.38
A0A4P8F6B8	Photosystem I P700 chlorophyll a apoprotein A2 OS=Triodia mallota	-0.73
A0A5P8FSR9	Photosystem II protein D1 OS=Bambusa variostriata	-0.94
A0A0E0QCR5	Plant heme peroxidase family profile domain-containing protein OS=Oryza rufipogon	-2.42
O64411	Polyamine oxidase 1 OS=Zea mays	-2.06
Q2QP54	Polyprotein of EF-Ts, chloroplastic OS=Oryza sativa subsp. japonica	-1.62
A0A0E0NUQ9	Potassium transporter OS=Oryza rufipogon	-1.01
Q2RAK2	Pyruvate kinase 1, cytosolic OS=Oryza sativa subsp. japonica	1.01
A0A0E0HXE6	Pyruvate kinase OS=Oryza nivara	-1.6
A0A3B5Y1F9	Pyruvate, phosphate dikinase OS=Triticum aestivum	2.17

A0A2S3ID39	Receptor-like serine/threonine-protein kinase OS=Panicum hallii	-1.92
A0A2T7CH14	Ribulose-phosphate 3-epimerase OS=Panicum hallii var. hallii	-1.18
A0A0E0D0N3	RING-type E3 ubiquitin transferase OS=Oryza meridionalis	-0.99
A0A0E0F9Y5	RNA cytidine acetyltransferase OS=Oryza meridionalis	0.65
A0A077RWS5	S-adenosylmethionine synthase OS=Triticum aestivum	-1.03
P46285	Sedoheptulose-1,7-bisphosphatase, chloroplastic OS=Triticum aestivum	-2
A0A0C4BJE5	Serine hydroxymethyltransferase OS=Triticum aestivum	-0.38
P49027	Small ribosomal subunit protein RACK1z OS=Oryza sativa subsp. japonica	-1.47
Q6YXW6	Sucrose-phosphatase 2 OS=Oryza sativa subsp. japonica	2.31
P09233	Superoxide dismutase [Mn] 3.1, mitochondrial OS=Zea mays	0.64
A0A3B6RMJ1	Thiamine thiazole synthase, chloroplastic OS=Triticum aestivum	-4
A0A0Q3NCX3	Thioredoxin reductase OS=Brachypodium distachyon	1.28
A0A3L6R8U7	threonine synthase OS=Panicum miliaceum	0.44
Q7SIC9	Transketolase, chloroplastic OS=Zea mays	-1.66
Q9ZRB0	Tubulin beta-3 chain OS=Triticum aestivum	3.26
A0A0U2GJM5	UDP-arabinopyranose mutase OS=Hordeum vulgare	1.58
Q6Z7B0	Heat shock 70 kDa protein BIP1 OS=Oryza sativa subsp. japonica	1.19
Q6Z058	Heat shock 70 kDa protein BIP5 OS=Oryza sativa subsp. japonica	2.23
A0A0E0PRJ8	very-long-chain 3-oxoacyl-CoA synthase	1.75
A0A1D6FIR4	V-type proton ATPase proteolipid subunit (Fragment) OS=Zea mays	-2.54
Q8L5C6	Xylanase inhibitor protein 1 OS=Triticum aestivum	1.59

Table S4.8 List of differentially expressed proteins with their accession ID, description and log2 fold change (logFC) when comparing heat stress condition against control condition for S11 729-10 at 14 d

Accession	Description	logFC
P30792	2,3-bisphosphoglycerate-independent phosphoglycerate mutase OS=Zea mays	-1.3
W5EP13	2-carboxy-D-arabinitol-1-phosphatase OS=Triticum aestivum	1.71
A0A3L6E9M0	4-coumarate--CoA ligase OS=Zea mays	-0.64
A0A2S3IJL2	5-methyltetrahydropteroyltriglutamate--homocysteine S-methyltransferase OS=Panicum hallii	-2.86
A0A3B6TBU2	6-phosphogluconate dehydrogenase, decarboxylating OS=Triticum aestivum	-0.86
A0A2T7DTW1	AAA+ ATPase domain-containing protein OS=Panicum hallii var. hallii	-1.4
A0A3B6NJT0	Acetyltransferase component of pyruvate dehydrogenase complex OS=Triticum aestivum	0.84
A0A0Q3F6L1	Aconitate hydratase OS=Brachypodium distachyon	-0.58
A0A194YR04	Adenosine kinase OS=Sorghum bicolor	-0.84
P32112	Adenosylhomocysteinase OS=Triticum aestivum	-2.45
A0A3B6JPU8	Adenylosuccinate synthetase, chloroplastic OS=Triticum aestivum	-0.99
A0A1D6HR58	alanine transaminase OS=Zea mays	-1.63
Q0DWH1	Alcohol dehydrogenase class-3 OS=Oryza sativa subsp. japonica	0.9
A0A1B6QHW4	Alpha-1,4 glucan phosphorylase OS=Sorghum bicolor	-1.56
Q9FXT4	Alpha-galactosidase OS=Oryza sativa subsp. japonica	-2.58
C6KEM4	Aminoaldehyde dehydrogenase 2 OS=Zea mays	-1.77
A0A453NS22	Aminopeptidase OS=Aegilops tauschii subsp. strangulata	-0.58
B8AU84	Arginase 1, mitochondrial OS=Oryza sativa subsp. indica	2.02
P37833	Aspartate aminotransferase, cytoplasmic OS=Oryza sativa subsp. japonica	-1.99
A0A1B6PGM0	aspartate carbamoyltransferase OS=Sorghum bicolor	0.7
A0A3B5ZZW5	assimilatory sulfite reductase (ferredoxin) OS=Triticum aestivum	-2.09
A0A2L0VAS4	ATP synthase subunit alpha, chloroplastic OS=Lamarckia aurea	-1.04
A0A2L0VAT4	ATP synthase subunit beta, chloroplastic OS=Lamarckia aurea	-1.48
P0C1M0	ATP synthase subunit gamma, chloroplastic OS=Zea mays	-1.11
A0A0H3V9P6	ATP-dependent Clp protease proteolytic subunit OS=Oryza glumipatula	0.65
A0A317YBF8	ATP-dependent DNA helicase OS=Zea mays	2.42
P16098	Beta-amylase OS=Hordeum vulgare	-3.44
Q84LK3	Betaine aldehyde dehydrogenase 2 OS=Oryza sativa subsp. japonica	-1.24
P04464	Calmodulin OS=Triticum aestivum	-1.03
A0A3B6KQP3	Catalase OS=Triticum aestivum	1.08

A0A1W0VZF1	CBM20 domain-containing protein OS=Sorghum bicolor	2.94
P29185	Chaperonin CPN60-1, mitochondrial OS=Zea mays	2.12
A0A0E0GTN2	Cysteine synthase OS=Oryza nivara	-1.49
A0A3G1AT48	Cytochrome b6 OS=Bromus vulgaris	-0.46
Q7X9A6	Cytochrome b6-f complex iron-sulfur subunit, chloroplastic OS=Triticum aestivum	-1.09
A0A0E0E626	Delta-aminolevulinic acid dehydratase OS=Oryza meridionalis	0.84
A0A0Q3FJF1	dihydroxy-acid dehydratase OS=Brachypodium distachyon	-0.75
A0A0E0JJD7	Endopeptidase Clp OS=Oryza punctata	-1.98
P36183	Endoplasmin homolog OS=Hordeum vulgare	1.4
A4KAG8	Ent-isokaur-15-ene synthase OS=Oryza sativa subsp. japonica	-1.27
Q6Z2Z4	Eukaryotic initiation factor 4A-3 OS=Oryza sativa subsp. japonica	-0.56
Q69RJ0	Ferredoxin-dependent glutamate synthase, chloroplastic	-1.29
P41344	Ferredoxin--NADP reductase, leaf isozyme 1, chloroplastic	-2.15
Q6ZFJ3	Ferredoxin--NADP reductase, leaf isozyme 2, chloroplastic	-2.65
A0A0E0N8J2	ferredoxin--NADP(+) reductase OS=Oryza rufipogon	-2.06
Q42997	Ferredoxin--nitrite reductase, chloroplastic OS=Oryza sativa subsp. japonica	-2.24
A0A1D5YQ12	Ferritin OS=Triticum aestivum	1.37
Q84N28	Flavone O-methyltransferase 1 OS=Triticum aestivum	-2.5
Q0JGZ6	Fructokinase-1 OS=Oryza sativa subsp. japonica	-0.84
Q0J8G4	Fructokinase-2 OS=Oryza sativa subsp. japonica	-2.33
A0A2K2DTT5	fructose-bisphosphatase OS=Brachypodium distachyon	-0.6
P17784	Fructose-bisphosphate aldolase 1, cytoplasmic OS=Oryza sativa subsp. japonica	-1.03
Q40677	Fructose-bisphosphate aldolase, chloroplastic OS=Oryza sativa subsp. japonica	0.7
Q7XN11	Gamma-aminobutyrate transaminase 1, mitochondrial OS=Oryza sativa subsp. japonica	-1.06
A3C4S4	GDP-mannose 3,5-epimerase 1 OS=Oryza sativa subsp. japonica	-1.41
Q6ZBZ2	Germin-like protein 8-14 OS=Oryza sativa subsp. japonica	-1.85
Q6AVT2	Glucose-1-phosphate adenylyltransferase large subunit 1, chloroplastic/amyloplastic OS=Oryza sativa subsp. japonica	-1.61
P55239	Glucose-1-phosphate adenylyltransferase large subunit 2 (Fragment) OS=Hordeum vulgare	-1.45
A0A3B6KSU0	Glucose-1-phosphate adenylyltransferase OS=Triticum aestivum	-1.29
A0A1D6I644	Glucose-6-phosphate isomerase OS=Zea mays	-0.96
Q33E23	Glutamate dehydrogenase 2, mitochondrial OS=Oryza sativa subsp. japonica	-1.75
I1HQF1	glutamate synthase (NADH) OS=Brachypodium distachyon	-2.91
P38562	Glutamine synthetase root isozyme 4 OS=Zea mays	-1.9
A0A1D6HW14	Glutaredoxin-dependent peroxiredoxin OS=Zea mays	-0.72
A0A3B6JM67	Glutathione reductase OS=Triticum aestivum	-0.94

P08735	Glyceraldehyde-3-phosphate dehydrogenase 1, cytosolic OS=Zea mays	-0.34
Q7FAH2	Glyceraldehyde-3-phosphate dehydrogenase 2, cytosolic OS=Oryza sativa subsp. japonica	-0.91
Q43247	Glyceraldehyde-3-phosphate dehydrogenase 3, cytosolic OS=Zea mays	-1.13
P09315	Glyceraldehyde-3-phosphate dehydrogenase A, chloroplastic OS=Zea mays	-0.5
Q10CE4	Glycolate oxidase 1 OS=Oryza sativa subsp. japonica	-1.4
B8B7C5	Glycolate oxidase 5 OS=Oryza sativa subsp. indica	-1.2
A0A0P0VLJ4	GrpE protein homolog OS=Oryza sativa subsp. japonica	0.98
A0A3L6RHP0	GTP 3',8-cyclase OS=Panicum miliaceum	-0.95
C5WVT9	Guanine nucleotide-binding protein alpha subunit OS=Sorghum bicolor	-1.5
Q0J4P2	Heat shock protein 81-1 OS=Oryza sativa subsp. japonica	0.93
P02276	Histone H2A.2.1 OS=Triticum aestivum	-2.02
P02277	Histone H2A.2.2 OS=Triticum aestivum	-1.98
A2WKT4	Histone H2B.5 OS=Oryza sativa subsp. indica	-2.28
P68428	Histone H3.2 OS=Triticum aestivum	-2.82
Q0JCT1	Histone H3.3 OS=Oryza sativa subsp. japonica	-2.66
P62787	Histone H4 OS=Zea mays	-2.62
A0A3B6LUD2	Inosine-5'-monophosphate dehydrogenase OS=Triticum aestivum	-0.9
O64437	Inositol-3-phosphate synthase 1 OS=Oryza sativa subsp. japonica	-1.98
A0A3B6GTN3	Isocitrate dehydrogenase [NADP] OS=Triticum aestivum	-0.43
A0A3B5Z5S1	Ketol-acid reductoisomerase OS=Triticum aestivum	-0.8
P17788	Large ribosomal subunit protein uL2cz/uL2cy OS=Zea mays	-1.1
Q9FE01	L-ascorbate peroxidase 2, cytosolic OS=Oryza sativa subsp. japonica	-0.48
Q6K669	Leucine aminopeptidase 2, chloroplastic OS=Oryza sativa subsp. japonica	-0.69
P24067	Luminal-binding protein 2 OS=Zea mays	1.18
Q9SE94	Methylenetetrahydrofolate reductase (NADH) 1 OS=Zea mays	-0.95
A0A0E0EWM9	Mevalonate kinase OS=Oryza meridionalis	-1.25
Q652L6	Monodehydroascorbate reductase 3, cytosolic OS=Oryza sativa subsp. japonica	-0.89
A0A0E0D501	Multifunctional fusion protein OS=Oryza meridionalis	0.74
Q8LK61	NADP-dependent glyceraldehyde-3-phosphate dehydrogenase OS=Triticum aestivum	-1.01
P43279	NADP-dependent malic enzyme, chloroplastic OS=Oryza sativa subsp. japonica	-3.19
B4FK49	Nucleoside diphosphate kinase 1 OS=Zea mays	-1.81
A0A0Q3RM53	ornithine aminotransferase OS=Brachypodium distachyon	2.02
A0A3B6LEJ3	Pectinesterase OS=Triticum aestivum	-3.49

Q336R9	Peptide methionine sulfoxide reductase A4, chloroplastic OS=Oryza sativa subsp. japonica	1.17
P27337	Peroxidase 1 OS=Hordeum vulgare	-1.11
A0A453APJ3	Peroxidase OS=Aegilops tauschii subsp. strangulata	-1.23
Q9FR35	Peroxiredoxin-2C OS=Oryza sativa subsp. japonica	-1.71
A0A0Q3JDL9	phosphoglucomutase (alpha-D-glucose-1,6-bisphosphate-dependent) OS=Brachypodium distachyon	-3.16
A0A3B6JK87	phosphoglycerate mutase (2,3-diphosphoglycerate-independent) OS=Triticum aestivum	-1.46
Q43007	Phospholipase D alpha 1 OS=Oryza sativa subsp. japonica	-1.32
A0A3B6HT18	Phosphomannomutase OS=Triticum aestivum	-2.86
A0A2U9DRJ5	Photosystem I P700 chlorophyll a apoprotein A1 OS=Campeiostachys nutans	-0.82
Q0J8R9	Photosystem II 22 kDa protein 2, chloroplastic OS=Oryza sativa subsp. japonica	-0.88
A0A218LWN1	Photosystem II CP43 reaction center protein OS=Triticum monococcum	-0.69
A0A0S1S3S5	Photosystem II D2 protein OS=Stipa lipskyi	-0.84
A0A5P8FSR9	Photosystem II protein D1 OS=Bambusa variostriata	-0.93
A0A0E0QCR5	Plant heme peroxidase family profile domain-containing protein OS=Oryza rufipogon	-1.72
Q2QP54	Polyprotein of EF-Ts, chloroplastic OS=Oryza sativa subsp. japonica	-1.55
Q6H6D2	Porphobilinogen deaminase, chloroplastic OS=Oryza sativa subsp. japonica	-1.69
A0A0E0NUQ9	Potassium transporter OS=Oryza rufipogon	-2.29
P80607	Probable UDP-arabinopyranose mutase 1 OS=Zea mays	-1.87
O22655	Profilin-4 OS=Zea mays	-1.53
P17070	Proliferating cell nuclear antigen OS=Oryza sativa subsp. japonica	-0.88
A0A3B6RCJ8	Proteasome subunit beta OS=Triticum aestivum	-0.97
A0A0E0NKR5	Pyruvate dehydrogenase E1 component subunit alpha OS=Oryza rufipogon	-0.83
A0A0E0HXE6	Pyruvate kinase OS=Oryza nivara	-1.51
A0A2S3ID39	Receptor-like serine/threonine-protein kinase OS=Panicum hallii	-1.48
A0A3L6DQ42	Ribokinase OS=Zea mays	-1.95
A0A8A6P3J7	Ribulose bisphosphate carboxylase large chain OS=Sphenopholis intermedia	0.62
A0A0E0MLI8	Ribulose bisphosphate carboxylase small subunit, chloroplastic OS=Oryza punctata	0.65
A0A2T7CH14	Ribulose-phosphate 3-epimerase OS=Panicum hallii var. hallii	-1.21
A0A0E0D0N3	RING-type E3 ubiquitin transferase OS=Oryza meridionalis	-0.98
A0A077RWS5	S-adenosylmethionine synthase OS=Triticum aestivum	-2.22
P46285	Sedoheptulose-1,7-bisphosphatase, chloroplastic OS=Triticum aestivum	-2.27

A0A0C4BJE5	Serine hydroxymethyltransferase OS=Triticum aestivum	-1.13
P49027	Small ribosomal subunit protein RACK1z OS=Oryza sativa subsp. japonica	-1.86
A0A1D6Q567	Succinate--CoA ligase [ADP-forming] subunit beta, mitochondrial OS=Zea mays	-0.44
P30298	Sucrose synthase 2 OS=Oryza sativa subsp. japonica	-0.69
A0A3B6RMJ1	Thiamine thiazole synthase, chloroplastic OS=Triticum aestivum	-3.86
A0A0Q3NCX3	Thioredoxin reductase OS=Brachypodium distachyon	0.4
Q7SIC9	Transketolase, chloroplastic OS=Zea mays	-1.99
P46225	Triosephosphate isomerase, chloroplastic OS=Secale cereale	-1.38
Q9ZRB0	Tubulin beta-3 chain OS=Triticum aestivum	0.53
A0A0Q3KYB0	Ubiquitin-like domain-containing protein OS=Brachypodium distachyon	-0.62
Q8H8T0	UDP-arabinopyranose mutase 1 OS=Oryza sativa subsp. japonica	-1.91
J3LV62	UMP-CMP kinase OS=Oryza brachyantha	-2.35
Q6Z7B0	Heat shock 70 kDa protein BIP1 OS=Oryza sativa subsp. japonica	0.72
Q6Z058	Heat shock 70 kDa protein BIP5 OS=Oryza sativa subsp. japonica	1.36
A0A0E0PRJ8	very-long-chain 3-oxoacyl-CoA synthase OS=Oryza rufipogon	0.6
P49087	V-type proton ATPase catalytic subunit A (Fragment) OS=Zea mays	-0.96
A0A1D6FIR4	V-type proton ATPase proteolipid subunit (Fragment) OS=Zea mays	-1.31

Table S4.9 List of differentially expressed proteins with their accession ID, description and log2 fold change (logFC) when comparing heat stress condition against control condition for S11 729-10 at 28 d

Accession	Description	logFC
P30792	2,3-bisphosphoglycerate-independent phosphoglycerate mutase OS=Zea mays	-1
W5EP13	2-carboxy-D-arabinitol-1-phosphatase OS=Triticum aestivum	2.61
Q337M4	2-oxoadipate dioxygenase/decarboxylase, chloroplastic/amyloplastic OS=Oryza sativa subsp. japonica	2.27
Q6AVG6	4-hydroxy-3-methylbut-2-enyl diphosphate reductase, chloroplastic OS=Oryza sativa subsp. japonica	0.66
A0A2S3IJL2	5-methyltetrahydropteroyltriglutamate--homocysteine S-methyltransferase OS=Panicum hallii	-2.17
A0A3B6TBU2	6-phosphogluconate dehydrogenase, decarboxylating OS=Triticum aestivum	-0.59
A0A3B6NJT0	Acetyltransferase component of pyruvate dehydrogenase complex OS=Triticum aestivum	1.82
P32112	Adenosylhomocysteinase OS=Triticum aestivum	-2.06
A0A3B6JPU8	Adenylosuccinate synthetase, chloroplastic OS=Triticum aestivum	-0.82
A0A1D6HR58	alanine transaminase OS=Zea mays	-1.76
A0A1B6QHW4	Alpha-1,4 glucan phosphorylase OS=Sorghum bicolor	-1.63
Q9FXT4	Alpha-galactosidase OS=Oryza sativa subsp. japonica	-1.87
B8AU84	Arginase 1, mitochondrial OS=Oryza sativa subsp. indica	2.47
P37833	Aspartate aminotransferase, cytoplasmic OS=Oryza sativa subsp. japonica	-1.81
A0A1B6PGM0	aspartate carbamoyltransferase OS=Sorghum bicolor	1.25
A0A0E0D753	aspartate-semialdehyde dehydrogenase OS=Oryza meridionalis	0.68
A0A3B5ZZW5	assimilatory sulfite reductase (ferredoxin) OS=Triticum aestivum	-2.2
A0A2L0VAT4	ATP synthase subunit beta, chloroplastic OS=Lamarckia aurea	-1.43
P0C1M0	ATP synthase subunit gamma, chloroplastic OS=Zea mays	-1.19
A0A317YBF8	ATP-dependent DNA helicase OS=Zea mays	3.78
P16098	Beta-amylase OS=Hordeum vulgare	-3.45
A0A3B5Y061	Branched-chain-amino-acid aminotransferase OS=Triticum aestivum	0.65
B9EXM2	Carbamoyl-phosphate synthase large chain, chloroplastic OS=Oryza sativa subsp. japonica	0.97
A0A3B6KQP3	Catalase OS=Triticum aestivum	1.98
A0A1W0VZF1	CBM20 domain-containing protein OS=Sorghum bicolor	3.88
P29185	Chaperonin CPN60-1, mitochondrial OS=Zea mays	3.25
A2XJ35	Chlorophyll a-b binding protein, chloroplastic OS=Oryza sativa subsp. indica	0.51
A0A0E0GTN2	Cysteine synthase OS=Oryza nivara	-0.61
Q0JM17	DEAD-box ATP-dependent RNA helicase 56 OS=Oryza sativa subsp. japonica	0.87

A0A0E0JJD7	Endopeptidase Clp OS=Oryza punctata	-1.46
P36183	Endoplasmin homolog OS=Hordeum vulgare	1.39
Q69RJ0	Ferredoxin-dependent glutamate synthase, chloroplastic OS=Oryza sativa subsp. japonica	-1.18
P41344	Ferredoxin--NADP reductase, leaf isozyme 1, chloroplastic OS=Oryza sativa subsp. japonica	-1.96
Q6ZFJ3	Ferredoxin--NADP reductase, leaf isozyme 2, chloroplastic OS=Oryza sativa subsp. japonica	-2.47
A0A0E0N8J2	ferredoxin--NADP(+) reductase OS=Oryza rufipogon	-1.86
Q42997	Ferredoxin--nitrite reductase, chloroplastic OS=Oryza sativa subsp. japonica	-1.56
A0A1D5YQ12	Ferritin OS=Triticum aestivum	1.03
Q84N28	Flavone O-methyltransferase 1 OS=Triticum aestivum	-2.29
A0A4V6DBK4	Formate dehydrogenase, mitochondrial OS=Setaria viridis	1.65
Q0JGZ6	Fructokinase-1 OS=Oryza sativa subsp. japonica	-0.42
A0A2K2DTT5	fructose-bisphosphatase OS=Brachypodium distachyon	-0.47
Q40677	Fructose-bisphosphate aldolase, chloroplastic OS=Oryza sativa subsp. japonica	1.35
Q6AVT2	Glucose-1-phosphate adenylyltransferase large subunit 1, chloroplastic/amyloplastic OS=Oryza sativa subsp. japonica	-1.08
A0A3B6KSU0	Glucose-1-phosphate adenylyltransferase OS=Triticum aestivum	-1.06
A0A1D6I644	Glucose-6-phosphate isomerase OS=Zea mays	-0.99
Q33E23	Glutamate dehydrogenase 2, mitochondrial OS=Oryza sativa subsp. japonica	-1.98
I1HQF1	glutamate synthase (NADH) OS=Brachypodium distachyon	-3.15
P38562	Glutamine synthetase root isozyme 4 OS=Zea mays	-2.04
A0A3B6JM67	Glutathione reductase OS=Triticum aestivum	-0.59
Q10CE4	Glycolate oxidase 1 OS=Oryza sativa subsp. japonica	-0.97
B8B7C5	Glycolate oxidase 5 OS=Oryza sativa subsp. indica	-0.83
A0A0P0VLJ4	GrpE protein homolog OS=Oryza sativa subsp. japonica	1.46
C5WVT9	Guanine nucleotide-binding protein alpha subunit OS=Sorghum bicolor	-1.26
Q0J4P2	Heat shock protein 81-1 OS=Oryza sativa subsp. japonica	1.66
P02276	Histone H2A.2.1 OS=Triticum aestivum	-1.78
A2WKT4	Histone H2B.5 OS=Oryza sativa subsp. indica	-1.67
P68428	Histone H3.2 OS=Triticum aestivum	-2.51
Q0JCT1	Histone H3.3 OS=Oryza sativa subsp. japonica	-2.06
P62787	Histone H4 OS=Zea mays	-2.26
F8RP11	Hsp70-Hsp90 organizing protein OS=Triticum aestivum	1.46
P17788	Large ribosomal subunit protein uL2cz/uL2cy OS=Zea mays	-1.17
A0A3B6PVU5	L-ascorbate peroxidase OS=Triticum aestivum	1.12
P24067	Luminal-binding protein 2 OS=Zea mays	1.71
Q652L6	Monodehydroascorbate reductase 3, cytosolic OS=Oryza sativa subsp. japonica	-0.66

A0A0E0D501	Multifunctional fusion protein OS=Oryza meridionalis	1.04
P43279	NADP-dependent malic enzyme, chloroplastic OS=Oryza sativa subsp. japonica	-2.52
A0A0Q3RM53	ornithine aminotransferase OS=Brachypodium distachyon	2.19
A0A3B6LEJ3	Pectinesterase OS=Triticum aestivum	-2.9
Q336R9	Peptide methionine sulfoxide reductase A4, chloroplastic OS=Oryza sativa subsp. japonica	1.18
A0A3B6HT18	Phosphomannomutase OS=Triticum aestivum	-1.73
Q943K1	Photosystem II 22 kDa protein 1, chloroplastic OS=Oryza sativa subsp. japonica	0.74
A0A218LWN1	Photosystem II CP43 reaction center protein OS=Triticum monococcum	-0.63
A0A0S1S3S5	Photosystem II D2 protein OS=Stipa lipskyi	-0.71
A0A5P8FSR9	Photosystem II protein D1 OS=Bambusa variostriata	-0.79
O64411	Polyamine oxidase 1 OS=Zea mays	-1.29
Q67UK9	Probable glutathione S-transferase DHAR2, chloroplastic OS=Oryza sativa subsp. japonica	1.16
Q69SV0	Probable L-ascorbate peroxidase 8, chloroplastic OS=Oryza sativa subsp. japonica	0.96
P80607	Probable UDP-arabinopyranose mutase 1 OS=Zea mays	-1.35
O22655	Profilin-4 OS=Zea mays	-1.4
A0A3B6RCJ8	Proteasome subunit beta OS=Triticum aestivum	-0.77
A0A0E0NKR5	Pyruvate dehydrogenase E1 component subunit alpha OS=Oryza rufipogon	-0.77
A0A0E0HXE6	Pyruvate kinase OS=Oryza nivara	-1.45
A0A2S3ID39	Receptor-like serine/threonine-protein kinase OS=Panicum hallii	-1.29
A0A0E0MLI8	Ribulose bisphosphate carboxylase small subunit, chloroplastic OS=Oryza punctata	0.34
A0A0E0F9Y5	RNA cytidine acetyltransferase OS=Oryza meridionalis OX=40149 PE=3 SV=1	1.22
A0A077RWS5	S-adenosylmethionine synthase OS=Triticum aestivum	-1.72
P46285	Sedoheptulose-1,7-bisphosphatase, chloroplastic OS=Triticum aestivum	-2.09
P49027	Small ribosomal subunit protein RACK1z OS=Oryza sativa subsp. japonica	-1.79
B9F3B6	Succinate-semialdehyde dehydrogenase, mitochondrial OS=Oryza sativa subsp. japonica	1.03
A0A0D3H388	Superoxide dismutase [Cu-Zn] OS=Oryza barthii	-1.03
P09233	Superoxide dismutase [Mn] 3.1, mitochondrial OS=Zea mays	1.32
A0A3B6RMJ1	Thiamine thiazole synthase, chloroplastic OS=Triticum aestivum	-3.32
Q7SIC9	Transketolase, chloroplastic OS=Zea mays	-1.83
P46225	Triosephosphate isomerase, chloroplastic OS=Secale cereale	-1.13
Q9ZRB0	Tubulin beta-3 chain OS=Triticum aestivum	2.06
Q8H8T0	UDP-arabinopyranose mutase 1 OS=Oryza sativa subsp. japonica	-1.03
J3LV62	UMP-CMP kinase OS=Oryza brachyantha	-1.59

Q6Z058	Heat shock 70 kDa protein BIP5 OS=Oryza sativa subsp. japonica	2.43
A0A0E0PRJ8	very-long-chain 3-oxoacyl-CoA synthase OS=Oryza rufipogon	1.07
P49087	V-type proton ATPase catalytic subunit A (Fragment) OS=Zea mays	-0.6
A0A1D6FIR4	V-type proton ATPase proteolipid subunit (Fragment) OS=Zea mays	-1.6

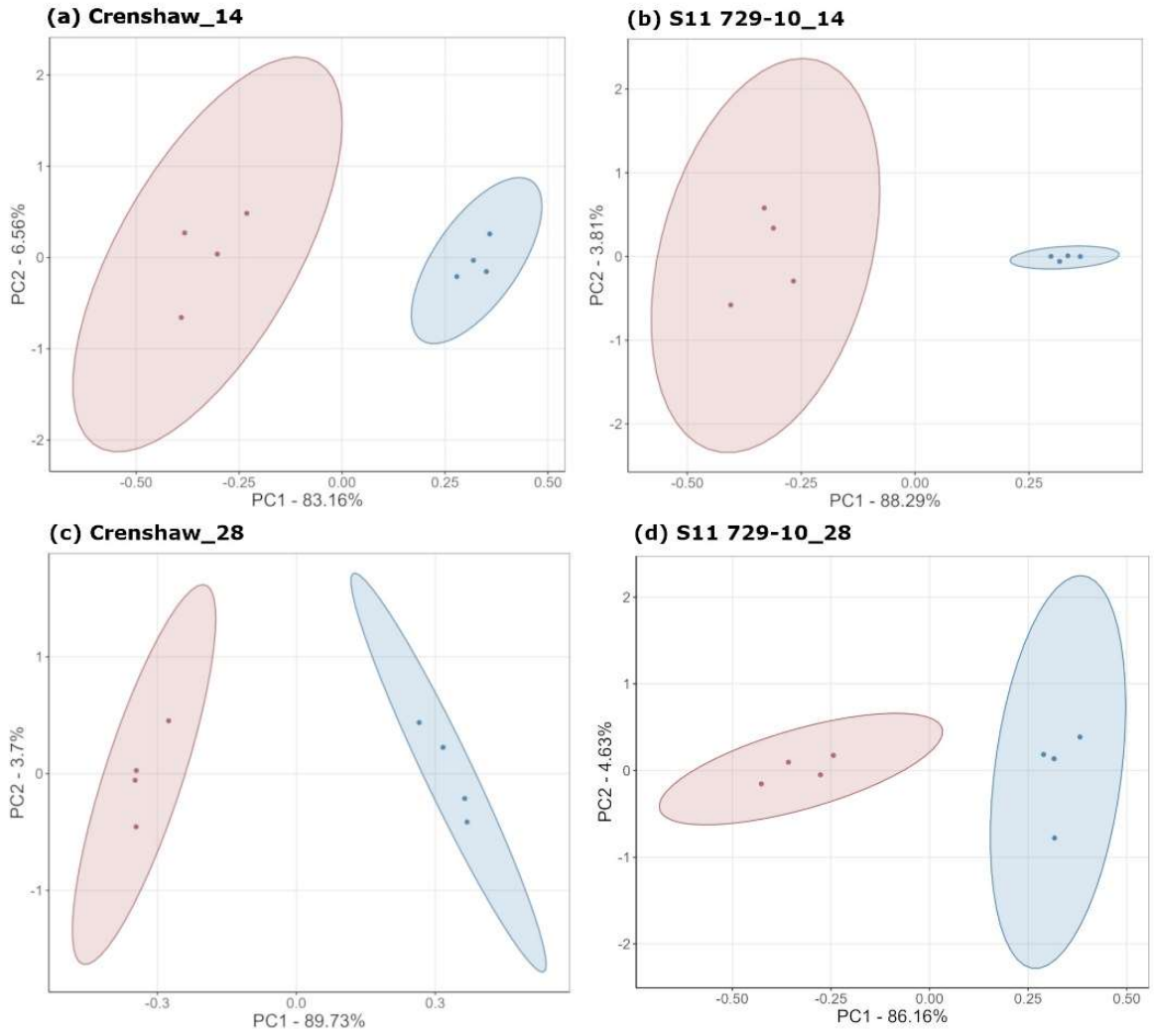

Figure S4.1 Principal component analysis for differentially expressed proteins of two creeping bentgrass lines (Crenshaw and S11 729-10) at 14 d (a, b) and 28 d (c, d). The red circle represented the control group while the blue circle represented the heat-stressed group within each plot.

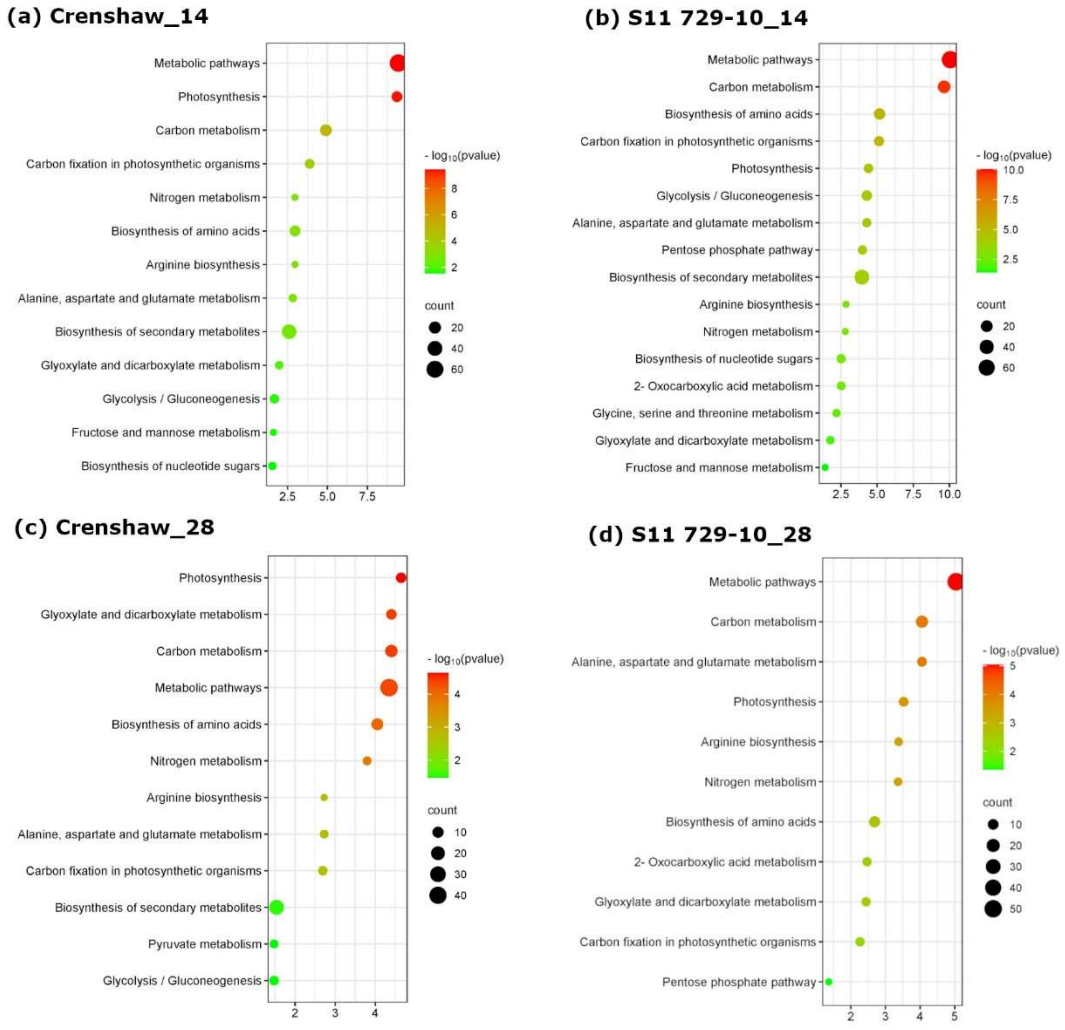

Figure S4.2 Kyoto Encyclopedia of Genes and Genomes (KEGG) analysis for differentially expressed proteins of two creeping bentgrass lines (Crenshaw and S11 729-10) at 14 d (a, b) and 28 d (c, d) responding to heat stress. The X axis represented the values of -log$_{10}$(pvalue).

CHAPTER 5

SUMMARY

Creeping bentgrass (*Agrostis stolonifera* L.) is an economically important turfgrass, which has been widely used in high-value sports areas like golf courses and tennis courts. It's highly prized for its superior turf qualities, like fine leaf texture, tolerance to close mowing and quicky recovery from traffic. However, as a cool-season grass, creeping bentgrass has only low to moderate tolerance to heat stress, resulting in poor performance in summer months, with damage being further exacerbated with the increasing trend of global warming. This has led to the conversion of many golf courses from creeping bentgrass to warm-season species. As creeping bentgrass is still desired by turfgrass superintendents, there is a critical need for the improvement of its heat tolerance.

A series of physiological damage can de induced in response to temperature elevation, including photosynthetic inhibition as a consequence of chlorophyll breakdown and reduced photosystem II (PSII) activity, oxidative stress due to overproduction of reactive oxygen species (ROS), as well as the interruption in protein metabolism. More tolerant cultivars or genotypes typically exhibit better maintenance of these cellular activities. Creeping bentgrass shows considerable intraspecific diversity among different lines for its tolerance to heat. Previous research has identified several experimental lines with exceptional summer performance. Nevertheless, the specific mechanisms involved in their enhanced tolerance to heat have not yet been clearly revealed at both physiological and molecular levels. A more complete understanding

of the mechanisms conferring improved thermotolerance is essential for the efficient development of elite cultivars. Hence, the central theme of this dissertation is to explore the heat stress mechanism in selected creeping bentgrass germplasm.

The second chapter aimed to screen a collection of creeping bentgrass germplasm (five cultivars and five experimental lines) for heat tolerance and determine the physiological mechanism leading to the differential tolerance levels. A number of measurements were taken to indicate plants' responses regarding photosynthetic ability, oxidative stress and protein metabolism. Principal component analysis and clustering analysis were then performed to rank stress performance and divide lines into different groups according to their tolerance similarities, respectively. Specifically, S11 729-10 and BTC032 were in the most thermotolerant group while BTC011, AU Victory and Penncross were in the second most thermotolerant group; Crenshaw belonged to the most heat-sensitive group while S11 675-02 and Pure Eclipse were in the second most heat-sensitive group; The group containing Penn A4 and GCB202-1 was intermediate in their tolerance ranking. The exceptional thermotolerance in S11 729-10 and BTC032 was mainly associated with their greater abilities to maintain integrity of cellular membranes, as well as protein metabolism, and the ability to minimize oxidative damages. In addition, among various light-harvesting steps, energy trapping, dissipation and electron transport from Q_A to PQ were more heat-sensitive than electron transport from Q_A to final PSI acceptors. Moreover, strong significant correlations were detected among multiple OJIP parameters and other stress-related factors. Along with the strong correlations between multiple OJIP parameters and other traits, it reveals that OJIP fluorescence could be a valuable tool for dissection of photosynthetic processes and identification of the critical steps responsible for photosynthetic declines, enabling a more targeted heat-stress screening. The findings indicated that variability in the level of heat tolerance and associated

mechanisms in creeping bentgrass germplasm could be utilized to develop new cultivars with improved thermotolerance.

Proteins are major drivers of cellular activities. However, responding to heat stress, protein will be denatured due to direct damage of extreme temperatures or oxidized due to overproduced ROS. These damaged proteins have to be removed. Otherwise, they can accumulation and form toxic aggregates, which can interfere with normal metabolic activities like aforementioned photosynthesis and oxidative defense, accelerating cellular aging and even death. One major approach to remove these damaged proteins is to degrade them into amino acids through proteolytic pathways, mainly proteases and the ubiquitin-proteasome system (UPS). Unlike normal conditions where there is a balance of proteins constantly being degraded and synthesized, protein degradation is typically accelerated relative to protein synthesis under heat stress, suggesting untimely replacement of degraded proteins by newly synthesized proteins. This will lead to decreases in total protein contents, eventually impairing normal metabolic activities and contributing to reduced tolerance level. Differential accumulations of total proteins were detected in association with varying levels of tolerance in our Chapter 2. However, the specific pathways responsible for protein degradation, the changes in individual protein accumulation that are driving the differences in heat tolerance, as well as the identification of substrate proteins taking specific proteolytic pathway, particularly the UPS, remained to be documented. Therefore, for the rest of my projects, a special focus was put on the investigation of protein metabolism by utilizing the identified heat-tolerant and -sensitive creeping bentgrass lines from Chapter 2.

Chapter 3 aimed to identify pathways for increased protein degradation by quantifying proteolytic activity and associated gene expression and understand the associated differences between heat-tolerant and -sensitive lines. It was found that protein degradation was enhanced

under heat as demonstrated by significant increases in protease activity and the UPS activity over time. A more heat-tolerant line, S11 729-10, maintained lower activities of both protease and the UPS, contributing to its higher protein contents, and thereby greater thermotolerance. Additionally, cysteine protease was more heat-inducible than serine protease during the midpoint phase of leaf senescence. This is the first time that the roles of protease activity and the UPS activity in heat stress were simultaneously analyzed in a perennial grass species. Chapter 4 aimed to estimate change in global protein accumulations by performing gel-free proteomics and identify proteins that have been polyubiquitinated and targeted to the UPS pathway via polyubiquitin-omics in contrasting creeping bentgrass lines exposed to heat stress. It was concluded that heat-tolerant S11 729-10 was able to maintain less severe downregulation of the proteins involved the light reactions of photosynthesis, while enhancing the upregulation of antioxidant proteins, particularly during the later phase of stress. These contributed to its improved physiological performance including greater cell membrane integrity as well as healthier light harvesting components, eventually leading to greater thermotolerance in S11 729-10. For the first time, polyubiquitin-omics analysis was applied to turfgrass research and it as found that the faster turnover of key polyubiquitinated antioxidant proteins in S11 729-10 likely represents a critical mechanism for protecting against oxidative damage and enhancing tolerance under prolonged heat stress. Our findings suggest the powerfulness of gel-free proteomics and polyubiquitin-omics in improving the understanding of global protein accumulation and degradation though the UPS, as well as their associated physiological responses, providing deeper insights into the molecular basis of heat tolerance.

Overall, this dissertation examined multiple regulatory levels—biochemical, global protein, and ubiquitin-tagged proteins—to investigate protein degradation and metabolism in heat-stressed plants. This approach provides a deeper understanding of the physiological performance

of plants, contributing to a greater insight into the thermotolerance mechanisms in creeping bentgrass. The identified key proteins and pathways plus unique germplasm can be utilized to develop new cultivars with enhanced tolerance to increasing temperature, thereby maintaining economic productivity in the face of climate change. Further studies on transcriptomics and protein turnover rates are needed to gain a more complete picture of how protein metabolism is regulated at different levels.